Role of liver cells in bacterial antigen metabolism and MAIT cell activation

Inauguraldissertation

zur

Erlangung der Würde eines Doktors der Philosophie vorgelegt

der Philosophisch-Naturwissenschaftlichen Fakultät der

Universität Basel

von

Martin LETT

2021

Genehmigt von der Philosophisch-Naturwissenschaftlichen Fakultät

auf Antrag von:

PD Dr. med. Dr. phil. Magdalena Filipowicz Sinnreich, Erstbetreuerin

Prof. Dr. med. Dr. phil. Christoph Hess, Zweitbetreuer

Prof. Dr. phil. Christian Münz, Externer Experte

Prof. Dr. Martin Spiess, Dekan

Basel, 23.06.2020

Acknowledgements

First, I would like to express my sincere gratitude to my supervisor: PD Dr. Magdalena Filipowicz-Sinnreich for her continuous and unrestricted support during my PhD study. Her supervision clued me in all the time of research and writing this thesis. Thanks for her constructive comments, and valuable feedbacks. With her trust, she gave me the opportunity to work in the stimulating environment of the Department of Biomedicine, and to join the renowned University of Basel.

I am truthfully thankful to my colleagues in the Lab: Dr Tina Jaeger and Dr Maxime Jacquet many thanks for the help and the fun. A special word for my oldest colleague Tina, thank you for bringing original perspective and for the encouragements.

I am deeply grateful to my PhD committee members for sharing their experience, for their valuable advices and relevant inputs: Prof. Dr. med. Christoph Hess, and Prof. Dr. phil. Christian Münz.

My thankfulness to Experimental Immunology actual and past laboratory members for sharing knowledge and experience. Thank you to Prof. Gennaro De Libero for hosting us in his lab. Particular attention for Dr Tobias Rutishauser, and Dr Mathias Schmaler for the entertaining scientific discussions.

I want to acknowledge the people I worked with before starting my PhD, at the university of Strasbourg, with a special thank you to Dr Emilie Sick. Her curiosity and critical thinking strength my will to persevere in science.

I am grateful to my parents to whom I dedicated this work, thank you for supporting and encouraging me during all these years. Thanks to my sister for 29 years of complicity.
Finally thank you to my wife for being marvelous, for bringing more music and new color to my life. To my daughter, keep laughing, keep smiling, it makes everything different…

List of Abbreviations:

5-A-RU: 5-amino-6-D-ribitylaminouracil
5-F-SA: 5-formyl-salicylic acid
5-OP-RU: 5-(2-oxopropylideneamino)-6-D-ribitylaminouracil
6-FP: 6-formylpterin
Ab: Antibody
ACKR1: Atypical chemokine receptor 1
ADA: Adenosine Deaminase
ADCC: Antibody-dependent cellular cytotoxicity
Ag: Antigen
AIH: Autoimmune hepatitis
ALD: Alcoholic liver disease
ALT: alanine aminotransferase
APC: Antigen presenting cell
APTES: (3-Aminopropyl)triethoxysilane
ASH: Alcoholic steatohepatitis
AST: aspartate aminotransferase
BCG: Bacillus Calmette–Guérin
BEC: Biliary epithelial cell
BSEP: Bile salt export pump
CCL#: Chemokine (C-C motif) ligand #
CCR#: C-C chemokine receptor type #
CDCA: Chenodeoxycholic acid
CDR: Complementarity-determining regions
CFU: colony forming unit
CLEC2D: C-type lectin domain family 2 member D
CXCL#: Chemokine (C-X-C motif) ligand #
CXCR#: C-X-C chemokine receptor type #
C/EBP: CCAAT-enhancer-binding proteins
DAMP: Damage-associated molecular pattern
DC: Dendritic cell
DN: double negative
DPPIV: Dipeptidyl peptidase-4
EC50: Effective concentration 50
EOMES: Eomesodermin
ER: Endoplasmic reticulum
FcRγIIIa: Fc receptor gamma III
FXR: Farnesoid X receptor
GLP-1: Glucagon-like peptide-1
GGT: Gamma-glutamyl transferase
GPR#: G-protein coupled receptor
HBV: Hepatitis B virus
HCV: Hepatitis C virus
HIV: Human immunodeficiency viruses
HTLV: Human T-lymphotropic virus,
HPLC: High performance liquid chromatography
HSC: Hepatic stellate cell
IFN-γ: Interferon gamma
IF: Immunofluorescence

IG: Immunoglobulin
IL: Interleukin
iNKT: Invariant natural killer T cell
ITAM: Immunoreceptor tyrosine-based activation motif
ITIM: Immunoreceptor tyrosine-based inhibition motif
KLRB1: Killer cell lectin-like receptor subfamily B, member 1
LARC: Liver and activation-regulated chemokine
LCA: Lithocholic acid
LCK: Lymphocyte-specific protein tyrosine kinase
LLT-1: Lectin-like transcript 1
LPAR1: Lysophosphatidic acid receptor 1
LSEC: Liver sinusoidal endothelial cell
MAIT: Mucosal-associated invariant T cell
MCP: Monocyte chemoattractant protein
MHC: Major histocompatibility complex
MR1: MHC class I-related protein 1
MS: Mass spectrometry
NEAA: Non-essential amino acids
NAFL: Non-alcoholic fatty liver
NAFLD: Non-alcoholic fatty liver disease
NASH: Non-alcoholic steatohepatitis
NCAM: Neural cell adhesion molecule
NF-κB: Nuclear factor-kappa B
NK: Natural killer
NPCs: Non-parenchymal cells
OCIL: Osteoclast inhibitory lectin
PAMP: Pathogen-associated molecular pattern
PBC: Primary biliary cholangitis
PBMCs: Peripheral blood mononuclear cells
PDITC: p-Phenylene diisothiocyanate
PDMS: Polydimethylsiloxane
PFA: Para-formaldehyde
PHA: Phyto-hemagglutinin
PLZF: Promyelocytic leukaemia zinc finger protein
P/S: Penicillin/Streptomycin
PSC: Primary sclerosing cholangitis
PLVAP: Plasmalemma vesicle associated protein
RORγT: RAR-related orphan receptor gamma
RL-7-Me: 7-methyl-8-ribityllumazine
RT: room temperature
SCFA: Short-chain fatty acids
SCID: Severe combined immunodeficiency
SHP-1: Src homology region 2 domain-containing phosphatase-1
STAT: Signal transducer and activator of transcription
TCR: T cell receptor
TLR: Toll-like receptor
TNBS: Trinitrobenzene sulfonic acid
TNF: Tumor necrosis factor
UDCA: Ursodeoxycholic acid
UV: ultraviolet

I. Summary

Background and rationale: Mucosal-associated invariant T (MAIT) cells are an evolutionary conserved subset of T cells with a partially invariant T cell receptor (TCR). The recent discovery of their antigen (Ag), and MR1 as the Ag-presenting molecule, demonstrated their microbial restriction and stimulated their study in humans. Changes in their phenotype have been observed in infectious and autoimmune diseases. Decreases in MAIT cell frequency have been observed in several chronic inflammatory diseases. These alterations are particularly observed in the liver, where MAIT cells represent the most abundant T cell population in healthy humans. Moreover, studies conducted in animal models showed a deleterious effect of activated MAIT cells in liver fibrosis. The process leading to MAIT cell activation remains largely unexplored, and only biliary cells have been shown to be able to present Ag to them in the liver environment. Here we assessed the activation of MAIT cells by various human primary liver cell types. We also investigated the capacity of liver cells to generate active Ag from bacteria-derived precursor, and studied the influence of molecular cell-cell interactions and MR1-inhibitors on MAIT cell activation.

Results: Primary human parenchymal and non-parenchymal cells efficiently present bacterial and synthetic Ag to MAIT cells. The comparison between the cells shows that hepatocytes are most efficient in inducing IFNγ secretion by MAIT cells. This effect is not mediated by IL-18, IL-12 or IL-23. Primary liver cells are capable of generating the active antigen 5-OP-RU from its precursor 5-A-RU. This is of interest regarding our *in silico* data which predict passive diffusion of both compounds with a better score for 5-A-RU, the precursor. Liver cell-mediated MAIT cell activation is seen both in a MAIT cell clone derived from peripheral blood and in liver-derived MAIT cell lines, and leads to downregulation of the TCR, as well as IFNγ and IL-17A secretion. The incubation of primary liver cells with MR1 blocking ligands leads to a drastic diminution of the activation. I also identify CLEC2D as a potent regulator of MAIT cell activation, the surface over-expression of which is strongly inhibiting MAIT cell activation, as well as leading to CD161 downregulation.

Discussion: Considering the hypothesized role of activated MAIT cells in the vicious circle of liver fibrosis, the identification of their activation mechanism is decisive. We established that all tested primary liver cells are prone to present bacteria derived Ag to MAIT cells. Additionally, we observed that hepatocytes, the most abundant liver cells, are the most efficient ones, as seen by the more pronounced cytokine secretion they induced in MAIT cells. With such myriad of APCs surrounding them, the availability of MAIT cell antigen in the liver is critical. Our *in silico* model suggests that active Ag and precursor can reach the liver. This is of particular importance regarding our evidence that primary liver cells can generate active Ag from precursor. The deleterious action of activated MAIT cells in the liver argues for the study of approaches preventing their stimulation. We demonstrated that the use of MR1 blocking ligands was efficient *in vitro,* using primary human liver cells. Furthermore, our investigation of the mechanism behind the discordances of Ag presentation between liver cells lead us to consider the role of the ligand of CD161, CLEC2D. We demonstrated a CLEC2D dependent inhibition of IFNγ secretion associated with a downregulation of CD161 on MAIT cells. We do not know yet whether this mechanism explains the difference observed in Ag presentation. Nevertheless, these findings place CLEC2D as a new potential therapeutic target in immune regulation, especially in the liver, where the majority of T cells express CD161. Overall, this work increases our understanding of MAIT cell activation in the human liver. The diffusion of MAIT cell Ag to the human liver has yet to be proven, but would argue for a central role of the intestinal microbiota and the integrity of the gut barrier in liver health. The study of the presence of MAIT cell stimulatory Ag in the circulation and liver in the liver disease context will help us understand better the pathophysiology of liver inflammatory diseases.

II. Introduction

A. MAIT cells

1. Discovery and definition

The existence of T cells bearing a partially invariant T cell receptor (TCR) was first postulated in 1993 by Porcelli and colleagues(Porcelli et al., 1993). In this publication the authors purified CD4/CD8 double negative T cells. The rearrangement of their TCR was analyzed by random cloning of single chain PCR. Two semi-invariant alpha chain rearrangements were identified, one using Vα24, the other Vα7.2. In the 90s the T cells expressing the Vα24 chain were profoundly studied, their restriction to CD1d was demonstrated in 1997, and they have been termed invariant natural killer T cells (iNKT)(Exley et al., 1997). Probably because of their sparsity in mouse, the Vα7.2 invariant T cells remained mysterious until Lantz and colleagues formally proved their restriction to the non-polymorphic MHC-I like molecule MR1(Treiner et al., 2003). The same laboratory chose the name Mucosal Associated Invariant T (MAIT) cells for the cells, as they found them to be enriched in the intestinal mucosa. The antigen (Ag) was at the time still unknown but the development of an antibody (Ab) against the Vα7.2 chain permitted the characterization of MAIT cells, at the time defined as CD3+ Vα7.2+ CD161high(Martin et al., 2009). A study using transgenic mice over-expressing Vα19 (ortholog to Vα7.2) show that MAIT cells are present in the gut lamina propria and can secrete TNF, IFN-γ, IL-10 and IL-4(Kawachi et al., 2006). In humans, MAIT cells were shown to be capable to react to several bacteria and to produce IFN-γ and TNF(Gold et al., 2010; Le Bourhis et al., 2010). In adults MAIT cells show an effector memory phenotype with no surface expression of CCR7 but expression of CD45RO; these features are not present in human cord blood where a naïve phenotype can be seen(Dusseaux et al., 2011). On the transcription level MAIT cells were shown to co-express T-bet and RORγt(Billerbeck, 2010; Dusseaux et al., 2011).

Evolutionary studies have shown that MR1 and MAIT cells are highly conserved in evolution. Moreover, interspecies cross presentation is frequent, human MAIT cells can recognize bovine and rat MR1, and the absence of recognition of mouse MR1 is because of a single amino-acid exchange(Goldfinch et al., 2010; Huang et al., 2009). Huang and colleagues showed the endocytic pathway to require late endosome, but to be independent of the proteasome, indicating that the Ag might be non-peptidic despite the high homology between MR1 and MHC-I(Huang et al., 2009). The Ag nature mystery was finally solved in 2012, when the team of Prof. J. McCluskey could show that denatured MR1 was able to refold in the presence of 6-formyl-pterin (6-FP), an UV-degradation product of folic acid. Hence, this study shows two surprising properties of MR1: it binds small organic polar ligands, and this binding is covalent(Kjer-Nielsen et al., 2012). 6-FP, although very affine for MR1, could not activate MAIT cells, but the same publication highlighted other vitamin B metabolites with this capacity: 6-hydroxymethyl-8-D-ribityllumazine (rRL-6-CH2OH) and 6,7-dimethyl-8-D-ribityllumazine (RL-6,7-diMe). Both ligands were capable of activating MAIT cells at µM levels, without covalently binding MR1. Two years later the same laboratory demonstrated the existence of much more potent MAIT cell activating molecules, capable of covalently binding MR1, namely 5-(2-oxopropylideneamino)-6-D-ribitylaminouracil (5-OP-RU) and 5-(2-oxoethylideneamino)-6-D-ribitylaminouracil (5-OE-RU). Both molecules can activate MAIT cells at a concentration below one nanomolar. The same team used this Ag to generate MR1 tetramer capable of staining MAIT cell TCR, establishing a non-ambiguous MAIT cell identification system(Corbett et al., 2014).

Hence, MAIT cells are defined as T cells expressing a TCR Vα7.2 chain reacting to 5-OP-RU presented by MR1.

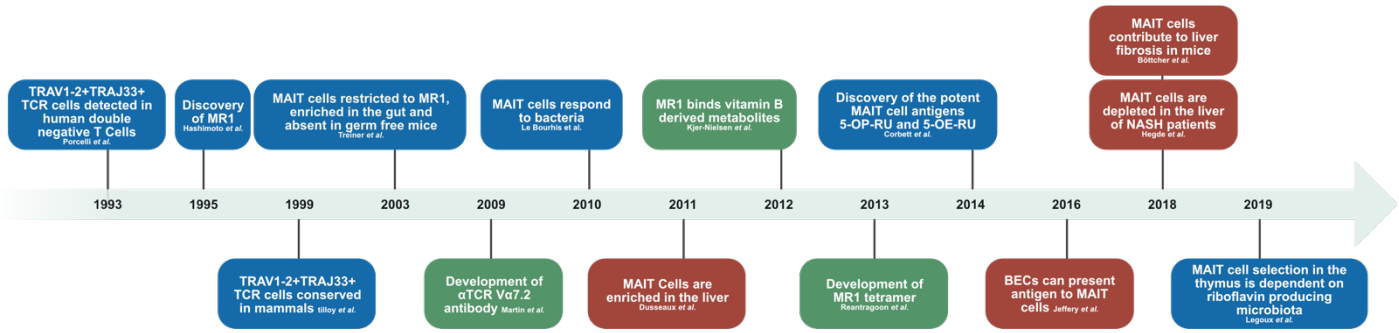

Figure 1: Timeline highlighting some of the most relevant findings in the study of the role of MAIT cells in the liver. Findings in blue are crucial for the whole MAIT cell field, the green boxes show crucial tool development, and in red studies concerning the liver and MAIT cell are depicted.

2. Antigen recognition by MAIT cells

Several MAIT cell Ags have been discovered, so far all derived from the riboflavin (Vitamin B2) biosynthesis intermediate 5-amino-6-D-ribitylaminouracil (5-A-RU). The most powerful ones are the two closely related 5-OP-RU and 5-OE-RU, both derived from the condensation of the Ag precursor 5-A-RU with methylglyoxal and glyoxal, respectively (Fig. 2)(Corbett et al., 2014). Before 5-OP-RU was discovered, it was already shown that MAIT cells react only to Ag derived from some bacteria but not others like *Listeria monocytogenes*, and not to several viruses *in vitro*(Gold et al., 2010). The discovery that riboflavin biosynthesis was indispensable for the generation of all MAIT cell Ags unmasked why MAIT cells react to some bacteria and not to others(Corbett et al., 2014).

MAIT cell Ag is by definition not synthesized by mammalian cells, hence the Ag precursor 5-A-RU is also absent in human cells, thus permitting the distinction between "self" and "non-self" for MAIT cells. In contrary, plants, fungi and many bacteria are capable of producing riboflavin. 5-A-RU is found in most commensal and pathogenic bacteria, although with differences between phyla(Corbett et al., 2014; Magnúsdóttir et al., 2015). The amount of riboflavin produced by an organism varies depending on the context, the availability of riboflavin in the environment, and the amount of riboflavin transporter expressed(Cisternas et al., 2017; Mack et al., 1998; Schmaler et al., 2018). Moreover, riboflavin catabolism can vary among serotypes of a single strain, accordingly, Hartmann and colleagues showed that a distinct serotype of *Streptococcus pneumoniae* with lower riboflavin synthesis capacity was less activatory for MAIT cells *in vivo.* The authors hypothesize that modulation of riboflavin synthesis could be an immune escape mechanism(Hartmann et al., 2018).

MAIT cell Ags have unusual properties compared to other T cell Ags. Conventional T cells respond to peptide Ags presented by MHC-I or MHC-II, whereas CD1-restricted T cells recognize lipids. In both cases the molecules weigh usually between 1000 and 3000 Daltons and are stable in the absence of specific degradation enzymes. 5-OP-RU in contrast weights only 330 Da and is chemically unstable in solution, with a half-life in aqueous solution of approximately 2 hours(Corbett et al., 2014). Despite its instability, 5-OP-RU can be absorbed through the intestine and the skin and it is 5-OP-RU derived from the gut microbiota which is presented to thymocytes in the thymus and indispensable for MAIT cell development, hence

explaining the absence of MAIT cells in germ free animals(Legoux et al., 2019; Treiner et al., 2003). Moreover, as opposed to conventional Ags, 5-OP-RU and 5-OE-RU are covalently bound in the hydrophilic pocket of MR1, which can explain their very high potency with their EC50 being in the picomolar range(Awad et al., 2020; Schmaler et al., 2018). This binding makes it almost impossible to displace these Ags in physiologic conditions without denaturing MR1. Interestingly, the covalent binding relies on a single amino acid lysine in position 43, which is conserved in every species possessing a functional MR1 gene. Mutated MR1 proteins with alanine replacement of this lysine are still capable of capturing Ags but with weaker affinity. What is more, they are capable of refolding in the absence of Ag, but in this case cannot bind the MAIT cell TCR(Reantragoon, 2013). A further singularity of MR1 compared to any other Ag presenting protein, is the existence of blocking ligands. Like for MHC-I, binding to its ligand results in MR1 targeting to the plasma membrane, and in the case of MR1, to its upregulation at the membrane as the normal levels are very low(Kjer-Nielsen et al., 2012; Raghavan et al., 2008). But opposite to MHC-I, several MR1 blocking ligands have been described, capable of covalently binding and stabilizing MR1, thereby promoting its membrane trafficking; however, they neither interact enough with the TCR to activate MAIT cells, nor do they bind MAIT cell TCRs when used in tetramer staining. Moreover, as opposed to endogenous peptides in MHC-I, these metabolite ligands cannot be displaced from MR1 without degradation. Several aforementioned blocking ligands have been described, the most potent ones being the folate derivate 6-FP and its acetylated derivative Acetyl-6-FP, and the aspirin derivative 3-formyl-salycilic acid(Keller et al., 2017).

The exact mechanism of MR1 loading, trafficking to the plasma membrane, and recycling is not fully understood, yet two pathways have been described. The first pathway, demonstrated with the use of exogenous Ag, showed that MR1 presentation of Ag is not sensitive to inhibitors of vesicle acidification. The large majority of MR1 was retained in the endoplasmic reticulum (ER) and associated with β2M after binding the ligand which reached the ER without endocytosis. The complex was then targeted to the Golgi and then to the plasma membrane(McWilliam et al., 2016; Ussher et al., 2016). The second model was established in studies on the presentation of Ags derived from *M. tuberculosis*. In this case, although the majority of MR1 was retained in the ER, the Ag presentation was dependent on the pool of MR1 in endosomes, and thus blocked by endosome acidification inhibitors.

In this model, MAIT cell response to *M. tuberculosis* was increased when the cells were primed with acetyl-6-FP. This priming likely lead to the delivery of MR1 from the ER to the membrane, and the later recycling made MR1 available for the intracellular bacterial Ags, which could then be loaded in the endosomes(Karamooz et al., 2018, 2019). Both pathways probably exist in parallel with probable differences depending on the APC type. MR1 loading on the cell surface is possible as well *in vitro*, but its relevance *in vivo* is so far not determined(Karamooz et al., 2018).

Several crystal structures of the TCR-MR1 complex loaded with 6-FP or with 5-OP-RU have been published, the presence of the blocking ligand slightly modifying but not preventing the complementarity-determining region (CDR)3β of the MAIT TCR to interact with MR1. The alteration is more pronounced with the CDR3α, which is the only interacting motif between the MAIT cell TCR and activating Ags; when MR1 is loaded with 6-FP this interaction is weakened. The CDR3α is the highly conserved between MAIT cell clones and among species, with a consensus motif CAXXDSNYQL. The most important amino acid in the CDR3α is tyrosine 95, which is highly interacting with MR1 jaws, but also with the Ag in the pocket *via* a hydrogen bond(Eckle et al., 2014; López-Sagaseta et al., 2013). The CDR3β is much more variable although originating from oligoclonal recombination, and mostly interacting with MR1 jaws, similar also to both CDR1 and CDR2(Lepore et al., 2014; Reantragoon et al., 2012). Interestingly, the described Ags occupy only a small fraction of the volume of the MR1 groove which is approximately 760 Å, moreover MR1 possesses two pockets, the basic hydrophilic A' pocket and the mysterious F' pocket(López-Sagaseta et al., 2013). It is thus probable that MR1 could bind and present larger Ags, or, as the Ag in the A' pocket is very strongly bound, accommodate a second Ag in the F' pocket.

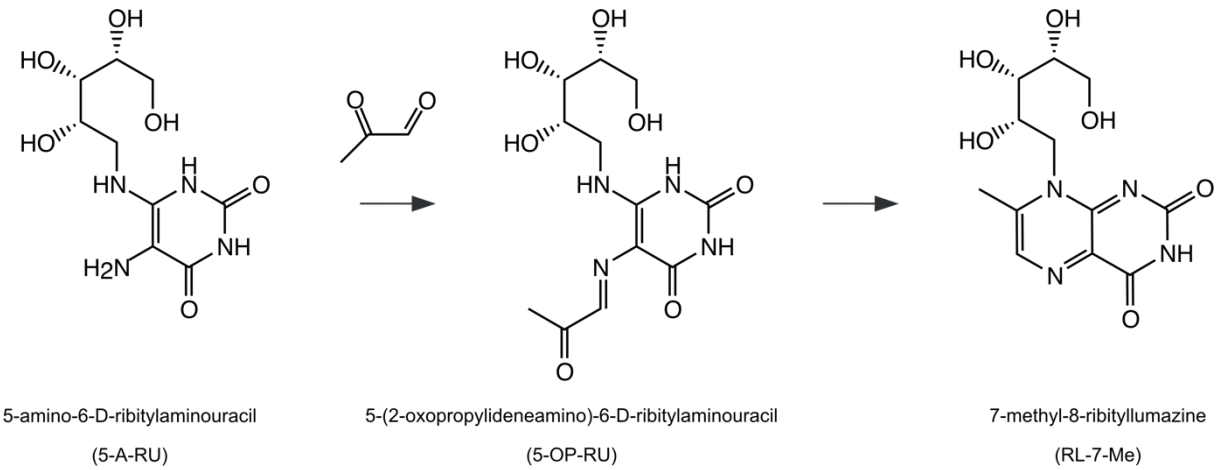

Figure 2: Chemical formation of pyrimidines and lumazines from condensation of methylglyoxal with 5-A-RU. 5-amino-6-D-ribitylaminouracil (5-A-RU) non enzymatically reacts with methylglyoxal to form the compelling antigen 5-(2-oxopropylideneamino)-6-D-ribitylaminouracil (5-OP-RU), which can undergo spontaneous cyclization into the 1000 times weaker antigen 7-methyl-8-ribityllumazine (RL-7-Me).

3. MAIT cell profile

Besides their Ag reactivity, MAIT cells express a unique combination of surface receptors, transcription factors and effectors which are not ubiquitous among T cells and inform us about their function. Some of these are universally expressed on MAIT cells, while others are tissue- or activation-dependent. MAIT cells all express TCR Vα7.2, CD26, IL-18 receptor, and a high level of CD161. Moreover, MAIT cells express several proteins usually found on natural killer (NK) cells, like CD56, and CD16a, associated with the chemokine receptors CCR2, CCR5, CCR6 and CXCR6. The next chapter will describe these proteins and how their role in other immune cells can open perspectives about their function in MAIT cells.

a) CD26

CD26, also called dipeptidyl peptidase IV (DPPIV), is a serine protease which can be expressed on the external surface of the cell as well as in a soluble form. Hepatocytes, epithelial cells in the small intestine, and endothelial cells express it(Balaban et al., 2007; Itou et al., 2013; Pala et al., 2003). Because of its degradation capacity of glucagon-like peptide 1 (GLP-1), CD26 has been extensively studied in diabetes, and DPPIV inhibitors are part of the routine treatment for type 2 diabetes(Idris and Donnelly, 2007). CD26 is also expressed by immune cells, first characterized as an activation marker on T cells and NK cells, the protein was later shown on B cells(Aliyari Serej et al., 2017). The protease is also expressed in the myeloid compartment by macrophages and dendritic cells (DCs)(Waumans et al., 2015). Studies in mice and severe combined immunodeficiency (SCID) patients, which have only tiny levels of lymphocytes, suggest that they are the major source of soluble CD26 in the circulation(Casrouge et al., 2018). Besides expression on activated lymphocytes, CD26 is mainly expressed on subsets of resting CD4 memory cells(Aliyari Serej et al., 2017; Bailey et al., 2017). Knock out studies in mice suggest its important role in T cell proliferation and T cell dependent Ab secretion(Yan et al., 2003). We can explain this by two characteristics of the enzyme, it can cleave terminal moieties of several cytokines, and act as a co-stimulatory signal for T cells. CD26 by its enzymatic activity can strongly affect the potency of many chemokines, or modulate their receptor spectrum.

For example, after cleavage CCL3 and CCL5 show decreased affinity for CCR3 but increased avidity for CCR1 and CCR2 respectively(Metzemaekers et al., 2016; Struyf et al., 1998). The co-stimulatory aspect is independent of its catalytic activity; cross linking of CD26 on the T cell surface induces stimulation in a TCR dependent manner(Hegen et al., 1993, 1997). This cross-linking can be induced by the binding of caveolin present at the surface of the Ag-presenting cell (APC)(Ohnuma et al., 2007). Interestingly, the binding of CD26 to caveolin will induce intracellular signaling in the APC leading to CD86 upregulation and hence an increased T cell stimulation(Ohnuma et al., 2004). Another pro-stimulatory aspect of surface CD26 expression for T cells is its binding of the enzyme adenosine deaminase (ADA) which degrades adenosine into inosine. As adenosine is an inhibitor of T cell activation, this is an additional pro-stimulatory mechanism(Linnemann et al., 2009). The combination of all these features explains why CD26 is critical for many T cell functions, like their recruitment into tissue(Rai et al., 2012).

The role of CD26 on MAIT cells is not well studied, but they represent by far the largest population of CD8 T cells expressing constitutively high levels of CD26(Sharma et al., 2015). Hence, higher levels suggest more co-stimulation potential mediated by caveolin-1, which is interesting because, opposite to many other co-stimulatory ligands, caveolin-1 is constitutively expressed on non-professional APCs, whereas most co-stimulation ligands are not(Goronzy and Weyand, 2008). MAIT cells can produce CCL5 (RANTES), a known substrate of DPPIV/CD26; hence, it is possible that CCL5 secreted by MAIT cells is post-translationally modified by CD26. As the cleavage mediated by CD26 diminishes affinity of CCL5 for CCR3, it will increase CCL5 signaling toward CCR2 and CCR5 instead(Maekawa et al., 2018; Metzemaekers et al., 2016). This would lead to flawed chemotaxis towards monocytes and lymphocytes compared to eosinophils(Bertrand and Ponath, 2000; Fantuzzi et al., 2019). The exact role of CD26 needs to be more precisely assessed in future studies.

b) IL-18 receptor

IL-18 receptor is a heterodimer composed of IL-18 receptor α chain (IL18 Rα; also called CD218) and IL-18 receptor β chain. In humans the receptor is highly expressed on NK cells, and also on approximately 1/3 of T cells, mostly on Th1(Gherardin et al., 2018; Yoshimoto et al., 1998). Naïve T cells, basophils, mast cells, and CD4 natural killer T (NKT) cells primed with IL-12 upregulate IL-18 receptor(Nakanishi et al., 2001). IL-18Rα binds IL-18 with a low affinity but this permits the heterodimerization of the receptor with IL-18Rβ, leading to a conformational change increasing the affinity and signaling through MyD88, TRAF and NF-κB(Yasuda et al., 2019). IL-18Rα can also bind IL-37 and dimerize with IL-1R8 leading to an inhibitory signal through STAT3. IL-18 was first discovered on Kupffer cells, but later shown to be produced by many cells belonging or not to the immune compartment. IL-18 is produced as an inactive precursor called pro-IL-18 in a similar fashion as IL-1β(Fantuzzi et al., 1998; Ushio et al., 1996). This precursor needs to be processed by the inflammasome to form the active IL-18(Shi et al., 2017). Hence, the production of active IL-18 is highly dependent on the inflammasome, which can be induced by pro-inflammatory signaling, mediated through pathogen-associated molecular patterns (PAMPs) and damage-associated molecular patterns (DAMPs). Additional enzymes can process pro-IL-18, like proteinase-3, or granzyme B, which is produced by MAIT and other cytotoxic T cells upon activation. Hence, when a MAIT cell kills its effector target, if the cytosol of these cells contained pro-IL-18, the killing will deliver active IL-18 into the surrounding(Catalfamo and Henkart, 2003; Omoto et al., 2010). After signaling through its receptor, IL-18 has pro-inflammatory effects, increasing the secretion of IL-13 in mast cells, and up-regulating adhesion molecules on endothelial cells, as examples. In T cells, IL-18 increases IFN-γ secretion and in combination with IL-12 is capable of activating subsets of T cells in a TCR independent manner. Because of this characteristic, these T cells are named innate-like T cells, which comprise some γδ T cells, iNKT and MAIT cells(Gutierrez-Arcelus et al., 2019). MAIT cells constitutively express high levels of IL-18Rα, and this expression is used to detect them, by flow cytometry or in tissue sections. IL-18 alone is not sufficient to induce MAIT cell activation, but needs to be associated with another signal, the best studied is the combination with IL-12(Jo et al., 2014; Ussher et al., 2014).

Other cytokine combinations have been shown to be capable to act in synergy with IL-18: type-I IFNs, TNF, and IL-15(Loh, 2016; Sattler et al., 2015; van Wilgenburg et al., 2016). Moreover, IFN-γ produced by MAIT cells can induce TNF and IL-18 secretion by the APCs, likely representing a positive feedback(Meierovics and Cowley, 2016; Sattler et al., 2015). This cytokine activation mechanism allows MAIT cells to respond to non-riboflavin producing bacteria and to viral infection, which induces cytokine production by APCs, via activation of toll-like receptors (TLRs)(Jo et al., 2014; Ussher et al., 2018). Cytokine activation of MAIT cells is also suspected to be an important mechanism of their deleterious effect in several autoimmune diseases(Chiba, 2017; Hayashi, 2016). Interestingly, MAIT cells activated by TCR alone, cytokines, or a combination of both display non-overlapping functions. The response to TCR stimulation is quick and short whereas the cytokine stimulation takes more time and lasts longer(Lamichhane et al., 2019). MAIT cells stimulated only by their TCR, produce and secrete proteins involved in tissue repair and in epithelial barrier function, cytokines and chemokines, among them CCL4, CCL3, and CCL20(Hinks et al., 2019; Lamichhane et al., 2019). "TCR only" stimulated MAIT cells increase wound healing *in vitro,* and in humans have been shown to be localized close to epithelial cells in the intestine(Leng et al., 2019). This tissue repair function has so far not been studied enough, but this particular function could explain the interest of harboring a high population of MAIT cells in tissues. Moreover, this singular function among T cells could stem from the unique transcription factor combination found in MAIT cells. MAIT cells co-express RORγt, PLZF, EOMES, Blimp-1 and T-bet, a combination not seen in any other T cell type, some of these transcription factors being usually mutually exclusive(Dias et al., 2019; Gibbs, 2017; Lantz and Legoux, 2018). Moreover the expression of C/EBPδ by MAIT cells, unique among lymphocytes, could be of importance in the tissue repair function(Lee et al.; Provine and Klenerman, 2020).

c) CD161 / KLRB1

KLRB1 was first discovered in rat as a cell surface expressed homodimer, which, once triggered by an Ab, would increase NK cell cytotoxicity(Chambers et al., 1989). Multiple homologues were discovered in mice and a single one in humans called KLRB1, or more recently CD161(Lanier et al.). In humans, the transmembrane homodimer is expressed on the majority of NK cells and approximately 1/4 of T cells including both CD4 and CD8(Lanier et al.). Interestingly, three populations at least can be characterized for CD161 surface expression: CD161 negative, low and high. Differences in gene expression between these three populations have been demonstrated(Fergusson, 2016; Fergusson et al., 2014). CD161 signaling has been shown to decrease NK cell cytotoxicity, and cytokine production, in humans and mice(Aldemir et al., 2005; Aust et al., 2009). Studies in T cells are more controversial, some studies implied a co-stimulatory role with an increased cytokine secretion, whereas others showed the opposite(Exley et al., 1998; Rosen et al., 2008). However, many studies used anti-CD161 Ab without clearly characterizing whether its effect is activating, inhibitory, or Fc-receptor mediated(Llibre et al., 2016a). Moreover, studies conducted in mice should be considered with caution, as human CD161 lacks the LCK binding motif present in the murine version(Exley et al., 1998). The natural ligand for CD161 in humans is a protein coded by the CLEC2D gene (C-type lectin domain family 2 D) also called OCIL (osteoclast inhibitory lectin), CLAX (C-type lectin activation expressed) or LLT-1 (lectin-like transcript 1). The main transcript codes for a transmembrane protein, but several soluble isoforms have been described(Boles et al., 1999). CLEC2D is expressed by various cells, among them monocytes, DCs, subsets of B cells, subsets of T cells, and non-immune cells(Mathew et al., 2004) Moreover, its surface expression is increased on B cells by TLR or IFN-γ signaling (Llibre et al., 2016b). The interaction between CLEC2D on the surface of a myeloid cell and CD161 on a lymphocyte results in signaling in both cells(Bambard et al., 2010; Llibre et al., 2016a). The binding of CLEC2D on the surface of an APC to CD161, present on NK cells, will result in an inhibition of cytotoxicity, and cytokine secretion(Aldemir et al., 2005; Aust et al., 2009; Rosen et al., 2008). The exact signaling cascade is not clear in humans, but the main hypothesis is that the intra-cellular part of CD161 would act as a weak inhibitory ITIM motif, hence activating the phosphatase SHP-1, which counteracts the activation of a receptor with ITAM motif(Kirkham and Carlyle, 2014;

Rosen et al., 2008). This inhibition of NK cells is used by several tumor cells, which have been show to overexpress CLEC2D on the surface(Marrufo et al., 2018; Mathew et al., 2016; Santos-Juanes et al., 2019). Besides its function on modulating T cells and NK cells, CLEC2D has been shown to have a cell signaling function itself(Llibre et al., 2016c). B cells in the germinal center express high levels of CLEC2D on the surface, and its signaling promotes their activation(Llibre et al., 2016b). MAIT cells represent the largest population of CD161high T cells in adults, and the combined surface expression of their TCR α chain Vα7.2 with a high expression of CD161 has been part of their definition for years(Negrotto et al., 2015; Provine and Klenerman, 2020). Interestingly, although CD161high expression is the principal MAIT cell characteristic, only few studies have assessed its functional role(Freeman et al., 2017; Le Bourhis et al., 2013). The study by Freeman and colleagues shows a decreased expression of CD161 on T cells, especially on MAIT, in HIV-infected patients. This fact questions many previous studies claiming loss of MAIT cells in the periphery during viral infection, as these studies based their MAIT definition on high surface expression of CD161(Dias et al., 2019; Paquin-Proulx et al., 2017). Concerning the modulation of MAIT cell function by CD161, a single study performed concluded that CD161 multimerization diminishes their cytotoxicity without affecting their cytokine secretion(Le Bourhis et al., 2013). This work was conducted using CD161 Abs, hence the effect of the natural ligand is not clear yet. Studying this interaction would be of great interest regarding the diversity of cells expressing CLEC2D, its regulation by pro-inflammatory signals, and the expression of CD161 by other T cells. Moreover, recent work suggests that CLEC2D is a receptor for extracellular histones released upon cell death, which could influence the binding of CD161 (Lai et al., 2020).

In addition to CD161, CD26, and IL-18Rα, which are constantly present on all MAIT cells, various surface proteins are expressed proportionally on more MAIT than conventional T cells. Among these are the chemokine receptors CXCR4, CCR5, CCR6, CXCR6, and receptors shared with NK cells (CD16, CD56) or with subsets of T cells (CD8, CD45RO).

d) CD8

CD8 is the generic name given to two surface proteins called CD8α and CD8β. Both are transmembrane glycoproteins belonging to the immunoglobulin (Ig) family, and can serve as a co-receptor upon TCR activation. T cells are the most notable CD8 expressing cells, but CD8 is also found on subsets of NK cells, macrophages and DCs(Baba et al., 2006; Shortman and Heath, 2010; Suck et al., 2007). The protein is always present as a dimer on the cell membrane, most cells expresses the αβ heterodimer, but αα homodimers can be found as well. In peripheral blood, between 1/4 and 1/3 of T cells express the CD8αβ dimer in both the memory and the naïve compartment, while CD8αα homodimers are fairly rare, and only present on memory cells(Magalhaes, 2015). Certain tissues are enriched for the CD8αα homodimer, like the skin and the intestine(Jarry et al., 1990; Zhu et al., 2013a). CD8αβ has been clearly shown to interact with the α3 domain of MHC-I, hence increasing the probability of interaction between the TCR and the α1 and α2 domains of MHC(Garcia et al., 1996). Moreover, the molecules also act as a co-activation receptor upon TCR activation(Jarry et al., 1990; Zhu et al., 2013a). In adults, 80% of MAIT cells express CD8α, among the CD8 negatives most are not expressing CD4, hence are called “double negative” (DN), and a small fraction of 1-2% express CD4 on the surface, although the existence of true CD4 MAIT cells is debated(Chen et al., 2019). Among the CD8α, around 60% of MAIT cells are CD8αα, and 40% are CD8αβ(Chen et al., 2019; Walker et al., 2012). Whether CD8 plays the same role regarding the interaction with MR1 as it does with MHC-I, is not established, but several clues point to that direction. There is a certain level of homology between the α3 domain of HLA-A/B/C in the CD8β binding region and the MR1 equivalent(Riegert et al., 1998). Moreover, anti-CD8 blocking Abs have been shown to abrogate the activation of certain MAIT cell clones reacting to *M. tuberculosis*, and to diminish polyclonal MAIT cell responses to *E. coli*(Gold et al., 2013; Kurioka et al., 2017). The exact interaction between CD8 and MR1 and the involved residues are undiscovered yet in the absence of crystallographic analyses, but studies suggest distinct properties between CD8 and DN MAIT. Dias and colleagues suggested an increased sensitivity for apoptosis in DN MAIT and a differential gene expression signature between the two subsets(Dias, 2018).

e) CD56

Neural cell adhesion molecule (NCAM), also called CD56, is a glycoprotein belonging to the Ig family. It is an adhesion molecule involved in homophilic interaction, present on the surface of neurons but also on NK cells, subsets of T cells and DCs(Van Acker et al., 2017). In immunology it is used as a marker for NK cells, where its dim or bright expression defines the two main transcriptionally distinct NK subsets.

The fraction of αβ T cells expressing CD56 is around 5% and is dependent on IL-12 signaling(Guia et al., 2008). Expression of CD56 on αβ T cells is correlated to cytotoxicity and correlates with the expression of other NK markers like CD16 and NKG2D; CD56 positive CD8 T cells can secrete IFN-γ in response to cytokine stimulation(Chan et al., 2013; Guia et al., 2008). The expression of CD56 can be induced *in vitro* on T cells by IL-15(Correia et al., 2011). CD56 is expressed by approximately 1/3 of MAIT cells in the periphery, thus suggesting that many previous studies on CD56+ CD8 T cells performed before characterization of MAIT cells, present in high frequencies in peripheral blood, might have been conducted on a population highly enriched in MAIT cells(Brozova et al., 2016; Dias, 2018). The role of CD56 on MAIT cells is still enigmatic, as it is the case for its role in conventional cytotoxic T cells.

Taken together, the expression of NCAM could be the sign of a recent activation, a recent interaction with an APC, or manifestation of a pro-migratory capacity, as NCAM is essential for NK cell motility(Mace et al., 2016). Moreover, because of its homophilic interaction, NCAM on the T cell can bind NCAM present on the APCs. Interestingly, it has been shown that NCAM expressing DCs induce preferential activation of CD56 expressing T cells(Nieda et al., 2015).

f) CD16a

CD16a, also called Fc fragment receptor IIIa (FcγRIIIa) is a low affinity transmembrane receptor binding the Fc fragment of antibodies. The protein is present on the surface of neutrophils, monocytes, macrophages, NK cells and subset of T cells. On NK cells, the receptor mediates antibody-dependent cellular cytotoxicity (ADCC), and is a strong inducer of NK cell activation. It was shown that CD16 is the only receptor capable of inducing NK cell degranulation without the activation of a second receptor(Bryceson et al., 2006). CD16 is expressed by the majority of T cells bearing a γδ TCR and a small fraction (1-2%) of αβ T cells(Braakman et al., 1992; Clémenceau et al., 2011). Like in NK cells, CD16 crosslinking on T cells induces activation and ADCC; this is true for both αβ and γδ T cells, although these processes are much less studied in T cells than in NK cells(Clémenceau et al., 2011). In the periphery, CD16 is expressed by approximately 10-30% of MAIT cells with a higher frequency in the CD8 positive MAIT cells(Brozova et al., 2016). How CD16 modulates MAIT cell activation is unknown, but regarding its general effect on T cells one could hypothesize that crosslinking of the receptor increases MAIT cell activation.

g) Chemokine receptors

Among their particularities compared to other T cells, MAIT cells express an uncommon chemokine receptor pattern (Fig. 3). The majority of MAIT cells constitutively express CCR2 and CCR5 on the surface whereas the latter is only expressed by 1% of CD8 T cells(Lee et al.; Sand et al., 2013). Both receptors allow detection of the chemokines CCL2, CCL3, and CCL5, among others, hence allowing the migration of MAIT cells towards inflammation sites(Ward et al., 1998). MAIT cells all express high levels of CCR6, which contributes to their tissue homing, which is very unusual for circulating CD8 T cells. Indeed, CCR6 surface expression is only seen in a minority of CD8 memory T cells. CCR6 is the only receptor for CCL20, produced in mucosal tissue and in the liver. Hence, CCR6 is believed to home T cells to the mucosa and liver, two tissues highly enriched for MAIT cells(Kondo et al., 2007; Provine and Klenerman, 2020).

Indeed, the chemokine CCL20 was first named “liver activation regulated chemokine” (LARC), because of all tissues tested the expression was highest in the liver(Hieshima et al., 1997). The CCL20-CCR6 axis is also a key factor in the formation of mucosal lymphoid tissues like Peyer’s patches; whether MAIT cells are involved in this process is not known(Randall and Mebius, 2014). Besides, half of the circulating MAIT cells express CXCR6 on their surface, which is uncommon in circulating memory CD8 T cells(Lee et al.). The ligand for CXCR6 is CXCL16, which is the biggest CXC chemokine in humans, and the only one existing as a transmembrane form(Heesch et al., 2014; Radtke et al., 2015). The CXCR6-CXCL16 axis is another homing signal directed to the liver where the expression of CXCR6 has been shown to favor CD8 T cell survival by an unknown mechanism(Heesch et al., 2014). Hence, the dual expression of CCR6 and CXCR6 with the absence of CCR7 is likely to be part of the mechanism explaining the very high abundance of MAIT cells in the human liver.

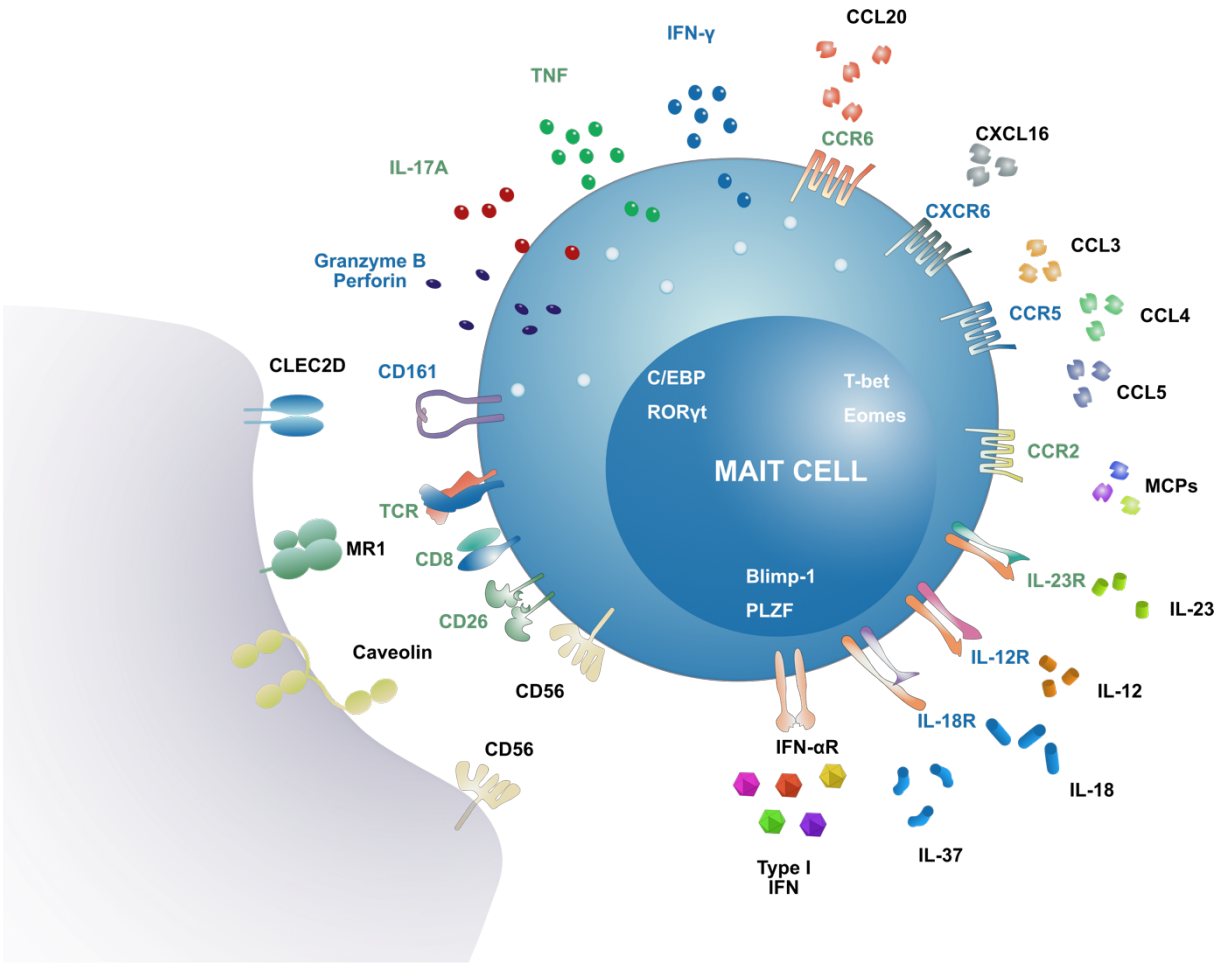

Figure 3: Surface receptors and secreted proteins characterizing MAIT cells. Names in blue represent proteins expressed in NK and T cells, names in green represent proteins expressed mostly on T cells, names in black represent proteins expressed by various cells. An antigen presenting cell is represented in grey. Transcription factors are depicted in the nucleus of the MAIT cell. MCP: Monocyte Chemoattractant protein, a family of chemokines comprising CCL2, CCL7, CCL8 and CCL13.

4. MAIT cell distribution and role in homeostasis and disease

Besides their uncommon expression of proteins, the key element making MAIT cells different from conventional T cells is their recognition of MR1-bound bacterial Ag. Recently, several studies suggested the existence of other MR1 restricted T cells not reacting to bacterial Ag; their Ag is however so far unknown, and they represent less than 1/5000 peripheral T cells(Crowther et al., 2020; Lepore et al., 2017). Because of their high frequency in blood and in tissue, MAIT cells represent by far the most abundant MR1-restricted T cell population discovered so far (Fig. 4). Although first shown to be enriched in the mucosa, which is the origin of their name, MAIT cells are also numerous in the circulation, where they represent approximately 3% of all T cells. MAIT cells are depleted in secondary lymphoid organs compared to tissues, where they usually represent between 2 and 10% of total T cells(Dusseaux et al., 2011; Voillet, 2018). One organ categorically out-competes the rest of the human body in terms of MAIT cell frequency: the liver, where in adults MAIT cells represent up to 40% of total T cells(Dusseaux et al., 2011; Ghazarian et al., 2017; Tang et al., 2013). MAIT cells have been shown to be protective in some diseases and deleterious in others, moreover their frequency among T cells is altered in many conditions(Toubal et al., 2019). Because of their Ag restriction, MAIT cells are expected to be part of the immune defense against several pathogens. This has been confirmed in numerous infections. In patients infected with *M. tuberculosis,* MAIT cells accumulate in the lungs and are consequently depleted in the periphery(Gold et al., 2010; Le Bourhis et al., 2010). MAIT cells migrating to infected tissues have also been suggested by an elegant study conducted by the laboratory of Prof. V. Cerundolo: Healthy volunteers were challenged orally with *Salmonella enterica*, and their circulating MAIT cells were analyzed pre-infection, during infection and after successful antibiotic treatment. The authors could show an oligoclonal proliferation of MAIT cells, a decrease in their frequency in circulation followed by a recovery after treatment(Howson et al., 2015). Similar findings were discovered with *Shigella dysenteriae* oral vaccine, and non-human primates had an accumulation of proliferative MAIT cells at the site of BCG vaccination(Greene, 2017; Le Bourhis et al., 2013). All these studies point towards an immune-protective role of MAIT cells in bacterial infections, which is underpinned by the study of Grimaldi and colleagues showing that patients with lower MAIT cell frequency had

the worst outcome in sepsis(Grimaldi, 2014). Viruses cannot synthesize riboflavin, hence are not producing MAIT cell Ag. Yet, MAIT cell frequency and function are altered in different viral infections, and a protective role of MAIT cells is even suggested in this context(Ussher et al., 2018). MAIT cells are activated during acute HBV, HCV, HTLV-1, dengue fever and influenza infection; this was shown by their increased surface expression of PD-1, CD69, or CD38. Interestingly, in all these infections except dengue fever, MAIT cell frequency in the periphery was decreased, an effect usually reversed by treatment(Barathan, 2016; Billerbeck, 2010; Bolte, 2017; Hengst, 2016; Loh, 2016; Paquin-Proulx et al., 2017; van Wilgenburg et al., 2016). The unusual increase in frequency, seen in the periphery during dengue fever, seems opposite to the findings in all previously cited viral diseases. If the change in frequency is however due to migration towards the infected site, associated with local proliferation, then the increased MAIT cell frequency observed in peripheral blood could be due to dengue virus infecting blood cells, hence the inflamed site being the circulation. To date, a protective effect of MAIT cells in viral infection has only been shown in a mouse model of influenza(Wilgenburg, 2018). Several mouse models have shown this protective effect in bacterial infections, which is of major interest regarding the low MAIT cell frequency in rodents; together with the data obtained in patients, the results suggest a similar function of MAIT cells in humans(Georgel et al., 2011; Meierovics et al., 2013; Wang, 2018).

Because of their TCR-independent activation capacity, MAIT cells can also take part in sterile inflammation; studies conducted in patients or disease models have reported beneficial or harmful capacity depending on the context(Toubal et al., 2019). In ankylosing spondylitis, the frequency of MAIT cells is decreased in the blood, enriched in the synovial fluid, and they secrete more IL-17A(Gracey, 2016; Toussirot et al., 2018). This secretion of IL-17 is interpreted as a deleterious effect, as the cytokine is pro-inflammatory and associated with numerous autoimmune diseases(Kuwabara et al., 2017). The same cytokine is the reason why MAIT cell activation is associated with a harmful effect in asthma. The frequency of IL-17 secreting and activated MAIT cells is associated with the severity of asthma in young children(Ishimori, 2017; Lezmi, 2018). Activated and secreting MAIT cells are also seen in systemic lupus erythematosus, psoriatic skin, and in the circulation of type 2 diabetic patients.

In all conditions their activation is suspected to be damaging(Chiba, 2017; Cho, 2014; Magalhaes, 2015; Teunissen et al., 2014). Protective roles have been demonstrated as well,

for most part in mouse models. In NOD mice, MAIT cells participate in the protection of the gut integrity, whereas in human type 1 diabetic patients they were histologically shown to be absent from pancreatic lesions(Kuric, 2018; Rouxel, 2017). In a colitis model, transfer of MAIT cells into 2,4,6-trinitrobenzenesulfonic acid (TNBS) challenged mice resulted in lower disease activity in the recipient(Ruijing, 2012). These findings have to be interpreted with vigilance, as alternative conclusions can be taken from a human study showing increased IL-17 producing MAIT cells in the circulation of IBD patients(Serriari, 2014). Regarding their high proportions, MAIT cells should be a major regulator of inflammation in the liver. Indeed, in a cohort of patients with type 1 autoimmune hepatitis, MAIT cells were shown to be the most altered immune population in the liver(Renand et al., 2018). The study conducted by Böttcher and colleagues on all autoimmune liver diseases found a lower frequency of MAIT cells in liver and circulation. This depletion was correlated with the fibrosis score in the tissue and the remaining cells secreted IL-17A, which is shown to activate hepatic stellate cells (HSCs), the main drivers of liver fibrosis generation(Böttcher et al., 2018). The study published by Setsu and colleagues on primary biliary cholangitis (PBC) patients, shows similar depletion of MAIT cells in the liver and the blood, interestingly this depletion was partially reversed after ursodeoxycholic acid (UDCA) treatment. In this paper, liver MAIT cells are also shown to express lower levels of IL-7 and IL-18 receptors compared to controls, and frequency of CD69+ MAIT cells in the circulation correlated with the level of liver enzymes(Setsu et al., 2018). Jiang and colleagues assessed MAIT cell phenotype and function in liver and blood of a large cohort of PBC patients (Jiang et al., 2018). The results show decreased MAIT cell frequency in patient blood associated with a more apoptotic phenotype. Interestingly, a slight increase in absolute numbers of MAIT cells in the liver is shown; the authors assessed them by *in situ* microscopical evaluation, whereas every other study in human liver assesses MAIT cell frequency *versus* CD3+ by flow cytometry, which might explain the discrepancy to studies reporting decreased MAIT cell frequencies in the liver. Like in the previous study, 6 months of UDCA therapy partially restored the MAIT cell frequency in the blood. The treatment also decreased their apoptosis propensity and their CD25 surface expression, which could be a sign of lower activation. Moreover, the authors showed an increased serum IL-7 level in PBC patients and demonstrated an increased IL-7, IL-12 and IL-23 secretion by a hepatocyte cell line upon stimulation of the Farnesoid X Receptor (FXR) with agonists. Hence, the authors speculate on

a role of cholic acid, an FXR agonist, in the deleterious role of MAIT cells, as IL-7 induces higher granzyme expression in activated MAIT cells(Jiang et al., 2018). To date few studies have been conducted on MAIT cells in non-alcoholic fatty liver disease (NAFLD), and their results are inconsistent. The study published by Hedge and colleagues, shows a decreased frequency of MAIT cells in the circulation of NAFLD patients, and a pro-fibrogenic role of MAIT cells in a fibrosis model (CCL4 induced liver injury), using either control, MAIT-deficient or MAIT-enriched mice(Hegde et al., 2018). The study of Li and colleagues - though showing the same decrease in circulation - shows a protective effect of MAIT cells in mice fed a methionine/choline deficient diet. This effect was mediated through the secretion of IL-4 and IL-10(Li et al., 2018). Therefore, more studies need to be conducted to conclude on the role of MAIT cells in NAFLD. Interestingly, bile acids can modulate MAIT cell function through IL-7 induction(Jiang et al., 2018). A very recent article found major differences between conjugated and non-conjugated biliary acids, the ratio of which is highly dependent on the entero-hepatic cycle, hence on the liver and the microbiota. Clearly, the relation between liver MAIT cells and gut microbiota has been neglected so far and would need to be elucidated in relation with liver diseases(Mendler et al.).

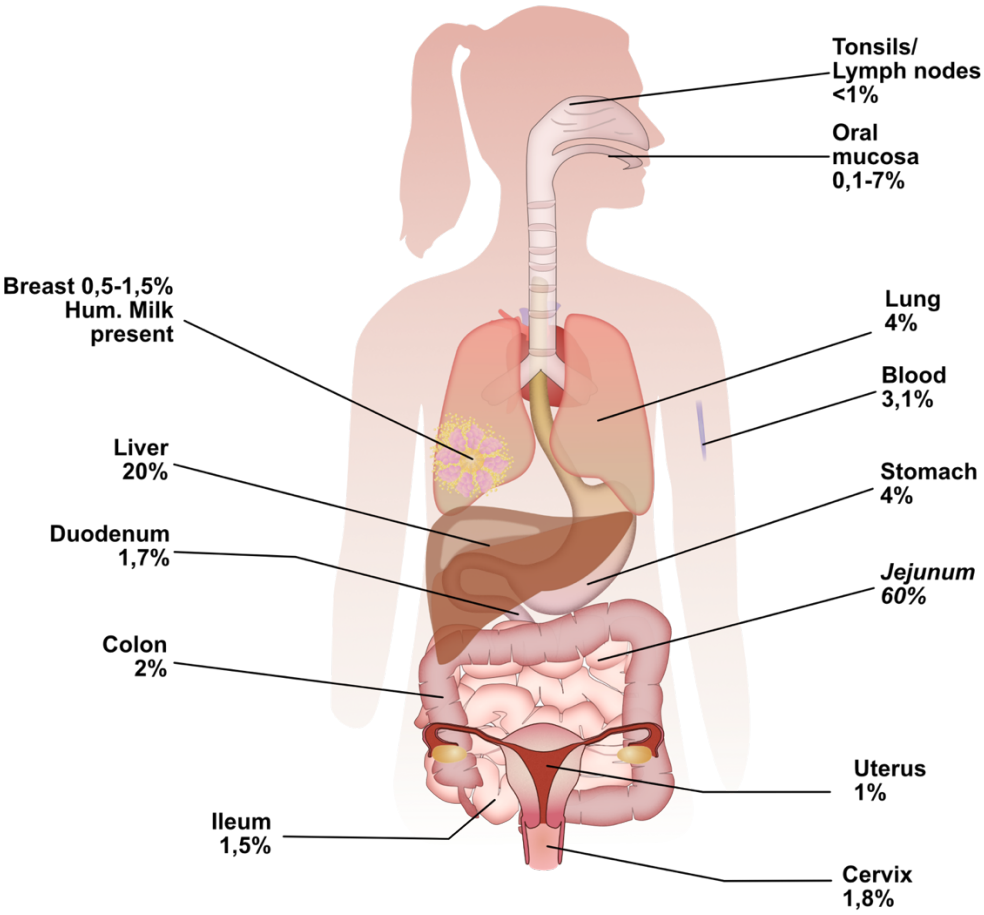

Figure 4: Distribution of MAIT cells in human tissues. The frequency of MAIT cells in the tissues of a healthy adult as mean of multiple studies, reviewed by Provine and Klenerman, additional data from Bedin and colleagues and Zumwalde and colleagues (Bedin et al., 2019; Provine and Klenerman, 2020; Zumwalde et al., 2018).

B. Liver microenvironment

1. Liver structure microanatomy

The liver is the largest internal organ of the human body representing 2.5 – 3.5% of the total body mass, and receiving 1/3 of the blood flow.(Clemente Carmine D.; Karlstadt et al., 2004). On the cellular level, hepatocytes represent 80% of the liver volume, and 60% of the cells. Non-parenchymal cells are mostly endothelial cells which represent 20% of liver cells, lymphocytes representing 10%, and Kupffer cells, the liver resident macrophages, representing around 8%(Racanelli and Rehermann, 2006). In lower proportion, the liver is populated by biliary epithelial cells draping bile ducts, and HSCs, residing under the endothelial layer of the sinudoids. HSCs are highly specialized pericytes, which secrete cytokines and store the majority of the vitamin A in the human body. They are a major regulator of wound healing and key players in fibrogenesis(Puche et al., 2013). The human liver carries out a large amount of physiologic functions covering production of bile, hormones and plasma proteins, storage of glycogen and vitamins, removal of toxic substances, and homeostatic regulation of the plasma constituents(Kalra and Tuma, 2020). With these specific functions comes a captivating anatomical singularity: the liver is the only organ supplied by both venous and arterial blood, with the venous blood coming from the intestine through the portal vein. Thus, the liver is the first organ reached by digestion-derived products, which facilitates their metabolism, and their storage. Anatomically the liver is divided into two lobes, themselves histologically divided into lobules. A liver lobule is a hexagonal unit with a branch of a portal venule, a hepatic artery and a bile duct at each corner (Fig. 5). The association of the three vessels is named the portal triad. The center of each lobule contains a central vein which collects the blood coming from the hepatic artery and the portal vein, after its mixing in the small fenestrated capillary-like structures called the liver sinusoids. The bile, secreted by hepatocytes, flows in the opposite direction towards the portal fields and is collected into bile canaliculi (Fig. 5).

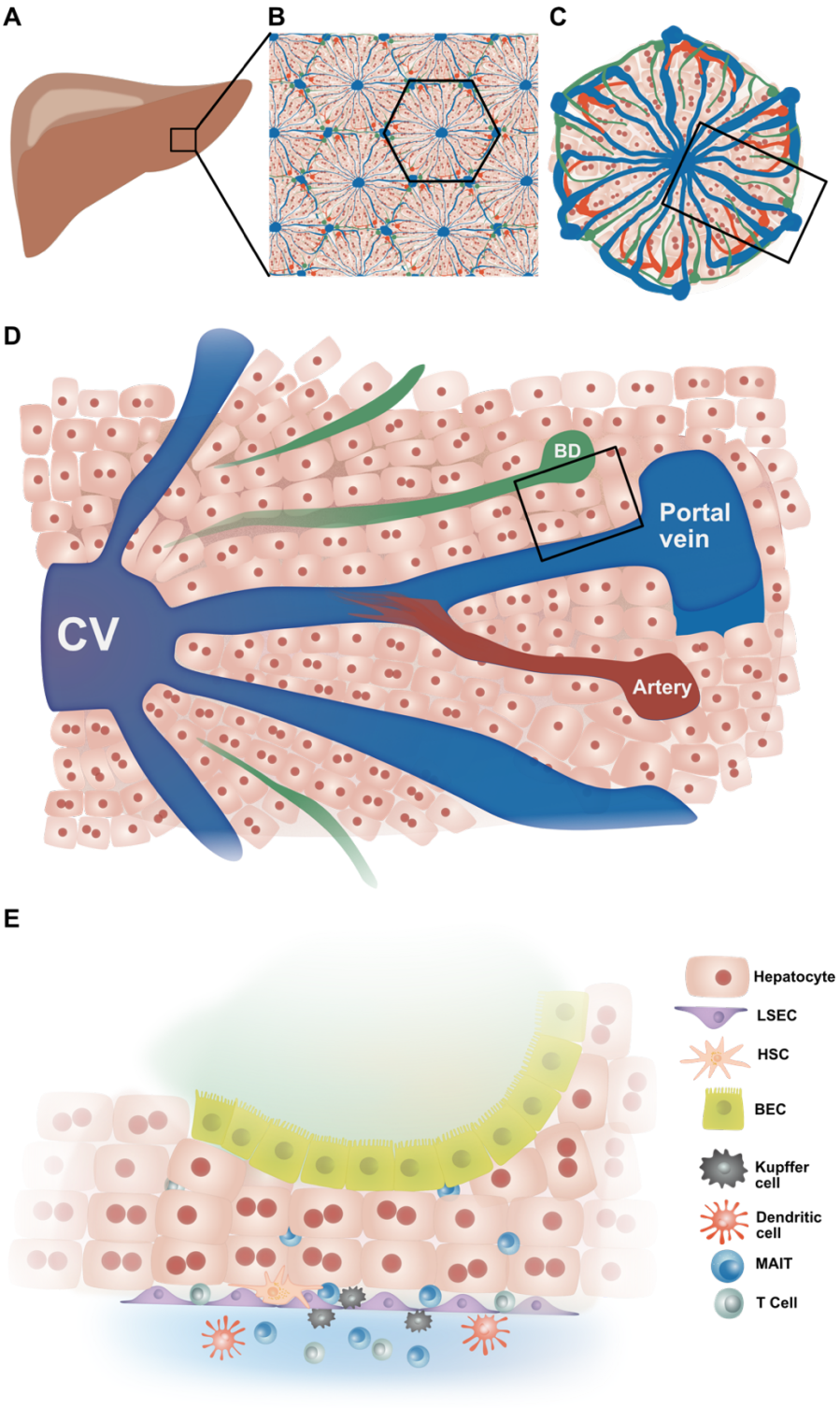

Figure 5: Microanatomy of the liver. Representation of a human liver (A) structure of the liver's functional units, the lobules (B&C). Zoom into a part of a liver lobule (D): Blood enters through branches of the portal vein and hepatic artery, then flows through sinusoids. Bile is secreted by hepatocytes and flows into the opposite direction and is collected in bile ductules. Closer look at the cellular players present in the liver (E).

2. Gut-liver axis

The gut-liver axis designates the interconnexion between the intestine, its microbiota and the liver through the portal vein in one direction and through the bile in the other.

a) The microbiota

The gut microbiota consists of an elaborate microbial community of over 100 trillion microorganisms in the gut, making it by far the densest microbial community, with the colon containing two thirds of the microbes in/on the human body. It is composed of all kinds of microorganisms: fungi, archaea, viruses, protozoans and bacteria, the last being the most prevalent(Sekirov et al., 2010). This metabolically active gut microbial community is an indispensable partner for the human digestive system, allowing the degradation of dietary products outside of the human digestive enzyme spectrum(Sakanaka et al., 2019). Besides, the gut microbiota is an essential source of metabolites, neuro-mediators and hormones that directly regulate gut function and influence extra-intestinal organs such as the liver, brain, and kidneys(McIntyre et al., 2011; Niwa, 2011; Quesada-Vázquez et al., 2020; Yano et al., 2015). For decades culture based microbial analysis gave a wrong picture of the digestive tract flora, as an example the stomach was long thought to be sterile in healthy individuals(Nardone and Compare, 2015). The development of 16s ribosomal RNA sequencing granted culture-independent microbiota definition(Weisburg et al., 1991). The recent depreciation in sequencing cost opened the way to microbial definition of important cohorts in multiple microbial niches. Microbial composition and concentration is highly variable along the digestive system. The stomach contains around 100 microorganisms per gram of content. When healthy, the organ contains mostly *Firmicutes* from the *Streptococcus* and *Lactobacillus* geni and *Actinobacterium* commonly from the *Propionibacterium* genus. The colonization by *H. pylori* alters this ecosystem and is harmful for the host.

The duodenum directly adjacent to the stomach contains a similar to slightly higher concentration of microorganism with around 10^2 to 10^3 colony forming units (CFUs) per mL (O'Hara and Shanahan, 2006). *Firmicutes*, *Proteobacteria*, *Bacteroidetes* and *Actinobacteria* all together represent 99% of the present phyla, with *Firmicutes* and *Proteobacteria*

representing 60% and 20%, respectively. At the genus level, most *Firmicutes* belong to the *Bacilli* genus, and *Pseudomonas* represent the most abundant *Proteobacteria*(Mei et al., 2018; Nistal et al., 2016).

The microbe density keeps increasing along the digestive track, in the jejunum the number of microbes per mL reaches 10^4 to 10^5. Along with this topographic increase comes diversification, with the apparition of phylum *Fusobacteria* in significant amounts, representing 7% of all organisms(Sundin et al., 2017). The evolution of the microbiota continues along the small intestine until the ileum, which contains 10^7 bacteria/mL. Ribosomal RNA sequencing of mucosal samples reveals an evolution towards aerotolerant and anaerobic bacteria, with *Firmicutes* representing the by far best represented phylum followed by *Actinobacteria*(Villmones et al., 2018). Microbiota in the jejunum and the ileum show the highest donor to donor fluctuation in the digestive tract, however the limited number of studies advocate for prudence in interpretations(Booijink et al., 2010). In the colon, microbial density reaches its highest concentration in the human body from 10^8 CFU/mL in the cecum to 10^{11} CFU/mL in the rectum. All phyla represented elsewhere in the digestive tract, namely *Firmicutes*, *Bacteroidetes*, *Actinobacteria*, *Proteobacteria*, *Fusobacteria*, and *Verrucomicrobia* are represented in the colon. Present in equivalent proportion, *Firmicutes* and *Bacteroidetes* are the most abundant and together represent close to 90% of all bacteria. Several studies reported the presence of *Cyanobacteria*, a phylum usually present in oceans and the soil. To date, no specimen has been isolated and cultivated; Di Rienzi and colleagues suggested the existence of a new phylum closely related to *Cyanobacteria*, based on their whole genome reconstruction. They named the phylum *Melainabacteria*, showing once more that study of the microbiota can lead to unexpected discoveries(Di Rienzi et al., 2013). Most studies concerning colon microbiota were conducted by sequencing 16s ribosomal RNA in feces. Although informative concerning the composition of the microbes living in the human gut, these studies give a very inaccurate picture of the bacteria in contact with the intestinal epithelium. Hence, biopsy-based or mucosa-based sequencing methods are superior towards this aim. Therefore, it is the above mentioned approach that we are currently using in the laboratory in order to analyze changes in microbiota associated with NAFLD.

b) Gut influence on the liver

(1) Polysaccharide depolymerisation

Hosting the intestinal microbiota has multiple advantages for the host. Mammals lack the enzymatic machinery to digest most complex carbohydrates. By themselves they cannot take advantage of most polysaccharides, or dietary fibers, like pectin, several forms of amylose or cellulose. Interestingly, the host indirectly selects for organisms beneficial in this regard, hence the gut population is enriched in microbial proteins capable of breaking down dietary polysaccharides(Gill et al., 2006). The study of complex sugar degradation by intestinal bacteria started more than 40 years ago and has focused mainly on *Bacteroidetes*(Salyers et al., 1977). The model organism used to study carbohydrate metabolism is *Bacteroides thetaiotaomicron.* According to transcriptome and genome analysis of *B. thetaiotaomicron*, 18% of the bacterial genome is dedicated to polysaccharide degradation(Martens et al., 2008). More recently, *Firmicutes* have been shown to play an important role in carbohydrate degradation as well. *Ruminococcaceae* like *R. bromii* show better ability to degrade resistant starch and promote starch utilization by other commensal bacteria from the *Eubacterium* and *Bifidobacterium* genus(Flint et al., 2012; Ze et al., 2012).

(2) Short chain fatty acids

The liberation of monosaccharides from their corresponding polymer makes them available for the host to use them as an energy source or building block. Part of them are used by the bacteria themselves and fermented. The main intermediary products are ethanol, succinate, and lactate. These are further modified mostly in the colon to form the principal end product: short-chain fatty acids (SCFAs). Their concentration is dependent on the amount of fiber ingested but is between 90 and 120 mM in the colon with a higher proportion of acetate. Interestingly, SCFAs are absorbed at 90%. Acetate and propionate are used as building blocks in the liver, for lipogenesis and gluconeogenesis respectively. Butyrate is preferably used as an energetic substrate by colonic epithelial cells. On top of their metabolic utility, SCFAs also have important signaling properties.

Butyrate modifies gene expression by inhibiting histone deacetylase (Lazarova et al., 2013). SCFAs can signal through GRP41 and GPR43, largely expressed in the digestive system. In hepatocytes, GPR43 signaling diminishes HBV-mediated inflammation(He et al., 2020).

(3) Secondary bile acids

Bile acids secreted by the liver into the duodenum decrease the proliferation of sensitive microbes and are indispensable for fat digestion. These detergents are also crucial for the absorption of lipids and hydrophobic vitamins, namely vitamin A, D, E and K. Moreover, bile acids can signal through the liver X receptor (LXR), the FXR, and the G-protein-coupled receptor TGR5(Jia et al., 2019; Yamagata et al., 2004). The two bile acids synthesized in hepatocytes from cholesterol, cholic acid (CA) and chenodeoxycholic acid (CDCA), are called primary bile acids. CDCA and CA are mostly secreted in a conjugated form with glycine or taurine. This conjugation is removed in the intestine by the commensal microorganisms increasing the pool of unconjugated bile acids. These can be metabolized by gut bacteria into so called secondary bile acids. The main representatives are deoxycholic acid (DCA) and lithocholic acid (LCA), formed by dihydroxylation of CA and CDCA, respectively. Both primary and secondary bile acids are reabsorbed in the colon, forming an entero-hepatic cycle(Ridlon et al., 2006). Secondary bile acid levels and their composition are important for humans. They bind the classical bile acid receptor and bile acid transporter with a different affinity than their respective precursors. Moreover, LCA was suspected to be a partial FXR antagonist, and decreases the expression of the bile salt export pump (BSEP), this mechanism contributing to its cholestatic effect(Yu et al., 2002). DCA is implicated in the pathogenesis of NAFLD and inhibits NF-κB signaling in hepatocytes thus inducing their apoptosis(Rodrigues et al., 2015).

(4) Other plant metabolites

Human diet contains an enormous quantity of non-energetic plant secondary metabolites, among these polyphenols are the most abundant antioxidants(Grootaert et al., 2015). Polyphenols and flavonoids have been reported to exert beneficial health effects, increasing interest in the study of their bioavailability, and biological activities(Clavel et al., 2006). Most polyphenols are glycosylated in the diet and converted by the microbiota, the unglycosylated form is the only bioavailable one(D'Archivio et al., 2010). Hence, the microbiota strongly affect the absorption of these active molecules, with diverse biological repercussions. Local effects happen already at the intestinal epithelium where terpenoid like Andrographolide increase the secretion of anti-microbial peptide β-defensin(Sechet et al., 2018). Different flavonoids like apigenin have hepato-protective effects in mice undergoing LPS-induced liver failure, with more than 50% reduction in mortality(He et al., 2019). Similar hepato-protection was demonstrated in diet-induced inflammation, where apigenin reduced the severity of NAFLD(Feng et al., 2017). In a broader perspective, polyphenol and flavonoids have been proposed as a therapeutic hit for the treatment of colitis and autoimmune diseases. Genistein, a polyphenol discovered in Genista tinctorial, has been used as a supplement in a clinical trial with NAFLD patients. The compound improved insulin resistance and significantly decreases serum levels of IL-6 and TNF(Amanat et al., 2018).

(5) Amino acid derivatives

High-protein diet results in an increased level of amino acids in the colon, hence also increasing their degradation products. Among these, branched-chain amino acids (BCAAs), derivative phenyl acetic acid and kynurenine are of major interest for human health. The effect of BCAAs and their microbial fermented counterpart BCAs is controversial. In a large cohort of diabetic patients insulin resistance was associated with a higher level of BCAs(Pedersen et al., 2016). Similar findings have been shown in obese adults where BCA serum levels are higher than in lean subjects(Newgard et al., 2009).

On the other hand, several studies conducted in humans have shown that BCAA dietary supplementation ameliorates symptoms, prognosis and the quality of life of cirrhotic patients(Kawaguchi et al., 2011; Kitajima et al., 2018). Aromatic amino acid metabolism is a source of interesting metabolites as well. Tryptophan degradation by gut bacteria generates a mixture of indole compounds which have been shown to have pharmacological activities(Hendrikx and Schnabl, 2019). The best studied indole derivative receptor in humans is the aryl hydrocarbon receptor (AHR), which is eminently expressed on immune cells but likewise outside of the immune compartment, in hepatocytes and in melanocytes(Aizarani et al., 2019; Esser et al., 2013). In the intestine, indole binding to AHR induce mucin expression and strengthens the mucosal barrier by increasing epithelial tight junctions(Bansal et al., 2010; Shimada et al., 2013). In NAFLD patients, tryptophan supplementation reduced serum levels of inflammatory cytokines and improved LDL as well as γ-glutamyltransferase levels(Celinski et al., 2014).

(6) Vitamins

Vitamins are small organic molecules belonging to the essential nutrients along with essential minerals, essential amino acids and essential fatty acids. They differ from the first by their organic nature, and from the two latter by their low abundance. Unlike essential amino and fatty acids, vitamins are needed in lower quantity and are not used as building blocks. According to their structure, vitamins are classified into two groups, hydrophilic and lipophilic vitamins. Lipophilic vitamins include the retinol family (vitamin A), the calcitriol family (vitamin D), the tocopherol family (vitamin E) and the quinone family (vitamin K). Vitamin A is indispensable for the function of several proteins like rhodopsin in the retina. Moreover, like vitamin D, vitamin A plays a hormone-like function. The function of vitamin E seems to be related to its fat-soluble antioxidant properties, whereas vitamin K is an enzymatic cofactor indispensable for many enzymes mostly in the coagulation cascade(Furie et al., 1999). Hydrophilic vitamins are water soluble co-factors, composed of vitamin C and the B vitamin family which encompasses 8 members, thiamin, riboflavin, niacin, pantothenic acid, pyridoxin, biotin, folate, and cyanocobalamin.

Vitamins from the B group are all enzyme co-factors used in every living organism, with exceptions concerning vitamin B12, absent in many plants. Nearly all animals are deficient for the biosynthesis of this family. Oppositely, almost every animal but anthropoid primates can generate ascorbic acid, a necessary co-factor for multicellular organisms and an important anti-oxidant(Smirnoff, 2018).

The importance of the gut microbiota in the vitamin income is now well established. The first evidence in this direction was generated in 1947, when Rosen and colleagues show that nicotinic acid excretion by rats was increased when they were given the same quantity of tryptophan orally *versus* parenterally(Rosen et al., 1946). It was later shown that germ-free rats raised without vitamin K supplementation developed hemorrhage because of thrombin deficiency, whereas control rats were fine without supplement(Gustafsson et al., 1962). Many microorganisms can produce vitamins from the vitamin B family, but not all of them. Moreover, very few bacteria have the capacity to produce the complete group, which is interesting regarding the fact that they are not dispensable. Magnúsdóttir and colleagues generated a systematic genome-based prediction of 256 common human gut bacteria for the presence of biosynthesis pathways for the eight B vitamins(Magnúsdóttir et al., 2015). They could show that vitamin sufficiency is relatively conserved in phyla, but variable among them. Most *Bacteroidetes* are capable of synthesizing all vitamins, a minority are deficient for vitamin B12, and very few are also deficient for riboflavin. *Fusobacteria* are all deficient for pantothenate and most for pyridoxal production. *Firmicutes* represent the phylum with the highest variability among species, but all tested were auxotroph for at least 1 pathway. On the vitamin point of view, riboflavin and nicotinamide biosynthesis were the most conserved among all microbiota-derived bacteria. Riboflavin is generally present in *Bacteroidetes*, *Proteobacteria*, and *Fusobacteria*, yet it is only synthesized in 50% of the *Firmicutes* and rarely in *Actinobacteria*(Magnúsdóttir et al., 2015). Globally they estimated that most of the host's need in pyridoxine is covered by the microbiota, and approximately one third of the need in cobalamin, folate and niacin. The existence of these biosynthetic pathways implies that not only the vitamins themselves will be transported through the portal vein but also all catabolism intermediates. Some of these intermediates are biologically active, shikimic acid and derivatives have a positive action on oligodendrocyte differentiation and bone resorption(Chen et al., 2018; Lu et al., 2019). Another intermediate was recently discovered

to be part of the gut-liver axis. 5-amino-6-(D-ribitylamino) uracil (5-A-RU) is an intermediate of the riboflavin biosynthesis in microorganisms and plants(Neuberger and Bacher, 1986). This small water-soluble molecule can react with glyoxal or methyl-glyoxal, two abundant products in the gut, synthesized by the microbiota(Baskaran et al., 1989; Eadala et al., 2011). The condensation of 5-A-RU with methylglyoxal will form 5-OP-RU, an antigenic molecule for the recently discovered MAIT cells, which are the most abundant T cells in the liver. Hence, 5-A-RU might be a so far neglected important player within the gut-liver axis.

c) Human shaping of gut microbiota

(1) Bile acids

Bile acid secretion because of its anatomical location and its composition is a major player in the liver-dependent shaping of the gut microbiota. Bile is an aqueous solution of organic and inorganic compounds whose major constituents include bile acids, cholesterol, phospholipids and the pigment biliverdin responsible for its yellow-brown color(Begley et al., 2005). Although for a long time neglected, bile also contains 100 different proteins, many derived from plasma, but several are enriched in the bile(Kristiansen et al., 2004).

The best studied component of bile influencing the gut microbiota are the bile acids themselves. Because of their amphiphilic nature, bile acids are capable of cell membrane destabilization or dissolution(De Boever et al., 2000; Noh and Gilliland, 1993). If the concentration is high enough, membrane dissolution takes place leading to instant death of bacteria. This powerful effect is responsible for the low colonization in the duodenum compared to the rest of the intestine. Microbes are unequal regarding their sensitivity to bile salts, several gram positive aerobes and most gram-negative aerobes show improved resistance(Chou and Weimer, 1999; Floch et al., 1971; Kimoto et al., 2002).

In addition to the alteration of cell walls, bile acids can alter the secondary structure of proteins and nucleic acids. In bacteria, alteration in RNA secondary structure as well as protein denaturation was demonstrated. In some strains these lead to a general stress response with induction of chaperon proteins(Flahaut et al., 1996). The stress response is resulting from the signaling of bile salt specific proteins, showing once again the great co-evolution between the microbiome and its host(Leverrier et al., 2003)(Begley et al., 2005).

(2) IgA

The bile contains on top of the bile salts an important amount of proteins. Among them, Immunoglobulin A (IgA) has been shown to exert important influence on the microbiome. IgA is the second most abundant secreted Ig in the serum with a concentration of approximately 2 mg/mL, but its concentration is much higher at mucosal sites, making it the most abundant produced Ig in humans with a secretion of 66 mg/kg body weight/day, exceeding the daily synthesis of all other isotypes together(Reinholdt and Husby, 2013). IgA is secreted into bile at a concentration close to 0,1 mg/mL(Sung et al., 1995). Once in the intestine, its affinity for the germs allows it to strongly attach to their surface. This binding will decrease bacterial motility, prevent adhesion to epithelium, and agglutinate bacteria, thereby increasing their clearance with intestinal peristalsis(Aagaard et al., 1996; Sung et al., 1992). The shaping of the microbiota by Abs and particularly by IgA has been established several decades ago, but the mechanism of action only starts to be unveiled(Macpherson and Uhr, 2004). IgA can be divided in two classes, the natural and the specific Abs. Natural Abs are poly-reactive because they are directed against shared molecular patterns, they can be secreted by B cells without the help of a T cell. Specific Abs bind to specific Ags and hence - oppositely to the natural Abs - require previous immunization, and T cell help. Hence, natural Abs have the characteristic of an immunological tool preventing bacterial overgrowth, but specific ones can lead to the selective pressure on certain species. Although the intestinal sub-epithelial space is an important provider of IgA, it has been shown that B cells primed in the gut migrate to the liver and secrete IgA into the bile (Moro-Sibilot et al., 2016). Hence, this mechanism could provide a way to selectively eliminate microbes, which had crossed the mucosal barrier.

This is supported by several studies showing that, in gut and feces, selective phyla and taxa are coated with IgA(Bunker et al., 2017; Kau et al., 2015). Interestingly, the two most abundant phyla, *Bacteroidetes* and *Firmicutes* are the ones showing the lowest IgA coating. Ab secretion is modulated by cytokines and inflammatory factors, which themselves are influenced by microbiota-derived factors. An interesting example is IL-17, a cytokine secreted by T cells in the gut and the liver, in response to TCR or cytokine activation. IL-17 was recently shown to increase humoral responses, and this mechanism is used by commensals to promote their survival illustrating the bi-directional communication between the host and the microbiota(Lécuyer et al., 2014; Mitsdoerffer et al., 2010).

(3) Mucus

Mucus is a polymer in aqueous secretion covering many mucosal surfaces in evolved animals. The human intestinal lumen is covered by a mucus physically separating the epithelium from the microbiota. Mucus structure and composition evolve along the digestive tract. The stomach and colon have a two-layered mucus, whereas the small intestine has only one(Hansson, 2012). In the intestine, the inner mucus layer is mostly made of the highly glycosylated protein mucin MUC2, which is attached to the epithelium in the colon but not in the small intestine. Mucin glycosylations are branched and imply an important number of sugar bonds, hence their complete degradation would require a vast amount of different specific enzymes. This complexity provides microbiota with various substrates, but also prevents complete degradation of the mucus(Larsson et al., 2009). The mucus also traps anti-microbial peptides, which increase its efficiency as a barrier(Dupont et al., 2014). By on one hand preventing bacterial contact, and on the other hand providing interesting energetic substrates to them, mucus secretion has an important role in shaping the microbial composition in the digestive tract. Although the mechanism is not fully elucidated yet, it is clear that microbes with mucin adhesion capacity, or able to utilize mucus-derived sugars as energetic resources will be advantaged. Modification in mucin glycosylation profile translates into differences in the microbial colonization(Huang et al., 2011; Martens et al., 2018). The importance of mucin as a bacterial fuel is well illustrated by the discovery of the species *Akkermansia muciniphila* in 2004, using solely mucin as a carbon source(Derrien et al., 2004).

Much evidence suggests that this interaction is positive for the host, and that evolution shaped microorganisms adapted to the gut microenvironment, and mammals capable of hosting beneficial microbiota. One striking example is the abundance of oligosaccharide in human milk, molecularly resembling mucin glycomotifs, but not digestible by human enzymes. These are of no nutritional value for the newborn without the presence of its microbiome, and hence might function as a natural probiotic(Gnoth et al., 2000; Marcobal et al., 2011). All these features show the necessity of a regulated mucosal secretion. Modulating factors are derived from the microbiome itself - it is established that germ-free mice have a perturbed mucus layer - but also from the liver with a known pro-secretory effect of bile. Indeed bile acid are known to increase mucus secretion and intestinal motility, placing mucus as a key player of the gut-liver axis(Barcelo et al., 2001; Kim et al., 2017).

3. NASH/NAFLD

a) **Definition**

Non-alcoholic fatty liver disease (NAFLD) refers to a condition where there is an aggregation of excess fat in the liver not caused by excessive alcohol consumption. This heterogeneous disease encompasses non-alcoholic steatohepatitis (NASH), the accumulation of fat in the organ associated with local inflammation, hepatocyte ballooning and often scaring, and the usually less serious condition named non-alcoholic fatty liver (NAFL) when lipid accumulation is seen without inflammation/ballooning or only with one or the other(Brunt et al., 2015).
NAFLD is strongly associated with metabolic disorders. NAFLD is a liver manifestation of the metabolic syndrome, consequently is highly prevalent in obese people and patients with type 2 diabetes(Targher et al., 2007; Wanless and Lentz, 1990).

b) **Alterations in the gut microbiome associated with NAFLD**

There is a well-established link between the metabolic syndrome and changes in the gut microbiome(Tilg and Kaser, 2011). Alterations of the microbiota are associated with NAFLD in mice and humans. Germ-free mice fed a high-fat diet display a lower level of fat accumulation in the liver than the colonized ones(Rabot et al., 2010). Microbiome from insulin resistant mice, when transferred into germ-free animals, led to the development of NAFLD in the recipient, whereas microbiome from healthy mice was harmless(Le Roy et al., 2013). The same publication described over- and under-representation of specific microbial species in NAFLD animals compared to controls. The same associations were found in children with NAFLD with an increased abundance of *Gammaproteobacteria* and *Prevotella* compared with BMI-matching individuals(Michail et al., 2015). Studies in adult patients with NAFLD demonstrated an accumulation of *Bacteroides* and *Escherichia*(Boursier et al., 2016; Zhu et al., 2013b). *Klebsiella pneumoniae* and *Helicobacter pylori* colonization have been shown to increase the risk and the severity of the disease(Ning et al., 2019; Yuan et al., 2019). On the other hand, the abundance of certain species in the gut have been suggested to play a protective role, as fatty liver disease patients showed decreased levels of *Faecalibacterium prausnitzii* in their

intestine, and beneficial dietary intervention in patients with type 2 diabetes was associated with an increased abundance of this microorganism(Medina-Vera et al., 2019; Munukka et al., 2014). *Akkermansia muciniphila* colonization in mice improved the metabolic profile and ameliorated the liver function(Nishiyama et al., 2020; Zhao et al., 2017). A clinical trial recently conducted in obese adults suggested weight loss and decreased insulin resistance in *Akkermansia muciniphila*-supplemented subjects(Depommier et al., 2019). All these changes in the microbiota indubitably result in changes in the gut-liver axis, thereby modulating the metabolic environment within the liver. This could have a large impact on the most abundant liver resident T cells, the MAIT cells, which recognize bacterial metabolite-derived Ags. Interestingly, these metabolites are not produced by all bacteria, and they can diffuse from the gut to the bloodstream, rendering parallel studies of liver MAIT cells and microbiota in NAFLD patients interesting.

c) **Liver heterogeneity argues for studies at single cell level**

At the cellular level, the liver displays for its resident cells a highly heterogenous environment with a gradient of oxygen, gut derived-nutrients and metabolites. This variability in conditions translates into cellular heterogeneity, long established for hepatocytes, but relevant as well for non-parenchymal cells(Geerts, 2001; Glaser et al., 2006; Jungermann and Keitzmann, 1996). This heterogeneity is also observed in liver resident immune cells, therefore arguing for studies at the single cell level(Blériot and Ginhoux, 2019). The recent development of single cell RNA sequencing techniques opens the possibility to combine the single cell level with an unbiased approach(Macosko et al., 2015). It permits to compare and cluster cells according to the differential expression of thousands of genes, hence bypassing the heterogeneity issue within a cell population and revealing unexpected implicated partners(Zheng et al., 2018). Recent single cell analysis in mouse healthy and fibrotic liver revealed heterogeneity in HSCs according to their proximity to central veins. Interestingly the authors could show that central vein-associated HSCs were the main drivers of fibrosis in their mouse model, and their analysis revealed LPAR1 as a therapeutic target to treat liver fibrosis(Dobie et al., 2019). Analysis conducted in human healthy or cirrhotic liver revealed the expansion of CD9+ pro-fibrogenic macrophages, and scar-associated endothelial cells expressing ACKR1 and PLVAP which

promote leucocyte transmigration(Ramachandran et al., 2019). High cellular heterogeneity among hepatocytes, endothelial cells and Kupffer cells has been revealed in a study constructing a human liver atlas from 9 donors, but to date no studies have used this approach to compare liver lymphocytes in human NAFLD patients and healthy subjects(Aizarani et al., 2019). Regarding their central role in the gut-liver axis, a study centered on MAIT cells seems promising. The development of high throughput techniques increased the impact and the feasibility of the aforesaid approach.

Among these, the Seq-well procedure is of interest, because, unlike other techniques, it is not based on droplet emulsion but on the use of a microwell chip(Gierahn et al., 2017). This approach permits diminishing the cost per sample, and to increase the number of detected genes per cell(Hughes et al., 2019), thus allowing for an increase in the number of samples analyzed, and in the quality of the data obtained. The use of this method on the highly relevant population of MAIT cells in NAFLD might be of major interest for the understanding of the pathophysiology of the disease.

Because of their high frequency in the liver, their implication in several liver diseases, their response to liver-derived cytokines, and their Ag, MAIT cells are in the center of the gut-liver axis. Hence, studies of the gut-liver axis require examination of liver MAIT cells, and any new findings on liver MAIT cells will inform us about the interplay between the gut microbiome and the liver.

AIMs of this study

AIM N°1: Characterizing interactions between MAIT cells and liver antigen presenting cells

AIM N°2: MAIT cell characterization in NAFLD/NASH patients at single-cell level

III. Aim n°1: Characterizing interactions between MAIT cells and liver antigen presenting cells

Despite their high frequency in the human liver, the interaction between MAIT cells and liver cells was largely neglected at the time this PhD project started. Only primary biliary epithelial cells (BECs) were shown to be capable of presenting Ags in an MR1 dependent manner.

A. Materials and Methods (Experimental procedures)

1. Preparation of primary cells from human samples

Primary liver cells were prepared from liver samples from patients undergoing liver resection at the University Hospitals in Basel and Bern. Written informed consent was obtained from each patient included in the study. The study protocol conforms to the ethical guidelines of the 1975 Declaration of Helsinki, and was approved by the local ethics committee (Ethikkommission Nordwestschweiz; EKNZ; permit number EKNZ BASEC 2016-01188). Human hepatocytes were isolated from fresh liver tissue according to a published protocol(Portmann et al., 2013). Isolation of BECs and LSECs was carried out by positive immunomagnetic selection with anti-EpCAM and anti-CD31 respectively. Hepatic myofibroblasts/stellate cells (HSCs) were isolated by outgrowth from a suspension of liver derived non-parenchymal cells (NPCs), after hepatocyte depletion. Detailed methods for the isolation of HSCs, LSECs and BECs, and the maintenance and characterisation of all primary cell types by microscopy and/or FACS can be found in the supplementary methods of the attached manuscript.

2. Immunofluorescence staining of human liver sections

Cryopreserved human liver biopsy samples from the biobank at the Department of Biomedicine (Basel, Switzerland, ethics approval EKNZ BASEC 2016-01188) were used in this study. Sections of 8 µm thickness were mounted on microscopy slides and fixed in 4% formaldehyde for 10 min at room temperature (RT).

Slides were then washed twice for 10 min in PBS and blocked in blocking buffer for 1 h at RT [blocking buffer: 1% Normal donkey serum (Jackson Immuno Research, Ely, UK), 2% fish

gelatin, 0.15% Triton-X-100 in PBS]. Slides were incubated with primary Abs, diluted in blocking buffer, at 4°C overnight, washed with PBS, and then incubated with secondary Abs at RT for 1 h. After washing with PBS, slides were mounted in mounting solution containing 300 µM DAPI. Abs used were anti-IL-18Rα, anti-TCR Vα7.2 and anti-CD3. Secondary Abs were donkey-anti-goat-Cy3, donkey-anti-mouse-A488, and donkey-anti-rabbit-A647. Fluorescence images were taken on the Olympus BX63 microscope (Olympus, Tokyo, Japan), using the 20x objective, and analysed with Image J (https://fiji.sc/).

For patient details, see table in Figure 1.

3. Cell lines and MAIT cell clones

In order to generate the K562-MR1 cell line, we transduced K562 cells with a lentivirus coding for human MR1 covalently linked with β2M; this construct was generously provided by Prof. Gennaro De Libero, Department of Biomedicine, University Hospital Basel, Switzerland(Lepore et al., 2017). We confirmed MR1 overexpression and cell surface display by flow cytometry, after staining the cells with mouse-anti-MR1 (clone 26.5; monoclonal Ab purified from a hybridoma kindly provided by Prof. Marina Cella, Washington University School of Medicine in St. Louis)(Huang et al., 2005).

Human MAIT cell clone SMC3 was also kindly provided by Prof. Gennaro De Libero(Lepore et al., 2017). This clone was generated from the peripheral blood of a healthy donor. In brief, sorted MAIT cells were cloned by limiting dilution using PHA (1 µg/ml), human IL-2 (100 IU/ml) and irradiated PBMCs (5×10^5/ml). The SMC3 MR1-restricted T cell clone was cultured and re-stimulated periodically as described by Lepore et al(Lepore et al., 2014), and maintained in complete RPMI-1640 medium containing 5% AB^+ human serum, and 100 IU/ml IL-2.

4. Generation of liver-derived MAIT cell lines

Non-parenchymal cells (NPCs) obtained from normal liver tissue samples of two patients undergoing surgery for colorectal cancer metastasis were used to generate two liver-derived MAIT cell lines, designated MAIT-BEL-10 and MAIT-BSL-19.

The NPC fraction was obtained after perfusion of the liver wedge with “collagenase buffer” (684 mM NaCl, 13 mM KCl, 3 mM Na_2PO_4 $2H_2O$, 125 mM HEPES, 25 mM $CaCl_2$; pH 7.4; containing 200 IU/ml collagenase type IV), and low speed centrifugation to deplete

hepatocytes. Liver-associated mononuclear cells were isolated by density gradient centrifugation on Ficoll. MAIT cells were then FACS-sorted based on expression of CD3 and staining by MR1 Tetramer and expanded by stimulation with phytohemagglutinin (PHA) and human IL-2 (100 IU/ml) in the presence of irradiated peripheral blood mononuclear cells (PBMCs) (40 Gray) as feeder cells. T cells were maintained in RPMI 1640 medium supplemented with 5% AB^+ human serum, IL-2 (100 IU/ml), P/S, L-glutamine, pyruvate and non-essential amino acids (NEAA).

5. Preparation of bacterial products and synthetic MAIT cell Ag

Synthetic Ag 5-(2-oxopropylideneamino)-6-D-ribitylaminouracil (5-OP-RU) was generated according to the protocol published by Corbett et al (Corbett et al., 2014). In brief, Ag precursor 5-amino-6-D-ribitylaminouracil (5-A-RU; Toronto chemicals, CA) was mixed with 10 molar equivalents of methylglyoxal and incubated for 5 min on ice. The resulting 5-OP-RU was used immediately upon preparation to prevent its transformation into 7-Hydroxy-6-methyl-8-ribityl lumazine (RL-6-Me-7-OH) or 7-methyl-8-D-ribityllumazine (Fig. 2).

E. coli lysate: The DH5α strain was grown in LB medium. Cells were harvested during exponential growth and washed three times with cold 0.9% NaCl. Before the last wash, an aliquot was removed to determine the CFU. The pellet was subsequently resuspended in 70% ethanol and the cells were disrupted by two consecutive French press rounds. After centrifugation (15,000 x g for 20 min at 4°C), supernatant was lyophilized overnight and the concentration was adjusted to an equivalent of 5 x 10^{11} CFU/ml. The lysate was stored at −80°C.

6. Ag presentation assays

For Ag presentation with bacterial lysate/synthetic Ag, all assays with primary cell subtypes were performed in RPMI medium containing 10%, to exclude unspecific effects of variable cell media. APCs were seeded and kept for 4 h at 37°C to allow for attachment/adaptation.

Following this, *E. coli* lysate/synthetic Ag was added and cells were incubated for 2 h prior to the addition of MAIT cells, at an APC to T cell ratio of 1:4. Primary MAIT cells were used right

after isolation and the MAIT cell clone SMC3 at day 14 after re-stimulation. MAIT cell activation as well as cytokine secretion was evaluated after 16 h of co-culture.

To perform blocking experiments, cells were incubated with Ag and the corresponding blocking Abs (10 ng/ml anti-MR1, 5 µg/ml anti-IL-12 or 4 µg/ml anti-IL-18) were added after 1 h, followed by a 1-h incubation step before the addition of MAIT cells. To test the blocking potential of non-activating MR1 ligands, 6-formylpterin (6-FP; 50 µM), acetyl-6-FP (5 µM) or 20 - 100 µM 5-formyl-salicylic acid (5-F-SA) was added 1 h before the addition of 5-OP-RU.

7. Mass spectrometry analysis

5-OP-RU was analysed in cell extracts and cell supernatants by liquid chromatography (LC: Shimadzu, Kyoto, Japan) tandem mass spectrometry (MS/MS: API 4000, AB Sciex, Concor, Canada). A Synergi Polar-RP analytical column (Phenomenex, Torrance, USA) was used as stationary phase, while the mobile phase consisted of water (mobile A) and methanol (mobile B), both supplemented with 0.1% acetic acid. 5-OP-RU eluted at 2.14 min when using the following gradient program: 0 - 0.5 min 20% B, 0.5 - 1.5 min 20-95% B, 1.5 - 2.5 min 95% B, 2.5 - 3 min 20% B. The sample was online diluted during the first 0.5 min with mobile phase A via a t-union, which was connected in front of the analytical column. The flow rate was kept constant (0.8 ml/min). Aliquots of cell supernatant (50 µl) or cell extract (from 1.5 million cells) were extracted with 150 µl 100% methanol and 200 µl 75% methanol, respectively. After centrifugation, supernatants (20 µl) of extracts were injected into the LC-MS/MS system.

5-OP-RU was analysed by electrospray ionization and selected reaction monitoring in the negative mode using the mass transition 329.0 m/z → 190.9 m/z (declusting potential: -110 V, entrance potential: -10V, collision energy: -24 V, collision cell exit potential: -9 V, gas: N2). Analyst software 1.6.2 (AB Sciex, Concord, Canada) was used to analyse the data and to operate the LC-MS/MS system.

8. Quantitative real-time RT-PCR (RT-qPCR)

RNA was purified from primary liver cell types with Nucleo Spin RNA II kit (Macherey- Nagel, Germany) according to manufacturer's instructions. RNA was reverse transcribed by Moloney murine leukemia virus reverse transcriptase (Promega Biosciences, Inc., Wallisellen, Switzerland) in the presence of random Primers (Promega) and deoxynucleoside triphosphates, according to manufacturer's instructions. All reactions were performed in triplicates on an ABI 7500 Real-Time PCR System (Applied Biosystems, Faster City (CA), USA) using SYBR green fluorescence (FastStart Universal SYBR® green; Roche, Basel, Switzerland) as read out. mRNA expression levels of the MR1 transcript, were normalized to GAPDH mRNA levels using the ΔCt method. The primers were designed across exon-intron junctions to prevent contribution from genomic DNA amplification (MR1_F: 5'-TGCGGTGTCCAC ATGGTTCT-3', MR1_R: 5'-TTTGCTCTCGGGGCCTTCT-3'; GAPDH_F: 5'-AAGTAT GACAACAGCCTCAAGAT-3', GAPDH_R: 5'-CATGAGTCCTTCCACGATACC-3').

9. Enzyme-linked immunosorbent assay (ELISA)

For the ELISA, analysis plates (Maxisorp, NUNC) were coated overnight at 4°C with 2.5 µg/ml capture Ab for IFN-γ (Clone MD-1) or IL-17A (Clone BL-23). The next day, unspecific sites were blocked with 0.5% fractionated gelatine for 1 h at RT. The samples were incubated for 2 h, followed by 1 h incubation step with biotinylated Ab, either 1 µg/ml anti-IFN-γ or 0.3 µg/ml anti-IL-17A, and 1 h incubation with either 0.25 µg/ml Streptavidin-HRP (BioLegend) for the IFN-γ or 0.1 µg/ml Streptavidin- PolyHRP80 (SDT GmbH, Baesweiler Germany) for the IL-17A ELISA. In between each step, the plate was rinsed 3 times with PBS 0.05% Tween. Revealing was performed after incubation with OPD (SIGMAFASTTM), by reading absorbance at λ=490 nm.

10. Flow cytometry analysis

For the intracellular staining, cells were washed with PBS and stained with Live/Dead Cell Stain (Thermo Fisher Scientific) for 15 min, followed by a 10 min fixation step with 4% PFA prior to permeabilising the cells for 10 min.

For the surface staining, Mononuclear cells were washed in PBS and rinsed once in staining buffer (PBS with 0.5% human albumin and 3 mM sodium azide), then incubated 20 minutes in blocking buffer (50% human AB+ serum in staining buffer), followed by incubation in staining buffer containing the Ab cocktail. Data were acquired on the LSRFortessaTM (BD Biosciences, Allschwil, Switzerland) and analyzed with FlowJo 10.0.7 (TreeStar, Ashland (OR), USA).

11. Lentiviral vector generation

Lentiviral vectors were generated by a transient three-plasmid vector packaging system. Briefly, HEK293T cells were co-transfected with VSV-G construct pMD2G (Addgene plasmid #12259), pCMVR8.74 (Addgene plasmid #22036), both gifts from Didier Trono, and our construct plasmid generated by inserting CLEC2D isoform 1 cDNA in construct pUltra-Chili (Addgene plasmid #48687). pUltra-Chili was a gift from Malcolm Moore.

12. Statistical analysis

Unless indicated otherwise, all graphs presented in the figures represent data from three or more independent experiments. Exact numbers of repetitions are indicated in the figure legends. Unless indicated otherwise, values plotted in the graphs are means ± SD. All statistical analyses were performed in GraphPad Prism7. Analysis of statistical significance was conducted with the tests specified in the figure legends.

B. Results

1. MAIT cells are dispersed within the parenchyma in healthy human liver

We investigated whether MAIT cells are present in the sinusoidal environment of the liver, where they might be activated by contact with parenchymal and non-parenchymal cells that potentially function as liver APCs capable of presenting gut-derived bacterial Ags. We analysed, by immunofluorescence (IF) staining, human liver samples from 8 donors, lacking significant hepatic histopathological abnormalities (Fig. 6D). MAIT cells were identified as cells positive for CD3, TCR Vα7.2 and IL-18Rα, a robust combination of markers as IL-18Rα parallels high CD161 expression on MAIT cells(Le Bourhis et al., 2010). MAIT cells localized dispersedly to the parenchymal space in the liver (Fig. 6A and 5A). They were found in or in the immediate proximity of the sinusoids, occasionally also within the portal fields. There was no zonal distribution that would confine MAIT cells to either of the three zones of the hepatic lobule. Our analysis, indicating that MAIT cells represent 8-33% of total liver T cells (Fig. 6C), confirmed that MAIT cells are highly abundant in human liver, considerably exceeding the frequency of Vα7.2-positive conventional T cells. Their proximity to parenchymal and non-parenchymal cells within the sinusoidal environment is likely to facilitate interaction of MAIT cells with liver cells taking up blood-borne liver-directed Ags.

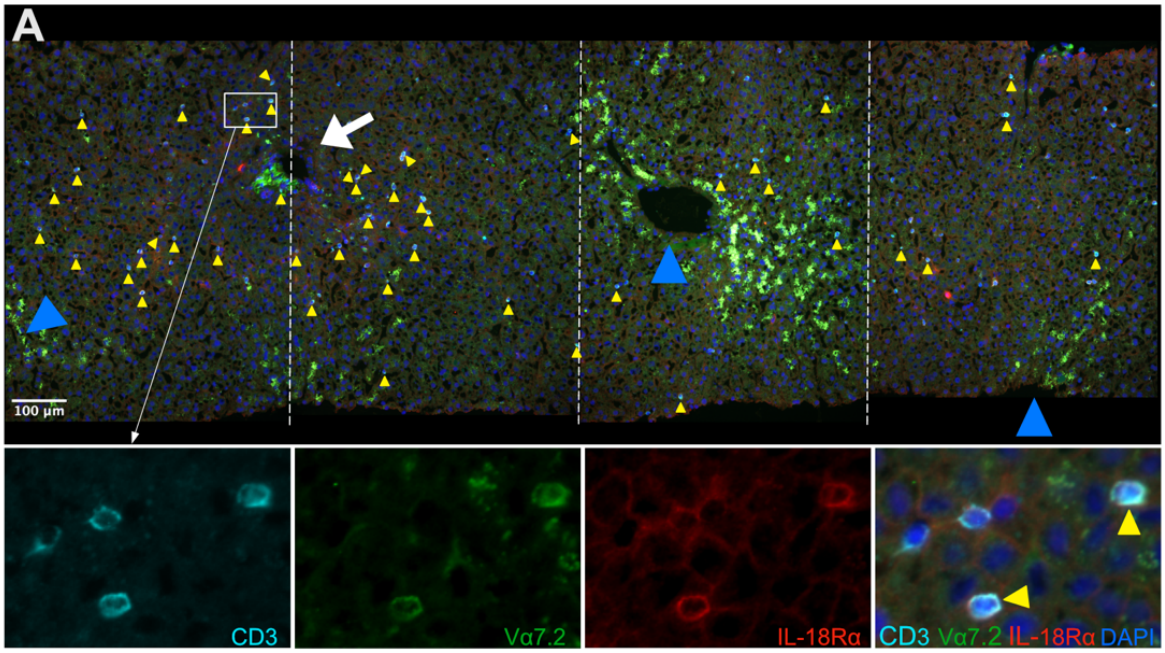

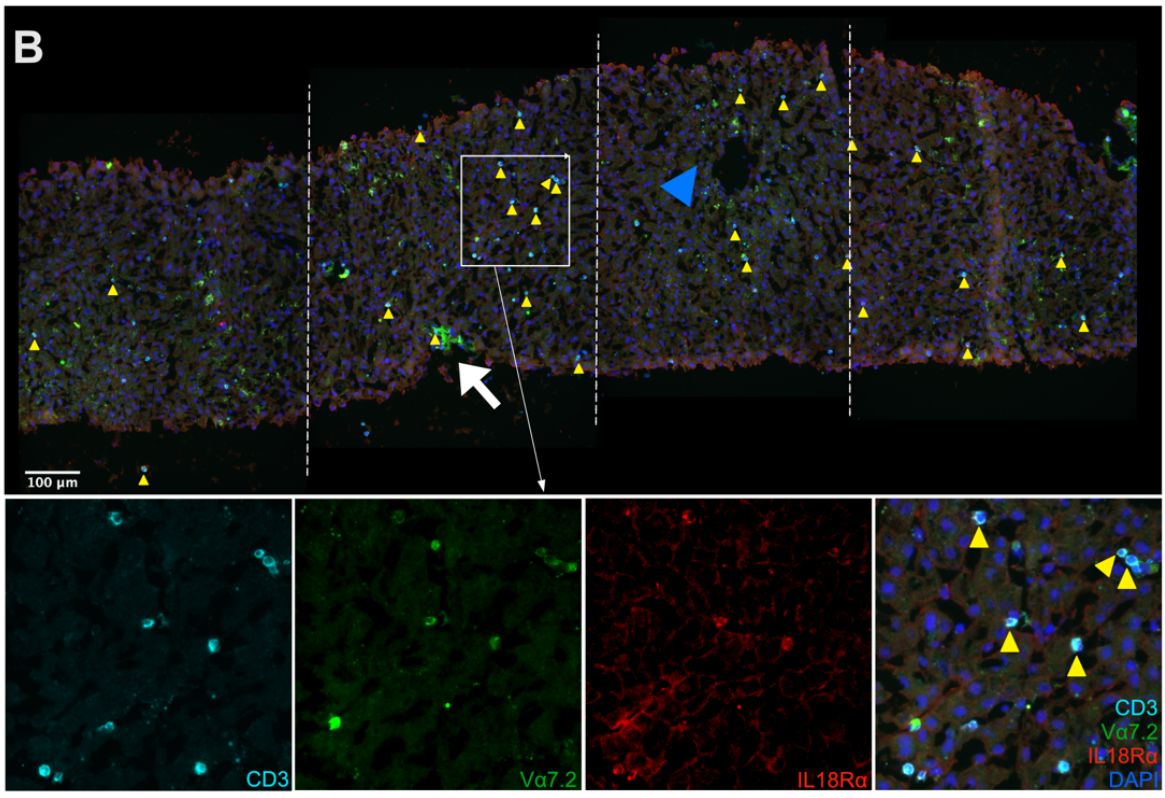

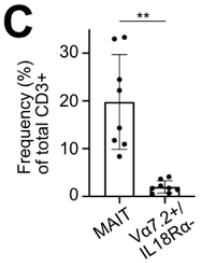

D

Patient ID	Age	% MAIT/ CD3	% Vα7.2+ IL18Rα-/ CD3	ALAT [U/l]	ASAT [U/l]	GGT [U/l]	AP [U/l]	Bilirubin [µmol/l]	Reason for biopsy	Biopsy result
C369	36	14.33	1.75	88	33	447	111	4	Suspicion of medication induced hepatotoxicity	Liver parenchyma without pathological changes.
C491	43	10.95	1.41	35	23	116	71	10	Isolated GGT increase	Liver parenchyma without pathological changes.
C545	54	32.97	3.62	91	49	216	204	8	Increased Transaminases/ GGT/AP	Liver parenchyma without pathological changes.
B927	60	22.22	1.71	15	22	20	41	12	Calcified liver mass	Liver parenchyma without pathological changes.
C28	50	24.48	0.69	43	39	406	150	9	Focal nodular hyperplasia	Liver parenchyma without major pathological changes. Minimal steatosis <10%.
C145	42	33.33	4.10	56	24	154	84	21	Increased Transaminases/GGT	Liver parenchyma without major pathological changes. Minimal unspecific lymphocytic infiltrates, minimal sinusoidal dilation.
C192	35	8.38	2.23	42	26	137	76	4	Increased Transaminases	Liver parenchyma without major pathological changes. Minimal reactive hepatitis.
B113	27	11.73	0.51	21	29	14	62	10	Increased Transaminases (normal again at time-point of biopsy)	Liver parenchyma without major pathological changes. Minimal unspecific lobular inflammation.

Figure 6. MAIT cells localize dispersedly to the parenchymal space in healthy human liver. Representative IF analysis of tissue section from a liver biopsy without histopathological abnormalities patient C545(A) C145(B). Co-localization of CD3, TCR Vα7.2 and IL18-Rα (see higher magnification lower panels) identifies MAIT cells (yellow arrow heads). White arrow and blue arrow heads point at portal field and central veins, respectively. Lower panels also show MAIT cells in proximity of TCR Vα7.2- and IL18-Rα-negative T cells. (C) Percentages of MAIT cells and non-MAIT Vα7.2^{+} cells *versus* total CD3^{+} T cells in healthy human liver (n = 8), assessed as shown in (A). ** $P < 0.01$, non-paired Welch t-test. (D) Patient characteristics of liver biopsy samples used for assessment of MAIT cell localization in normal human liver by IF staining.

2. Robust MAIT cell activation by primary human liver cell subsets

Given the potential of MAIT cells to interact with any liver cells according to their dispersion in tissue, we next investigated their ability to interact *in vitro* with different liver parenchymal and non-parenchymal primary cells isolated from human liver tissue. We isolated hepatocytes and hepatic myofibroblasts/HSCs ourselves, and obtained BECs, Liver sinusoidal endothelial cells (LSECs) and additional hepatocytes and myofibroblasts/HSCs from our collaborators, the laboratory of Visceral Surgery of Prof. D. Stroka at the University of Bern. Cells were isolated from surgically removed liver specimens and their identities were assessed by FACS and/or microscopy (Fig. 7A-C). All of these cell types represent potential non-professional APCs unique to the liver environment. Importantly, we observed MR1 expression in primary human hepatocytes, which at approximately 60% constitute the main liver cell population, but also in BECs, LSECs and HSCs both at the RNA level and by surface staining assessed by cytometry (Data not shown and Fig. 7D).

Primary hepatocytes, when incubated with *E. coli* lysate, activated MAIT cell clone SMC3 in an MR1-dependent manner as shown by IFN-γ secretion (Fig. 7E) upregulation of MAIT cell activation markers CD69, CD137 and PD-1 (Fig. 7F). K562-MR1 human myeloid leukaemia cells stably transfected with a β2M-MR1 construct, and thus over-expressing MR1, were used as positive control APCs (Figs 6E and 6I). The results of robust MAIT cell activation by hepatocytes acting as APCs were verified using pure synthetic Ag 5-OP-RU instead of the *E. coli* lysate (Fig. 4D and Supplementary Fig. 5B).

HSCs are the main drivers of fibrogenesis in the liver, efficiently producing proteins involved in extracellular matrix formation upon activation(Tsuchida and Friedman, 2017). As MAIT cells were recently linked to liver fibrosis(Böttcher et al., 2018; Hegde et al., 2018), we asked whether HSCs are able to directly activate MAIT cells. Using primary HSCs as APCs and treating them with either the *E. coli* lysate or 5-OP-RU, we demonstrated MR1-dependent activation of MAIT cells measured by IFN-γ secretion (Fig. 7H-I) and expression of activation markers CD69, CD25 and CD137, as well as TCR downregulation (Fig. 7K-L).

We also tested the ability of blood-derived FACS-sorted MAIT cells to induce pro-fibrotic genes in HSCs upon stimulation with Ag and found a fibrogenic response (data not shown). This observation is in line with recent published findings(Böttcher et al., 2018; Hegde et al., 2018). Taken together, the results implicate direct interaction between HSCs and MAIT cells as a factor contributing to the mechanism of their fibrogenic activity.

MR1-expressing primary cell populations of BECs and LSECs were also able to present *E. coli*-derived and synthetic 5-OP-RU Ag to MAIT cells (Figs 6J and 7A). This aspect is of particular importance as both cell types represent a barrier between the liver, the intestine and the circulation respectively. In summary, the data demonstrate that cells from the sinusoidal environment in the liver, as well as BECs, have a capacity to present bacteria-derived and pure Ag to MAIT cells.

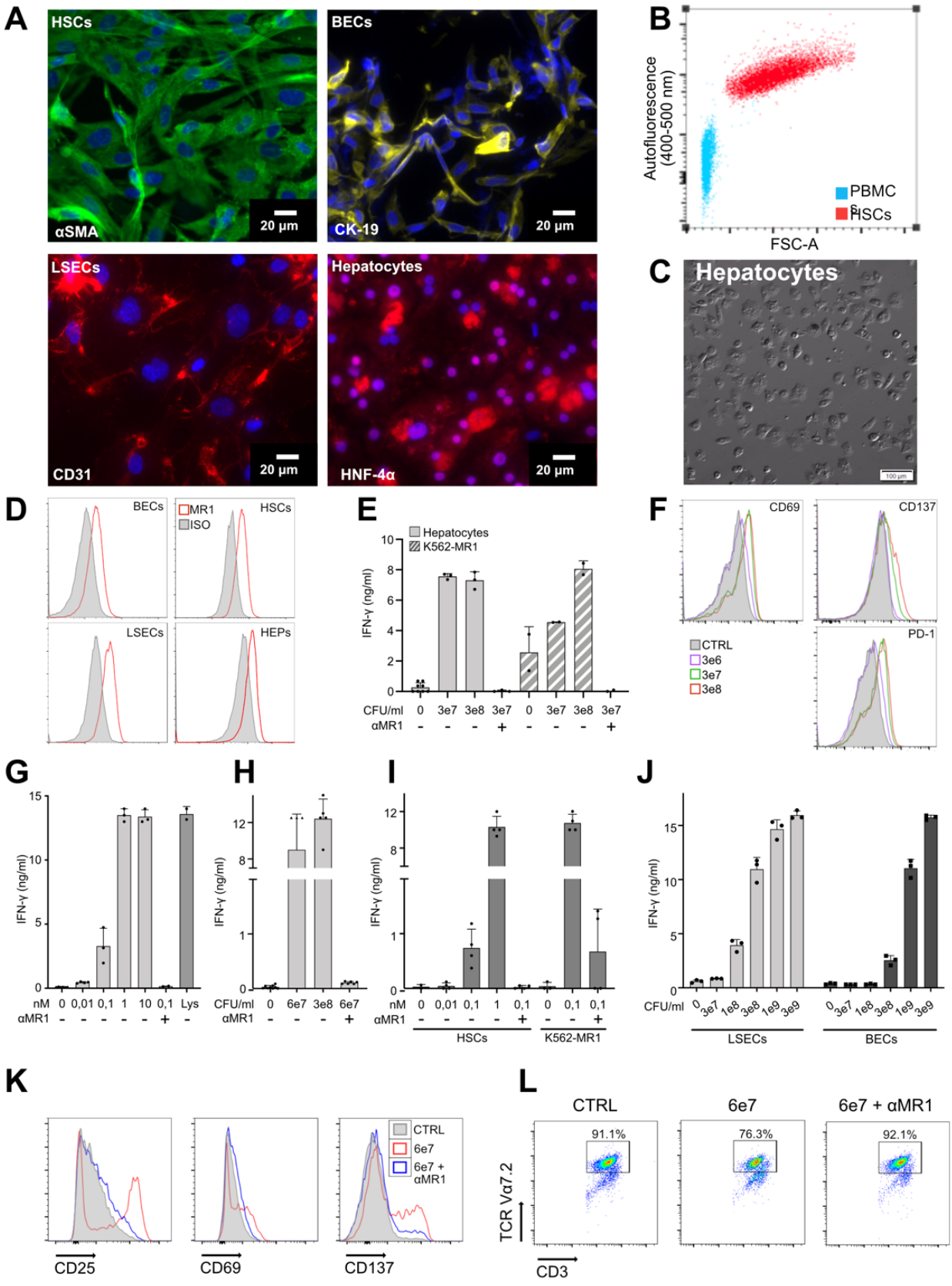
A
HSCs
αSMA
20 µm
BECs
CK-19
20 µm
LSECs
CD31
20 µm
Hepatocytes
HNF-4α
20 µm
B
Autofluorescence (400-500 nm)
FSC-A
PBMC
HSCs
C
Hepatocytes
100 µm
D
BECs
HSCs
LSECs
HEPs
MR1
ISO
E
Hepatocytes
K562-MR1
IFN-γ (ng/ml)
CFU/ml 0 3e7 3e8 3e7 0 3e7 3e8 3e7
αMR1 - - - + - - - +
F
CD69
CD137
PD-1
CTRL
3e6
3e7
3e8
G
IFN-γ (ng/ml)
nM 0 0,01 0,1 1 10 0,1 Lys
αMR1 - - - - - + -
H
IFN-γ (ng/ml)
CFU/ml 0 6e7 3e8 6e7
αMR1 - - - +
I
IFN-γ (ng/ml)
nM 0 0,01 0,1 1 0,1 0 0,1 0,1
αMR1 - - - - + - - +
HSCs
K562-MR1
J
IFN-γ (ng/ml)
CFU/ml 0 3e7 1e8 3e8 1e9 3e9 0 3e7 1e8 3e8 1e9 3e9
LSECs
BECs
K
CD25
CD69
CD137
CTRL
6e7
6e7 + αMR1
L
CTRL
6e7
6e7 + αMR1
91.1%
76.3%
92.1%
TCR Vα7.2
CD3

Figure 7. Primary human parenchymal and non-parenchymal liver cells express MR1 and present Ag to MAIT cells.

(A) Isolated primary cells were analyzed by IF for expression of indicated markers. Formalin-fixed cells grown on chamber slides were stained for DAPI and α-SMA for HSCs, CK-19 for BECs, CD31 for LSECS and HNF4α for hepatocytes. (B) Flow cytometry analysis of unstained HSCs compared with PBMCs. The characteristic autofluorescence of HSCs appears in the violet channel (λ= 400.500 nm). (C) Representative preparation of primary human hepatocytes (partially binucleated) used in Ag presentation experiments, visualized by bright fields microscopy. (D) Flow cytometry histograms showing primary BECs, LSECs, HSCs and hepatocytes (HEPs) expressing MR1, stained with anti-MR1 (red) or isotype-matched control antibody (filled grey). (E) MAIT cell clone SMC3 IFN-γ production upon co-culture with hepatocytes incubated with *E. coli* lysate (3e7 or 3e8 CFU/ml). (n = 4). (F) Representative flow cytometry histograms, showing indicated markers on clone SMC3 in response to hepatocytes incubated with *E. coli* lysate (3e6 – 3e8 CFU/ml). Filled grey histograms correspond to negative controls (CTRL) lacking lysate. (G - J) IFN-γ production by clone SMC3 in response to incubation with indicated liver cells and Ags. (G) Hepatocytes incubated with 5-OP-RU (0.01 - 10 nM). *E. coli* lysate (Lys; 3e8 CFU/ml) served as positive control (n = 7). (H) HSCs incubated with *E. coli* lysate (6e7 or 3e8 CFU/ml) (n = 5). (I) HSCs incubated with 5-OP-RU (0.01 - 1 nM) (n = 9). (J) LSECs and BECs incubated with *E. coli* lysate (3e7 – 3e9 CFU/ml) (n = 6). In panels B, D, E, F and G, the data (means ± SD of measurements from three independent wells originating from the same patient) exemplify representative experiments out of 4 - 9 performed with cells obtained from at least 3 different donors. IFN-γ was measured by ELISA. (K) Representative FACS histograms showing upregulated activation markers CD69, CD25 and CD137, and (L) FACS plots showing downregulated TCR Vα7.2 on clone SMC3 in response to HSCs incubated with *E. coli* lysate (6e7 CFU/ml). Controls are lacking the lysate (CTRL). MR1 dependence of activation was assessed by anti-MR1 blocking Ab clone 26.5 (Fig. E & G-L). IFNγ secretion was assessed by ELISA.

3. Hepatocytes are the most efficient non-professional Ag-presenting cells to MAIT cells in the liver

We found pronounced differences in presentation capacity between the investigated cell types, with hepatocytes being the most efficient liver-derived APCs, (Fig. 8A-D), as assessed by the pure Ag or bacterial lysate concentration needed to reach an EC50 of IFN-γ production by MAIT cell clone SMC3. Differences in the liver APC-induced activation of MAIT cells in the presence of Ag persisted when either IL-12 or IL-18 was blocked (Fig. 8D-J) Inclusion of exogenous IL-12 or IL-18 increased MAIT cell activation, a known effect synergistic with TCR-dependent stimulation(Turtle et al., 2011; Ussher et al., 2014). The effect decreased upon addition of blocking antibodies against the respective cytokines, thus confirming the blocking effectiveness (Fig. 8L). Taken together, our results demonstrate robust MR1-dependent Ag presentation capabilities of intrahepatic cell types, most prominently hepatocytes, leading to the activation of MAIT cells.

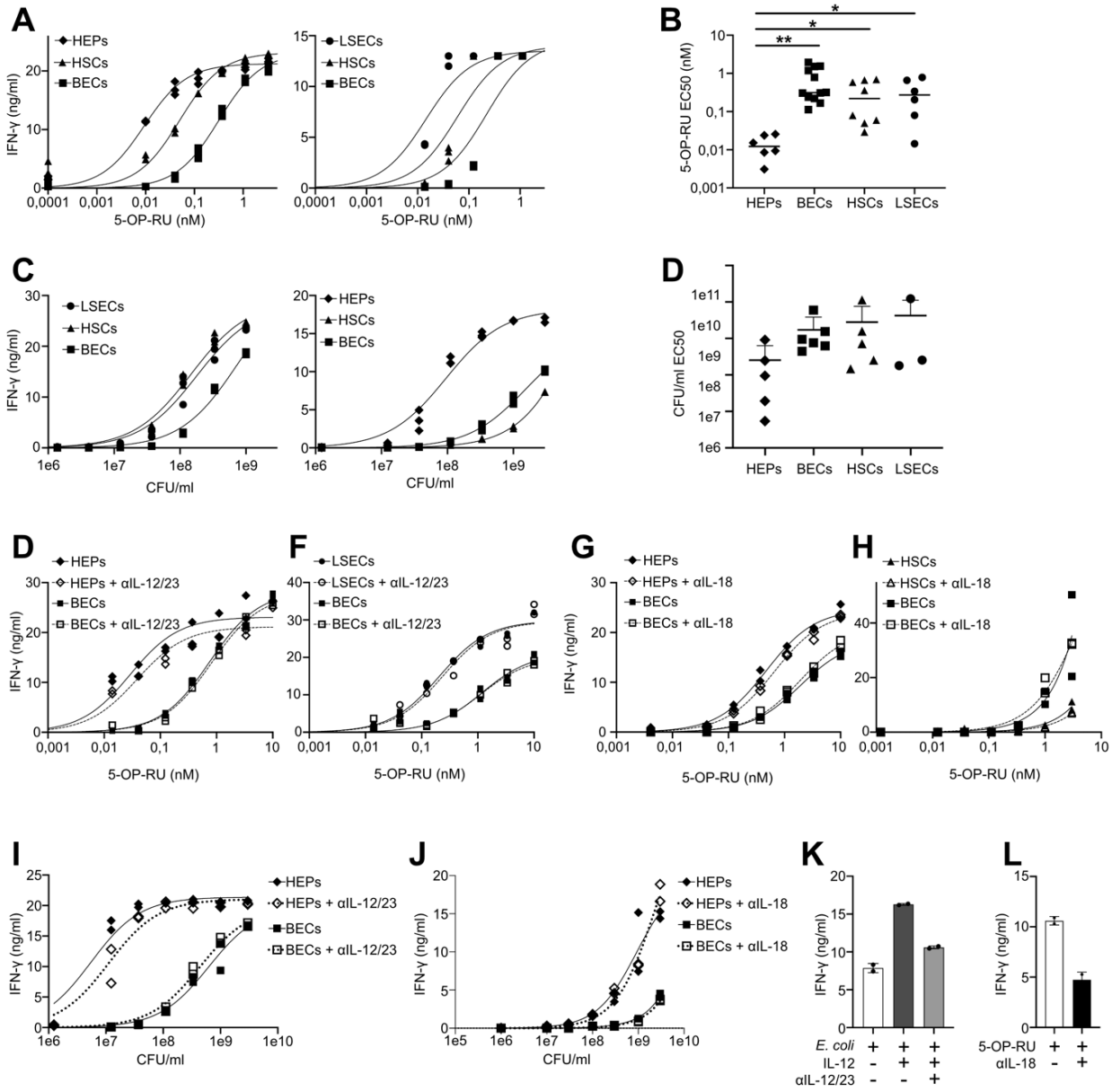
A
HEPs
HSCs
BECs
IFN-γ (ng/ml)
5-OP-RU (nM)
LSECs
B
5-OP-RU EC50 (nM)
HEPs BECs HSCs LSECs
C
CFU/ml
D
CFU/ml EC50
D
HEPs + αIL-12/23
BECs + αIL-12/23
F
LSECs + αIL-12/23
G
HEPs + αIL-18
BECs + αIL-18
H
HSCs + αIL-18
I
J
K
E. coli
IL-12
αIL-12/23
L
5-OP-RU
αIL-18

Figure 8. Hepatocytes represent potent liver-derived APCs activating MAIT cells.
(A) Two representative examples of synthetic Ag 5-OP-RU titration (0.01 - 3 nM) on liver APCs. Three independent measurements per dose are depicted. (B) Pooled results of all experiments performed as in panel (A). Shown are concentrations of 5-OP-RU needed to reach EC50 of IFN-γ secretion. (C) Two representative examples of *E.coli* lysate titration on liver APCs. (D). Pooled results of all experiments performed as in panel (C). Shown are equivalent CFU of Lysate needed to reach EC50 of IFN-γ secretion. Statistical significance was determined by paired Student's t-test. ** $p < 0.01$, * $p < 0.05$. (E-H) Representative examples of 5-OP-RU (0.01 - 10 nM) titration on liver APCs, in the absence or presence of Abs blocking either IL-12/23 (E and F) or IL-18 (G and H). One representative experiment out of 2 is shown in each panel. Other details are as in panel (A). (I and J) Representative examples of E. coli lysate (3e6 – 6e9 CFU/ml) titration using primary hepatocytes/HEPs and BECs as APCs, either in the absence or presence of IL-12/23 (I) or IL-18 (J) blocking Abs. (K) Confirmation of blocking efficiency of the anti-IL-12/23 Ab. BECs were stimulated with *E. coli* lysate (1e6 CFU/ml) in the absence or presence of IL-12 and anti-IL-12/23 Ab. (L) Confirmation of blocking efficiency of the anti-IL-18 Ab. THP-1 cells were stimulated with 1 nM 5-OP-RU in the absence or presence of Ab blocking IL-18.

4. Primary liver cells generate active MAIT cell Ag when provided with its precursor

In view of the strong intrahepatic interactions involving MAIT cells, we investigated whether liver APCs can generate active MAIT cell-stimulatory Ag endogenously. It has been reported that the Ag precursor 5-A-RU is not able to bind to MR1 and activate MAIT cells.(7) However, we found that exposure of liver APCs (hepatocytes, BECs, LSECs) to 5-A-RU for 2 or 5 h led to MAIT cell activation (Fig. 9A-B), suggesting that the activatory 5-OP-RU is formed by the liver APCs. To investigate the formation of 5-OP-RU, Liquid chromatography tandem mass spectrometry (LC-MS/MS) analysis of cell culture supernatants following exposure of THP-1 to 5-A-RU was set (Fig. 9C-D), and a time course experiement confirm the formation of 5-OP-RU (Fig. 9E). We then used the same method on primary liver cells, and the antigen formation observed corroborated the data obtained previously in the activation experiment. MS analysis indicated that all tested primary liver cell types generated 5-OP-RU in a dose-dependent manner when provided with the precursor 5-A-RU (Fig. 9F). Collectively, these results demonstrate that primary liver cell subtypes can form active MAIT cell Ag when provided with the precursor 5-A-RU. This indicates that the process of activation of liver MAIT cells, encompassing both production of specific Ag molecules and their presentation by nearby liver APCs, can occur in a local liver environment.

5-A-RU conversion to active Ag *in vivo* in liver depends upon 5-A-RU crossing the intestinal barrier. Indeed, a compound with a molecular mass corresponding to the MAIT cell Ag precursor 5-A-RU was detected in the circulation and liver of mice(Uchimura et al., 2018). To assess the probability of 5-A-RU crossing an intact intestinal barrier, we performed *in silico* modelling by applying a published method that uses a combination of physico-chemical parameters(Lipinski et al., 2001; Martin, 2005). Applying this method to the Ag 5-OP-RU and its precursor 5-A-RU, we identified that of these two chemically very similar compounds the precursor has a higher probability of passive intestinal absorption than the active 5-OP-RU product (Fig. 9G).

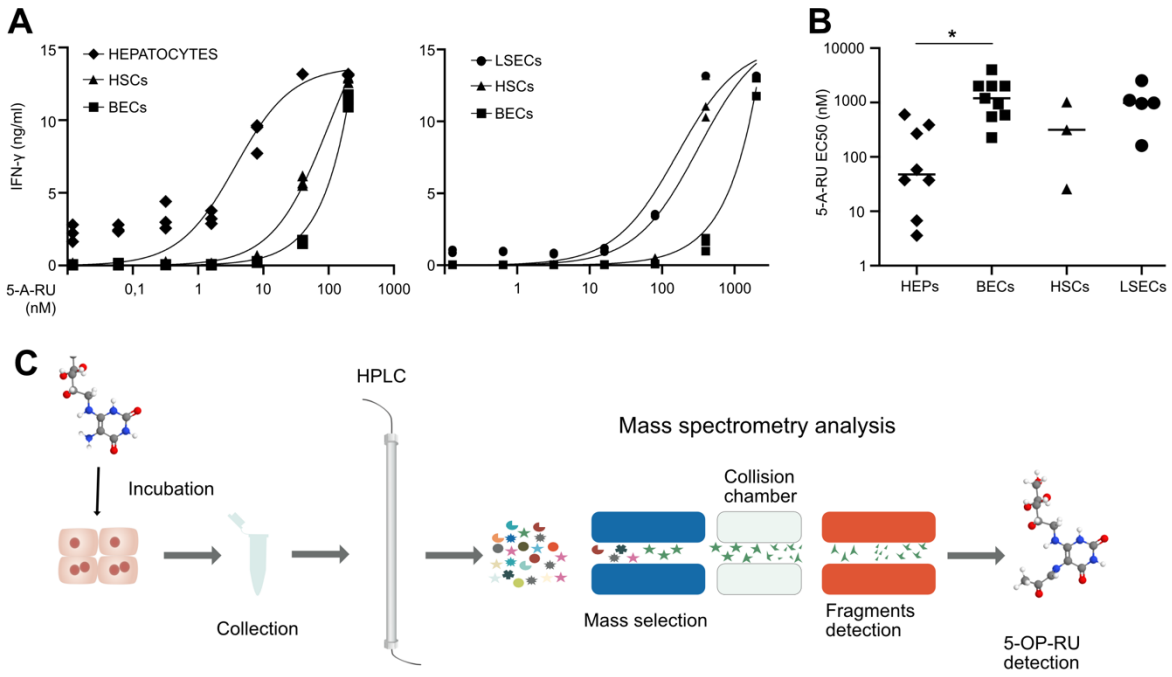

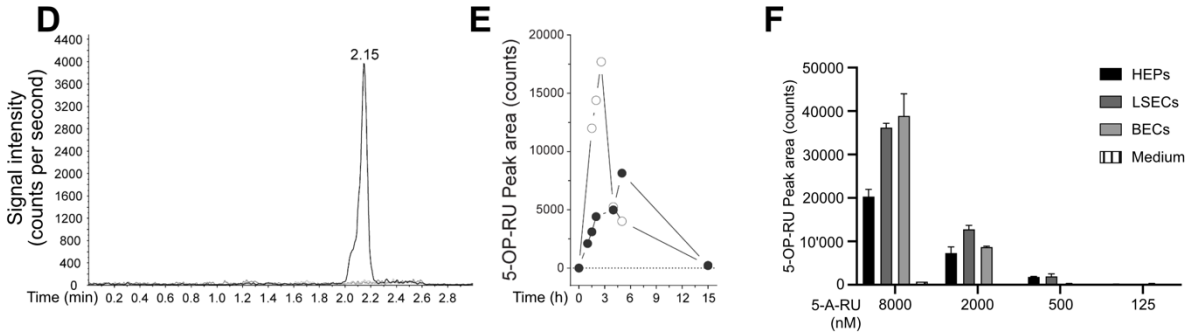

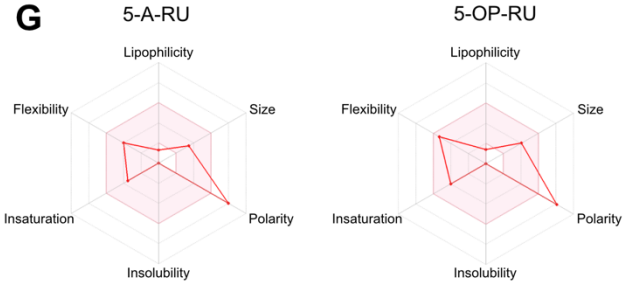

Molecular weight	276.3 Da
LogP	-2.3
TPSA	184 Å²
Lipinski's rule	1 violation
Bioavailability score	**0.55**

Molecular weight	330.3 Da
LogP	-1.7
TPSA	188 Å²
Lipinski's rule	2 violations
Bioavailability score	**0.17**

Figure 9. Liver-derived primary APCs have the capacity to generate active Ag endogenously. (A) Representative experiment of MAIT cell Ag precursor 5-A-RU (0.01 – 2000 nM) titration using different liver primary cells as APCs. IFN-γ production by MAIT cell clone SMC3 was assessed by ELISA. Three independent replicates per dose are depicted. (B) Pooled results of all experiments performed as shown in panel (A), using cells originating from at least 3 different donors per cell type as APCs. Shown are concentrations of 5-A-RU needed to reach EC50 of IFN-γ production. Statistical significance determined by paired Student's t-test. *$p < 0.05$.(C) Schematic representation of the analytical strategy used to assess the generation of 5-OP-RU from 5-A-RU in the presence of cells. (D) Overlay of three LC-MS/MS chromatograms of 5-OP-RU determined in cell supernatant of THP-1 cells (black, 5-OP-RU following 2.6 h incubation; light grey, 5-OP-RU following 15 h incubation; dark grey, pure methanol injection). (E) LC-MS/MS analysis of cell extracts and the corresponding culture supernatants following incubation of THP-1 cells with 1 μM 5-A-RU. Shown are time-course accumulation curves of 5-OP-RU in cell lysate (black circles) and cell culture supernatant (open circles). (F) Quantification of 5-OP-RU by LC-MS/MS in cell culture supernatants derived from indicated liver primary cells harvested after treatment with indicated doses of 5-A-RU (125 – 8000 nM). RPMI medium without inclusion of cells served as negative control (Medium).

5. The degree of activation of polyclonal blood- and liver-derived MAIT cells varies with the APC

To investigate whether the findings for the MAIT cell clone SMC3 apply to primary polyclonal MAIT cell populations, we isolated and tested MAIT cells from human peripheral blood and liver tissue. Starting with PBMCs, which contain 2-5% MAIT cells, negative magnetic bead selection using Abs against CD45RA, CD62L, CD19, CD14, CD36 and TCRγδ, depleted naïve T cells, B cells, monocytes, dendritic cells, platelets and γδ T cells, resulting in four- to sevenfold enrichment for MAIT cells (Fig. 10A). Activation of the enriched polyclonal MAIT cells was assessed upon exposure to Ag-loaded primary liver cells. TCR expression was downregulated in response to distinct liver-derived APCs exposed to 5 nM 5-OP-RU, with hepatocytes again being the most potent APCs (Fig. 10B).

To assess activation of polyclonal liver-derived MAIT cells, we generated two liver MAIT cell lines (MAIT-BEL-10 and MAIT-BSL-19) from two patient donors. Both cell lines produced IFN-γ and IL-17 and showed upregulation of several activation markers, including CD107a and CD137, in response to different human liver-derived APCs exposed to synthetic 5-OP-RU, including hepatocytes, BECs and HSCs (Figs 9C-D and 9F, and data not shown). Presentation capacity varied between the liver APCs, as assessed by IFN-γ secretion and upregulation of activation markers by the MAIT-BEL-10 and MAIT-BSL-19 cells (Figs 9C and 9F). To mimic an inflammatory context in which increased amounts of bacterial products and inflammatory cytokines reach the liver, the synthetic Ag in some experiments was spiked into *E. coli* lysate (Fig. 10E). In this state, hepatocytes remained as efficient APCs (Fig. 7D) and this was paralleled by cytotoxicity elicited by liver-derived MAIT cell line MAIT-BSL-19 (Fig. 7E).
Thus, as a proof of concept, we demonstrated that hepatocytes can be killed *in vitro* following Ag-mediated activation of liver-derived MAIT cells. Taken together, our experiments demonstrate that human polyclonal MAIT cells derived from peripheral blood and liver respond to Ag presentation by different liver cells, most prominently hepatocytes.

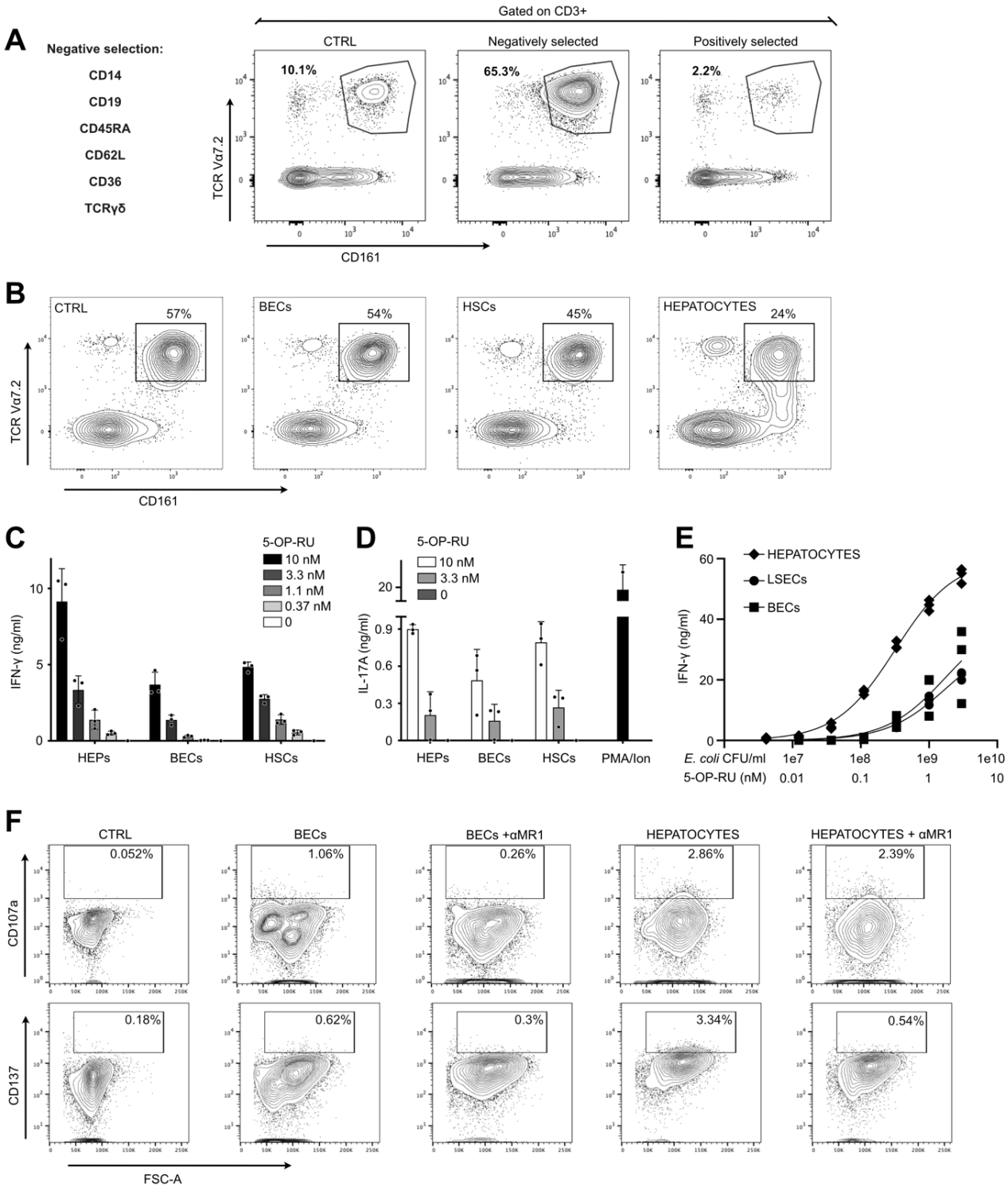
A
Negative selection:
CD14
CD19
CD45RA
CD62L
CD36
TCRγδ
Gated on CD3+
CTRL
Negatively selected
Positively selected
10.1%
65.3%
2.2%
TCR Vα7.2
CD161
B
CTRL
57%
BECs
54%
HSCs
45%
HEPATOCYTES
24%
TCR Vα7.2
CD161
C
5-OP-RU
10 nM
3.3 nM
1.1 nM
0.37 nM
0
IFN-γ (ng/ml)
HEPs
BECs
HSCs
D
5-OP-RU
10 nM
3.3 nM
0
IL-17A (ng/ml)
HEPs
BECs
HSCs
PMA/Ion
E
HEPATOCYTES
LSECs
BECs
IFN-γ (ng/ml)
E. coli CFU/ml
1e7
1e8
1e9
1e10
5-OP-RU (nM)
0.01
0.1
1
10
F
CTRL
BECs
BECs +αMR1
HEPATOCYTES
HEPATOCYTES + αMR1
0.052%
1.06%
0.26%
2.86%
2.39%
CD107a
0.18%
0.62%
0.3%
3.34%
0.54%
CD137
FSC-A

Figure 10. Robust activation of polyclonal MAIT cells in response to interactions with primary human liver cell subsets.

(A) Representative cytometry plot showing the frequency of Vα7.2^{+} CD161^{++} among CD3+ lymphocytes before (CTRL) and in both fractions after magnetic enrichment with indicated markers. (B) PBMCs, enriched like in (A) were co-cultured with indicated liver APCs exposed to 5 nM 5-OP-RU. Representative example of cell surface expression of CD161 and TCR Vα7.2, as measured by flow cytometry (n=2). Dot plots are gated on CD3^{+} cells. (C and D) Production of IFN-γ (C) and IL-17 (D) by liver-derived MAIT cell line MAIT-BEL-10, measured by ELISA, in response to interaction with different liver APCs exposed to indicated concentrations of 5-OP-RU. Stimulation of MAIT cells with PMA/ionomycin (PMA/Ion) served as positive control. (E) IFN-γ production by liver-derived MAIT cell line MAIT-BSL-19, stimulated by indicated liver APCs exposed to increasing concentrations of *E. coli* lysate spiked in with 5-OP-RU. Three replicates per dose are shown. (F) Cell surface staining for CD107a and CD137 on MAIT-BSL-19 cells, stimulated by either hepatocytes or BECs exposed to 5 nM 5-OP-RU. MR1 dependence of activation was assessed with anti-MR1 blocking antibody (αMR1). Negative control (CTRL) in panel A and E lacks the APC.

6. Inhibition of liver APC-mediated MAIT cell activation by small molecules

To approach the prevention of MAIT cell activation in the liver, we explored the blocking of MR1 occupancy with non-activating MR1 ligands. These ligands occupy the bed of the MR1 A' groove similarly to the activating one but their distal moiety - regarding the covalent association with MR1- is shorter and poke out of the MR1 jaws in smaller magnitude (Fig.10A-B). The consequence is a weaker interaction with the TCR and no MAIT cell activation, 6-formylpterin (6-FP), derived from the folate degradation pathway, and acetyl-6-FP were first the non-activating MR1 ligands described(Awad et al., 2020; Keller et al., 2017). We found that MAIT cell activation by Ag-exposed primary liver cells (hepatocytes, BECs and HSCs) can be prevented in a dose dependent manner by pre-treating the liver cells with 6-FP or acetyl-6-FP (Figs 10C-D). Other molecules, e.g. the acetylsalicylic acid derivative 5-formyl-salicylic acid (5-F-SA), were found previously to stabilize MR1 on the cell surface; however, they did not stimulate Jurkat T cells overexpressing the MAIT TCR(Keller et al., 2017). MAIT cell activation by liver APCs was prevented by 5-F-SA (Fig. 11D). This indicates that liver APC-induced MAIT cell activation can be inhibited by small molecular-weight compounds that specifically interfere with MR1 activity on the surface of APCs.

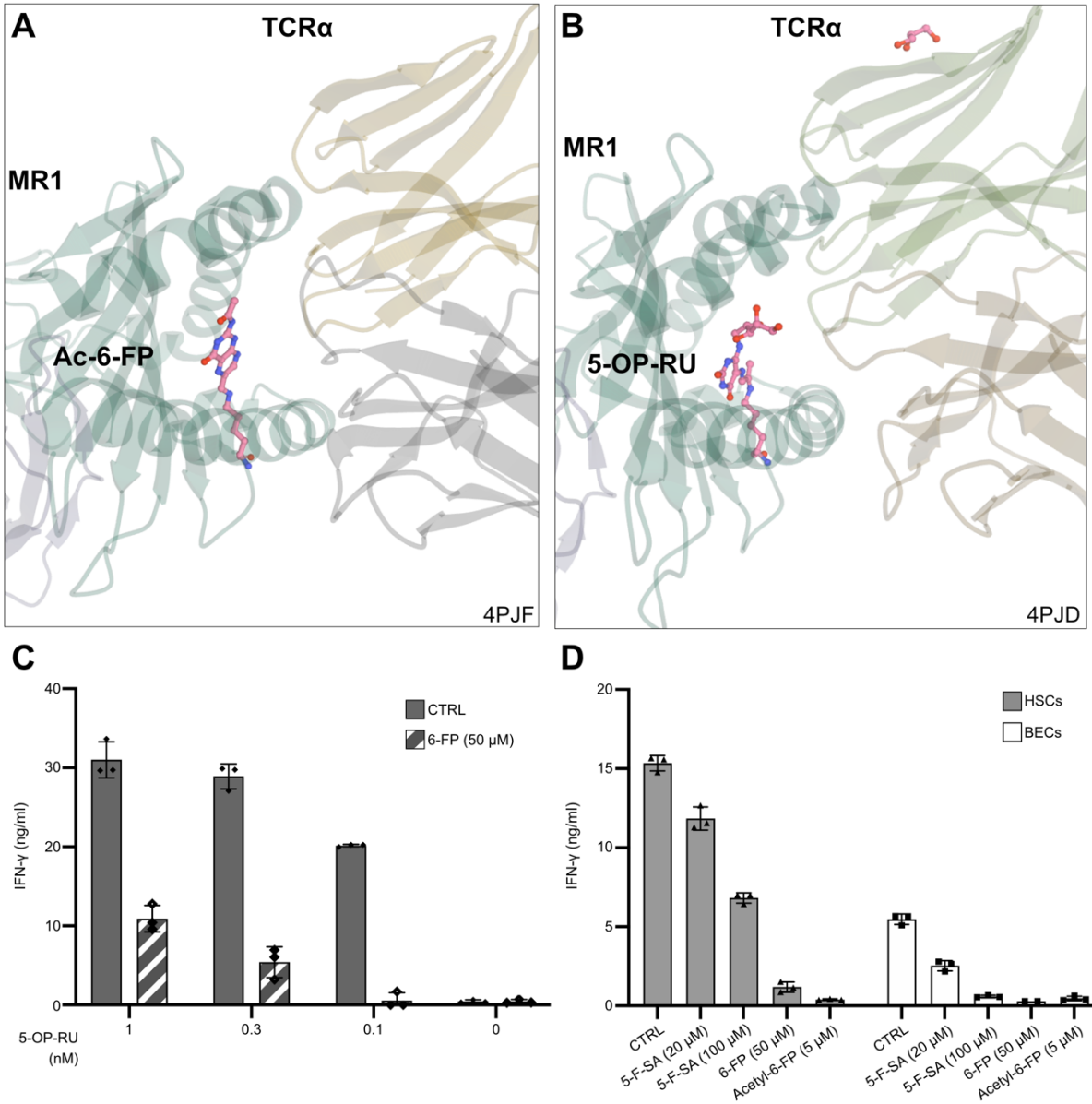
A
TCRα
MR1
Ac-6-FP
4PJF
B
TCRα
MR1
5-OP-RU
4PJD
C
CTRL
6-FP (50 μM)
IFN-γ (ng/ml)
40
30
20
10
0
5-OP-RU (nM)
1
0.3
0.1
0
D
HSCs
BECs
IFN-γ (ng/ml)
20
15
10
5
0
CTRL
5-F-SA (20 μM)
5-F-SA (100 μM)
6-FP (50 μM)
Acetyl-6-FP (5 μM)
CTRL
5-F-SA (20 μM)
5-F-SA (100 μM)
6-FP (50 μM)
Acetyl-6-FP (5 μM)

Figure 11. Non-activating MR1 ligands prevent MAIT cell activation by liver-derived APCs. 3D Representation of MR1 crystal structure with non-activating (A) or activating (B) ligand. Representation of human MR1 loaded with Acetyl-6-FP (A), or 5-OP-RU (B) co-crystalized with human MAIT TCR C10. Cristal structure generated by Birkinshaw, R.W. and Rossjohn, J, representation generated on the PDB website, PDB number indicated in the lower right corner. (C-D) MAIT cell clone SMC3 was co-cultured with indicated liver cells pre-treated with different non-activating MR1 ligands for 1 h before addition of 5-OP-RU. IFN-γ secretion was assessed by ELISA. (C) Hepatocytes either treated with 0.1-1 nM 5-OP-RU alone (CTRL) or pre-treated with 50 µM of 6-FP before adding 5-OP-RU. (D) HSCs and BECs either treated with 5-OP-RU alone (1 nM; CTRL), or pre-treated with indicated concentrations of 6-FP, Acetyl-6-FP, or 5-formyl-salicylic acid (5-F-SA) before 5-OP-RU addition. The mean ± SD of measurements of three independent wells originating from the same patient's cells is shown. One representative experiment out of 2, originating from two different donors, is shown.

7. CLEC2D over-expression on APCs downregulates CD161 on MAIT cells

To investigate the impact of surface CLEC2D expression by APCs on MAIT cell function, we generated cell lines with different levels of stable membrane expression of isoform 1 of CLEC2D. H69 and THP-1 cell lines over-expressing CLEC2D were generated using a lentiviral vector integrating the cDNA coding for dTomato and CLEC2D transmembrane isoform 1 under the ubiquitin promoter (Fig. 12A). The infected cells were sorted by cytometry according to their level of dTomato expression (Fig. 12B), subsequently their CLEC2D surface expression was verified by surface staining after expansion (Fig. 12C). CLEC2D being the ligand for CD161, the interaction between both partners could modulate their expression, as is seen for other surface receptors like GPCR, or the TCR(Utzny et al., 2006; von Zastrow, 2001). Thus, we cultured MAIT cell clone SMC3 with H69 cells expressing a high level of surface CLEC2D for 16h and analysed MAIT surface CD161 expression (Fig. 12D-E). We observed CD161 downregulation on the MAIT cell clone, and also observed the same phenomenon on primary T cells (Fig. 12F). The downregulation argues for an interaction between CD161 and CLEC2D, which would lead to CD161-initiated signalling, thereby initiating its internalisation.

8. CLEC2D expression on APCs modulates MAIT cell activation

To examine the effect of surface CLEC2D expression by APCs on MAIT cell cytokine secretion and proliferation, we used THP-1 and H69 cell lines with a different level of CLEC2D expression in Ag presentation assays with 5-OP-RU. MAIT cell clone SMC3 secreted lower amounts of IFN-γ when activated by THP-1 or H69 cell lines expressing a high level of CLEC2D on the surface, independently of the concentration of Ag used to activate them (Fig. 12G). The effect seems to be dependent on the CLEC2D level on the surface of APCs used, as THP-1 cells expressing less CLEC2D induce IFN-γ secretion more efficiently that THP-1 cells expressing more CLEC2D (Fig. 12H). This Inhibitory effect can be prevented by the addition of a polyclonal CLEC2D antibody, arguing for a cell to cell interaction between CLEC2D and its partner CD161 on MAIT cells.

We investigated the effect of CLEC2D expression on MAIT cell proliferation by co-culturing the SMC3 clone with H69 cells expressing high levels of CLEC2D and staining MAIT cells with a proliferation dye. After 6 days, we observed a decreased proliferation of the clones activated by CLEC2D overexpressing cells (Fig. 12J-K), whereas no differences were observed in the absence of Ag (Fig. 12K). This indicates that expression of CLEC2D on the surface of the APC reduces Ag-induced proliferation of MAIT cells.

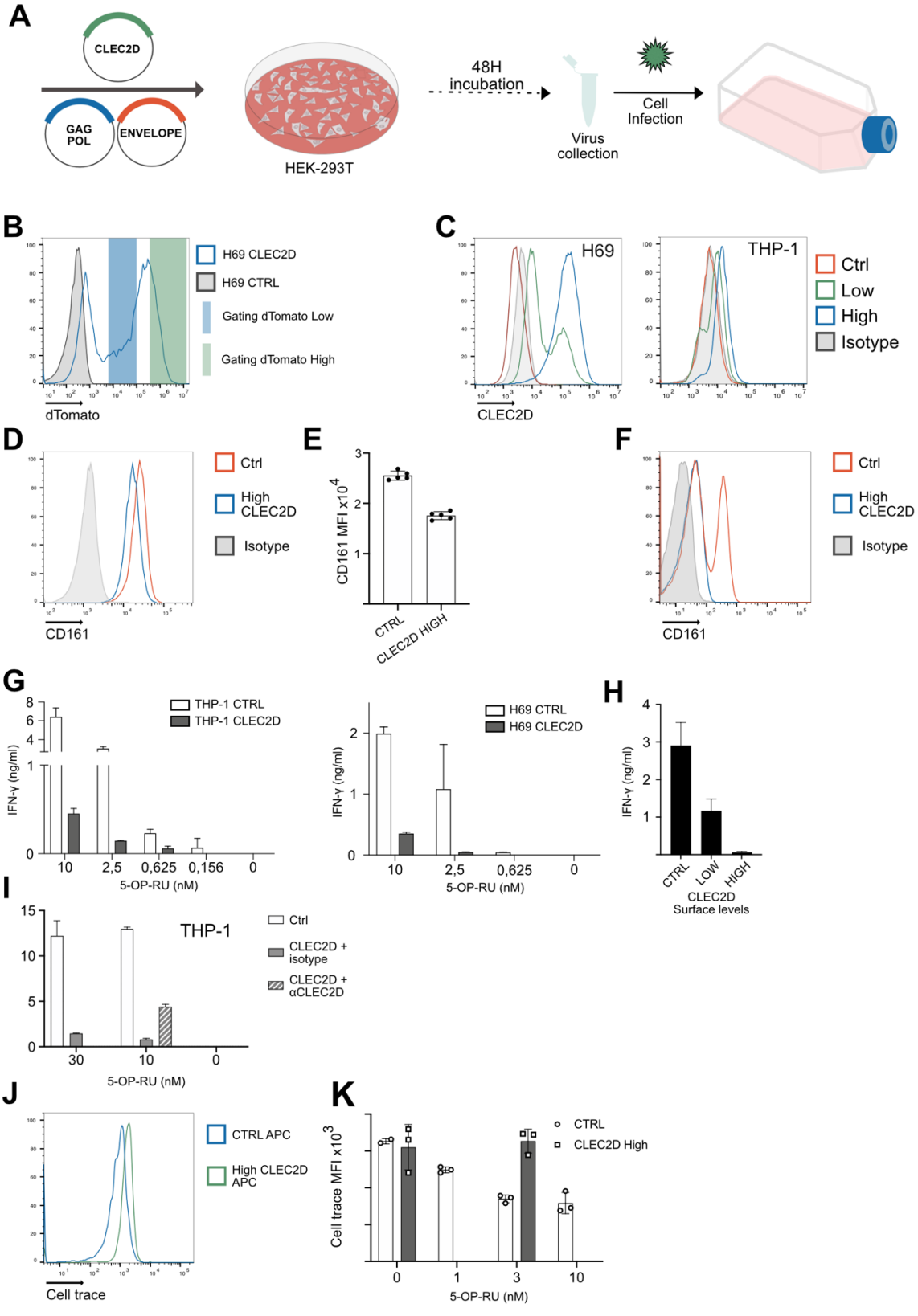
A
CLEC2D
GAG POL
ENVELOPE
HEK-293T
48H incubation
Virus collection
Cell Infection
B
H69 CLEC2D
H69 CTRL
Gating dTomato Low
Gating dTomato High
dTomato
C
H69
THP-1
Ctrl
Low
High
Isotype
CLEC2D
D
Ctrl
High CLEC2D
Isotype
CD161
E
CD161 MFI x10^4
CTRL
CLEC2D HIGH
F
Ctrl
High CLEC2D
Isotype
CD161
G
THP-1 CTRL
THP-1 CLEC2D
IFN-γ (ng/ml)
10
2,5
0,625
0,156
0
5-OP-RU (nM)
H69 CTRL
H69 CLEC2D
IFN-γ (ng/ml)
10
2,5
0,625
0
5-OP-RU (nM)
H
IFN-γ (ng/ml)
CTRL
LOW
HIGH
CLEC2D Surface levels
I
THP-1
Ctrl
CLEC2D + isotype
CLEC2D + αCLEC2D
30
10
0
5-OP-RU (nM)
J
CTRL APC
High CLEC2D APC
Cell trace
K
Cell trace MFI x10^3
CTRL
CLEC2D High
0
1
3
10
5-OP-RU (nM)

Figure 12. Modulation of MAIT cell function by CLEC2D expressed on antigen presenting cells.

(A) Schematic representation of the method used for the establishment of stable cell lines expressing CLEC2D on the surface. HEK-293T cell line was used to produce the lentiviral vector used to integrate CLEC2D isoform 1 and dTomato in H69 and THP-1 cells. (B) Flow cytometry histograms showing the expression of dTomato on H69 cells 3 days after infection, with the gating strategy used to generate H69 CLEC2D low (blue) and high (green); a similar strategy was used with THP-1 cells. (C) Flow cytometry histograms showing the expression of CLEC2D on the sorted cells 3 days after sorting, comparing the cells sorted for dTomato high, low and untransfected control. (D) Flow cytometry histograms displaying the downregulation of CD161 on MAIT cell clone SMC3 after overnight culture with H69 CLEC2D high cells (blue) compared to SMC3 cultured with H69 ctrl (red). (E) Mean fluorescence intensity (MFI) of 5 replicates of the experiment in (D) represented as bar plot. (F) Flow cytometry histograms displaying the downregulation of CD161 on CD3+ PBMCs after overnight culture with H69 CLEC2D high cells (Blue) compared to CD3+ PBMC after culture with H69 control (ctrl) cells (Red). (G) IFN-γ production by clone SMC3 in response to incubation with 5-OP-RU primed THP-1 (left) or H69 (right) cells overexpressing or not CLEC2D. (H) IFN-γ production by clone SMC3 in response to culture with THP-1 cells expressing different levels of CLEC2D, primed with 3 nM 5-OP-RU. (I) IFN-γ production by clone SMC3 in response to incubation with 5-OP-RU primed H69 cells overexpressing CLEC2D in presence of a CLEC2D blocking antibody (polyclonal goat, 2 µg/mL) or isotype control. (J) Flow cytometry histograms of cell trace red fluorescence on clone SMC3 6 days after activation with 3 nM 5-OP-RU, incubated with THP-1 cells overexpressing CLEC2D compared to control THP-1 cells. (K) MFI of independent wells in experiment (J) with indicated 5-OP-RU concentrations; overexpressing cells were only used with 3 nM and 0 nM of 5-OP-RU.

C. Discussion

The study presented here demonstrates that hepatocytes, LSECs, HSCs and BECs can present Ags to MAIT cells in a MR1-dependent manner, and are able to generate Ag from its non-antigenic precursor. Moreover, among all the non-immune liver resident cells, hepatocytes manifest the highest efficiency in Ag presentation to MAIT cells. We also observed that non-stimulatory MR1 ligands can prevent MAIT cell activation by liver-derived APCs. Moreover, the modulation of MAIT cell activation through CLEC2D over-expression revealed here constitutes a so far neglected aspect of MAIT cell physiology. Our findings are important for a better understanding of the role of MAIT cells both in liver physiology and in the pathogenesis of fibrosis. They are also relevant for the development of strategies to prevent the profibrogenic activity of MAIT cells in human liver.

We found that purified primary human cells present in the liver environment, namely hepatocytes, BECs, LSECs and HSCs, can specifically activate MAIT cells in an MR1-dependent manner, albeit to different degrees (Figs 6 and 7). To date, within the liver environment only BECs have been shown to present Ag to MAIT cells(Jeffery et al., 2016). Other hepatic cell types including hepatocytes, LSECs and HSCs were also reported to serve as liver-resident APCs but through non-MR1-mediated Ag presentation(Knolle, 2016). Hepatocytes were the strongest inducers of MAIT cell activation, requiring very low (picomolar) concentrations of the activating MAIT cell Ag, 5-OP-RU. The effect was MRI dependent and mildly potentiated by cytokines (Fig. 8) Importantly, our results demonstrate for the first time MR1-dependent MAIT cell activation by HSCs (Fig. 7H-L), providing functional significance to the previous finding of MR1 expression on HSCs(Hegde et al., 2018). In line with their ability to produce fibrogenic and proinflammatory cytokines, MAIT cells were shown recently to promote profibrogenic HSC activation(Böttcher et al., 2018; Hegde et al., 2018). Furthermore, a study performed in $MR1^{-/-}$ mice demonstrated that lack of MAIT cells is protective in mouse models of liver fibrosis(Hegde et al., 2018). In these studies, MAIT cells induced proliferation and collagen secretion by hepatic myofibroblasts, and directed macrophages towards a pro-inflammatory phenotype in vitro. Our results suggest that the interaction between HSCs and MAIT cells reciprocally potentiates pro-fibrotic properties of both cell types.

We also demonstrate MR1 expression as well as MAIT cell activation by LSECs (Figs 6D and 6J), which are in the immediate proximity of Ag-rich blood flowing through the sinusoids. The fenestrations in the layer of LSECs allow Ags also to reach hepatocytes, making our findings of efficient MR1-mediated Ag presentation by hepatocytes of potential physiological importance. We cannot exclude that cells contaminating our primary liver cell preparations contribute to the observed differences in APC activity. However, the procedures used for primary cell isolation and purification of the cells, with assessment by microscopy IF staining and cytometry, argue against this possibility (Fig. 7A-C). The protocol used for isolation of LSECs yields not only endothelial cells of sinusoidal origin but also endothelial cells originating from the liver vasculature, the latter possibly contributing to Ag presentation by LSECs to MAIT cells.

Studies on MAIT cell localization in normal human liver yielded divergent results(Böttcher et al., 2018; Hegde et al., 2018; Jeffery et al., 2016). The findings ranged from MAIT cells being either found exclusively in the sinusoidal space, to their predominant localisation within portal tracts(Hegde et al., 2018; Jeffery et al., 2016). Our results obtained by staining sections originating from livers lacking apparent histopathological abnormalities, using three different markers, indicate that MAIT cells are in a minority in the portal fields, with most of them localized dispersedly in the sinusoidal environment (Fig. 6). Thus, MAIT cells are in close contact with hepatocytes, LSECs (lining the surface of the sinusoids) and HSCs (residing in the space of Dissé between the hepatocytes and the LSECs), and also with BECs (forming the bile ducts within the portal fields). Our results argue for an extensive interaction potential of MAIT cells with abundant liver cell types, both in the sinusoidal and the portal environment, a property likely to have implications for both liver physiology and the pathogenesis of liver diseases.

We present evidence that all the primary liver cell types investigated generate active Ag 5-OP-RU in a dose-dependent manner when provided with the inactive precursor 5-A-RU (Fig. 9). As a signal corresponding to 5-A-RU was detected in the blood of “healthy” mice, i.e. not suffering from colitis or another condition disrupting integrity of the gut epithelium and/or endothelium, it is likely that bacterial metabolites produced in the gut regularly reach the

liver(Uchimura et al., 2018). Our analysis of chemical properties of the metabolite 5-A-RU further supports its diffusion through the gut epithelium (Fig. 9G). Moreover, very recent work has demonstrated that Ag sufficient for thymic selection of MAIT cells is derived from bacteria and therefore passes the gut epithelial and endothelial barriers(Legoux et al., 2019). The liver uptake of the 5-A-RU precursor and its in situ conversion to the active 5-OP-RU in the liver environment may be physiologically relevant, since stability of 5-OP-RU when not protected by binding to MR1 is very limited at body temperature(Corbett et al., 2014). 5-OP-RU is converted rapidly to 7-hydroxy-6-methyl-8-ribityl lumazine (RL-6-Me-7-OH) and 7-methyl-8-D-ribityllumazine (Fig. 5), and indeed a compound with a mass corresponding to RL-6-Me-7-OH was present in the dataset obtained for the mouse blood and liver(Uchimura et al., 2018). It remains to be determined whether 5-A-RU conversion to active 5-OP-RU occurs within liver cells or whether 5-OP-RU is generated by methylglyoxal released by the cells and then loaded onto MR1 present on the cell surface(McWilliam et al., 2016). Furthermore, this conversion might be influenced by the APCs metabolic state. Methylglyoxal is constantly produced in mammalian cells from lipid peroxidation and glycolysis, the latter being the principal source(Chaplen et al., 1998). Moreover, external signals can modulate methylglyoxal levels in cells, an interesting example being its increase induced by TNF signalling(Van Herreweghe et al., 2002). Consequently, the cells molecular microenvironment and energy consumption might modulate the pool of methylglyoxal available to react with 5-A-RU, thereby influencing its conversion to 5-OP-RU.

The findings that bacterial metabolites produced in the gut reach the circulation and the liver, where they may be converted to active Ag, suggest that MAIT cells present in the parenchyma are in a continuous low activation state. This is supported by high expression of activation and exhaustion markers CD38, CD39, PD-1, and TIM3 on liver MAIT cells(Böttcher et al., 2018; Hegde et al., 2018; Tang et al., 2013).

Thus, low level MAIT cell activation and upregulation of tissue residency markers such as CD69 may contribute to maintaining a constant pool of MAIT cells in the liver. The proliferative capacity of MAIT cells is lower than of conventional T cells, which is also reflected by our finding of a dispersed rather than clustered localization of MAIT in healthy liver (Fig. 6)(Dusseaux et al., 2011; Gutierrez-Arcelus et al., 2019).

The high frequency and dispersed distribution of MAIT cells in an alerted, “ready to act” state in liver tissue might protect the liver from incoming pathogens or increased amounts of microbial products. Antibacterial and immunomodulatory activity of MAIT cells has been clearly demonstrated by various studies of bacterial and viral infections(Le Bourhis et al., 2010, 2013; Loh, 2016).

A constant low activation of MAIT cells and their close contact with hepatocytes could also have implications for tissue homeostasis in the liver. Recent studies performed with MAIT cells isolated from gut, lung or blood have shown that activation of MAIT cells via their TCR, as opposed to cytokines, is associated with induction of a tissue-repair gene expression program(Hinks et al., 2019; Lamichhane et al., 2019; Leng et al., 2019). Consistently, MAIT cells were found to promote tissue repair either in vitro or in vivo in a mouse model of skin injury(Constantinides et al., 2019; Leng et al., 2019).

In contrast to “homeostatic” stimulation via TCR ligands, full (and potentially deleterious) activation of MAIT cells requires additional cytokine-mediated signaling(Hinks et al., 2019; Leng et al., 2019). Such a condition is likely to occur when higher amounts of microbial products enter the liver via the portal vein in the context of a disrupted gut epithelial and/or endothelial barrier. Human and mouse studies show that liver disease is coupled to alterations in the gut mucosa and gut dysbiosis(Henao-Mejia et al., 2012; Spadoni et al., 2015). In response to increased stimulatory signals derived from the gut, activated MAIT cells might enhance liver inflammation and contribute to immune-mediated liver pathologies, including liver fibrogenesis. Indeed, liver-derived MAIT cells produce large amounts of pro-inflammatory cytokines and the pro-fibrogenic cytokine IL-17 when stimulated by liver-residing APCs (Fig. 10C-D). This could be an important factor that initiates and/or perpetuates development of fibrosis.

It was shown that secretion of IL-17 by MAIT cells increases in response to IL-7 produced by hepatocytes under inflammatory conditions(Sawa et al., 2009; Tang et al., 2013). Our finding that hepatocytes act as strong APCs suggests that, under inflammatory conditions in a pathophysiological context, hepatocytes could activate MAIT cells and skew them towards an

IL-17 phenotype. The increased IL-7 secretion caused by cholic acid activation of Farnesoid X receptor on hepatocytes might increase this phenomenon, hence contributing to bile toxicity in chronic liver diseases(Jiang et al., 2018). It is also possible, that under conditions of liver inflammation the reported tissue repair activity of MAIT cells may be mis-regulated and contribute to the development of fibrosis.

We also considered TCR-independent alteration of MAIT cell activation. Although high expression of CD161 on the surface of MAIT cells is part of their definition, the functional effects of its abundant presence are largely unknown. Thus, we examined the consequences of binding of CD161 to its ligand CLEC2D (Fig. 12). By using two cell lines overexpressing CLEC2D on the surface as APCs, we could demonstrate the downregulation of CD161 on MAIT cells after co-culture (Fig. 12D-F). This downregulation, as it is seen for various other receptors including the TCR, might be part of negative regulatory mechanism, as the internalisation of CD161 could prevent further signalling. Moreover, APCs expressing high levels of CLEC2D induced less IFN-γ secretion by MAIT cells after TCR dependent activation (Fig. 12G). This effect was attenuated by the addition of a polyclonal CLEC2D Ab, hence confirming CLEC2D dependency (Fig. 12I). We could also show that the expression of CLEC2D diminished the activation-induced proliferation of MAIT cells (Fig. 12J-K). More experiments need to be conducted to confirm our findings and elucidate the underlying mechanisms as well as the *in vivo* implications. CLEC2D expression might protect APCs from MAIT cell cytotoxicity as is seen for NK cells(Aldemir et al., 2005). The interaction between CLEC2D and CD161 might function as checkpoint in a similar manner to PD1-PD1L, preventing overactivation of T cells; A major difference being that opposite to PD1, CD161 is constitutively highly present on the surface of MAIT cells, arguing for a role in steady states. The CLEC2D-CD161 axis represents a yet underexplored interesting aspect of MAIT cell biology with therapeutic potential regarding the implication of MAIT cells in human diseases.

With these considerations in mind, we explored possibilities for blocking MR1 with non-activating ligands and so preventing excessive MAIT cell activation in the liver in response to Ag presentation by abundant liver-derived APCs. We found that MAIT cell activation by Ag-exposed primary liver cells can be alleviated by pre-treating them with 6-FP or acetyl-6-FP, as well as the acetylsalicylic acid derivative 5-F-SA (Fig. 10). Of note, acetyl-6-FP and 3-F-SA (a compound with a similar characteristic to 5-F-SA), were previously shown to have an inhibitory effect on MAIT cells in a mouse model mimicking lung infection(Keller et al. 2017). Our findings corroborate the prospect of using inactive MR1 ligands as therapeutic agents to prevent involvement of MAIT cells in the fibrogenic process. The effectiveness of hepatocytes and other liver cells in presenting Ag to MAIT cells makes this approach of particular importance, both for anti-fibrotic treatment and for fibrosis prevention in patients at risk. Detailed mechanistic insights into hepatic MAIT cell activation are crucial because of their pro-fibrogenic properties. Our study reveals novel mechanisms of immune interactions in human liver and uncovers possible novel targets for immunotherapy.

IV. Aim n°2: MAIT cell characterization in NAFLD/NASH patients at single-cell level

A. Materials and Methods (Experimental procedures)

1. Tissue sample processing

Liver, colon and ileum biopsies were collected in a tube containing sterile RPMI. Small cylinders of liver tissue or colon biopsies were cut in small pieces in petri dishes with 1 mL of digestion medium (RPMI containing 200 IU/mL collagenase type IV, 100 IU/ml DNAse, 0,25µg/mL Amphotericin B). The pieces were then transferred into digestion medium pre-warmed at 37°C, using a sterile glass Pasteur pipette. The tube was then placed into the water bath at 37°C for 2 h and gently mixed every 20 minutes during the incubation. The cell suspension from the digested pieces was then flushed through a 40 µm cell strainer, and remaining tissue was further mechanically dissociated on the cell strainer using the piston of a 2 mL syringe. The cells in suspension were counted and 4% of cells were collected for cytometric analysis, the rest being frozen in FCS containing 10% DMSO.

2. PBMCs isolation and staining

Buffy coats for isolation of peripheral blood mononuclear cells (PBMCs) were obtained at the centre for blood donations in Basel. PBMCs were isolated by density gradient centrifugation on Ficoll (Lymphoprep®; Axonlab, Baden, Switzerland), using a standard protocol.4

Flow cytometry analysis

Mononuclear cells were washed in PBS and rinsed once in staining buffer (PBS with 0.5% human albumin and 3 mM sodium azide), then incubated 20 minutes in blocking buffer (50% human AB+ serum in staining buffer), followed by incubation in staining buffer containing the Ab cocktail. Data were acquired on the LSRFortessaTM (BD Biosciences, Allschwil, Switzerland) and analyzed with FlowJo 10.0.7 (TreeStar, Ashland (OR), USA). After excluding doublets and DAPI-, MAIT cells were identified as $CD3^{+}CD161^{high}Va7.2^{+}$.

3. Seq-well array synthesis

The protocol for array synthesis was provided to us by the laboratory of Prof. Shalek at MIT and can be found online (http://shaleklab.com).

Sylgard base was combined and mixed with Sylgard crosslinker at a 10:1 ratio creating the PDMS master mix. The master mix was put into vacuum at 0,3 atm for 20 minutes to remove air bubbles. 50 mL of the master mix were then injected into the mold, manufactured by FlowJEM according to the protocol, containing standard glass slides and the PDMS was cured at 70°C for 2,5 hrs.

The arrays were then removed from the mold, trimmed and washed with ethanol. The arrays were then treated in a Harrick PDC-002-HP plasma oven, with a high power air generated plasma at a 0,5 mBar for 5 minutes. The total surface of the array was then functionalized with 0.05% 3-aminopropyl-triethoxysilane APTES in 95% ethanol for 15 minutes, dried and further functionalized with p-phenylene diisothiocyanate (PDITC). The surface of the arrays was then functionalized with a 0.2% chitosan solution in water at room pressure, and later the inner part of the wells was modified with a 20 ug/mL aspartic acid solution at 0,3 atm.

4. Seq-well doublet rate estimation

After functionalization, the arrays were loaded with a mixture (1:1 ratio) of 4T1 cell lines expressing GFP or mCherry, kindly provided to us by Prof. N. Aceto, Department of Biomedicine, Basel. After sealing with a cover slide, the arrays were imaged by fluorescent microscopy and the number of wells containing either single or double fluorescent cells were counted.

B. Results

1. Establishment of a documented patient biobank

We generated a human tissue biobank from patients with NAFLD, alcoholic steatohepatitis (ASH), and autoimmune liver diseases as well as healthy control samples. For all included patients we collected serum, isolated PBMCs, and tissue resident lymphocytes from the liver and/or the colon. We obtained liver tissue from patients undergoing diagnostic liver biopsy or therapeutic liver resection at the University Hospital Basel or the University Medical Clinic in Liestal. Colon and ileum biopsies were collected from patients undergoing screening colonoscopies. Control liver tissue was obtained from healthy liver tissue surrounding surgically resected cancer metastasis. Anonymous clinical data including lab values and results from histopathological evaluation were collected for all patients. After cell isolation, we stained a small fraction of the cells for CD45, CD19, CD3, CD4, CD8, CD161, and TCR Vα7.2, allowing us to quantify and classify the MAIT cells in our samples.

We included 174 patients in our biobank, for 125 patients we collected PBMCs, serum and liver tissue, for 49 patients we collected PBMCs, serum, colon and ileum biopsies; some patients are included into both cohorts allowing MAIT cell characterization in 3 organs within the same patient (Fig. 13A). The staining of a fraction of each sample allows us to know the frequency of MAIT cells in the tissues of our patients, and to correlate this frequency with histopathological classification determined by the pathologists. We show that patients with NASH, ASH or autoimmune liver disease have significantly less MAIT cells in the circulation compared to control patients (Fig. 13B). Moreover, the MAIT cell frequency is diminished in the liver of patients with chronic liver inflammation (Fig. 13C). These findings are corroborating studies previously published on NAFLD and AIH(Böttcher et al., 2018; Jeffery et al., 2016). The same approach applied to our colon biopsy collection, with our preliminary analysis showing a decreased MAIT cell frequency in peripheral blood of NAFLD patients, but no differences in the colon and ileum between NAFLD patients and healthy control subjects. We also included histopathological scores into our analysis.

The frequency of MAIT cells in PBMCs and liver was significantly decreased in patients with higher fibrotic stages (Fig. 13E-F). When assessing MAIT cell frequency according to the inflammation score, we observed significantly decreased frequency of liver MAIT cells in patients with higher liver inflammation, the tendency being similar in peripheral blood but not reaching statistical significance. We evaluated the correlation between MAIT cell frequency and histologically assessed steatosis and observed a solid inverted correlation between MAIT cell frequency in the liver and the level of steatosis (Fig. 13I), this relation being less evident in the circulation (Fig. 13J). Taken together, these preliminary results suggest a decrease in MAIT cell frequency along with the disease progression, as shown in previous work(Böttcher et al., 2018; Hegde et al., 2018). This might be due to infiltration of other T cells, or MAIT cell apoptosis; the staining of our biobank with a broader panel should give more clues concerning the mechanism behind this change.

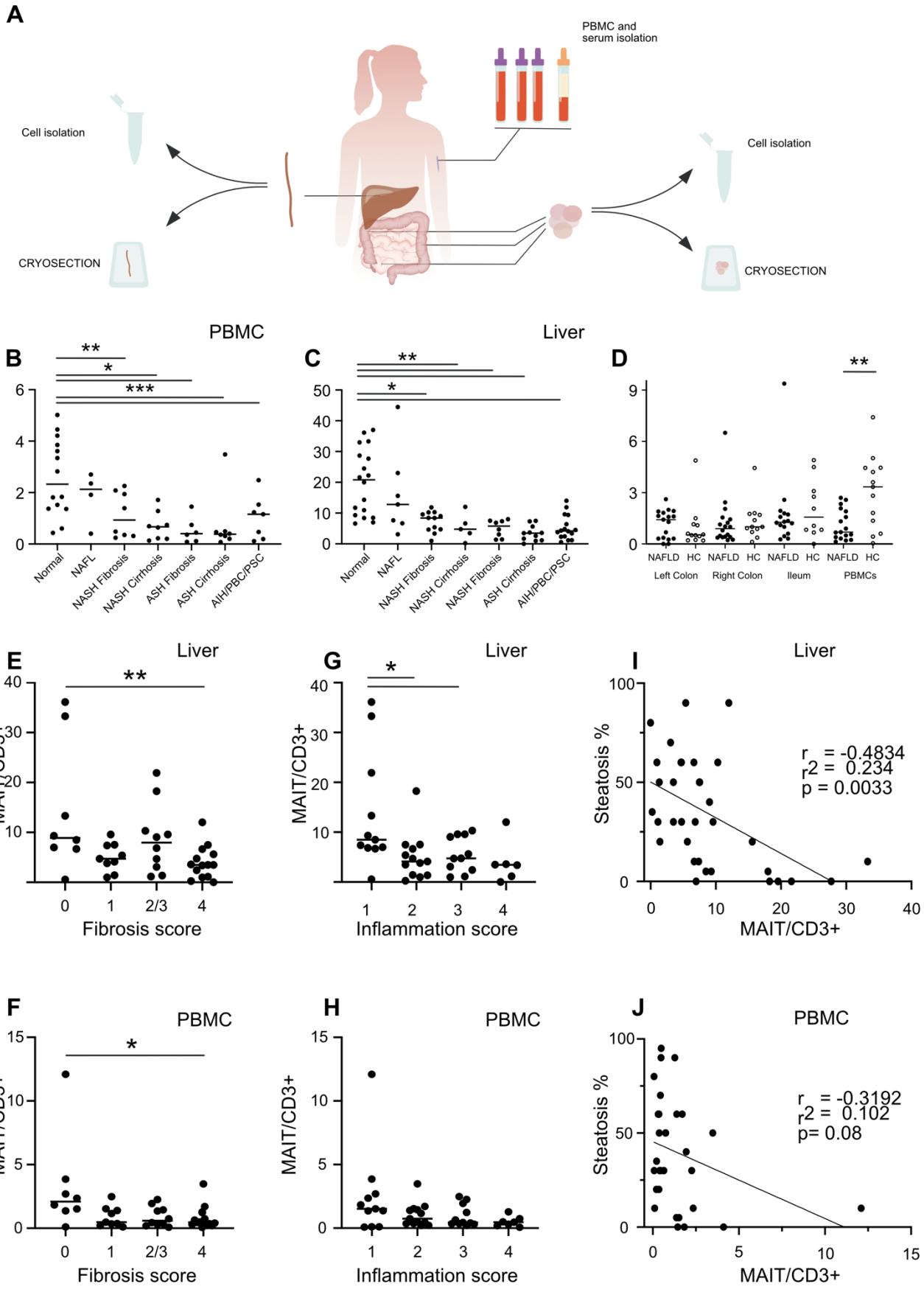
A
PBMC and serum isolation
Cell isolation
CRYOSECTION
Cell isolation
CRYOSECTION
B
PBMC
C
Liver
D
Normal
NAFL
NASH Fibrosis
NASH Cirrhosis
ASH Fibrosis
ASH Cirrhosis
AIH/PBC/PSC
NAFLD HC NAFLD HC NAFLD HC NAFLD HC
Left Colon
Right Colon
Ileum
PBMCs
E
Liver
MAIT/CD3+
Fibrosis score
G
Liver
Inflammation score
I
Liver
Steatosis %
MAIT/CD3+
r = -0.4834
r2 = 0.234
p = 0.0033
F
PBMC
Fibrosis score
H
PBMC
Inflammation score
J
PBMC
Steatosis %
MAIT/CD3+
r = -0.3192
r2 = 0.102
p= 0.08

Figure 13. Generation and analysis of a patient tissue biobank.

(A) Schematic representation of sample collection of patients undergoing liver biopsy or screening colonoscopy. Patients included the liver study are enrolled at time of diagnostic biopsy and donate a liver biopsy part that is used for cell isolation and embedded for cryosectioning. Patients included into the colon study are enrolled at the time of screening colonoscopy and donate ileal, left and right colon biopsies used for cell isolation and embedded for cryosectioning. The patients also donate blood which is used for PBMC and serum isolation. (B) MAIT cell frequency among CD3+ cells in PBMCs of patients with various liver diseases as a function of the histopathological diagnosis (NAFL: Non-alcoholic fatty liver; NASH: Non-alcoholic steatohepatitis; ASH: Alcoholic steatohepatitis; AIH: Autoimmune hepatitis; PBC: Primary biliary cholangitis; PSC: Primary sclerosing cholangitis). (C) MAIT cell frequency among CD3+ cells in liver of patient with various liver diseases and different fibrotic stages. (D) MAIT cell frequency among CD3+ cells in different tissues/tissue locations from patients with non-alcoholic fatty liver disease (NAFLD) versus healthy control (HC) subjects. (E) MAIT cell frequency in the liver of patients with AIH, alcoholic liver disease (ALD), PBC, PSC, or NAFLD, according to the histological fibrosis score; 0: no fibrosis, 1: portal fibrosis 2: Portal fibrosis with few septa 3: portal fibrosis with many septa and bridging, 4: cirrhosis. (F) MAIT cell frequency in PBMCs of patients as in previous figure. (G) MAIT cell frequency in the liver of patients allocated according to the histological inflammation score; 1: minimal, 2: mild, 3: middle and 4: strong. (H) MAIT cell frequency in PBMCs of patients allocated according to the same liver histological inflammation score (I) Pearson correlation between MAIT cell frequency in the liver and the degree of steatosis in the liver of patients with ALD, NAFLD or HC subjects. (J) Pearson correlation between MAIT cell frequency in PBMCs and the degree of steatosis in the liver of patients with ALD, NAFLD or HC subjects. MAIT cell frequencies were evaluated by flow cytometry among CD3+ lymphocytes. Statistical significance was assessed by unpaired Student test for all figures except I and J.

2. Establishment of Seq-well

In order to sequence some representative samples of our biobank at single cell level we established in our lab the Seq-well method developed by the laboratory of Prof. Shalek at the MIT (Fig. 14). The method is based on the trapping of cells in microwells with RNA capturing beads. The use of a semi-permeable membrane at one face of the well allows buffer exchange and *in situ* cell lysis. We generated Seq-well arrays by pouring and curing Polydimethylsiloxane (PDMS) on a silicon wafer support imprinted with the negative mask of the 40 µm nanowells. The process generated regular 40 µm wells as confirmed by bright field microscopy (Fig. 14A). After surface functionalization we could seal the arrays with polycarbonate membranes allowing sequestration of cells, beads and later RNA on one hand, and buffer exchange on the other. By using a 1:1 mixture of cell lines expressing GFP and mCherry we could evaluate the cell doublet rate for different cell array ratios (Fig. 14B). Our results suggest that our doublet rate corresponds to the one published previously and fits the standard of commercially available methods. The observed capturing efficiency was 25%, again in line with published results, which is sufficient for us to recover enough cells from our patient samples (Fig. 14C).

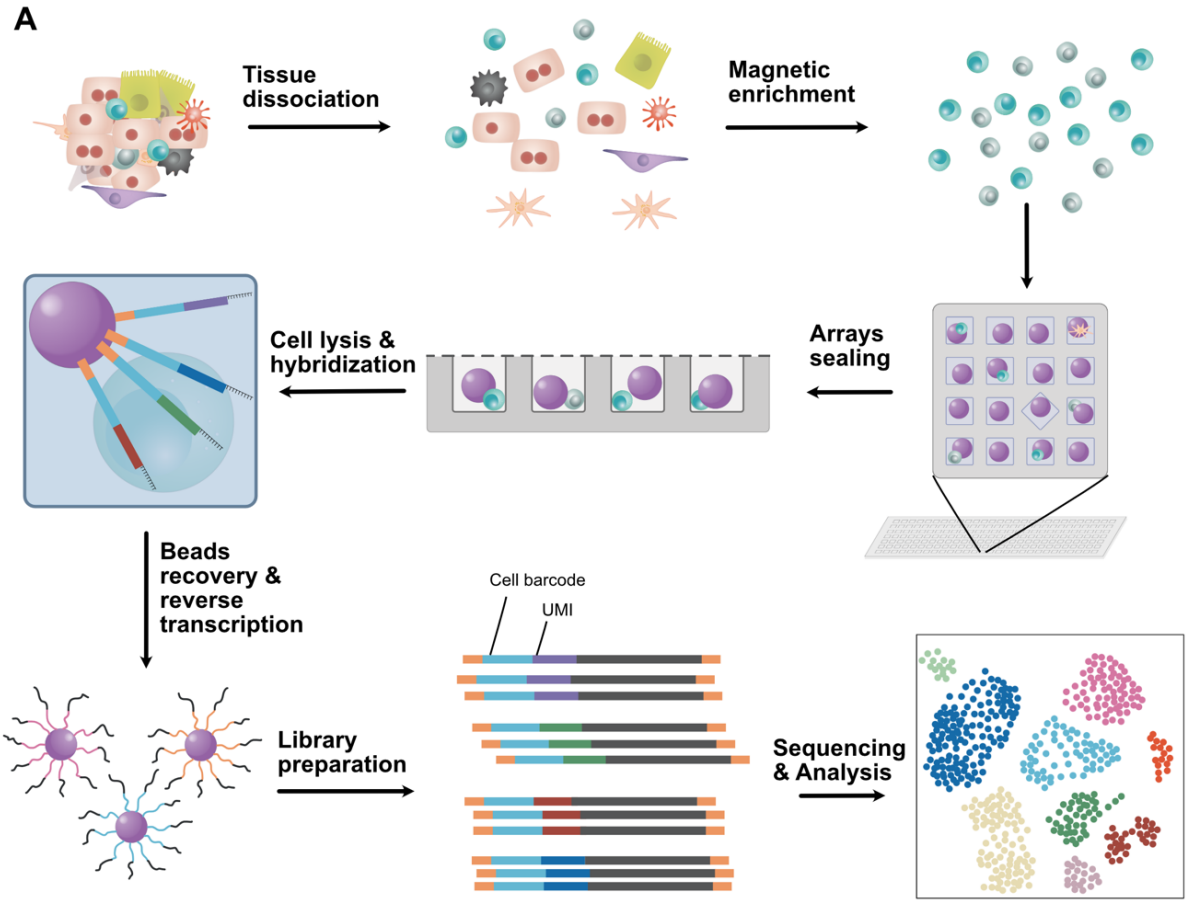

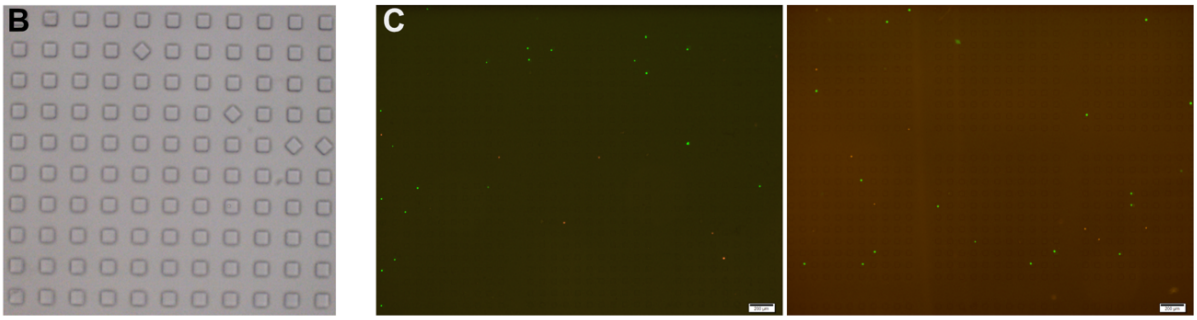

D

Number of cells loaded on the array	10 000	20 000
Number GFP positive wells	138	476
Number mCherry positive wells	83	257
Doublet rate	<1%	0,023
Capturing efficiency	0.23	0.43

Figure 14. Seq-well establishment

(A) Schematic representation of the Seq-well method workflow. Each RNA-capturing bead is bearing multiple unique oligo with a UMI (Unique molecular identifiers) allowing to retrieve the number of capture molecule for every sequence and a cell barcode unique to each bead, but shared by all the attached oligo allowing to assign all sequences to the cell of origin. At the free end all oligos bear a poly-T sequence for RNA capturing by pairing with poly-A.

(B) Bright field microscopy picture showing the regular square shaped wells generated in the laboratory. (C) Two representative fluorescent microscopy pictures showing arrays loaded with a mixture of GFP+ and mCherry+ cells used for the doublet rate evaluation. (D) Summary table depicting the doublet rates and capturing efficiencies obtained when arrays were loaded with either 10 000 or 20 000 cells.

C. Discussion

We have established a biobank of 175 patients from which we have serum, isolated PBMCs, isolated tissue cells and tissue cryosections available. The use of a minor fraction of the cells to characterize the tissues by flow cytometry confirms that regarding the MAIT cell frequencies the samples fit with published data(Böttcher et al., 2018; Hegde et al., 2018; Jeffery et al., 2016). Moreover, we can observe correlations between MAIT cell frequencies in blood and tissue and disease severity (Fig. 13). To date we have not proceeded to sample analysis, but we have established all required methods and staining panels. The establishment of Seq-well in our lab will permit us to sequence RNA at single cell level of tissue and circulating MAIT cells from 50 samples originating from approximately 10 NASH patients and 5 healthy control subjects. The high cell capturing efficiency added to the numerous recovered transcripts associated to this method will improve data accuracy (Fig. 14). The establishment of negative selection-based magnetic enrichment for resident memory T cells allows us to increase the proportion of MAIT cells in the specimens before sequencing (Fig. 9). Furthermore, by sequencing cells from colon, liver and peripheral blood of the same patient we will interrogate both localization- mediated differential gene expression and disease associated alterations. The biobank will then allow us to assess the changes observed in transcripts at the protein level by cytometry, and *in situ* by IF microscopy. In parallel, in the laboratory we are studying the microbiota from the patients from which we obtain colon samples. To avoid the bias associated with stool microbiota sequencing, we use tissue biopsies taken during the endoscopy on which we apply 16S rRNA sequencing. This will allow us to assess whether changes in intestinal microbiome parallel changes in MAIT cell phenotype in patients with NAFLD. All findings will then be correlated to clinical parameters. The histological and serological data will allow us to not only challenge our findings regarding the patient diagnosis but also regarding the disease severity. This multiparameter methodology should allow us to better understand the pathophysiology of NAFLD, and to detect variations of subpopulations of MAIT cells associated with it. Moreover, this will increase the understanding of MAIT cell function and regulation in healthy and diseased subjects.

V. General conclusion

The initial part of our work presents a broad analysis of the activation of intrahepatic MAIT cells by liver cells in a MR1-dependent manner. We also explored the capacity of liver cells in the metabolism of converting inactive Ag precursor into its effective form. We observed that hepatocytes, BECs, HSCs, and LSECs all express MR1 on the surface. We determined for the first time that these primary liver cell types can present Ag to MAIT cells and established that hepatocytes are the most efficient non-professional APCs for MAIT cells in the liver. This capacity was proven using bacterial lysate and pure synthetic Ag. Moreover, we assessed for the first time the potential of primary cells to condensate 5-A-RU, the Ag precursor, with methylglyoxal to form the active 5-OP-RU. We demonstrated that all primary cells tested can generate 5-OP-RU, when provided with 5-A-RU, without addition of exogenous methylglyoxal. These findings are of particular relevance regarding the high abundance of MAIT cells in the liver and their significance in liver diseases(Böttcher et al., 2018; Hegde et al., 2018). Our data demonstrate that MAIT cells can interact with any liver resident cell, hence any MAIT cell in the liver is virtually surrounded by APCs. Moreover, the capacity of liver cells to generate Ag from its precursor sustains the hypothesis that MAIT cells are constantly activated by low levels of active Ags. This is particularly interesting regarding the recent report suggesting that TCR activated MAIT cells exert tissue repair functions in the colon and the skin. To date, no study addressing the liver in this context has been published, however the pro-fibrogenic role of MAIT cells found in some diseases could be an exaggerated pathological side of this function(Constantinides et al., 2019; Hegde et al., 2018; Leng et al., 2019). This effect is missing when the cells are co-stimulated with cytokines. Together these findings suggest that both the abundance of Ags and the nature of the co-stimulation are crucial to modulate MAIT cell function. Pro-inflammatory molecules can typically reach the liver in case of a leaky endothelial barrier in the intestine, this leaky gut might consequently switch MAIT cell function from tissue healing to tissue damage(Llorente and Schnabl, 2015). In this context it seems imperative to approach MAIT cell physiology in a global perspective. Our preliminary investigation on the function of CLEC2D expression by APCs is aimed towards this goal. We found that CLEC2D can downregulate CD161, thus questioning results from studies that are using high CD161 expression as definition for MAIT cells in a situation where CLEC2D could be

highly upregulated, e.g. viral infection(Oa et al., 2019; Satkunanathan et al., 2014). We also observed that the surface expression of CLEC2D diminishes MAIT cell proliferation and IFN-γ secretion, highlighting the CD161-CLEC2D interaction as an underestimated regulator of MAIT cell activity. Further work is required in the lab to verify our initial findings and study the reciprocity and the signals involved in this interaction. How this interaction guides MAIT cells towards tissue repair or other effector functions remains unknown and is of great interest in further studies.

Taken together, the evidence produced in this first part of our work demonstrates two things: In the liver MAIT cells are surrounded by MR1-sufficient interacting partners, and MAIT cell Ag is potentially constantly diffusing and generated *in situ*. This raises the possibility that MAIT cell phenotype could be altered in disorders in which Ag abundance and the molecular milieu are distorted, like NAFLD. Comparing liver and blood MAIT cells in NAFLD patients and healthy control subjects is the ambition of our second study. We collected a large biobank of patient material and quantified the amount of MAIT cells in the samples by sacrificing only a very small fraction of the samples. Now that we established the Seq-well method, we will generate transcriptomic data on several representative patient and control sampes at single cell level. This should allow us to identify disease- and tissue-associated changes at the population level, that we can later assess by flow cytometry on the rest of the biobank. These findings will then be combined with localization data of MAIT cells in the liver thanks to the use of patient tissue cryosections that we are currently analyzing. This study, by the combination of an unbiased approach in multiple tissues, reinforced by functional examination, should allow us to better understand the underling pathophysiology and the implication of MAIT cells in NAFLD.

VI. Submitted manuscript

The following manuscript has been submitted in 2019. Except for the second figure, all figures and conclusions were included in the thesis. The exception concerning figure 2 is motivated given that the data were generated by the group of Prof. P. Klenerman, our collaborators in Oxford.

Robust MAIT cell activation by primary human liver cells: Implications for liver physiology and disease

Martin Lett[1]*, Hema Mehta[2]*, Adrian Keogh[3], Tina Jaeger[1], Marie-Anne Meier[4,5], Isabel Fofana[4], Otto Kollmar[6], Urs Duthaler[7], Markus Heim[4,5], Paul Klenerman[2,8], Deborah Stroka[3], Magdalena Filipowicz Sinnreich[1, 9]

[1] Liver Immunology, Department of Biomedicine, University Hospital Basel and University of Basel, Switzerland
[2] Peter Medawar Building for Pathogen Research, University of Oxford, UK
[3] Clinic of Visceral Surgery and Medicine, University Hospital Bern, Department of Biomedical Research, University of Bern, Switzerland
[4] Hepatology, Department of Biomedicine, University Hospital Basel and University of Basel, Switzerland
[5] Division of Gastroenterology and Hepatology, Clarunis, University Center for Gastrointestinal and Liver Diseases, Basel, Switzerland
[6] Division of Visceral Surgery, Clarunis, University Center for Gastrointestinal and Liver Diseases, Basel, Switzerland
[7] Clinical Pharmacology, Department of Biomedicine, University Hospital Basel and University of Basel, Switzerland
[8] Oxford NIHR Biomedical Research Centre, The John Radcliffe Hospital, Oxford, UK
[9] Department of Gastroenterology and Hepatology, Basel University Medical Clinic, Liestal, Switzerland

* These authors contributed equally to the manuscript

Key words: MR1, bacterial metabolites, gut-liver axis, hepatocytes, liver fibrosis

Corresponding author:
Magdalena Filipowicz Sinnreich, MD, PhD
Liver Immunology
Department of Biomedicine
University Hospital Basel
Hebelstrasse 20
4031 Basel
Switzerland
tel +41 61 328 77 89 / fax +41 61 265 53 52
email: magdalena.filipowicz@unibas.ch

List of Abbreviations:

5-A-RU: 5-amino-6-D-ribitylaminouracil; 5-F-SA: 5-formyl-salicylic acid; RL-6-Me-7-OH: 7-Hydroxy-6-methyl-8-ribityl lumazine; 5-OP-RU: 5-(2-oxopropylideneamino)-6-D-ribitylaminouracil; 6-FP: 6-Formylpterin; Ab: antibody; Ag: antigen; APC: antigen presenting cell; BEC: biliary epithelial cell; CFU: colony forming unit; HSC: hepatic stellate cell; IFN-γ: interferon gamma; IF: immunofluorescence; IL: Interleukin; LB: lysogenic broth; LC: liquid chromatography; LSEC: liver sinusoidal endothelial cell; MAIT: mucosal-associated invariant T cell; MHC: major histocompatibility complex; MR1: MHC class I-related protein 1; MS: mass spectrometry; NEAA: non-essential amino acids; NPCs: non-parenchymal cells; PBMCs: peripheral blood mononuclear cells; PFA: para-formaldehyde; PHA: phyto-hemagglutinin; P/S: Penicillin/Streptomycin; RT: room temperature; TCR: T cell receptor; TIMP: tissue inhibitor of metalloproteinase; TNF-α: tumor necrosis factor alpha.

Financial support

Financial support for this study has been granted by grants to M.F.S. from the Goldschmidt-Jacobson Stiftung and the Swiss National Science Foundation (SNSF; grant number PZ00P3_167828), and by grants Wellcome Trust 109965MA, NIHR Biomedical Research Centre, Oxford, and NIHR Senior Fellowship to P.K.

Conflict of interest statement

The authors declare to have no conflict of interest.

Abstract

Background & Aims: Mucosal-associated invariant T (MAIT) cells are the most abundant T cell type in human liver. They respond to bacterial metabolites presented by MHC-like molecule MR1 on Ag-presenting cells (APCs). Activated liver MAIT cells are described as fibrogenic and MAIT cells from patients with liver cirrhosis show functional alterations consistent with pro-fibrotic activity. However, it remains unclear which liver cells are involved in MAIT cell activation and how their fibrogenic activity can be prevented. Likewise, little is known about the role of liver cells in the metabolism of bacterial MAIT cell antigens (Ags). *Approach & Results:* In our immunofluorescence analysis of human liver tissue, MAIT cells localized dispersedly in the liver parenchyma in the proximity of different liver cells. Human primary hepatocytes, hepatic myofibroblasts/stellate cells, liver endothelial cells and biliary epithelial cells were able to present Ags to blood- and liver-derived MAIT cells, with hepatocytes being the most efficient. Presentation was MR1-dependent and occurred in response to bacterial lysate and pure synthetic Ag 5-OP-RU. MAIT cell activation was prevented by non-activating MR1 ligands 6-formylpterin and acetylsalicylic acid-derivative 5-formyl-salicylic acid. Liver cells exposed to the bacterial Ag precursor had the capacity to generate active 5-OP-RU endogenously, as determined by mass spectrometry. *Conclusions:* The ability of different liver cells to act as APCs and their potential to generate active MAIT cell Ag provide new insights into the understanding of intrahepatic MAIT cell activation. The interaction between hepatic stellate cells and MAIT cells, and the production of pro-fibrotic cytokine IL-17 by MAIT cells, support a role for these cells in the development of fibrosis. Repression of MAIT cell activation by non-stimulatory MR1 ligands creates an opportunity to design anti-fibrotic therapies.

Mucosal-associated invariant T (MAIT) cells are the most abundant population of innate-like T cells in humans; they comprise up to 5% of T cells in peripheral blood and are found in high numbers in the liver and mucosal tissues.(1-3) Unlike conventional T cells, which recognize Ags presented by major histocompatibility complex (MHC) class I or II molecules, MAIT cells are restricted to the highly conserved MHC-class I related molecule MR1.(2) They express a semi-invariant T cell receptor (TCR) containing the Vα7.2 variable chain (Vα7.2-Jα33/12/20) paired with an oligoclonal TCRβ repertoire.(2, 4) MAIT cells recognize MR1-bound metabolites of the riboflavin (vitamin B2) biosynthesis pathway produced by many pathogenic and commensal bacteria.(2, 5, 6) The most potent stimulatory MAIT cell Ag is the pyrimidine 5-(2-oxopropylideneamino)-6-D-ribitylaminouracil (5-OP-RU). It is formed by non-enzymatic condensation of the bacteria-derived precursor 5-amino-6-ribitylaminouracil (5-A-RU) with methylglyoxal derived from the glycolysis pathway.(7) Upon specific TCR activation, MAIT cells rapidly secrete pro-inflammatory cytokines like interferon gamma (IFN-γ) and tumour necrosis factor alpha (TNF-α) and acquire potent killing capacity; they consequently exert important immunoregulatory and antimicrobial functions.(8, 9) MAIT cells are further characterized by high cell-surface expression levels of C-type lectin CD161, interleukin-18 receptor (IL-18R) and IL-12R. Thus they can be activated by respective cytokines in a TCR-independent manner.(1, 10-12) These features of MAIT cells generate protective innate immunity before an adaptive immune response has formed.

MAIT cells constitute up to 40% of T cells residing in human liver,(1, 3, 13, 14) indicating their importance in liver physiology and in the pathogenesis of liver diseases. Liver MAIT cells secrete large amounts of IFN-γ, TNF-α and, importantly, IL-17. Secretion of the latter follows repetitive IL-12 stimulation or occurs in response to IL-7, a cytokine produced by hepatocytes under inflammatory conditions.(13-17) IL-17 acts as a fibrogenic cytokine that activates hepatic

stellate cells (HSCs) and induces a pro-fibrotic state.(18) The aforementioned cytokine expression profile suggests a detrimental role of MAIT cells in liver inflammation and fibrogenesis. This notion is supported by a recent study with an $MR1^{-/-}$ mouse model in which the lack of MAIT cells protected against liver fibrosis, and by reports that MAIT cells from patients with liver cirrhosis show alterations consistent with pro-fibrotic activity.(16, 17)

Apart from the locally produced endogenous cytokines, the liver also receives cytokines and bacterial products originating from the gut and the systemic circulation via the portal vein and the liver artery. In addition, bacterial products may enter the liver via the biliary tree. Their responsiveness to bacterial products places MAIT cells at a central position in the immunological gut-liver axis, a notion supported by the finding that biliary epithelial cells (BECs) present *Escherichia coli*-derived Ag to MAIT cells.(14) Furthermore, in a study in mice colonized by *E. coli*, a compound with a molecular mass corresponding to the MAIT cell Ag precursor 5-A-RU was detected in the circulation, suggesting that 5-A-RU is able to cross the intestinal barrier.(19) This is also supported by a recent mouse study showing that MAIT cell Ag passes from mucosal surfaces to the thymus, where it induces development of MAIT cells.(20) These studies suggest that Ag exposure of MAIT cells may occur in the sinusoidal environment, including the subendothelial space of Dissé, where HSCs acting as main drivers of liver fibrogenesis are located.(18) It has been proposed that various hepatic parenchymal and non-parenchymal cell types act as liver-resident APCs, mainly for MHC class I/II and CD1d-dependent Ag-presentation.(14, 21) However, it has not yet been investigated whether cells from the sinusoidal environment, including hepatocytes, HSCs and liver sinusoidal endothelial cells (LSECs), i.e. cells that are in direct contact with the blood entering via the portal vein, can present metabolite Ags to MAIT cells.

In this present study, we show the localization of MAIT cells within the human liver and characterize cellular interactions of human liver-derived primary cells with MAIT cells. We demonstrate important differences in the capacity of liver-derived APCs to present stimulatory Ag to MAIT cells, with hepatocytes being the most efficient. Further, we characterize the capacity of human liver cells to generate active MAIT cell Ag from exogenously provided bacterial precursor. We demonstrate that MAIT cell activation by liver APCs can be blocked by non-stimulatory ligands binding to MR1. This creates a therapeutic opportunity to interfere with the pro-fibrogenic activity of MAIT cells.

Materials and Methods

Resources used are listed in Supplementary Table 1 (reagents), Table 2 (cell lines) and Table 3 (antibodies). Further details of resources and methods not described in the main text are in the Supplementary data file.

Preparation of primary cells from human samples

Primary liver cells were prepared from liver samples from patients undergoing liver resection at the University Hospitals in Basel and Bern. Written informed consent was obtained from each patient included in the study. The study protocol conforms to the ethical guidelines of the 1975 Declaration of Helsinki, and was approved by the local ethics committee (Ethikkommission Nordwestschweiz; EKNZ; permit number EKNZ BASEC 2016-01188). Human hepatocytes were isolated from fresh liver tissue according to a published protocol.(22) For the isolation of HSCs, LSECs and BECs, and the maintenance and characterisation of all primary cell types by microscopy and/or flow cytometry, see the Supplementary data file.

Immunofluorescence staining of human liver sections

Cryopreserved human liver biopsy samples from the biobank at the Department of Biomedicine (Basel, Switzerland, ethics approval EKNZ BASEC 2016-01188) were used in this study. For patient details and staining procedures, see Supplementary Table 4 and the Supplementary data file.

Cell lines and MAIT cell clones

For details, see the Supplementary data file. All cell lines and MAIT cell clones used were routinely tested for mycoplasma contamination.

Generation of liver-derived MAIT cell lines

Non-parenchymal cells (NPCs) obtained from normal liver tissue samples of two patients undergoing surgery for colorectal cancer metastasis were used to generate two liver-derived

MAIT cell lines, designated MAIT-BEL-10 and MAIT-BSL-19. The NPC fraction was obtained after perfusion of the liver wedge with “collagenase buffer” (684 mM NaCl, 13 mM KCl, 3 mM Na_2PO_4 $2H_2O$, 125 mM HEPES, 25 mM $CaCl_2$; pH 7.4; containing 200 IU/ml collagenase type IV), and low speed centrifugation to deplete hepatocytes (see details in the Supplementary data file). Liver-associated mononuclear cells were isolated by density gradient centrifugation on Ficoll. MAIT cells were then FACS-sorted based on expression of CD3 and staining by MR1 Tetramer and expanded by stimulation with phytohemagglutinin (PHA) and human IL-2 (100 IU/ml) in the presence of irradiated peripheral blood mononuclear cells (PBMCs) (40 Gray) as feeder cells. T cells were maintained in RPMI 1640 medium supplemented with 5% AB^+ human serum, IL-2 (100 IU/ml), Penicillin/Streptomycin (100 IU/ml; P/S), L-glutamine, pyruvate and non-essential amino acids (NEAA).

MAIT cell enrichment strategy

To enrich for MAIT cells, $CD8^+$ cells were isolated by positive selection using the Miltenyi positive selection kit (purity ≥85%), or a negative selection panel composed of Abs against CD45RA, CD62L, CD19, CD14, CD36 and TCRγδ was used. This allowed for depletion of naïve T cells, B cells, monocytes, dendritic cells, platelets and γδ T cells.

Preparation of bacterial products and synthetic MAIT cell Ag

The preparation of fixed bacteria or bacterial lysate and of synthetic Ag 5-OP-RU is described in the Supplementary data file.

Ag presentation assays

Details of Ag presentation assays are described in the Supplementary data file. To perform blocking experiments, cells were incubated with Ag and the corresponding blocking Abs (10 ng/ml anti-MR1, 5 µg/ml anti-IL-12 or 4 µg/ml anti-IL-18) were added after 1 h, followed by a 1-h incubation step before the addition of MAIT cells. To test the blocking potential of non-

activating MR1 ligands, 6-formylpterin (6-FP; 50 µM), acetyl-6-FP (5 µM) or 20 - 100 µM 5-formyl-salicylic acid (5-F-SA) was added 1 h before the addition of 5-OP-RU.

Statistical analysis

Unless indicated otherwise, all graphs presented in the figures represent data from three or more independent experiments. Exact numbers of repetitions are indicated in the figure legends. Unless indicated otherwise, values plotted in the graphs are means ± SD. All statistical analyses were performed in GraphPad Prism7. Analysis of statistical significance was conducted with the tests specified in the figure legends.

Results

MAIT cells are dispersed within the parenchyma in healthy human liver

We investigated whether MAIT cells are present in the sinusoidal environment of the liver, where they might be activated by contact with parenchymal and non-parenchymal cells that potentially function as liver APCs capable of presenting gut-derived bacterial Ags. We analysed, by immunofluorescence (IF) staining, human liver samples from 8 donors, lacking significant hepatic histopathological abnormalities (see Supplementary Table 4). MAIT cells were identified as cells positive for CD3, TCR Vα7.2 and IL-18Rα, a robust combination of markers as IL-18Rα parallels high CD161 expression on MAIT cells.(9) MAIT cells localized dispersedly to the parenchymal space in the liver (Fig. 1A and Supplementary Fig. 1A-B). They were found in or in the immediate proximity of the sinusoids, occasionally also within the portal fields. There was no zonal distribution that would confine MAIT cells to either of the three zones of the hepatic lobule. Our analysis, indicating that MAIT cells represent 8-33% of total liver T cells (Fig. 1B), confirmed that MAIT cells are highly abundant in human liver, considerably exceeding the frequency of Vα7.2-positive conventional T cells. Their proximity to parenchymal and non-parenchymal cells within the sinusoidal environment is likely to facilitate interaction of MAIT cells with liver cells taking up bloodborne liver-directed Ags.

Liver cell lines demonstrate a limited capacity to activate MAIT cells

Given the observation that MAIT cells reside dispersedly within the liver, both in the sinusoidal environment and occasionally within the portal fields, we next investigated their ability to interact *in vitro* with different liver parenchymal and non-parenchymal cell lines. We tested hepatoma cell lines HepG2 and Huh7, HSC lines TWNT-4 and LX-2, LSEC cell line TMNK-1 and BEC line H69. Using HepG2 and Huh7 cells, we stimulated MAIT cells ($CD8^{+}CD161^{++}Vα7.2^{+}$; Supplementary Fig. 2A) with riboflavin-synthesizing *E. coli*. We observed no IFN-γ or activation marker CD69 expression in MAIT cells co-cultured with either HepG2 or Huh7 cells exposed to a low concentration of *E. coli* (corresponding to 1.5e7

CFU/ml). In contrast, robust expression of both markers was found in response to the conventional APC cell line THP-1 used as control (Fig. 2A). Stimulation of MAIT cells by HepG2 or Huh7 cells exposed to higher CFUs of *E. coli* resulted in increased expression of CD69 but no marked IFN-γ or TNF-α production (Fig. 2B and Supplementary Fig. 2B).

Weak MAIT cell activation by HSC line TWNT-4 in response to *E. coli* was similar to that seen with the hepatoma cell lines (Fig. 2C-D). HSC line LX-2 also did not induce MAIT cell activation in response to *E. coli* lysate, as evidenced by the lack of IFN-γ secretion by MAIT cells (Supplementary Fig. 2D). In contrast to the hepatoma and HSC lines, LSEC cell line TMNK-1 activated MAIT cells in response to *E. coli*, though induction of IFN-γ and TNF-α was lower than that seen with THP-1 cells (Fig. 2C-D and Supplementary Fig. 2C). MAIT cell activation by LSEC cell line TMNK-1 was both MR1- and cytokine-dependent (Fig. 2E). Finally, when incubating BEC H69 cells with serial dilutions of *E. coli* lysate (Supplementary Fig. 2D), we found that these cells present Ag in an MR1-restricted manner. All liver-derived cell lines, except LX-2, responded to some extent to pure stimulatory Ag 5-OP-RU (Figs 2A, 2C and Supplementary Fig. 2E). Taken together, the results demonstrate that different types of liver-derived cell lines differ in their ability, in general limited, to activate MAIT cells via an MR1-restricted pathway.

Robust MAIT cell activation by primary human liver cell subsets

Given the Ag presentation differences seen in cell line experiments, we next investigated the stimulatory potential of primary cells isolated from human liver tissue. We isolated hepatocytes, BECs, hepatic myofibroblasts/HSCs and LSECs from surgically removed liver specimens and verified the identities of the cell populations by FLOW CYTOMETRY and/or microscopy (Supplementary Fig. 3A-C). All of these cell types represent potential non-professional APCs unique to the liver environment. Importantly, we observed MR1 expression in primary human

hepatocytes, which at approximately 60% constitute the main liver cell population, but also in BECs, LSECs and HSCs (Fig. 3A and Supplementary Fig. 3D).

Primary hepatocytes, when incubated with *E. coli* lysate, activated MAIT cell clone SMC3 in an MR1-dependent manner as shown by IFN-γ secretion (Fig. 3B) and upregulation of MAIT cell activation markers CD69, CD137 and PD-1 (Fig. 3C). Increased degranulation assessed by CD107a surface staining and TCR downregulation provided further evidence for T cell activation (Fig. 3C and Supplementary Fig. 4A). K562-MR1 human myeloid leukaemia cells stably transfected with a β2M-MR1 construct, and thus overexpressing MR1, were used as positive control APCs (Figs 3B and 3F). The results of robust MAIT cell activation by hepatocytes acting as APCs were confirmed using pure synthetic Ag 5-OP-RU instead of the *E. coli* lysate (Fig. 3D and Supplementary Fig. 4B).

HSCs are the main drivers of fibrogenesis in the liver, efficiently producing proteins involved in extracellular matrix formation upon activation.(18) As MAIT cells were recently linked to liver fibrosis,(16, 17) we asked whether HSCs are able to directly activate MAIT cells. Using primary HSCs as APCs and treating them with either the *E. coli* lysate or 5-OP-RU, we demonstrated MR1-dependent activation of MAIT cells measured by IFN-γ secretion (Fig. 3E-F) and expression of activation markers CD69, CD25 and CD137, as well as TCR downregulation (Supplementary Fig. 4C). We also tested the ability of blood-derived FACS-sorted MAIT cells to induce pro-fibrotic genes in HSCs upon stimulation with Ag and found a fibrogenic response (data not shown). This observation is in line with recent published findings.(16, 17) Taken together, the results implicate direct interaction between HSCs and MAIT cells as a factor contributing to the mechanism of their fibrogenic activity.

MR1-expressing primary cell populations of BECs and LSECs were also able to present *E. coli*-derived and synthetic 5-OP-RU Ag to MAIT cells (Figs 3G and 4A). In summary, the data presented here demonstrate that cells from the sinusoidal environment in the liver, as well as BECs, have a capacity to present bacteria-derived and pure Ag to MAIT cells.

Hepatocytes are the most efficient non-professional Ag-presenting cells to MAIT cells in the liver

We found marked differences in presentation capacity between the investigated cell types, with hepatocytes being the most efficient liver-derived APCs (Fig. 4A-B and Supplementary Fig. 5A-B), as assessed by the pure Ag or bacterial lysate concentration needed to reach an EC50 of IFN-γ production by MAIT cell clone SMC3. The killing capacity of the SMC3 clone differed depending on the APC used for stimulation (Supplementary Fig. 6A). Differences in the liver APC-induced activation of MAIT cells in the presence of Ag persisted when either IL-12 or IL-18 was blocked (Fig. 4C-D and Supplementary Fig. 5C-D). Inclusion of exogenous IL-12 or IL-18 increased MAIT cell activation, a known effect synergistic with TCR-dependent stimulation.(10, 23) The effect decreased upon addition of blocking antibodies against the respective cytokines, thus confirming the blocking effectiveness (Supplementary Fig. 5E-F and data not shown). Taken together, our results demonstrate robust MR1-dependent Ag presentation capabilities of intrahepatic cell types, most prominently hepatocytes, leading to the activation of MAIT cells.

Primary liver cells generate active MAIT cell Ag when provided with its precursor

In view of the strong intrahepatic interactions involving MAIT cells, we investigated whether liver APCs can generate active MAIT cell-stimulatory Ag endogenously. It has been reported that the Ag precursor 5-A-RU is not able to bind to MR1 and activate MAIT cells.(7) However, we found that exposure of liver APCs (hepatocytes, BECs, LSECs) to 5-A-RU for 2 or 5 h led to MAIT cell activation (Fig. 5A-B), suggesting that the activatory 5-OP-RU is formed by the

liver APCs. Liquid chromatography tandem mass spectrometry (LC-MS/MS) analysis of cell culture supernatants following exposure of different liver-derived primary APCs to 5-A-RU corroborated these findings. To standardize the system, we incubated THP-1 cells with 5-A-RU (Supplementary Fig. 7). We detected time-dependent accumulation of 5-OP-RU (and decay at later time points) by selected reaction monitoring (Supplementary Fig. 7). Importantly, MS analysis indicated that all tested primary liver cell types generated 5-OP-RU in a dose-dependent manner when provided with the precursor 5-A-RU (Fig. 5C). Collectively, these results demonstrate that primary liver cell subtypes can form active MAIT cell Ag when provided with the precursor 5-A-RU. This indicates that the process of activation of liver MAIT cells, encompassing both production of specific Ag molecules and their presentation by nearby liver APCs, can occur in a local liver environment.

5-A-RU conversion to active Ag *in vivo* in liver depends upon 5-A-RU crossing the intestinal barrier. Indeed, a compound with a molecular mass corresponding to the MAIT cell Ag precursor 5-A-RU was detected in the circulation and liver of mice.(19) To assess the probability of 5-A-RU crossing an intact intestinal barrier, we performed *in silico* modelling by applying a published method that uses a combination of physico-chemical parameters.(24, 25) Applying this method to the Ag 5-OP-RU and its precursor 5-A-RU, we found that of these two chemically very similar compounds the precursor has a higher probability of intestinal absorption than the active 5-OP-RU product (Supplementary Fig. 8).

The degree of activation of polyclonal blood- and liver-derived MAIT cells varies with the APC

To investigate whether the findings for the MAIT cell clone SMC3 apply to primary polyclonal MAIT cell populations, we isolated and tested MAIT cells from human peripheral blood and liver tissue. Starting with PBMCs, which contain 2-5% MAIT cells, negative magnetic bead selection using Abs against CD45RA, CD62L, CD19, CD14, CD36 and TCRγδ, depleted naïve

T cells, B cells, monocytes, dendritic cells, platelets and γδ T cells, resulting in four- to sevenfold enrichment for MAIT cells (data not shown). Activation of the enriched polyclonal MAIT cells was assessed upon exposure to Ag-loaded primary liver cells. TCR expression was downregulated in response to distinct liver-derived APCs exposed to 5 nM 5-OP-RU, with hepatocytes again being the most potent APCs (Fig. 6).

To assess activation of polyclonal liver-derived MAIT cells, we generated two liver MAIT cell lines (MAIT-BEL-10 and MAIT-BSL-19) from two patient donors. Both cell lines produced IFN-γ and IL-17 and showed upregulation of several activation markers, including CD107a and CD137, in response to different human liver-derived APCs exposed to synthetic 5-OP-RU, including hepatocytes, BECs and HSCs (Figs 6B-C and 6E, and data not shown). Presentation capacity differed between the liver APCs, as assessed by IFN-γ secretion and upregulation of activation markers by the MAIT-BEL-10 and MAIT-BSL-19 cells (Figs 6B and 6E). To mimic an inflammatory context in which increased amounts of bacterial products and inflammatory cytokines reach the liver, the synthetic Ag in some experiments was spiked into *E. coli* lysate (Fig. 6D and Supplementary Fig. 6B and Supplementary Videos). In this state, hepatocytes remained as efficient APCs (Fig. 6D) and this was paralleled by cytotoxicity elicited by liver-derived MAIT cell line MAIT-BSL-19 (Fig. 6B and Supplementary Videos). Thus, as a proof of concept, we demonstrated that hepatocytes can be killed *in vitro* following Ag-mediated activation of liver-derived MAIT cells. Taken together, our experiments demonstrate that human polyclonal MAIT cells derived from peripheral blood and liver respond to Ag presentation by different liver cells, most prominently hepatocytes.

Inhibition of liver APC-mediated MAIT cell activation by small molecules

To approach the prevention of MAIT cell activation in the liver, we explored the blocking of MR1 occupancy with non-activating MR1 ligands. 6-formylpterin (6-FP), derived from the folate degradation pathway, and acetyl-6-FP are known to bind MR1 but do not activate MAIT

cells.(5, 26) We found that MAIT cell activation by Ag-exposed primary liver cells (hepatocytes, BECs and HSCs) can be prevented in a dose dependent manner by pre-treating the liver cells with 6-FP or acetyl-6-FP (Fig. 7A-B). Other molecules, e.g. the acetylsalicylic acid derivative 5-formyl-salicylic acid (5-F-SA), were found previously to stabilize MR1 on the cell surface; however, they did not stimulate Jurkat T cells overexpressing the MAIT TCR.(26) MAIT cell activation by liver APCs was prevented by 5-F-SA (Fig. 7B). This indicates that liver APC-induced MAIT cell activation can be inhibited by small molecular-weight compounds that specifically interfere with MR1 activity on the surface of APCs.

Discussion

Here we present results of a comprehensive analysis of the activation of intrahepatic MAIT cells by liver cells, in a process mediated by MR1-bound bacterial Ags. We also examined the role of liver cells in the metabolism of bacterial Ags activating MAIT cells. We found that many primary liver cell types, most prominently hepatocytes, can present Ag to MAIT cells and that liver cells can generate active MAIT cell Ag when provided with its natural precursor molecule. We also observed that non-stimulatory MR1 ligands can prevent MAIT cell activation by liver-derived APCs. Our findings are important for a better understanding of the role of MAIT cells in liver physiology and in the pathogenesis of fibrosis. They are also relevant for the development of strategies to prevent the profibrogenic activity of MAIT cells in human liver.

We found that purified primary human cells present in the liver environment, namely hepatocytes, BECs, LSECs and HSCs, can specifically activate MAIT cells in an MR1-dependent manner, albeit to different degrees (Figs 3 and 4). To date, only BECs within the liver environment have been shown to present Ag to MAIT cells.(14) Other hepatic cell types including hepatocytes, LSECs and HSCs were also reported to serve as liver-resident APCs but through non-MR1-mediated Ag presentation.(21) Hepatocytes were the strongest inducers of MAIT cell activation, requiring very low (picomolar) concentrations of the activating MAIT cell Ag, 5-OP-RU. The effect was MRI dependent and mildly potentiated by cytokines (Fig. 4 and Supplementary Fig. 5). Importantly, our results demonstrate for the first time MR1-dependent MAIT cell activation by HSCs (Fig. 3E-F and Supplementary Fig. 4C), providing functional significance to the previous finding of MR1 expression on HSCs.(16) In line with their ability to produce fibrogenic and proinflammatory cytokines, MAIT cells were shown recently to promote profibrogenic HSC activation.(16, 17) Furthermore, a study performed in $MR1^{-/-}$ mice demonstrated that lack of MAIT cells is protective in mouse models of liver fibrosis.(16) In these studies, MAIT cells induced proliferation and collagen secretion by

hepatic myofibroblasts, and directed macrophages towards a pro-inflammatory phenotype *in vitro*. Our results suggest that the interaction between HSCs and MAIT cells reciprocally potentiates pro-fibrotic properties of both cell types.

We also demonstrate MR1 expression as well as MAIT cell activation by LSECs (Fig. 3A and 3G), which are in the immediate proximity of Ag-rich blood flowing through the sinusoids. The fenestrations in the layer of LSECs allow Ags also to reach hepatocytes, making our findings of efficient MR1-mediated Ag presentation by hepatocytes of potential physiological importance. We cannot exclude that cells contaminating our primary liver cell preparations contribute to the observed differences in APC activity. However, the procedures used for primary cell isolation and purification of the cells, with assessment by microscopy and IF staining, argue against this possibility. The protocol we used for isolation of LSECs yields not only endothelial cells of sinusoidal origin but also endothelial cells originating from the liver vasculature, the latter possibly contributing to Ag presentation by LSECs to MAIT cells. Notably, we showed that the LSEC-derived TMNK-1 cells and BEC H69 cells grown in culture were able to present Ag in an MR1-restricted manner to MAIT cells (Fig. 2 and Supplementary Fig. 2). Generally, the established cell lines, particularly hepatoma and stellate cell lines, were found to be less efficient in Ag presentation assays than primary cells.

Studies on MAIT cell localization in normal human liver yielded divergent results.(14, 16, 17) The findings ranged from MAIT cells being either found exclusively in the sinusoidal space, (16) to their predominant localisation within portal tracts.(14) Our results obtained by staining sections originating from livers lacking apparent histopathological abnormalities, using three different markers, indicate that MAIT cells are in a minority in the portal fields, with most of them localized dispersedly in the sinusoidal environment (Fig. 1 and Supplementary Fig. 1).

Thus, MAIT cells are in close contact with hepatocytes, LSECs (lining the surface of the sinusoids) and HSCs (residing in the space of Dissé between the hepatocytes and the LSECs), and also with BECs (forming the bile ducts within the portal fields). Our results argue for an extensive interaction potential of MAIT cells with abundant liver cell types, both in the sinusoidal and the portal environment, a property likely to have implications for both liver physiology and the pathogenesis of liver diseases.

We present evidence that all the primary liver cell types investigated generate active Ag 5-OP-RU in a dose-dependent manner when provided with the inactive precursor 5-A-RU (Fig. 5). As a signal corresponding to 5-A-RU was detected in the blood of “healthy” mice, i.e. not suffering from colitis or another condition disrupting integrity of the gut epithelium and/or endothelium,(19) it is likely that bacterial metabolites produced in the gut regularly reach the liver. Our analysis of chemical properties of the metabolite 5-A-RU further supports its diffusion through the gut epithelium (Supplementary Fig. 8). Moreover, very recent work has demonstrated that Ag sufficient for thymic selection of MAIT cells is derived from bacteria and therefore passes the gut epithelial and endothelial barriers.(20) The liver uptake of the 5-A-RU precursor and its *in situ* conversion to the active 5-OP-RU in the liver environment may be physiologically relevant, since stability of 5-OP-RU when not protected by binding to MR1 is very limited at body temperature.(7) 5-OP-RU is converted rapidly to 7-hydroxy-6-methyl-8-ribityl lumazine (RL-6-Me-7-OH) and 7-methyl-8-D-ribityllumazine (Supplementary Fig. 7A), and indeed a compound with a mass corresponding to RL-6-Me-7-OH was detected in the dataset obtained for the mouse blood and liver.(19) It remains to be determined whether 5-A-RU conversion to active 5-OP-RU occurs within liver cells or whether 5-OP-RU is generated by methylglyoxal released by the cells and then loaded onto MR1 present on the cell surface.(27)

The findings that bacterial metabolites produced in the gut reach the circulation and the liver, where they may be converted to active Ag, suggest that MAIT cells present in the parenchyma are in a continuous low activation state. This is supported by high expression of activation and exhaustion markers CD38, CD39, PD-1, and TIM3 on liver MAIT cells.(13, 16, 17) Thus low level MAIT cell activation and upregulation of tissue residency markers such as CD69 may contribute to maintaining a constant pool of MAIT cells in the liver. The proliferative capacity of MAIT cells is lower than of conventional T cells,(1, 28) which is also reflected by our finding of a dispersed rather than clustered localization of MAIT in healthy liver (Fig. 1 and Supplementary Fig. 1). The high frequency and dispersed distribution of MAIT cells in an alerted, “ready to act” state in liver tissue might protect the liver from incoming pathogens or increased amounts of microbial products. Antibacterial and immunomodulatory activity of MAIT cells has been clearly demonstrated by various studies of bacterial and viral infections.(9, 11, 29)

A constant low activation of MAIT cells and their close contact with hepatocytes could also have implications for tissue homeostasis in the liver. Recent studies performed with MAIT cells isolated from gut, lung or blood have shown that activation of MAIT cells via their TCR, as opposed to cytokines, is associated with induction of a tissue-repair gene expression program.(30-32) Consistently, MAIT cells were found to promote tissue repair either *in vitro* (30) or *in vivo* in a mouse model of skin injury.(33)

In contrast to “homeostatic” stimulation via TCR ligands, full (and potentially deleterious) activation of MAIT cells requires additional cytokine-mediated signaling.(30, 31) Such a condition is likely to occur when higher amounts of microbial products enter the liver via the

portal vein in the context of a disrupted gut epithelial and/or endothelial barrier. Human and mouse studies show that liver disease is coupled to alterations in the gut mucosa and gut dysbiosis.(34-36) In response to increased stimulatory signals derived from the gut, activated MAIT cells might enhance liver inflammation and contribute to immune-mediated liver pathologies, including liver fibrogenesis. Indeed, liver-derived MAIT cells produce large amounts of pro-inflammatory cytokines and the pro-fibrogenic cytokine IL-17 when stimulated by liver-residing APCs (Fig. 6B-D). This could be an important factor that initiates and/or perpetuates development of fibrosis. It was shown that secretion of IL-17 by MAIT cells increases in response to IL-7 produced by hepatocytes under inflammatory conditions.(13, 15) Our finding that hepatocytes act as strong APCs suggests that, under inflammatory conditions in a pathophysiological context, hepatocytes could activate MAIT cells and skew them towards an IL-17 phenotype. It is also possible, that under conditions of liver inflammation the reported tissue repair activity of MAIT cells may be mis-regulated and contribute to the development of fibrosis.

An additional consequence of MAIT cell activation may be the development of a potential to kill liver APCs, including hepatocytes. Indeed, our results suggest that direct killing of hepatocytes by activated MAIT cells may be an additional factor contributing to the pathogenesis of liver diseases (Supplementary Fig. 6 and Supplementary Videos).

With these considerations in mind, we explored possibilities for blocking MR1 with non-activating ligands and so preventing excessive MAIT cell activation in the liver in response to Ag presentation by abundant liver-derived APCs. We found that MAIT cell activation by Ag-exposed primary liver cells can be alleviated by pre-treating them with 6-FP or acetyl-6-FP, as well as the acetylsalicylic acid derivative 5-F-SA (Fig. 7). Of note, acetyl-6-FP and 3-F-SA (a

compound with a similar characteristic to 5-F-SA), were previously shown to have an inhibitory effect on MAIT cells in a mouse model mimicking lung infection.(26) Our findings corroborate the prospect of using inactive MR1 ligands as therapeutic agents to prevent involvement of MAIT cells in the fibrogenic process. The effectiveness of hepatocytes and other liver cells in presenting Ag to MAIT cells makes this approach of particular importance, both for anti-fibrotic treatment and for fibrosis prevention in patients at risk. Detailed mechanistic insights into hepatic MAIT cell activation are crucial because of their pro-fibrogenic properties. Our study reveals novel mechanisms of immune interactions in human liver and uncovers possible novel targets for immunotherapy.

Acknowledgements

We are grateful to the patients who agreed to donate biological material for research purposes. We acknowledge the surgeons and pathologists who helped in obtaining spare material from liver resections. We thank Prof. G. De Libero for sharing the MAIT cell clone SMC3 as well as the β2M-MR1 construct and Prof. M. Cella for sharing the MR1 Ab hybridoma (clone 26.5). We thank Prof. S. L. Friedman, Prof. D. Jefferson, and Prof. N Kobayashi for providing us with cell lines. We acknowledge the NIH Tetramer Core Facility, Emory University, Atlanta, GA, USA, for providing us with MR1-tetramer. The MR1 tetramer technology was developed jointly by Dr. James McCluskey, Dr. Jamie Rossjohn, and Dr. David Fairlie, and the material was produced by the NIH Tetramer Core Facility as permitted to be distributed by the University of Melbourne.

References

1. Dusseaux M, Martin E, Serriari N, Peguillet I, Premel V, Louis D, Milder M, et al. Human MAIT cells are xenobiotic-resistant, tissue-targeted, CD161hi IL-17-secreting T cells. Blood 2011;117:1250-1259.
2. Le Bourhis L, Mburu YK, Lantz O. MAIT cells, surveyors of a new class of antigen: development and functions. Curr Opin Immunol 2013;25:174-180.
3. **Billerbeck E**, **Kang YH**, Walker L, Lockstone H, Grafmueller S, Fleming V, Flint J, et al. Analysis of CD161 expression on human CD8+ T cells defines a distinct functional subset with tissue-homing properties. Proc Natl Acad Sci U S A 2010;107:3006-3011.
4. Lepore M, Kalinichenko A, Colone A, Paleja B, Singhal A, Tschumi A, Lee B, et al. Parallel T-cell cloning and deep sequencing of human MAIT cells reveal stable oligoclonal TCRbeta repertoire. Nat Commun 2014;5:3866.
5. Kjer-Nielsen L, Patel O, Corbett AJ, Le Nours J, Meehan B, Liu L, Bhati M, et al. MR1 presents microbial vitamin B metabolites to MAIT cells. Nature 2012;491:717-723.
6. Tastan C, Karhan E, Zhou W, Fleming E, Voigt AY, Yao X, Wang L, et al. Tuning of human MAIT cell activation by commensal bacteria species and MR1-dependent T-cell presentation. Mucosal Immunol 2018;11:1591-1605.
7. **Corbett AJ**, **Eckle SB**, **Birkinshaw RW**, **Liu L**, Patel O, Mahony J, Chen Z, et al. T-cell activation by transitory neo-antigens derived from distinct microbial pathways. Nature 2014;509:361-365.
8. **van Wilgenburg B**, **Scherwitzl I**, Hutchinson EC, Leng T, Kurioka A, Kulicke C, de Lara C, et al. MAIT cells are activated during human viral infections. Nat Commun 2016;7:11653.
9. Le Bourhis L, Martin E, Peguillet I, Guihot A, Froux N, Core M, Levy E, et al. Antimicrobial activity of mucosal-associated invariant T cells. Nat Immunol 2010;11:701-708.
10. **Ussher JE**, **Bilton M**, Attwod E, Shadwell J, Richardson R, de Lara C, Mettke E, et al. CD161++ CD8+ T cells, including the MAIT cell subset, are specifically activated by IL-12+IL-18 in a TCR-independent manner. Eur J Immunol 2014;44:195-203.
11. Loh L, Wang Z, Sant S, Koutsakos M, Jegaskanda S, Corbett AJ, Liu L, et al. Human mucosal-associated invariant T cells contribute to antiviral influenza immunity via IL-18-dependent activation. Proc Natl Acad Sci U S A 2016;113:10133-10138.
12. **Jo J**, **Tan AT**, Ussher JE, Sandalova E, Tang XZ, Tan-Garcia A, To N, et al. Toll-like receptor 8 agonist and bacteria trigger potent activation of innate immune cells in human liver. PLoS Pathog 2014;10:e1004210.
13. **Tang XZ**, **Jo J**, **Tan AT**, **Sandalova E**, Chia A, Tan KC, Lee KH, et al. IL-7 licenses activation of human liver intrasinusoidal mucosal-associated invariant T cells. J Immunol 2013;190:3142-3152.

14. **Jeffery HC**, **van Wilgenburg B**, Kurioka A, Parekh K, Stirling K, Roberts S, Dutton EE, et al. Biliary epithelium and liver B cells exposed to bacteria activate intrahepatic MAIT cells through MR1. J Hepatol 2016;64:1118-1127.
15. Sawa Y, Arima Y, Ogura H, Kitabayashi C, Jiang JJ, Fukushima T, Kamimura D, et al. Hepatic interleukin-7 expression regulates T cell responses. Immunity 2009;30:447-457.
16. Hegde P, Weiss E, Paradis V, Wan J, Mabire M, Sukriti S, Rautou PE, et al. Mucosal-associated invariant T cells are a profibrogenic immune cell population in the liver. Nat Commun 2018;9:2146.
17. Bottcher K, Rombouts K, Saffioti F, Roccarina D, Rosselli M, Hall A, Luong T, et al. MAIT cells are chronically activated in patients with autoimmune liver disease and promote profibrogenic hepatic stellate cell activation. Hepatology 2018;68:172-186.
18. Gao B, Friedman SL, Mehal Z: The immunopathogenesis of cirrhosis. In: Liver Immunology: Principles and Practice: Springer, 2014; 413-424.
19. **Uchimura Y**, **Fuhrer T**, **Li H**, Lawson MA, Zimmermann M, Yilmaz B, Zindel J, et al. Antibodies Set Boundaries Limiting Microbial Metabolite Penetration and the Resultant Mammalian Host Response. Immunity 2018;49:545-559 e545.
20. Legoux F, Bellet D, Daviaud C, El Morr Y, Darbois A, Niort K, Procopio E, et al. Microbial metabolites control the thymic development of mucosal-associated invariant T cells. Science 2019.
21. Knolle PA. Staying local-antigen presentation in the liver. Curr Opin Immunol 2016;40:36-42.
22. Portmann S, Fahrner R, Lechleiter A, Keogh A, Overney S, Laemmle A, Mikami K, et al. Antitumor effect of SIRT1 inhibition in human HCC tumor models in vitro and in vivo. Mol Cancer Ther 2013;12:499-508.
23. Turtle CJ, Delrow J, Joslyn RC, Swanson HM, Basom R, Tabellini L, Delaney C, et al. Innate signals overcome acquired TCR signaling pathway regulation and govern the fate of human CD161(hi) CD8alpha(+) semi-invariant T cells. Blood 2011;118:2752-2762.
24. Lipinski CA, Lombardo F, Dominy BW, Feeney PJ. Experimental and computational approaches to estimate solubility and permeability in drug discovery and development settings. Adv Drug Deliv Rev 2001;46:3-26.
25. Martin YC. A bioavailability score. J Med Chem 2005;48:3164-3170.
26. Keller AN, Eckle SB, Xu W, Liu L, Hughes VA, Mak JY, Meehan BS, et al. Drugs and drug-like molecules can modulate the function of mucosal-associated invariant T cells. Nat Immunol 2017;18:402-411.

27. McWilliam HE, Eckle SB, Theodossis A, Liu L, Chen Z, Wubben JM, Fairlie DP, et al. The intracellular pathway for the presentation of vitamin B-related antigens by the antigen-presenting molecule MR1. Nat Immunol 2016;17:531-537.
28. Gutierrez-Arcelus M, Teslovich N, Mola AR, Polidoro RB, Nathan A, Kim H, Hannes S, et al. Lymphocyte innateness defined by transcriptional states reflects a balance between proliferation and effector functions. Nat Commun 2019;10:687.
29. **Le Bourhis L**, **Dusseaux M**, Bohineust A, Bessoles S, Martin E, Premel V, Core M, et al. MAIT cells detect and efficiently lyse bacterially-infected epithelial cells. PLoS Pathog 2013;9:e1003681.
30. **Leng T**, **Akther HD**, **Hackstein CP**, Powell K, King T, Friedrich M, Christoforidou Z, et al. TCR and Inflammatory Signals Tune Human MAIT Cells to Exert Specific Tissue Repair and Effector Functions. Cell Rep 2019;28:3077-3091 e3075.
31. Hinks TSC, Marchi E, Jabeen M, Olshansky M, Kurioka A, Pediongco TJ, Meehan BS, et al. Activation and In Vivo Evolution of the MAIT Cell Transcriptome in Mice and Humans Reveals Tissue Repair Functionality. Cell Rep 2019;28:3249-3262 e3245.
32. Lamichhane R, Schneider M, de la Harpe SM, Harrop TWR, Hannaway RF, Dearden PK, Kirman JR, et al. TCR- or Cytokine-Activated CD8(+) Mucosal-Associated Invariant T Cells Are Rapid Polyfunctional Effectors That Can Coordinate Immune Responses. Cell Rep 2019;28:3061-3076 e3065.
33. Constantinides MG, Link VM, Tamoutounour S, Wong AC, Perez-Chaparro PJ, Han SJ, Chen YE, et al. MAIT cells are imprinted by the microbiota in early life and promote tissue repair. Science 2019;366.
34. **Henao-Mejia J**, **Elinav E**, **Jin C**, Hao L, Mehal WZ, Strowig T, Thaiss CA, et al. Inflammasome-mediated dysbiosis regulates progression of NAFLD and obesity. Nature 2012;482:179-185.
35. Boursier J, Diehl AM. Implication of gut microbiota in nonalcoholic fatty liver disease. PLoS Pathog 2015;11:e1004559.
36. Spadoni I, Zagato E, Bertocchi A, Paolinelli R, Hot E, Di Sabatino A, Caprioli F, et al. A gut-vascular barrier controls the systemic dissemination of bacteria. Science 2015;350:830-834.

Author names in bold designate shared co-first authorship.

Robust MAIT cell activation by primary human liver cells: Implications for liver physiology and disease

Martin Lett[1]*, Hema Mehta[2]*, Adrian Keogh[3], Tina Jaeger[1], Marie-Anne Meier[4,5], Isabel Fofana[4], Otto Kollmar[6], Urs Duthaler[7], Markus Heim[4,5], Paul Klenerman[2,8], Deborah Stroka[3], Magdalena Filipowicz Sinnreich[1, 9]

[1] Liver Immunology, Department of Biomedicine, University Hospital Basel and University of Basel, Switzerland
[2] Peter Medawar Building for Pathogen Research, University of Oxford, UK
[3] Clinic of Visceral Surgery and Medicine, University Hospital Bern, Department of Biomedical Research, University of Bern, Switzerland
[4] Hepatology, Department of Biomedicine, University Hospital Basel and University of Basel, Switzerland
[5] Division of Gastroenterology and Hepatology, Clarunis, University Center for Gastrointestinal and Liver Diseases, Basel, Switzerland
[6] Division of Visceral Surgery, Clarunis, University Center for Gastrointestinal and Liver Diseases, Basel, Switzerland
[7] Clinical Pharmacology, Department of Biomedicine, University Hospital Basel and University of Basel, Switzerland
[8] Oxford NIHR Biomedical Research Centre, The John Radcliffe Hospital, Oxford, UK
[9] Department of Gastroenterology and Hepatology, Basel University Medical Clinic, Liestal, Switzerland

* These authors contributed equally to the manuscript.

Corresponding author:

Magdalena Filipowicz Sinnreich, MD, PhD

Liver Immunology

Department of Biomedicine

University Hospital Basel

Hebelstrasse 20

4031 Basel

Switzerland

tel +41 61 328 77 89 / fax +41 61 265 53 52

email: magdalena.filipowicz@unibas.ch

List of Abbreviations:

5-A-RU: 5-amino-6-D-ribitylaminouracil; 5-F-SA: 5-formyl-salicylic acid; RL-6-Me-7-OH: 7-Hydroxy-6-methyl-8-ribityl lumazine; 5-OP-RU: 5-(2-oxopropylideneamino)-6-D-ribitylaminouracil; 6-FP: 6-Formylpterin; Ab: antibody; Ag: antigen; APC: antigen presenting cell; BEC: biliary epithelial cell; CFU: colony forming unit; HSC: hepatic stellate cell; IFN-γ: interferon gamma; IF: immunofluorescence; IL: Interleukin; LB: lysogenic broth; LC: liquid chromatography; LSEC: liver sinusoidal endothelial cell; MAIT: mucosal-associated invariant T cell; MHC: major histocompatibility complex; MR1: MHC class I-related protein 1; MS: mass spectrometry; NEAA: non-essential amino acids; NPCs: non-parenchymal cells; PBMCs: peripheral blood mononuclear cells; PFA: para-formaldehyde; PHA: phyto-hemagglutinin; P/S: Penicillin/Streptomycin; RT: room temperature; TCR: T cell receptor; TIMP: tissue inhibitor of metalloproteinase; TNF-α: tumor necrosis factor alpha.

Financial support

Financial support for this study has been granted by grants to M.F.S. from the Goldschmidt-Jacobson Stiftung and the Swiss National Science Foundation (SNSF; grant number PZ00P3_167828), and by grants Wellcome Trust 109965MA, NIHR Biomedical Research Centre, Oxford, and NIHR Senior Fellowship to P.K.

Conflict of interest statement

The authors declare to have no conflict of interest.

Abstract

Background & Aims: Mucosal-associated invariant T (MAIT) cells are the most abundant T cell type in human liver. They respond to bacterial metabolites presented by MHC-like molecule MR1 on Ag-presenting cells (APCs). Activated liver MAIT cells are described as fibrogenic and MAIT cells from patients with liver cirrhosis show functional alterations consistent with pro-fibrotic activity. However, it remains unclear which liver cells are involved in MAIT cell activation and how their fibrogenic activity can be prevented. Likewise, little is known about the role of liver cells in the metabolism of bacterial MAIT cell antigens (Ags). *Approach & Results:* In our immunofluorescence analysis of human liver tissue, MAIT cells localized dispersedly in the liver parenchyma in the proximity of different liver cells. Human primary hepatocytes, hepatic myofibroblasts/stellate cells, liver endothelial cells and biliary epithelial cells were able to present Ags to blood- and liver-derived MAIT cells, with hepatocytes being the most efficient. Presentation was MR1-dependent and occurred in response to bacterial lysate and pure synthetic Ag 5-OP-RU. MAIT cell activation was prevented by non-activating MR1 ligands 6-formylpterin and acetylsalicylic acid-derivative 5-formyl-salicylic acid. Liver cells exposed to the bacterial Ag precursor had the capacity to generate active 5-OP-RU endogenously, as determined by mass spectrometry. *Conclusions:* The ability of different liver cells to act as APCs and their potential to generate active MAIT cell Ag provide new insights into the understanding of intrahepatic MAIT cell activation. The interaction between hepatic stellate cells and MAIT cells, and the production of pro-fibrotic cytokine IL-17 by MAIT cells, support a role for these cells in the development of fibrosis. Repression of MAIT cell activation by non-stimulatory MR1 ligands creates an opportunity to design anti-fibrotic therapies.

Introduction

Mucosal-associated invariant T (MAIT) cells are the most abundant population of innate-like T cells in humans; they comprise up to 5% of T cells in peripheral blood and are found in high numbers in the liver and mucosal tissues.(1-3) Unlike conventional T cells, which recognize Ags presented by major histocompatibility complex (MHC) class I or II molecules, MAIT cells are restricted to the highly conserved MHC-class I related molecule MR1.(2) They express a semi-invariant T cell receptor (TCR) containing the Vα7.2 variable chain (Vα7.2-Jα33/12/20) paired with an oligoclonal TCRβ repertoire.(2, 4) MAIT cells recognize MR1-bound metabolites of the riboflavin (vitamin B2) biosynthesis pathway produced by many pathogenic and commensal bacteria.(2, 5, 6) The most potent stimulatory MAIT cell Ag is the pyrimidine 5-(2-oxopropylideneamino)-6-D-ribitylaminouracil (5-OP-RU). It is formed by non-enzymatic condensation of the bacteria-derived precursor 5-amino-6-ribitylaminouracil (5-A-RU) with methylglyoxal derived from the glycolysis pathway.(7) Upon specific TCR activation, MAIT cells rapidly secrete pro-inflammatory cytokines like interferon gamma (IFN-γ) and tumour necrosis factor alpha (TNF-α) and acquire potent killing capacity; they consequently exert important immunoregulatory and antimicrobial functions.(8, 9) MAIT cells are further characterized by high cell-surface expression levels of C-type lectin CD161, interleukin-18 receptor (IL-18R) and IL-12R. Thus they can be activated by respective cytokines in a TCR-independent manner.(1, 10-12) These features of MAIT cells generate protective innate immunity before an adaptive immune response has formed.

MAIT cells constitute up to 40% of T cells residing in human liver,(1, 3, 13, 14) indicating their importance in liver physiology and in the pathogenesis of liver diseases. Liver MAIT cells secrete large amounts of IFN-γ, TNF-α and, importantly, IL-17. Secretion of the latter follows repetitive IL-12 stimulation or occurs in response to IL-7, a cytokine produced by hepatocytes under inflammatory conditions.(13-17) IL-17 acts as a fibrogenic cytokine that activates hepatic stellate cells (HSCs) and induces a pro-fibrotic state.(18) The aforementioned cytokine expression profile suggests a detrimental role of MAIT cells in liver inflammation and fibrogenesis. This notion is supported by a recent study with an $MR1^{-/-}$ mouse model in which the lack of MAIT cells protected against liver fibrosis, and by reports that MAIT cells from patients with liver cirrhosis show alterations consistent with pro-fibrotic activity.(16, 17)

Apart from the locally produced endogenous cytokines, the liver also receives cytokines and bacterial products originating from the gut and the systemic circulation via the portal vein and the liver artery. In addition, bacterial products may enter the liver via the biliary tree. Their responsiveness to bacterial products places MAIT cells at a central position in the immunological gut-liver axis, a notion supported by the finding that biliary epithelial cells (BECs) present *Escherichia coli*-derived Ag to MAIT cells.(14) Furthermore, in a study in mice colonized by *E. coli*, a compound with a molecular mass corresponding to the MAIT cell Ag precursor 5-A-RU was detected in the circulation, suggesting that 5-A-RU is able to cross the intestinal barrier.(19) This is also supported by a recent mouse study showing that MAIT cell Ag passes from mucosal surfaces to the thymus, where it induces development of MAIT cells.(20) These studies suggest that Ag exposure of MAIT cells may occur in the sinusoidal environment, including the subendothelial space of Dissé, where HSCs acting as main drivers of liver fibrogenesis are located.(18) It has been proposed that various hepatic parenchymal and non-parenchymal cell types act as liver-resident APCs, mainly for MHC class I/II and CD1d-dependent Ag-presentation.(14, 21) However, it has not yet been investigated whether

cells from the sinusoidal environment, including hepatocytes, HSCs and liver sinusoidal endothelial cells (LSECs), i.e. cells that are in direct contact with the blood entering via the portal vein, can present metabolite Ags to MAIT cells.

In this present study, we show the localization of MAIT cells within the human liver and characterize cellular interactions of human liver-derived primary cells with MAIT cells. We demonstrate important differences in the capacity of liver-derived APCs to present stimulatory Ag to MAIT cells, with hepatocytes being the most efficient. Further, we characterize the capacity of human liver cells to generate active MAIT cell Ag from exogenously provided bacterial precursor. We demonstrate that MAIT cell activation by liver APCs can be blocked by non-stimulatory ligands binding to MR1. This creates a therapeutic opportunity to interfere with the pro-fibrogenic activity of MAIT cells.

Materials and Methods

Resources used are listed in Supplementary Table 1 (reagents), Table 2 (cell lines) and Table 3 (antibodies). Further details of resources and methods not described in the main text are in the Supplementary data file.

Preparation of primary cells from human samples

Primary liver cells were prepared from liver samples from patients undergoing liver resection at the University Hospitals in Basel and Bern. Written informed consent was obtained from each patient included in the study. The study protocol conforms to the ethical guidelines of the 1975 Declaration of Helsinki, and was approved by the local ethics committee (Ethikkommission Nordwestschweiz; EKNZ; permit number EKNZ BASEC 2016-01188). Human hepatocytes were isolated from fresh liver tissue according to a published protocol.(22) For the isolation of HSCs, LSECs and BECs, and the maintenance and characterisation of all primary cell types by microscopy and/or flow cytometry, see the Supplementary data file.

Immunofluorescence staining of human liver sections

Cryopreserved human liver biopsy samples from the biobank at the Department of Biomedicine (Basel, Switzerland, ethics approval EKNZ BASEC 2016-01188) were used in this study. For patient details and staining procedures, see Supplementary Table 4 and the Supplementary data file.

Cell lines and MAIT cell clones

For details, see the Supplementary data file. All cell lines and MAIT cell clones used were routinely tested for mycoplasma contamination.

Generation of liver-derived MAIT cell lines

Non-parenchymal cells (NPCs) obtained from normal liver tissue samples of two patients undergoing surgery for colorectal cancer metastasis were used to generate two liver-derived

MAIT cell lines, designated MAIT-BEL-10 and MAIT-BSL-19. The NPC fraction was obtained after perfusion of the liver wedge with “collagenase buffer” (684 mM NaCl, 13 mM KCl, 3 mM Na_2PO_4 $2H_2O$, 125 mM HEPES, 25 mM $CaCl_2$; pH 7.4; containing 200 IU/ml collagenase type IV), and low speed centrifugation to deplete hepatocytes (see details in the Supplementary data file). Liver-associated mononuclear cells were isolated by density gradient centrifugation on Ficoll. MAIT cells were then FACS-sorted based on expression of CD3 and staining by MR1 Tetramer and expanded by stimulation with phytohemagglutinin (PHA) and human IL-2 (100 IU/ml) in the presence of irradiated peripheral blood mononuclear cells (PBMCs) (40 Gray) as feeder cells. T cells were maintained in RPMI 1640 medium supplemented with 5% AB^+ human serum, IL-2 (100 IU/ml), Penicillin/Streptomycin (100 IU/ml; P/S), L-glutamine, pyruvate and non-essential amino acids (NEAA).

MAIT cell enrichment strategy

To enrich for MAIT cells, $CD8^+$ cells were isolated by positive selection using the Miltenyi positive selection kit (purity ≥85%), or a negative selection panel composed of Abs against CD45RA, CD62L, CD19, CD14, CD36 and TCRγδ was used. This allowed for depletion of naïve T cells, B cells, monocytes, dendritic cells, platelets and γδ T cells.

Preparation of bacterial products and synthetic MAIT cell Ag

The preparation of fixed bacteria or bacterial lysate and of synthetic Ag 5-OP-RU is described in the Supplementary data file.

Ag presentation assays

Details of Ag presentation assays are described in the Supplementary data file. To perform blocking experiments, cells were incubated with Ag and the corresponding blocking Abs (10 ng/ml anti-MR1, 5 µg/ml anti-IL-12 or 4 µg/ml anti-IL-18) were added after 1 h, followed by a 1-h incubation step before the addition of MAIT cells. To test the blocking potential of non-activating MR1 ligands, 6-formylpterin (6-FP; 50 µM), acetyl-6-FP (5 µM) or 20 - 100 µM 5-formyl-salicylic acid (5-F-SA) was added 1 h before the addition of 5-OP-RU.

Statistical analysis

Unless indicated otherwise, all graphs presented in the figures represent data from three or more independent experiments. Exact numbers of repetitions are indicated in the figure legends. Unless indicated otherwise, values plotted in the graphs are means ± SD. All statistical analyses were performed in GraphPad Prism7. Analysis of statistical significance was conducted with the tests specified in the figure legends.

Results

MAIT cells are dispersed within the parenchyma in healthy human liver

We investigated whether MAIT cells are present in the sinusoidal environment of the liver, where they might be activated by contact with parenchymal and non-parenchymal cells that potentially function as liver APCs capable of presenting gut-derived bacterial Ags. We analysed, by immunofluorescence (IF) staining, human liver samples from 8 donors, lacking significant hepatic histopathological abnormalities (see Supplementary Table 4). MAIT cells were identified as cells positive for CD3, TCR Vα7.2 and IL-18Rα, a robust combination of markers as IL-18Rα parallels high CD161 expression on MAIT cells.(9) MAIT cells localized dispersedly to the parenchymal space in the liver (Fig. 1A and Supplementary Fig. 1A-B). They were found in or in the immediate proximity of the sinusoids, occasionally also within the portal fields. There was no zonal distribution that would confine MAIT cells to either of the three zones of the hepatic lobule. Our analysis, indicating that MAIT cells represent 8-33% of total liver T cells (Fig. 1B), confirmed that MAIT cells are highly abundant in human liver, considerably exceeding the frequency of Vα7.2-positive conventional T cells. Their proximity to parenchymal and non-parenchymal cells within the sinusoidal environment is likely to facilitate interaction of MAIT cells with liver cells taking up bloodborne liver-directed Ags.

Liver cell lines demonstrate a limited capacity to activate MAIT cells

Given the observation that MAIT cells reside dispersedly within the liver, both in the sinusoidal environment and occasionally within the portal fields, we next investigated their ability to interact *in vitro* with different liver parenchymal and non-parenchymal cell lines. We tested hepatoma cell lines HepG2 and Huh7, HSC lines TWNT-4 and LX-2, LSEC cell line TMNK-1 and BEC line H69. Using HepG2 and Huh7 cells, we stimulated MAIT cells ($CD8^{+}CD161^{++}Vα7.2^{+}$; Supplementary Fig. 2A) with riboflavin-synthesizing *E. coli*. We observed no IFN-γ or activation marker CD69 expression in MAIT cells co-cultured with either HepG2 or Huh7 cells exposed to a low concentration of *E. coli* (corresponding to 1.5e7

CFU/ml). In contrast, robust expression of both markers was found in response to the conventional APC cell line THP-1 used as control (Fig. 2A). Stimulation of MAIT cells by HepG2 or Huh7 cells exposed to higher CFUs of *E. coli* resulted in increased expression of CD69 but no marked IFN-γ or TNF-α production (Fig. 2B and Supplementary Fig. 2B).

Weak MAIT cell activation by HSC line TWNT-4 in response to *E. coli* was similar to that seen with the hepatoma cell lines (Fig. 2C-D). HSC line LX-2 also did not induce MAIT cell activation in response to *E. coli* lysate, as evidenced by the lack of IFN-γ secretion by MAIT cells (Supplementary Fig. 2D). In contrast to the hepatoma and HSC lines, LSEC cell line TMNK-1 activated MAIT cells in response to *E. coli*, though induction of IFN-γ and TNF-α was lower than that seen with THP-1 cells (Fig. 2C-D and Supplementary Fig. 2C). MAIT cell activation by LSEC cell line TMNK-1 was both MR1- and cytokine-dependent (Fig. 2E). Finally, when incubating BEC H69 cells with serial dilutions of *E. coli* lysate (Supplementary Fig. 2D), we found that these cells present Ag in an MR1-restricted manner. All liver-derived cell lines, except LX-2, responded to some extent to pure stimulatory Ag 5-OP-RU (Figs 2A, 2C and Supplementary Fig. 2E). Taken together, the results demonstrate that different types of liver-derived cell lines differ in their ability, in general limited, to activate MAIT cells via an MR1-restricted pathway.

Robust MAIT cell activation by primary human liver cell subsets

Given the Ag presentation differences seen in cell line experiments, we next investigated the stimulatory potential of primary cells isolated from human liver tissue. We isolated hepatocytes, BECs, hepatic myofibroblasts/HSCs and LSECs from surgically removed liver specimens and verified the identities of the cell populations by FLOW CYTOMETRY and/or microscopy (Supplementary Fig. 3A-C). All of these cell types represent potential non-professional APCs unique to the liver environment. Importantly, we observed MR1 expression in primary human

hepatocytes, which at approximately 60% constitute the main liver cell population, but also in BECs, LSECs and HSCs (Fig. 3A and Supplementary Fig. 3D).

Primary hepatocytes, when incubated with *E. coli* lysate, activated MAIT cell clone SMC3 in an MR1-dependent manner as shown by IFN-γ secretion (Fig. 3B) and upregulation of MAIT cell activation markers CD69, CD137 and PD-1 (Fig. 3C). Increased degranulation assessed by CD107a surface staining and TCR downregulation provided further evidence for T cell activation (Fig. 3C and Supplementary Fig. 4A). K562-MR1 human myeloid leukaemia cells stably transfected with a β2M-MR1 construct, and thus overexpressing MR1, were used as positive control APCs (Figs 3B and 3F). The results of robust MAIT cell activation by hepatocytes acting as APCs were confirmed using pure synthetic Ag 5-OP-RU instead of the *E. coli* lysate (Fig. 3D and Supplementary Fig. 4B).

HSCs are the main drivers of fibrogenesis in the liver, efficiently producing proteins involved in extracellular matrix formation upon activation.(18) As MAIT cells were recently linked to liver fibrosis,(16, 17) we asked whether HSCs are able to directly activate MAIT cells. Using primary HSCs as APCs and treating them with either the *E. coli* lysate or 5-OP-RU, we demonstrated MR1-dependent activation of MAIT cells measured by IFN-γ secretion (Fig. 3E-F) and expression of activation markers CD69, CD25 and CD137, as well as TCR downregulation (Supplementary Fig. 4C). We also tested the ability of blood-derived FACS-sorted MAIT cells to induce pro-fibrotic genes in HSCs upon stimulation with Ag and found a fibrogenic response (data not shown). This observation is in line with recent published findings.(16, 17) Taken together, the results implicate direct interaction between HSCs and MAIT cells as a factor contributing to the mechanism of their fibrogenic activity.

MR1-expressing primary cell populations of BECs and LSECs were also able to present *E. coli*-derived and synthetic 5-OP-RU Ag to MAIT cells (Figs 3G and 4A). In summary, the data presented here demonstrate that cells from the sinusoidal environment in the liver, as well as BECs, have a capacity to present bacteria-derived and pure Ag to MAIT cells.

Hepatocytes are the most efficient non-professional Ag-presenting cells to MAIT cells in the liver

We found marked differences in presentation capacity between the investigated cell types, with hepatocytes being the most efficient liver-derived APCs (Fig. 4A-B and Supplementary Fig. 5A-B), as assessed by the pure Ag or bacterial lysate concentration needed to reach an EC50 of IFN-γ production by MAIT cell clone SMC3. The killing capacity of the SMC3 clone differed depending on the APC used for stimulation (Supplementary Fig. 6A). Differences in the liver APC-induced activation of MAIT cells in the presence of Ag persisted when either IL-12 or IL-18 was blocked (Fig. 4C-D and Supplementary Fig. 5C-D). Inclusion of exogenous IL-12 or IL-18 increased MAIT cell activation, a known effect synergistic with TCR-dependent stimulation.(10, 23) The effect decreased upon addition of blocking antibodies against the respective cytokines, thus confirming the blocking effectiveness (Supplementary Fig. 5E-F and data not shown). Taken together, our results demonstrate robust MR1-dependent Ag presentation capabilities of intrahepatic cell types, most prominently hepatocytes, leading to the activation of MAIT cells.

Primary liver cells generate active MAIT cell Ag when provided with its precursor

In view of the strong intrahepatic interactions involving MAIT cells, we investigated whether liver APCs can generate active MAIT cell-stimulatory Ag endogenously. It has been reported that the Ag precursor 5-A-RU is not able to bind to MR1 and activate MAIT cells.(7) However, we found that exposure of liver APCs (hepatocytes, BECs, LSECs) to 5-A-RU for 2 or 5 h led to MAIT cell activation (Fig. 5A-B), suggesting that the activatory 5-OP-RU is formed by the

liver APCs. Liquid chromatography tandem mass spectrometry (LC-MS/MS) analysis of cell culture supernatants following exposure of different liver-derived primary APCs to 5-A-RU corroborated these findings. To standardize the system, we incubated THP-1 cells with 5-A-RU (Supplementary Fig. 7). We detected time-dependent accumulation of 5-OP-RU (and decay at later time points) by selected reaction monitoring (Supplementary Fig. 7). Importantly, MS analysis indicated that all tested primary liver cell types generated 5-OP-RU in a dose-dependent manner when provided with the precursor 5-A-RU (Fig. 5C). Collectively, these results demonstrate that primary liver cell subtypes can form active MAIT cell Ag when provided with the precursor 5-A-RU. This indicates that the process of activation of liver MAIT cells, encompassing both production of specific Ag molecules and their presentation by nearby liver APCs, can occur in a local liver environment.

5-A-RU conversion to active Ag *in vivo* in liver depends upon 5-A-RU crossing the intestinal barrier. Indeed, a compound with a molecular mass corresponding to the MAIT cell Ag precursor 5-A-RU was detected in the circulation and liver of mice.(19) To assess the probability of 5-A-RU crossing an intact intestinal barrier, we performed *in silico* modelling by applying a published method that uses a combination of physico-chemical parameters.(24, 25) Applying this method to the Ag 5-OP-RU and its precursor 5-A-RU, we found that of these two chemically very similar compounds the precursor has a higher probability of intestinal absorption than the active 5-OP-RU product (Supplementary Fig. 8).

The degree of activation of polyclonal blood- and liver-derived MAIT cells varies with the APC

To investigate whether the findings for the MAIT cell clone SMC3 apply to primary polyclonal MAIT cell populations, we isolated and tested MAIT cells from human peripheral blood and liver tissue. Starting with PBMCs, which contain 2-5% MAIT cells, negative magnetic bead selection using Abs against CD45RA, CD62L, CD19, CD14, CD36 and TCRγδ, depleted naïve

T cells, B cells, monocytes, dendritic cells, platelets and γδ T cells, resulting in four- to sevenfold enrichment for MAIT cells (data not shown). Activation of the enriched polyclonal MAIT cells was assessed upon exposure to Ag-loaded primary liver cells. TCR expression was downregulated in response to distinct liver-derived APCs exposed to 5 nM 5-OP-RU, with hepatocytes again being the most potent APCs (Fig. 6).

To assess activation of polyclonal liver-derived MAIT cells, we generated two liver MAIT cell lines (MAIT-BEL-10 and MAIT-BSL-19) from two patient donors. Both cell lines produced IFN-γ and IL-17 and showed upregulation of several activation markers, including CD107a and CD137, in response to different human liver-derived APCs exposed to synthetic 5-OP-RU, including hepatocytes, BECs and HSCs (Figs 6B-C and 6E, and data not shown). Presentation capacity differed between the liver APCs, as assessed by IFN-γ secretion and upregulation of activation markers by the MAIT-BEL-10 and MAIT-BSL-19 cells (Figs 6B and 6E). To mimic an inflammatory context in which increased amounts of bacterial products and inflammatory cytokines reach the liver, the synthetic Ag in some experiments was spiked into *E. coli* lysate (Fig. 6D and Supplementary Fig. 6B and Supplementary Videos). In this state, hepatocytes remained as efficient APCs (Fig. 6D) and this was paralleled by cytotoxicity elicited by liver-derived MAIT cell line MAIT-BSL-19 (Fig. 6B and Supplementary Videos). Thus, as a proof of concept, we demonstrated that hepatocytes can be killed *in vitro* following Ag-mediated activation of liver-derived MAIT cells. Taken together, our experiments demonstrate that human polyclonal MAIT cells derived from peripheral blood and liver respond to Ag presentation by different liver cells, most prominently hepatocytes.

Inhibition of liver APC-mediated MAIT cell activation by small molecules

To approach the prevention of MAIT cell activation in the liver, we explored the blocking of MR1 occupancy with non-activating MR1 ligands. 6-formylpterin (6-FP), derived from the folate degradation pathway, and acetyl-6-FP are known to bind MR1 but do not activate MAIT

cells.(5, 26) We found that MAIT cell activation by Ag-exposed primary liver cells (hepatocytes, BECs and HSCs) can be prevented in a dose dependent manner by pre-treating the liver cells with 6-FP or acetyl-6-FP (Fig. 7A-B). Other molecules, e.g. the acetylsalicylic acid derivative 5-formyl-salicylic acid (5-F-SA), were found previously to stabilize MR1 on the cell surface; however, they did not stimulate Jurkat T cells overexpressing the MAIT TCR.(26) MAIT cell activation by liver APCs was prevented by 5-F-SA (Fig. 7B). This indicates that liver APC-induced MAIT cell activation can be inhibited by small molecular-weight compounds that specifically interfere with MR1 activity on the surface of APCs.

Discussion

Here we present results of a comprehensive analysis of the activation of intrahepatic MAIT cells by liver cells, in a process mediated by MR1-bound bacterial Ags. We also examined the role of liver cells in the metabolism of bacterial Ags activating MAIT cells. We found that many primary liver cell types, most prominently hepatocytes, can present Ag to MAIT cells and that liver cells can generate active MAIT cell Ag when provided with its natural precursor molecule. We also observed that non-stimulatory MR1 ligands can prevent MAIT cell activation by liver-derived APCs. Our findings are important for a better understanding of the role of MAIT cells in liver physiology and in the pathogenesis of fibrosis. They are also relevant for the development of strategies to prevent the profibrogenic activity of MAIT cells in human liver.

We found that purified primary human cells present in the liver environment, namely hepatocytes, BECs, LSECs and HSCs, can specifically activate MAIT cells in an MR1-dependent manner, albeit to different degrees (Figs 3 and 4). To date, only BECs within the liver environment have been shown to present Ag to MAIT cells.(14) Other hepatic cell types including hepatocytes, LSECs and HSCs were also reported to serve as liver-resident APCs but through non-MR1-mediated Ag presentation.(21) Hepatocytes were the strongest inducers of MAIT cell activation, requiring very low (picomolar) concentrations of the activating MAIT cell Ag, 5-OP-RU. The effect was MRI dependent and mildly potentiated by cytokines (Fig. 4 and Supplementary Fig. 5). Importantly, our results demonstrate for the first time MR1-dependent MAIT cell activation by HSCs (Fig. 3E-F and Supplementary Fig. 4C), providing functional significance to the previous finding of MR1 expression on HSCs.(16) In line with their ability to produce fibrogenic and proinflammatory cytokines, MAIT cells were shown recently to promote profibrogenic HSC activation.(16, 17) Furthermore, a study performed in $MR1^{-/-}$ mice demonstrated that lack of MAIT cells is protective in mouse models of liver fibrosis.(16) In these studies, MAIT cells induced proliferation and collagen secretion by

hepatic myofibroblasts, and directed macrophages towards a pro-inflammatory phenotype *in vitro*. Our results suggest that the interaction between HSCs and MAIT cells reciprocally potentiates pro-fibrotic properties of both cell types.

We also demonstrate MR1 expression as well as MAIT cell activation by LSECs (Fig. 3A and 3G), which are in the immediate proximity of Ag-rich blood flowing through the sinusoids. The fenestrations in the layer of LSECs allow Ags also to reach hepatocytes, making our findings of efficient MR1-mediated Ag presentation by hepatocytes of potential physiological importance. We cannot exclude that cells contaminating our primary liver cell preparations contribute to the observed differences in APC activity. However, the procedures used for primary cell isolation and purification of the cells, with assessment by microscopy and IF staining, argue against this possibility. The protocol we used for isolation of LSECs yields not only endothelial cells of sinusoidal origin but also endothelial cells originating from the liver vasculature, the latter possibly contributing to Ag presentation by LSECs to MAIT cells. Notably, we showed that the LSEC-derived TMNK-1 cells and BEC H69 cells grown in culture were able to present Ag in an MR1-restricted manner to MAIT cells (Fig. 2 and Supplementary Fig. 2). Generally, the established cell lines, particularly hepatoma and stellate cell lines, were found to be less efficient in Ag presentation assays than primary cells.

Studies on MAIT cell localization in normal human liver yielded divergent results.(14, 16, 17) The findings ranged from MAIT cells being either found exclusively in the sinusoidal space, (16) to their predominant localisation within portal tracts.(14) Our results obtained by staining sections originating from livers lacking apparent histopathological abnormalities, using three different markers, indicate that MAIT cells are in a minority in the portal fields, with most of them localized dispersedly in the sinusoidal environment (Fig. 1 and Supplementary Fig. 1).

Thus, MAIT cells are in close contact with hepatocytes, LSECs (lining the surface of the sinusoids) and HSCs (residing in the space of Dissé between the hepatocytes and the LSECs), and also with BECs (forming the bile ducts within the portal fields). Our results argue for an extensive interaction potential of MAIT cells with abundant liver cell types, both in the sinusoidal and the portal environment, a property likely to have implications for both liver physiology and the pathogenesis of liver diseases.

We present evidence that all the primary liver cell types investigated generate active Ag 5-OP-RU in a dose-dependent manner when provided with the inactive precursor 5-A-RU (Fig. 5). As a signal corresponding to 5-A-RU was detected in the blood of “healthy” mice, i.e. not suffering from colitis or another condition disrupting integrity of the gut epithelium and/or endothelium,(19) it is likely that bacterial metabolites produced in the gut regularly reach the liver. Our analysis of chemical properties of the metabolite 5-A-RU further supports its diffusion through the gut epithelium (Supplementary Fig. 8). Moreover, very recent work has demonstrated that Ag sufficient for thymic selection of MAIT cells is derived from bacteria and therefore passes the gut epithelial and endothelial barriers.(20) The liver uptake of the 5-A-RU precursor and its *in situ* conversion to the active 5-OP-RU in the liver environment may be physiologically relevant, since stability of 5-OP-RU when not protected by binding to MR1 is very limited at body temperature.(7) 5-OP-RU is converted rapidly to 7-hydroxy-6-methyl-8-ribityl lumazine (RL-6-Me-7-OH) and 7-methyl-8-D-ribityllumazine (Supplementary Fig. 7A), and indeed a compound with a mass corresponding to RL-6-Me-7-OH was detected in the dataset obtained for the mouse blood and liver.(19) It remains to be determined whether 5-A-RU conversion to active 5-OP-RU occurs within liver cells or whether 5-OP-RU is generated by methylglyoxal released by the cells and then loaded onto MR1 present on the cell surface.(27)

The findings that bacterial metabolites produced in the gut reach the circulation and the liver, where they may be converted to active Ag, suggest that MAIT cells present in the parenchyma are in a continuous low activation state. This is supported by high expression of activation and exhaustion markers CD38, CD39, PD-1, and TIM3 on liver MAIT cells.(13, 16, 17) Thus low level MAIT cell activation and upregulation of tissue residency markers such as CD69 may contribute to maintaining a constant pool of MAIT cells in the liver. The proliferative capacity of MAIT cells is lower than of conventional T cells,(1, 28) which is also reflected by our finding of a dispersed rather than clustered localization of MAIT in healthy liver (Fig. 1 and Supplementary Fig. 1). The high frequency and dispersed distribution of MAIT cells in an alerted, “ready to act” state in liver tissue might protect the liver from incoming pathogens or increased amounts of microbial products. Antibacterial and immunomodulatory activity of MAIT cells has been clearly demonstrated by various studies of bacterial and viral infections.(9, 11, 29)

A constant low activation of MAIT cells and their close contact with hepatocytes could also have implications for tissue homeostasis in the liver. Recent studies performed with MAIT cells isolated from gut, lung or blood have shown that activation of MAIT cells via their TCR, as opposed to cytokines, is associated with induction of a tissue-repair gene expression program.(30-32) Consistently, MAIT cells were found to promote tissue repair either *in vitro* (30) or *in vivo* in a mouse model of skin injury.(33)

In contrast to “homeostatic” stimulation via TCR ligands, full (and potentially deleterious) activation of MAIT cells requires additional cytokine-mediated signaling.(30, 31) Such a condition is likely to occur when higher amounts of microbial products enter the liver via the

portal vein in the context of a disrupted gut epithelial and/or endothelial barrier. Human and mouse studies show that liver disease is coupled to alterations in the gut mucosa and gut dysbiosis.(34-36) In response to increased stimulatory signals derived from the gut, activated MAIT cells might enhance liver inflammation and contribute to immune-mediated liver pathologies, including liver fibrogenesis. Indeed, liver-derived MAIT cells produce large amounts of pro-inflammatory cytokines and the pro-fibrogenic cytokine IL-17 when stimulated by liver-residing APCs (Fig. 6B-D). This could be an important factor that initiates and/or perpetuates development of fibrosis. It was shown that secretion of IL-17 by MAIT cells increases in response to IL-7 produced by hepatocytes under inflammatory conditions.(13, 15) Our finding that hepatocytes act as strong APCs suggests that, under inflammatory conditions in a pathophysiological context, hepatocytes could activate MAIT cells and skew them towards an IL-17 phenotype. It is also possible, that under conditions of liver inflammation the reported tissue repair activity of MAIT cells may be mis-regulated and contribute to the development of fibrosis.

An additional consequence of MAIT cell activation may be the development of a potential to kill liver APCs, including hepatocytes. Indeed, our results suggest that direct killing of hepatocytes by activated MAIT cells may be an additional factor contributing to the pathogenesis of liver diseases (Supplementary Fig. 6 and Supplementary Videos).

With these considerations in mind, we explored possibilities for blocking MR1 with non-activating ligands and so preventing excessive MAIT cell activation in the liver in response to Ag presentation by abundant liver-derived APCs. We found that MAIT cell activation by Ag-exposed primary liver cells can be alleviated by pre-treating them with 6-FP or acetyl-6-FP, as well as the acetylsalicylic acid derivative 5-F-SA (Fig. 7). Of note, acetyl-6-FP and 3-F-SA (a

compound with a similar characteristic to 5-F-SA), were previously shown to have an inhibitory effect on MAIT cells in a mouse model mimicking lung infection.(26) Our findings corroborate the prospect of using inactive MR1 ligands as therapeutic agents to prevent involvement of MAIT cells in the fibrogenic process. The effectiveness of hepatocytes and other liver cells in presenting Ag to MAIT cells makes this approach of particular importance, both for anti-fibrotic treatment and for fibrosis prevention in patients at risk. Detailed mechanistic insights into hepatic MAIT cell activation are crucial because of their pro-fibrogenic properties. Our study reveals novel mechanisms of immune interactions in human liver and uncovers possible novel targets for immunotherapy.

Acknowledgements

We are grateful to the patients who agreed to donate biological material for research purposes. We acknowledge the surgeons and pathologists who helped in obtaining spare material from liver resections. We thank Prof. G. De Libero for sharing the MAIT cell clone SMC3 as well as the β2M-MR1 construct and Prof. M. Cella for sharing the MR1 Ab hybridoma (clone 26.5). We thank Prof. S. L. Friedman, Prof. D. Jefferson, and Prof. N Kobayashi for providing us with cell lines. We acknowledge the NIH Tetramer Core Facility, Emory University, Atlanta, GA, USA, for providing us with MR1-tetramer. The MR1 tetramer technology was developed jointly by Dr. James McCluskey, Dr. Jamie Rossjohn, and Dr. David Fairlie, and the material was produced by the NIH Tetramer Core Facility as permitted to be distributed by the University of Melbourne.

Figure Legends

Figure 1

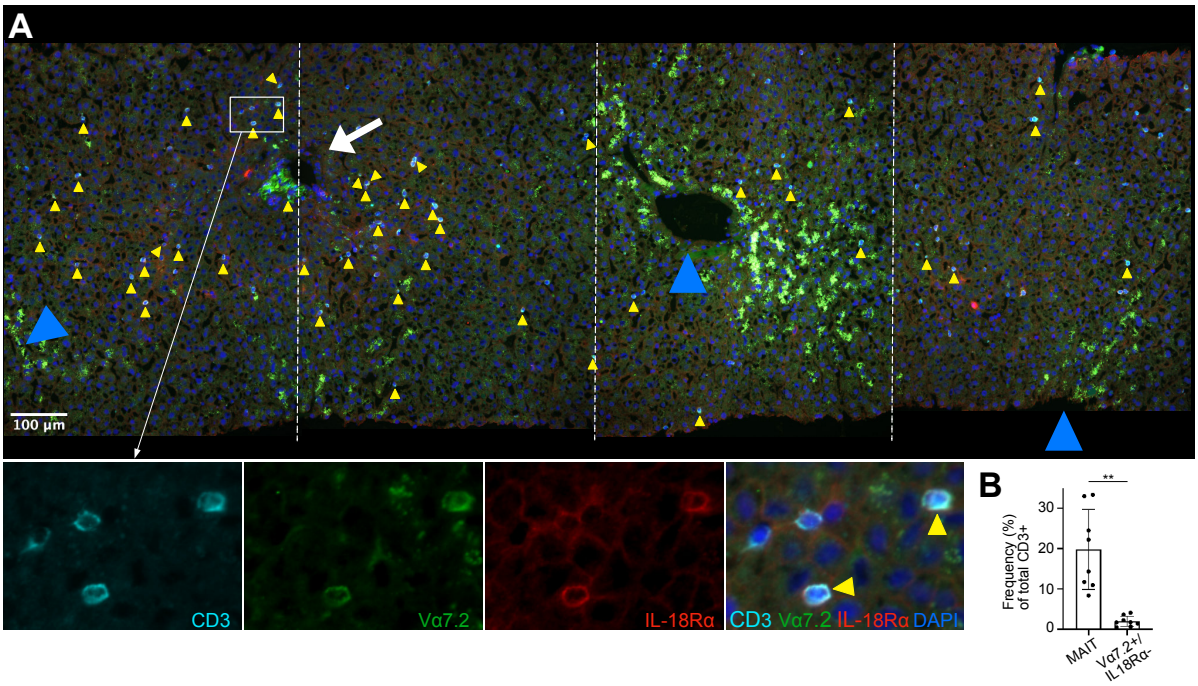

Figure 1. MAIT cells localize dispersedly to the parenchymal space in healthy human liver.

(A) Representative IF analysis of tissue section from a liver biopsy without histopathological abnormalities (patient C545). Co-localization of CD3, TCR Vα7.2 and IL18-Rα (see higher magnification lower panels) identifies MAIT cells (yellow arrow heads). White arrow and blue arrow heads point at portal field and central veins, respectively. Lower panels also show MAIT cells in proximity of TCR Vα7.2- and IL18-Rα-negative T cells. (B) Percentages of MAIT cells and non-MAIT Vα7.2^{+} cells *versus* total CD3^{+} T cells in healthy human liver (n = 8), assessed as shown in (A). ** P < 0.01, non-paired Welch t-test.

Figure 2

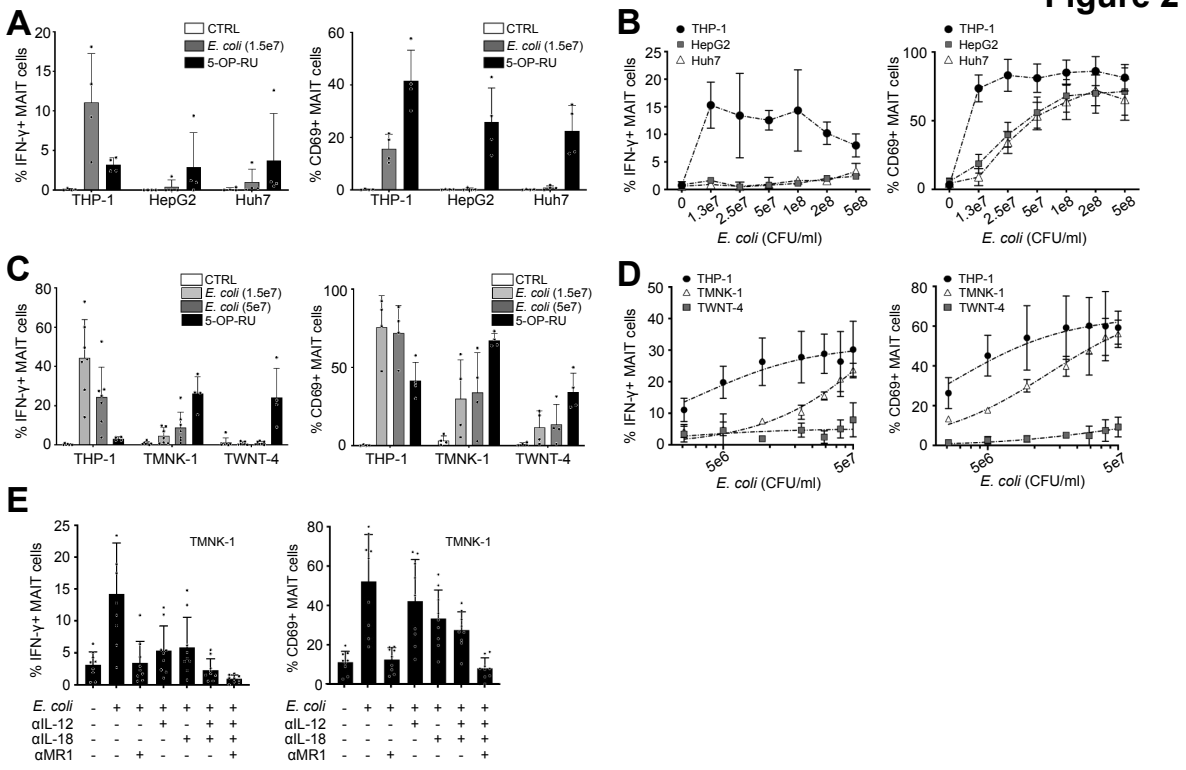

Figure 2. Liver cell lines exert limited capacity to activate MAIT cells.

MAIT cell expression of IFN-γ (left panels) and CD69 (right panels) measured by flow cytometry. CD8$^+$ T cells were co-cultured with different indicated cell lines in the presence of fixed *E. coli* or 5-OP-RU. (A) THP-1, HepG2 or Huh7 cells exposed to fixed *E. coli* (1.5e7 CFU/ml) or 10 nM 5-OP-RU (n = 4). (B) THP-1, HepG2 or Huh7 cells exposed to increasing concentrations of fixed *E. coli* (1.3e7 - 5e8 CFU/ml) (n = 3). (C) THP-1, LSEC TMNK-1 or stellate TWNT-4 cells exposed to fixed *E. coli* (1.5e7 or 5e7 CFU/ml) or 10 nM 5-OP-RU (n = 4). (D) TMNK-1 or TWNT-4 cells exposed to increasing concentrations of fixed *E. coli* (n = 3). (E) LSEC TMNK-1 cells in the presence of fixed *E. coli* (5e7 CFU/ml) exposed to different combinations of blocking Abs (n = 9).

Figure 3

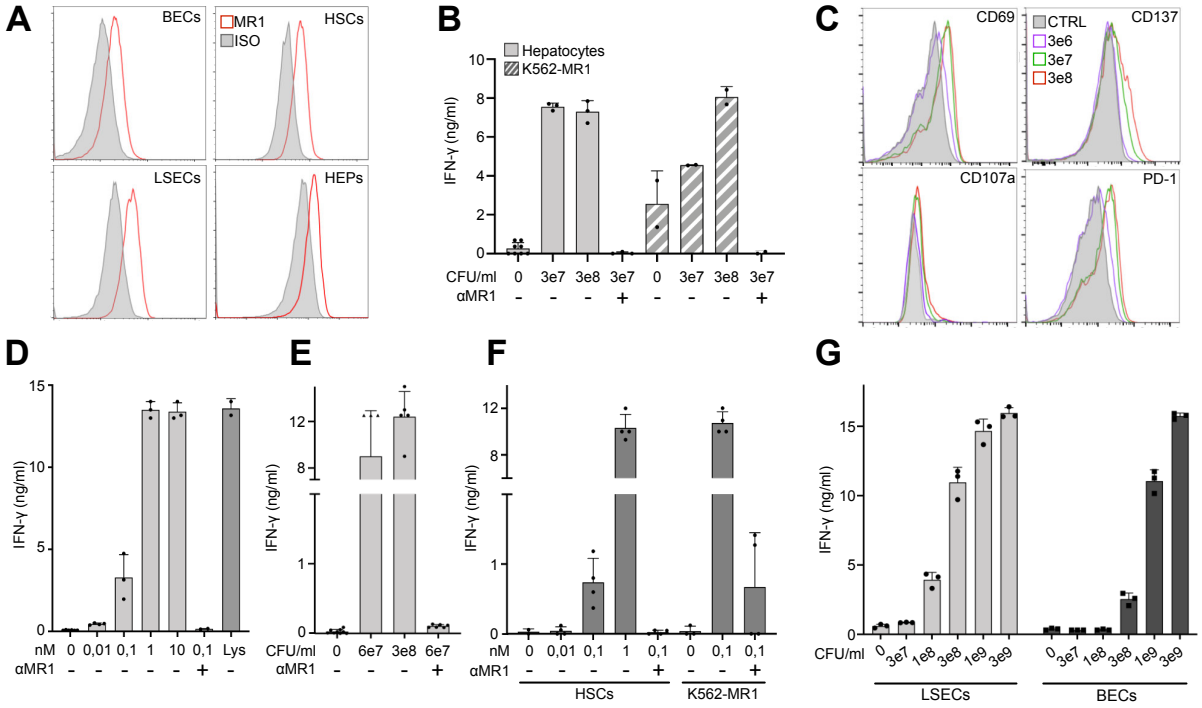

Figure 3. Primary human parenchymal and non-parenchymal liver cells express MR1 and present Ag to MAIT cells.

(A) Flow cytometry histograms showing primary BECs, LSECs, HSCs and hepatocytes (HEPs) expressing MR1, stained with anti-MR1 (red) or isotype-matched control antibody (filled grey). (B) MAIT cell clone SMC3 IFN-γ production upon co-culture with hepatocytes incubated with *E. coli* lysate (3e7 or 3e8 CFU/ml). (n = 4). (C) Representative flow cytometry histograms, showing indicated markers on clone SMC3 in response to hepatocytes incubated with *E. coli* lysate (3e6 – 3e8 CFU/ml). Filled grey histograms correspond to negative controls (CTRL) lacking lysate. (D - G) IFN-γ production by clone SMC3 in response to incubation with indicated liver cells and Ags. (D) Hepatocytes incubated with 5-OP-RU (0.01 - 10 nM). *E. coli* lysate (Lys; 3e8 CFU/ml) served as positive control (n = 7). (E) HSCs incubated with *E. coli* lysate (6e7 or 3e8 CFU/ml) (n = 5). (F) HSCs incubated with 5-OP-RU (0.01 - 1 nM) (n = 9). (G) LSECs and BECs incubated with *E. coli* lysate (3e7 – 3e9 CFU/ml) (n = 6). In panels B, D, E, F and G, the data (means ± SD of measurements from three independent wells originating from the same patient) exemplify representative experiments out of 4 - 9 performed with cells obtained from at least 3 different donors. IFN-γ was measured by ELISA. K562 cells overexpressing MR1 (K562-MR1) served as positive control APCs (B) and (F). Anti-MR1 antibody (αMR1) was used in panels (B) and (D - F).

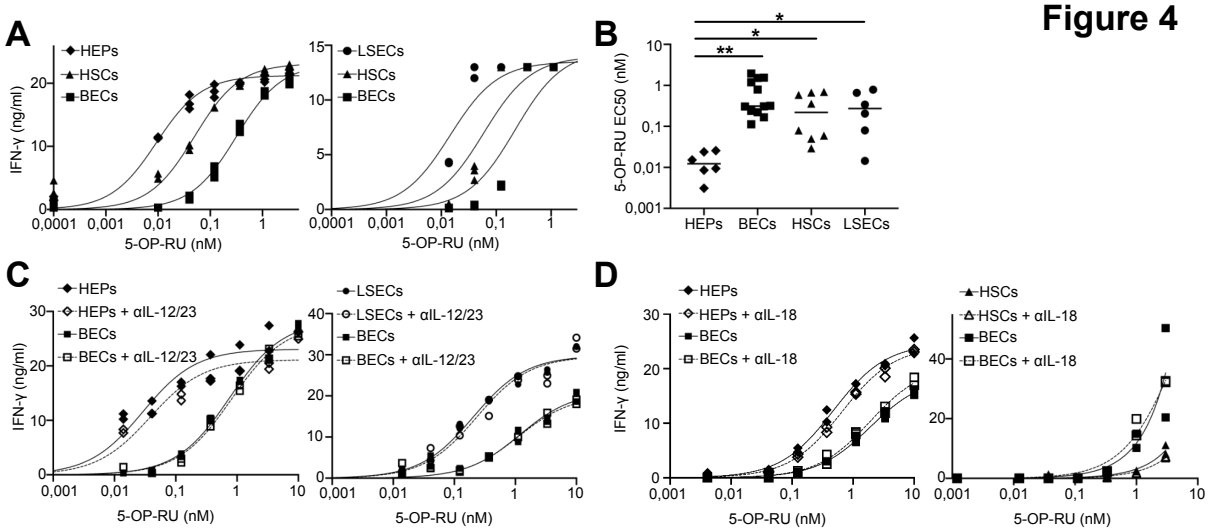

Figure 4

Figure 4. Hepatocytes represent potent liver-derived APCs activating MAIT cells.

(A) Two representative examples of synthetic Ag 5-OP-RU titration (0.01 - 3 nM) on liver APCs. IFN-γ production by MAIT cell clone SMC3 was measured by ELISA. Three independent measurements per dose are depicted. (B) Pooled results of all experiments performed as in panel (A). Shown are concentrations of 5-OP-RU needed to reach EC50 of IFN-γ secretion. Statistical significance was determined by paired Student's t-test. ** $p < 0.01$, * $p < 0.05$. (C and D) Representative examples of 5-OP-RU (0.01 - 10 nM) titration on liver APCs, in the absence or presence of Abs blocking either IL-12/23 (C) or IL-18 (D). One representative experiment out of 2 is shown in each panel. Other details are as in panel (A).

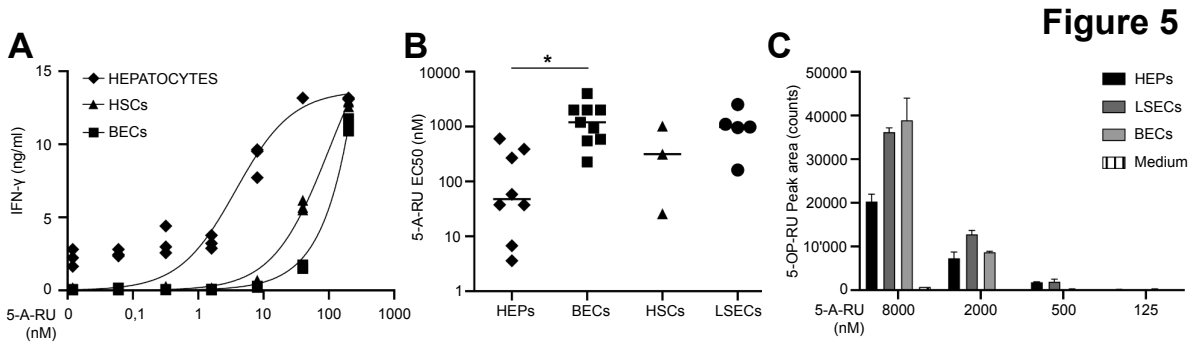

Figure 5. Liver-derived primary APCs have the capacity to generate active Ag endogenously.

(A) Representative experiment of MAIT cell Ag precursor 5-A-RU (0.01 – 2000 nM) titration using different liver primary cells as APCs. IFN-γ production by MAIT cell clone SMC3 was assessed by ELISA. Three independent replicates per dose are depicted. (B) Pooled results of all experiments performed as shown in panel (A), using cells originating from at least 3 different donors per cell type as APCs. Shown are concentrations of 5-A-RU needed to reach EC50 of IFN-γ production. Statistical significance determined by paired Student's t-test. *$p < 0.05$ (C) Quantification of 5-OP-RU by LC-MS/MS in cell culture supernatants derived from indicated liver primary cells harvested after treatment with indicated doses of 5-A-RU (125 – 8000 nM). RPMI medium without inclusion of cells served as negative control (Medium).

Figure 6

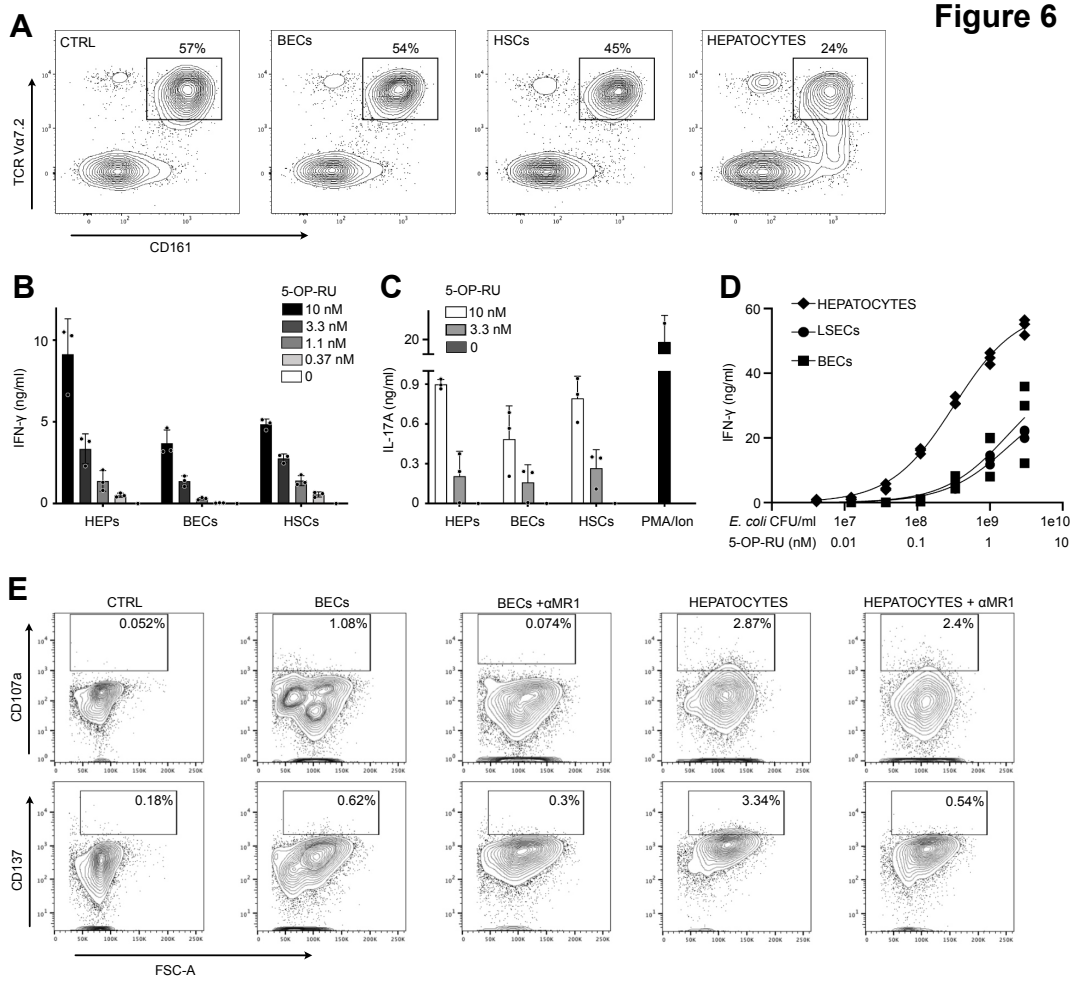

Figure 6. Robust activation of polyclonal MAIT cells in response to interactions with primary human liver cell subsets.

(A) PBMCs, enriched for Vα7.2^{+} CD161^{++} cells by negative selection (see Materials and Methods) were co-cultured with indicated liver APCs exposed to 5 nM 5-OP-RU. Representative example of cell surface expression of CD161 and TCR Vα7.2, as measured by flow cytometry (n=2). Dot plots are gated on CD3^{+} cells. (B and C) Production of IFN-γ (B) and IL-17 (C) by liver-derived MAIT cell line MAIT-BEL-10, measured by ELISA, in response to interaction with different liver APCs exposed to indicated concentrations of 5-OP-RU. Stimulation of MAIT cells with PMA/ionomycin (PMA/Ion) served as positive control. (D) IFN-γ production by liver-derived MAIT cell line MAIT-BSL-19, stimulated by indicated liver APCs exposed to increasing concentrations of *E. coli* lysate spiked in with 5-OP-RU. Three replicates per dose are shown. (E) Cell surface staining for CD107a and CD137 on MAIT-BSL-19 cells, stimulated by either hepatocytes or BECs exposed to 5 nM 5-OP-RU. MR1 dependence of activation was assessed with anti-MR1 blocking antibody (αMR1). Negative control (CTRL) in panel A and E lacks the APC.

Figure 7

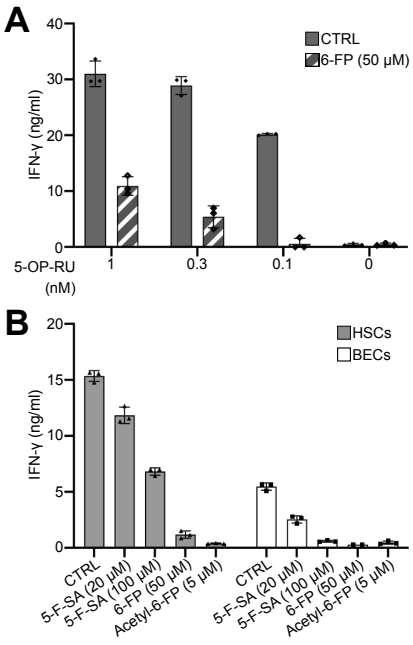

Figure 7. Non-activating MR1 ligands prevent MAIT cell activation by liver-derived APCs. MAIT cell clone SMC3 was co-cultured with indicated liver cells pre-treated with different non-activating MR1 ligands for 1 h before addition of 5-OP-RU. IFN-γ secretion was assessed by ELISA. (A) Hepatocytes either treated with 1nM 5-OP-RU alone (CTRL) or pre-treated with indicated concentrations of 6-FP before adding 5-OP-RU. (B) HSCs and BECs either treated with 5-OP-RU alone (CTRL), or pre-treated with indicated concentrations of 6-FP, Acetyl-6-FP, or 5-formyl-salicylic acid (5-F-SA) before 5-OP-RU addition. The mean ± SD of measurements of three independent wells originating from the same patient's cells is shown. One representative experiment out of 2, originating from two different donors, is shown.

Supplementary

Table of content

Supplementary Materials and Methods

Unless stated otherwise, all chemicals were received from Merck, Darmstadt, Germany.

Preparation of primary cells from human samples

For isolation of liver cell subsets, a wedge of encapsulated liver was perfused according to the protocol published by Portmann et al.(1) Hepatocytes were isolated by performing consecutive 50 x g centrifugation steps. Isolated hepatocytes were seeded (7 x 10^4 cell/cm^2) onto tissue culture plastic coated with rat tail collagen and were maintained in arginine-free Williams E medium, supplemented with insulin (0.015 IU/ml; Actrapid, Novo Nordisk Pharma, Switzerland), hydrocortisone (5 µm), penicillin / streptomycin (P/S; 100 IU per ml / 100 µg per ml), L-glutamine (2 mM; BioConcept, Allschwil, Switzerland), and ornithine (0.4 mM). 10% FCS (BioConcept) was added to the medium for 12 h following cell plating. After 12 h, medium was exchanged for medium lacking FCS and hepatocyte culture purity was assessed by microscopy; cells were then used for experiments. Brightfield microscopy of primary liver cells was performed on the Olympus IX81 microscope. IF staining of hepatocytes was performed using antibody against HNF-4α. Fluorescence images of primary cell populations were taken on the Nikon Ti2 microscope (Nikon, Tokyo, Japan).

Hepatic myofibroblasts/stellate cells (HSCs) were isolated by outgrowth from a suspension of liver derived non-parenchymal cells (NPCs), the fraction previously deprived of hepatocytes, plated in DMEM high glucose supplemented with 20% FCS, P/S, L-glutamine, 1 mM pyruvate, and Non-Essential Amino Acid (NEAA; BioConcept). After 24 h, the attached cells were washed once with PBS and cultured for additional 7 days. Mainly HSCs outlast this selection; their purity was assessed by flow cytometry

using their strong autofluorescence (due to Vitamin A storage) at λ=400-500 nm (violet channel) as readout, and by immunofluorescence (IF) staining using Ab against alpha-smooth muscle actin.

Isolation of Liver sinusoidal endothelial cells (LSECs) was carried out by positive immunomagnetic selection, according to the protocol of Shetty et al.(2) using a CD31 Ab conjugated to DYNABEADS (Thermo Fisher Scientific, Waltham (MA), USA). We use the term LSECs throughout the manuscript, although this protocol will yield not only endothelial cells of sinusoidal origin, but also endothelial cells originating from the liver vasculature. The cells were maintained in endothelial cell basal medium containing 10% human AB^+ serum (obtained from the blood donation centre, Basel, Switzerland), hepatocyte growth factor (10 ng/ml; PeproTech, Rocky Hill (NJ), USA), vascular endothelial growth factor (10 ng/ml; PeproTech), P/S, L-glutamine, pyruvate, and NEAA. The cells were grown in collagen-coated tissue culture plastic dishes. Identity of LSECs/endothelial cells were assessed by IF microscopy using a CD31 Ab, confirming the effectiveness of the isolation method.

Isolation of biliary epithelial cells (BECs) was performed by positive selection using EpCAM according to the protocol published previously.(3) BECs were maintained in epithelial cell medium composed of a 1:1 mix of DMEM low glucose and DMEM/F12-ham (Thermo Fisher Scientific, Waltham (MA), USA), supplemented with 10% FCS, P/S, adenine (18 µM), insulin (0.15 U/ml Humalog®, Eli Lilly SA, Switzerland), epinephrine (1 mg/ml), triiodothyronine-transferrin (1.1 µg/ml; 8.2 µg/ml), epidermal growth factor (10 ng/ml, PeproTech, Rocky Hill (NJ), USA), and hydrocortisone (13.4 µg/ml). BECs were assessed by IF microscopy using Ab against CK19.

Buffy coats for isolation of peripheral blood mononuclear cells (PBMCs) were obtained at the blood donation centre in Basel. PBMCs were isolated by density gradient centrifugation on Ficoll (Lymphoprep®; Axonlab, Baden, Switzerland), using a standard protocol.(4)

Immunofluorescence staining of human liver sections

Sections of 8 µm thickness were mounted on microscopy slides and fixed in 4% formaldehyde for 10 min at room temperature (RT). Slides were then washed twice for 10 min in PBS and blocked in blocking buffer for 1 h at RT [blocking buffer: 1% Normal donkey serum (Jackson Immuno Research, Ely, UK), 2% fish gelatin, 0.15% Triton-X-100 in PBS]. Slides were incubated with primary Abs, diluted in blocking buffer, at 4°C overnight, washed with PBS, and then incubated with secondary Abs at RT for 1 h. After washing with PBS, slides were mounted in mounting solution containing 300 µM DAPI. Abs used were anti-IL-18Rα, anti-TCR Vα7.2 and anti-CD3. Secondary Abs were donkey-anti-goat-Cy3, donkey-anti-mouse-A488, and donkey-anti-rabbit-A647. Fluorescence images were taken on the Olympus BX63 microscope (Olympus, Tokyo, Japan), using the 20x objective, and analysed with Image J (https://fiji.sc/).(5)

Cell lines and MAIT cell clones

All cell lines used are listed in Supplementary Table 2. LX2 cells were cultured in DMEM high glucose, and HepG2 and Huh7 cells in DMEM low glucose, supplemented with 10% FCS, P/S, L-glutamine, pyruvate and NEAA. TMNK-1 and TWNT-4 cell lines were grown in DMEM GlutaMax™ (Thermo Fisher Scientific) with P/S, pyruvate and NEAA. K562 and THP-1 cells were cultured in RPMI 1640 containing 10% FCS, P/S and L-glutamine, pyruvate, with or without NEAA, depending on the experiment. All cells were grown at 37°C under 5% CO_2 atmosphere.

In order to generate the K562-MR1 cell line, we transduced K562 cells with a lentivirus coding for human MR1 covalently linked with β2M; this construct was generously provided by Prof. Gennaro De Libero, Department of Biomedicine, University Hospital Basel, Switzerland.(6) We confirmed MR1 overexpression and cell surface display by flow cytometry, after staining the cells with mouse-anti-MR1 (clone 26.5; monoclonal Ab purified from a hybridoma kindly provided by Prof. Marina Cella, Washington University School of Medicine in St. Louis).(7)

Human MAIT cell clone SMC3 was also kindly provided by Prof. Gennaro De Libero.(6) This clone was generated from the peripheral blood of a healthy donor. In brief, sorted MAIT cells were cloned by limiting dilution using PHA (1 μg/ml), human IL-2 (100 IU/ml) and irradiated PBMCs (5×10^5/ml). The SMC3 MR1-restricted T cell clone was cultured and re-stimulated periodically as described by Lepore et al,(8) and maintained in complete RPMI-1640 medium containing 5% AB^+ human serum, and 100 IU/ml IL-2.

Preparation of bacterial products and synthetic MAIT cell Ag

Synthetic Ag 5-(2-oxopropylideneamino)-6-D-ribitylaminouracil (5-OP-RU) was generated according to the protocol published by Corbett et al.(9) In brief, Ag precursor 5-amino-6-D-ribitylaminouracil (5-A-RU; Toronto chemicals, CA) was mixed with 10 molar equivalents of methylglyoxal and incubated for 5 min on ice. The resulting 5-OP-RU was used immediately upon preparation to prevent its transformation into 7-Hydroxy-6-methyl-8-ribityl lumazine (RL-6-Me-7-OH) or 7-methyl-8-D-ribityllumazine (see Supplementary Figure 7A).

Fixed bacteria: *E. coli* (DH5α) was grown on lysogenic broth (LB) agar plates for 16 h at 37°C before fixing in 2% paraformaldehyde (PFA) for 20 min followed by

several PBS washing steps. Before fixation, bacteria were plated to determine number of colony forming units (CFUs). Concentration-adjusted stocks of fixed bacteria were re-suspended in PBS.

E. coli lysate: The DH5α strain was grown in LB medium. Cells were harvested during exponential growth and washed three times with cold 0.9% NaCl. Before the last wash, an aliquot was removed to determine the CFU. The pellet was subsequently resuspended in 70% ethanol and the cells were disrupted by two consecutive French press rounds. After centrifugation (15,000 x g for 20 min at 4°C), supernatant was lyophilized overnight and the concentration was adjusted to an equivalent of 5 x 10^{11} CFU/ml. The lysate was stored at −80°C.

Ag presentation assays

Ag presentation assays with fixed bacteria were performed by co-culturing cell lines and isolated $CD8^+$ T cells, at a ratio of 1:4, in 96 well flat bottom plates. Fixed bacteria were added at the concentration (CFU/ml) indicated, followed by 16 h incubation at 37°C. Brefeldin A (BioLegend, San Diego (CA), USA) and Monensin (BioLegend) were added for the final 4 h of incubation. $CD8^+$ T cells were subjected to flow cytometry analysis.

For Ag presentation with bacterial lysate/synthetic Ag, all assays with primary cell subtypes were performed in RPMI medium containing 10% FCS (supplemented as described above) to exclude unspecific effects of variable cell media. APCs were seeded and kept for 4 h at 37°C to allow for attachment/adaptation. Following this, *E. coli* lysate/synthetic Ag was added and cells were incubated for 2 h prior to the addition of MAIT cells, at an APC to T cell ratio of 1:4. Primary MAIT cells were used right after

isolation and the MAIT cell clone SMC3 at day 14 after re-stimulation. MAIT cell activation as well as cytokine secretion was evaluated after 16 h of co-culture.

Quantitative Real-Time PCR (RT-qPCR)

RNA was purified from primary liver cell types with Nucleo Spin RNA II kit (Macherey-Nagel, Germany) according to manufacturer's instructions. RNA was reverse transcribed by Moloney murine leukemia virus reverse transcriptase (Promega Biosciences, Inc., Wallisellen, Switzerland) in the presence of random Primers (Promega) and deoxynucleoside triphosphates, according to manufacturer's instructions. All reactions were performed in triplicates on an ABI 7500 Real-Time PCR System (Applied Biosystems, Faster City (CA), USA) using SYBR green fluorescence (FastStart Universal SYBR® green; Roche, Basel, Switzerland) as read out. mRNA expression levels of the MR1 transcript, were normalized to GAPDH mRNA levels using the ΔCt method. The primers were designed across exon-intron junctions to prevent contribution from genomic DNA amplification (MR1_F: 5'-TGCGGTGTCCAC ATGGTTCT-3', MR1_R: 5'-TTTGCTCTCGGGGCCTTCT-3'; GAPDH_F: 5'-AAGTAT GACAACAGCCTCAAGAT-3', GAPDH_R: 5'-CATGAGTCCTTCCACGATACC-3').

Enzyme-linked immunosorbent assay (ELISA)

For the ELISA, analysis plates (Maxisorp, NUNC) were coated overnight at 4°C with 2.5 µg/ml capture Ab for IFN-γ (Clone MD-1) or IL-17A (Clone BL-23). The next day, unspecific sites were blocked with 0.5% fractionated gelatine for 1 h at RT. The samples were incubated for 2 h, followed by 1 h incubation step with biotinylated Ab, either 1 µg/ml anti-IFN-γ or 0.3 µg/ml anti-IL-17A, and 1 h incubation with either 0.25 µg/ml Streptavidin-HRP (BioLegend) for the IFN-γ or 0.1 µg/ml Streptavidin-

PolyHRP80 (SDT GmbH, Baesweiler Germany) for the IL-17A ELISA. Between each step, the plate was rinsed 3 times with PBS 0.05% Tween. Revealing was performed after incubation with OPD (SIGMAFAST™) by reading absorbance at λ=490 nm.

Flow cytometry analysis

For the intracellular staining, cells were washed with PBS and stained with Live/Dead Cell Stain (Thermo Fisher Scientific) for 15 min, followed by a 10 min fixation step with 4% PFA prior to permeabilising the cells for 10 min. Cells were then incubated with the Ab cocktail (see Supplementary Table 3) for 20 min before washing and re-suspending in PBS for analysis on MACSQaunt analyser (Miltenyi Biotech, Germany).

For the surface staining, mononuclear cells were washed in PBS and stained with Live/Dead® Fixable Dead Cell Stain blue (Thermo Fisher Scientific), and rinsed once in staining buffer (PBS with 0.5% human albumin and 3 mM sodium azide), followed by incubation with Abs against cell-surface molecules. Data were acquired on the LSRFortessa™ (BD Biosciences, Allschwil, Switzerland) and analysed with FlowJo 10.0.7 (TreeStar, Ashland (OR), USA). After excluding doublets and DAPI- or LIVE/DEAD stain-positive cells, MAIT cells were identified as $CD3^{+}CD161^{high}V\alpha7.2^{+}$ and/or MR1 tetramer (APC-labeled MR1 5-OP-RU tetramer; NIH Tetramer Core Facility, Emory University, Atlanta (GA), USA) positive cells.

Mass spectrometry analysis

5-OP-RU was analysed in cell extracts and cell supernatants by liquid chromatography (LC: Shimadzu, Kyoto, Japan) tandem mass spectrometry (MS/MS: API 4000, AB Sciex, Concor, Canada). A Synergi Polar-RP analytical column (Phenomenex, Torrance, USA) was used as stationary phase, while the mobile phase consisted of water (mobile A) and methanol (mobile B), both supplemented with 0.1% acetic acid.

5-OP-RU eluted at 2.14 min when using the following gradient program: 0 - 0.5 min 20% B, 0.5 - 1.5 min 20-95% B, 1.5 - 2.5 min 95% B, 2.5 - 3 min 20% B. The sample was online diluted during the first 0.5 min with mobile phase A via a t-union, which was connected in front of the analytical column. The flow rate was kept constant (0.8 ml/min). Aliquots of cell supernatant (50 µl) or cell extract (from 1.5 million cells) were extracted with 150 µl 100% methanol and 200 µl 75% methanol, respectively. After centrifugation, supernatants (20 µl) of extracts were injected into the LC-MS/MS system. 5-OP-RU was analysed by electrospray ionization and selected reaction monitoring in the negative mode using the mass transition 329.0 m/z → 190.9 m/z (declusting potential: -110 V, entrance potential: -10V, collision energy: -24 V, collision cell exit potential: -9 V, gas: N2). Analyst software 1.6.2 (AB Sciex, Concord, Canada) was used to analyse the data and to operate the LC-MS/MS system.

Supplementary Tables

Supplementary Table 1. Key resources

Reagent or Material	Supplier	Identifier
Growth media / Supplements		
Adenine	Merck, Darmstadt, Germany	Cat# A8626
DMEM high glucose	Merck, Darmstadt, Germany	Cat# D6571
DMEM low glucose	Merck, Darmstadt, Germany	Cat# D5546
DMEM/F12-ham	Thermo Fisher Scientific, Waltham (MA), USA	Cat# 21331
DMEM GlutaMax™	Thermo Fisher Scientific	
Endothelial cell basal medium	Merck, Darmstadt, Germany	Cat# 210-500
Epidermal growth factor	PeproTech, Rocky Hill (NJ), USA	Cat# 100-15
Epinephrine	Merck, Darmstadt, Germany	Cat# E4250
Foetal Calf Serum, FCS	BioConcept, Allschwil, Switzerland	Cat# 2-01F10-I
Hepatocyte growth factor	PeproTech, Rocky Hill (NJ), USA	Cat# 100-39H
Hydrocortisone	Merck, Darmstadt, Germany	Cat# H-0888
IL-2, human	PeproTech, Rocky Hill (NJ), USA	Cat# 200-02
Insulin, ACTRAPID®	Novo Nordisk Pharma AG, Switzerland	
Insulin, HUMALOG®	Eli Lilly SA, Switzerland	Cat# VL7394
L-glutamine	BioConcept, Allschwil, Switzerland	Cat# 5-10K50-H
Non-Essential Amino Acid	BioConcept, Allschwil, Switzerland	Cat# 5-13K00-H
Ornithine		
Penicillin / Streptomycin	Merck, Darmstadt, Germany	Cat# P-4333
Phytohemagglutinin	Thermo Fisher Scientific, Waltham (MA), USA	Cat# 10082333
RPMI 1640 medium	Merck, Darmstadt, Germany	Cat# R0883
Triiodothyronine	Merck, Darmstadt, Germany	Cat# T6397
Transferrin	Merck, Darmstadt, Germany	Cat# T1147
Vascular endothelial growth factor	PeproTech, Rocky Hill (NJ), USA	Cat# 100-20
Williams E medium	Merck, Darmstadt, Germany	Cat# W4128
Reagents		
5-amino-6-D-ribitylaminouracil	Toronto chemicals, CA	Cat# A629245
5-formyl-salicylic acid	Merck, Darmstadt, Germany	Cat# F17601

6-Formylpterin	Schircks Laboratories, Switzerland	Cat# 11.415
Acetyl-6-Formylpterin	Schircks Laboratories, Switzerland	Cat# 11.418
Brefeldin A	BioLegend, San Diego (CA), USA	Cat# 420601
Casein buffer, biotin-free	SDT GmbH, Baesweiler, Germany	Cat# CBC1
Collagen	Merck, Darmstadt, Germany	Cat# C3867
Collagenase type IV	Merck, Darmstadt, Germany	Cat# C5138
Deoxynucleoside triphosphates	Promega Biosciences, Inc., Wallisellen, Switzerland	Cat# U1515
Ficoll, LYMPHOPREP®	Axonlab, Baden, Switzerland	Cat# 1114547
Fish gelatin	Merck, Darmstadt, Germany	Cat# G7041
Fractionated gelatine	Merck, Darmstadt, Germany	Cat# 37766
Live/Dead Cell Stain	Thermo Fisher Scientific, Waltham (MA), USA	Cat# L10119
LIVE/DEAD® Fixable Dead Cell Stain blue	Thermo Fisher Scientific, Waltham (MA), USA	Cat# L23105
Methylglyoxal	Merck, Darmstadt, Germany	Cat# R0252
Moloney murine leukemia virus reverse transcriptase	Promega Biosciences, Inc., Wallisellen, Switzerland	Cat# M1701
Monensin	BioLegend, San Diego (CA), USA	Cat# 420701
Normal donkey serum	Jackson Immuno Research	Cat# 017-000-121
o-Phenylenediamine dihydrochloride; SIGMAFAST™ OPD	Merck, Darmstadt, Germany	Cat# F4648
Random Primers	Promega Biosciences, Inc., Wallisellen, Switzerland	Cat# C1181
Streptavidin-HRP	BioLegend, San Diego (CA), USA	Cat# 405210
Streptavidin-PolyHRP80	SDT GmbH, Baesweiler, Germany	Cat# SP80C
SYBR green; FastStart Universal SYBR® green master	Roche, Basel, Switzerland	Cat# 28137500
Other		
DYNABEADS	Thermo Fisher Scientific, Waltham (MA), USA	
ELISA plates; Maxisorp	NUNC	Cat# 439454
Nucleo Spin RNA II kit	Macherey-Nagel, Germany	Cat# 740984
Miltenyi positive selection kit	Miltenyi Biotec	Cat# 130-096-495

Supplementary Table 2. Cell lines

Name	Description	Source	Reference
H69	SV40 T Ag transformed biliary cell line, derived from normal liver	Douglas Jefferson[1], provided by Christian Fingas[2]	(10)
HepG2 Huh7	Hepatocarcinoma cell lines	American Type Culture Collection	(11),(12)
K562	Chronic myeloid leukemia cell line	American Type Culture Collection	
K562-MR1	K562 cells constitutively expressing MR1-β2M		This study
LX2	SV40 T Ag immortalized stellate cell line	Scott L. Friedman[3]	(13)
SMC3	Human MAIT cell clone	Gennaro De Libero[4]	(6)
THP-1	Myelomonocytic leukemia cell line	American Type Culture Collection	
TMNK-1	LSEC cell line	Naoya Kobayashi[5]	(14)
TWNT-4	Stellate cell line	Naoya Kobayashi[5]	(14)

[1]New England Medical Center, Tufts University; [2]University Duisburg Essen, Germany; [3]Icahn School of Medicine at Mount Sinai, New York, USA; [4]Department of Biomedicine, University Hospital Basel, Switzerland; [5]Okayama University, Japan.

Supplementary Table 3. Antibodies

Antibody	Clone	Company	Cat#
Antibodies for Enrichment			
CD36	REA760	Miltenyi Biotec	130-110-738
TCR γδ	REA591	Miltenyi Biotec	130-113-510
CD4	REA623	Miltenyi Biotec	130-113-224
CD14	REA599	Miltenyi Biotec	130-110-517
CD19	REA675	Miltenyi Biotec	130-113-644
CD45RA	REA1047	Miltenyi Biotec	130-117-750
Antibody Cocktail used for the intracellular staining			
Near IR	NA	ThermoFisher	L10119
CD3	UCHT1	BioLegend	300430
CD8	BW135/80	Miltenyi	130-113-164
CD161	191B8	Miltenyi	130-113-593
Vα7.2	3C10	BioLegend	351708
IFN-γ	45-15	Miltenyi	130-091-641
TNF-α	MAb11	BioLegend	502930
CD69	FN50	Invitrogen	11-0699-42
Antibody Cocktail used for the surface staining			
CD107a	H4A3	Biolegend	328605
CD8α	RPA-T8	BD Biosciences	564804
CD3	UCHT1	Biolegend	300448
CD161	HP-3G10	Biolegend	339916
TCR Vα7.2	3C10	Biolegend	351722
CD279/PD-1	EH12.2H7	Biolegend	329918
CD137	4B4-1	Biolegend	309816
CD69	FN50	Biolegend	310914
Antibodies for Immunofluorescence staining			
α-SMA	1A4	Sigma	5228
CK-19	B170	Leica Biosystems	NCL-CK19
HNF-4α	POLYCLONAL	Santa Cruz	Sc-8987
CD31	WM59	Biolegend	303110
IL-18Rα	POLYCLONAL	R&D System	AF840
TCR Vα7.2	3C10	Biolegend	351702
CD3	POLYCLONAL	DAKO	A0452
Anti-Mouse	POLYCLONAL	Jackson Immuno Research	715-545-150

Anti-Rabbit	POLYCLONAL	Jackson Immuno Research	711-605-152
Anti-Goat	POLYCLONAL	Jackson Immuno Research	705-165-147
Blocking Antibodies			
IL12/IL23	C8.6	Biolegend	508804
IL-18	125-2h	MBL	D044-3
MR1	26.5	Biolegend	361108

Supplementary Table 4. Patient characteristics of liver biopsy samples used for assessment of MAIT cell localisation in normal human liver by IF staining (see Figs 1 and Supplementary Figure 1).

Patient ID	Age	% MAIT/ CD3	% Vα7.2$^+$ IL18Rα$^-$ /CD3	ALT [U/l]	AST [U/l]	GGT [U/l]	AP [U/l]	Bilirubin [µmol/l]	Reason for biopsy	Biopsy result
C369	36	14.33	1.75	88	33	447	111	4	Suspicion of medication induced hepatotoxicity	Liver parenchyma without pathological changes.
C491	43	10.95	1.41	35	23	116	71	10	Isolated GGT increase	Liver parenchyma without pathological changes.
C545	54	32.97	3.62	91	49	216	204	8	Increased Transaminases/ GGT/AP	Liver parenchyma without pathological changes.
B927	60	22.22	1.71	15	22	20	41	12	Calcified liver mass	Liver parenchyma without pathological changes.
C28	50	24.48	0.69	43	39	406	150	9	Focal nodular hyperplasia	Liver parenchyma without major pathological changes. Minimal steatosis <10%.
C145	42	33.33	4.10	56	24	154	84	21	Increased Transaminases/ GGT	Liver parenchyma without major pathological changes. Minimal unspecific lymphocytic infiltrates, minimal sinusoidal dilation.
C192	35	8.38	2.23	42	26	137	76	4	Increased Transaminases	Liver parenchyma without major pathological changes. Minimal reactive hepatitis.
B113	27	11.73	0.51	21	29	14	62	10	Increased Transaminases (normal again at time-point of biopsy)	Liver parenchyma without major pathological changes. Minimal unspecific lobular inflammation.

ALT: Alanine amino-transferase; AST: Aspartate amino-transferase; GGT: γ-glutamyltransferase; AP: Alkaline phosphatase

Supplementary Figures

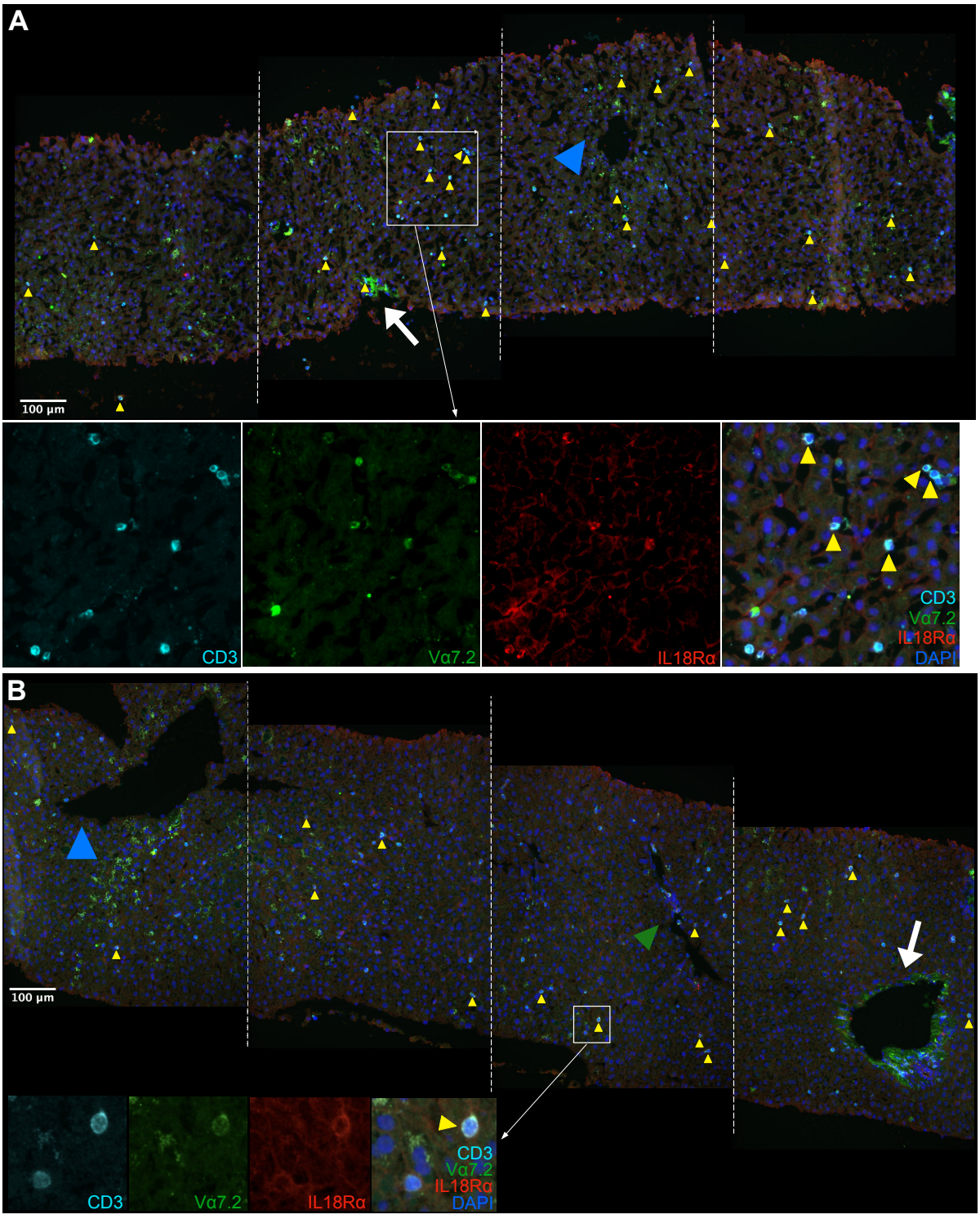

Supplementary Figure 1.
Dispersed MAIT cell localization in the parenchymal space of normal human liver. Two representative tissue sections from liver biopsies without histopathological abnormalities; patient identifiers C145 (A) and C369 (B). Co-localization of CD3, TCR Vα7.2 and IL-18Rα identifies MAIT cells (yellow arrow heads; see higher magnification lower panels) dispersed within the liver parenchyma. White arrows point towards portal fields, and blue arrow heads towards central veins. The green arrow points to a structure that is likely a central vein. The higher magnification panels also identify MAIT cells in the proximity of T cells negative for IL-18Rα and/or TCR Vα7.2 staining. Abs used for IF staining of cryosections are specified in higher magnification panels.

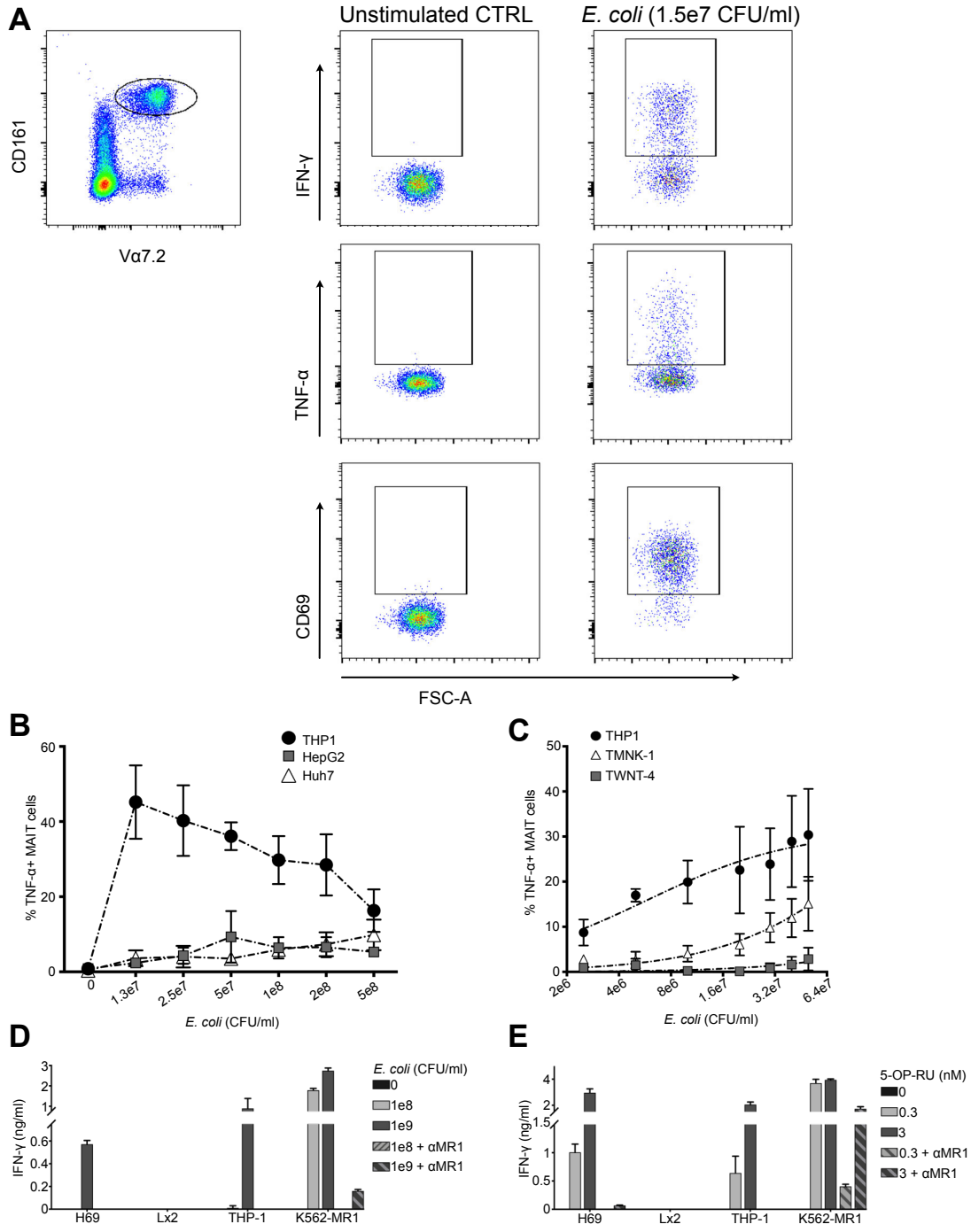

Supplementary Figure 2.
Liver-derived established cell lines exert limited capacity to activate MAIT cells. (A) Representative FACS plot showing MAIT cell identification as CD161^{++} Vα7.2^{+} cells within the CD8^{+} cell population (upper left panel). Remaining panels, gated on MAIT cells, represent staining of IFN-γ, TNF-α and CD69 in response to activation by THP-1 cells exposed to fixed *E. coli* (1.5e7 CFU/ml; right panels), compared to unstimulated cells (middle panels; CTRL). (B) Isolated CD8^{+} T cells co-cultured with THP-1 or hepatoma cell lines exposed to increasing concentrations of fixed *E. coli.* (C) Isolated CD8^{+} T cells co-cultured with THP-1, LSEC TMNK-1 or stellate TWNT-4 cells exposed to increasing concentrations of fixed *E. coli*. In (B) and (C) TNF-α expression values are means ± SD (n = 3). (D and E) SMC3 MAIT cell clone co-cultured with H69 or LX-2 cells exposed to *E. coli* lysate (D) or 5-OP-RU (E), with and without anti-MR1 blocking antibody (αMR1). THP-1 and K562-MR1 cells served as positive control. IFN-γ secretion values, measured by ELISA, are means ± SD from three independent measurements. One representative experiment out of three is shown.

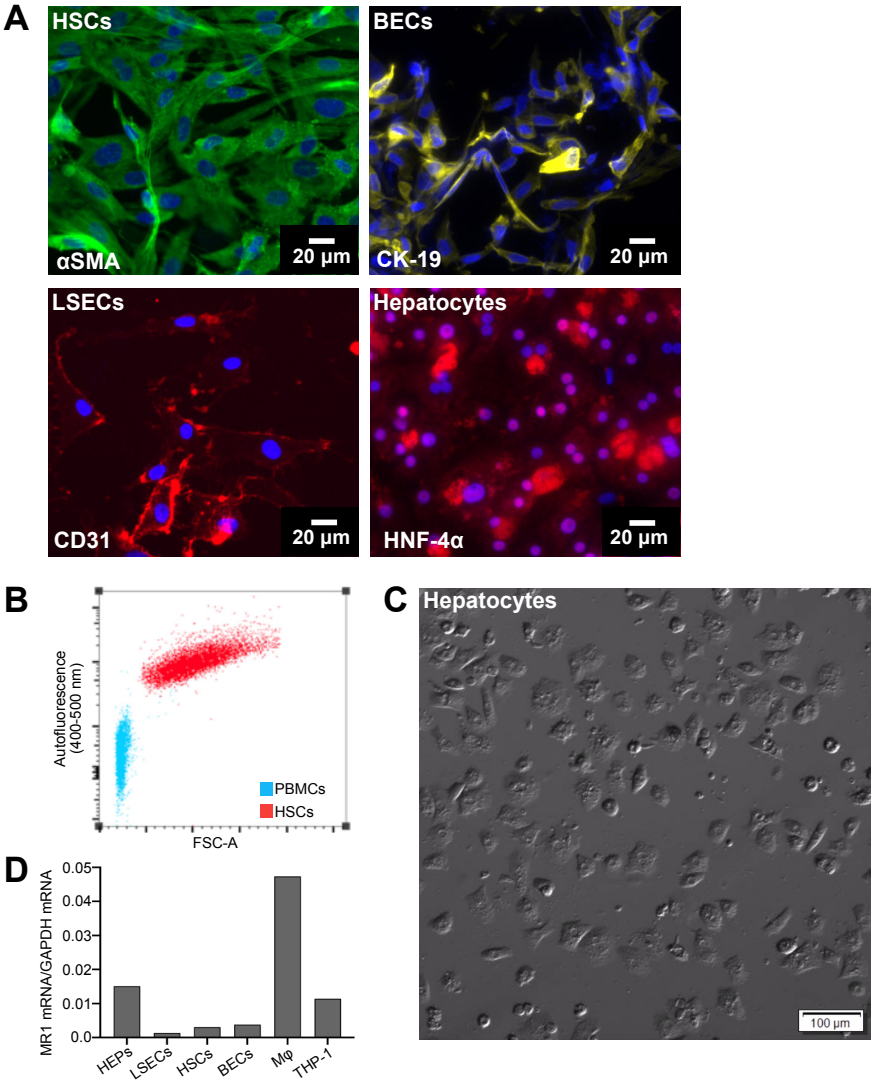

Supplementary Figure 3.
Characterization of primary liver-derived cell subpopulations and their MR1 expression. (A) Isolated primary cells were analysed by IF for expression of indicated markers. Formalin-fixed cells grown on chamber slides were stained for DAPI, and α-SMA for HSCs, CK-19 for BECs, CD31 for LSECs/liver endothelial cells and HNF-4α for hepatocytes (B) FACS analysis of unstained HSCs compared to human PBMCs. The characteristic autofluorescence of HSCs appears in the violet channel (λ = 400-500 nm). (C) Representative preparation of primary hepatocytes (partially binucleated), used in Ag presentation experiments. The cells were visualized by bright field microscopy. (D) RT-qPCR analysis of MR1 mRNA expression in investigated liver cell subpopulations: hepatocytes/HEPs, LSECs, HSCs and BECs, and in macrophages (Mϕ) and THP-1 control cells. MR1 mRNA levels are related to GAPDH mRNA.

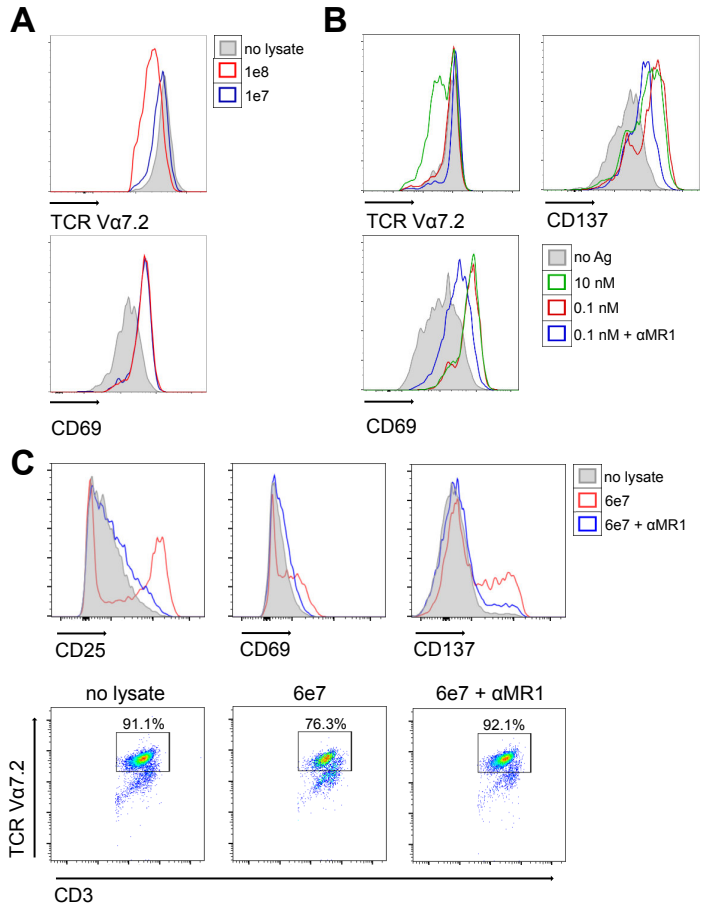

Supplementary Figure 4.
MAIT cell activation in response to Ag-exposed hepatocytes and HSCs. (A) Representative FACS histograms showing up-regulated activation marker CD69 and down-regulated TCR Vα7.2 on MAIT cell clone SMC3 in response to hepatocytes incubated with *E. coli* lysate (1e7 or 1e8 CFU/ml). (B) Representative FACS histograms showing up-regulated activation markers CD69 and CD137 and down-regulated TCR Vα7.2 on clone SMC3 in response to hepatocytes incubated with 0.1 or 10 nM 5-OP-RU. MR1 dependence of the activation was assessed by the use of anti-MR1 blocking Ab (αMR1). (C) Representative FACS histograms showing up-regulated activation markers CD69, CD25 and CD137, and FACS plots (lower row) showing down-regulated TCR Vα7.2, on clone SMC3 in response to HSCs incubated with *E. coli* lysate (6e7 CFU/ml). MR1 dependence of activation was assessed by anti-MR1 blocking Ab.

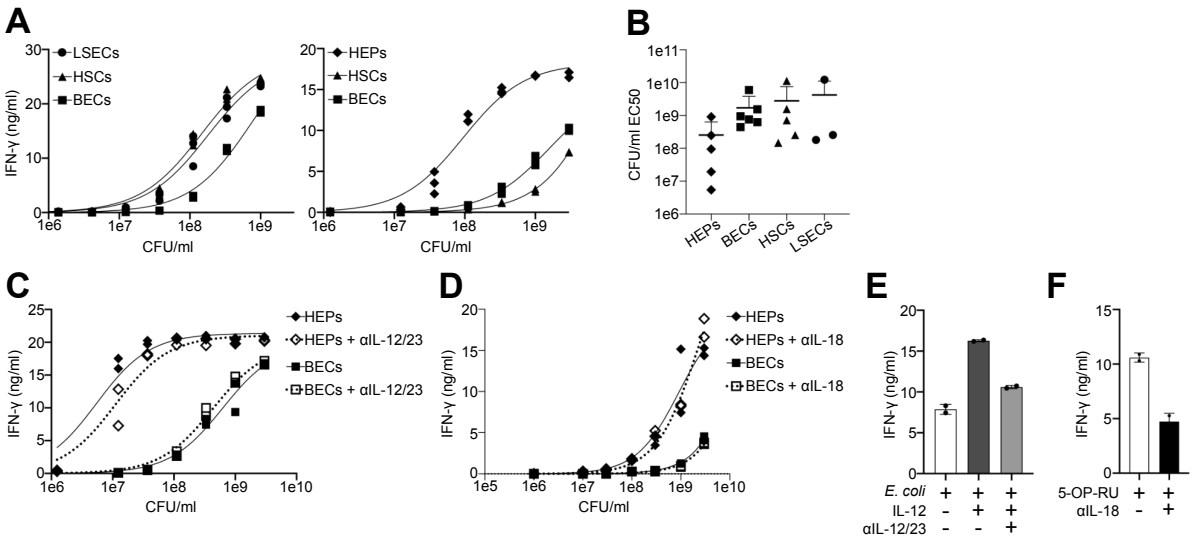

Supplementary Figure 5.
Characterisation of MR1-dependent Ag-presentation capabilities of primary liver cells exposed to *E. coli* lysate. In panels (A - F) IFN-γ production by MAIT cell clone SMC3 was measured by ELISA. (A) Two representative examples (left and right panels) of *E. coli* lysate (3e6 – 3e9 CFU/ml) titration using different primary cells (hepatocytes/HEPs, BECs, HSCs, and LSECs) as APCs. Three independent replicates per dose are depicted. (B) Pooled results of all experiments performed as shown in panel (A). Shown are concentrations of lysate needed to reach EC50 of IFN-γ secretion. Differences between APCs did not reach statistical significance as determined by paired Student's t-test. (C and D) Representative examples of *E. coli* lysate (3e6 – 6e9 CFU/ml) titration using primary hepatocytes/HEPs and BECs as APCs, either in the absence or presence of IL-12/23 (C) or IL-18 (D) blocking Abs. Other details are as in panel (A). (E) Confirmation of blocking efficiency of the anti-IL-12/23 Ab. BECs were stimulated with *E. coli* lysate (1e6 CFU/ml) in the absence or presence of IL-12 and anti-IL-12/23 Ab. (F) Confirmation of blocking efficiency of the anti-IL-18 Ab. THP-1 cells were stimulated with 1 nM 5-OP-RU in the absence or presence of Ab blocking IL-18.

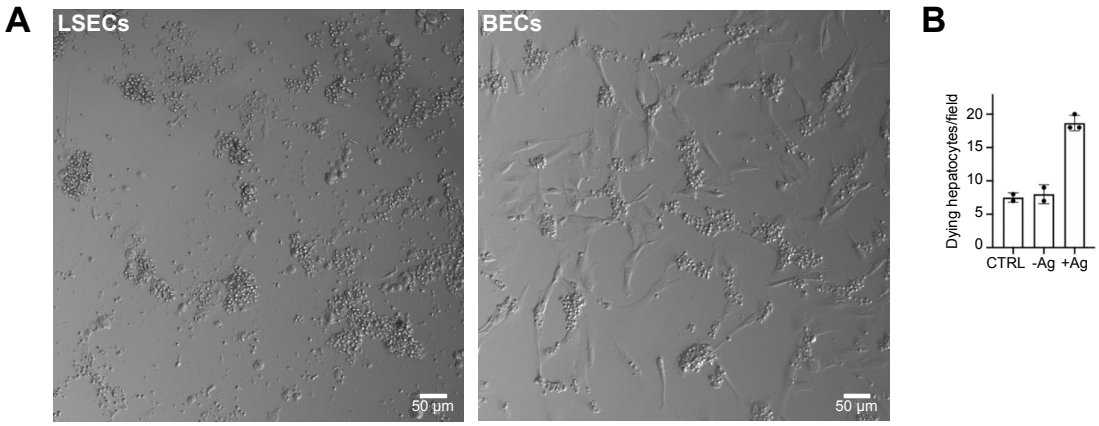

Supplementary Figure 6.
Killing efficiency of MAIT cells in response to activation by liver APCs. (A) Representative pictures of LSECs and BECs, exposed to 3 nM 5-OP-RU for 2 h, and then co-cultured with MAIT cell clone SMC3 for 36 h. The LSECs of this patient were very efficiently activating MAIT cell clone SCM3 (corresponding data shown in Fig. 4B, lowest point in the LSEC column), paralleled by an efficient killing of the LSECs. In contrast, most BECs were surviving the co-culture, consistent with a less efficient MAIT cell activation and killing capacity. (B) Quantification of hepatocyte killing, as visualized by time-lapse microscopy (as shown in the Supplementary Videos), by the liver-derived MAIT cell line MAIT-BSL-19, following activation using mixture of 3 nM 5-OP-RU and *E. coli* lysate (3e9 CFU/ml) (+ Ag). Hepatocytes alone (CTRL) and hepatocytes co-cultured with MAIT-BSL-19 cells, without any Ag (- Ag), served as negative controls.

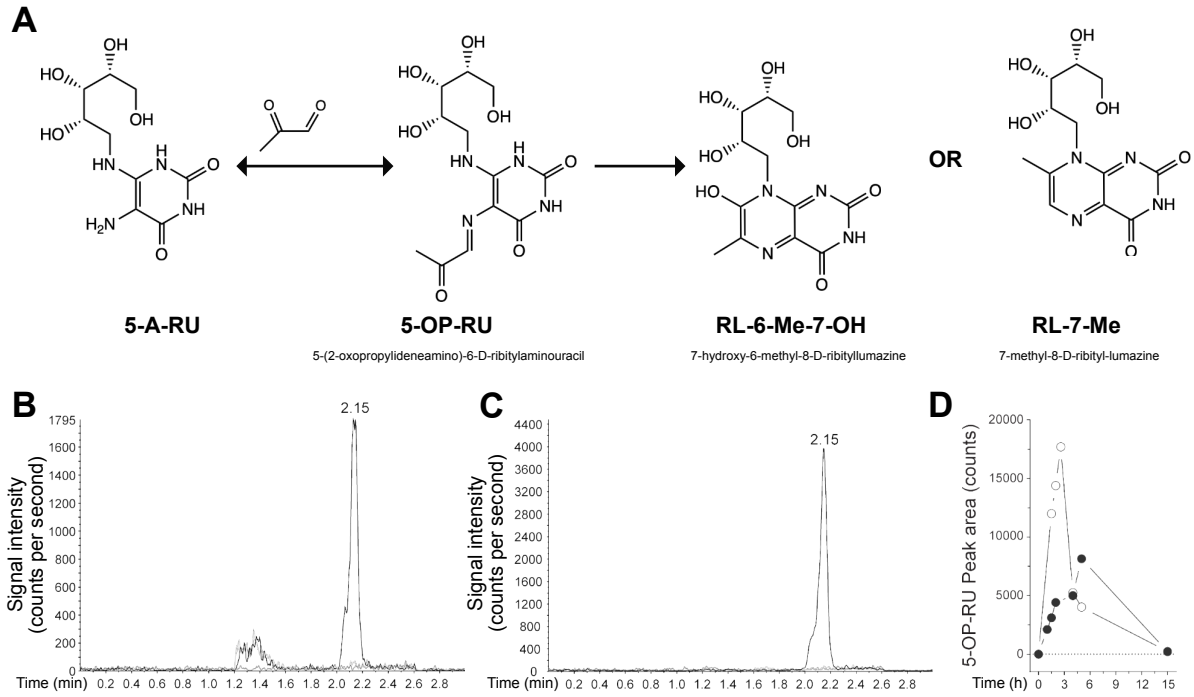

Supplementary Figure 7.
Scheme of 5-OP-RU formation and its detection by LC-MS/MS. (A) Scheme of generation of 5-OP-RU from 5-A-RU and methylglyoxal, and of catabolism of 5-OP-RU, adapted from Corbett et al. (9) (B) Overlay of three LC-MS/MS chromatograms of 5-OP-RU determined in cell lysate of THP-1 cells (black, 5-OP-RU following 5 h incubation; light grey, 5-OP-RU following 15 h incubation; dark grey, pure methanol injection). 5-OP-RU exhibited a retention time of 2.14 min and was detected by selected reaction monitoring in the negative mode (mass transition: 329.0 m/z → 190.9 m/z). (C) Overlay of three LC-MS/MS chromatograms of 5-OP-RU determined in cell supernatant of THP-1 cells (black, 5-OP-RU following 2.6 h incubation; light grey, 5-OP-RU following 15 h incubation; dark grey, pure methanol injection). (D) LC-MS/MS analysis of cell extracts and the corresponding culture supernatants following incubation of THP-1 cells with 1 M 5-A-RU. Shown are time-course accumulation curves of 5-OP-RU in cell lysate (black circles) and cell culture supernatant (open circles).

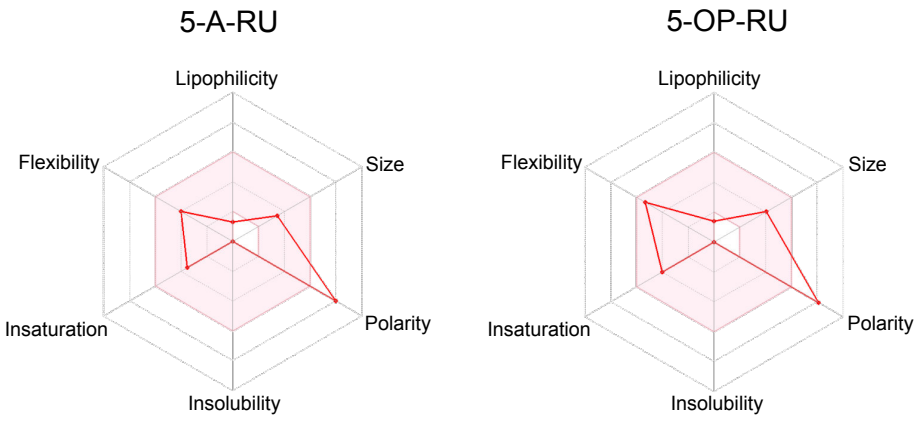

Molecular weight	276.3 Da
LogP	-2.3
TPSA	184 Å^2
Lipinski's rule	1 violation
Bioavailability score	**0.55**

Molecular weight	330.3 Da
LogP	-1.7
TPSA	188 Å^2
Lipinski's rule	2 violations
Bioavailability score	**0.17**

Supplementary Figure 8.
***In silico* modeling and bioavailability scores of 5-A-RU and 5-OP-RU.** *In silico* modeling was performed by applying a published method using a combination of physico-chemical parameters to the Ag 5-OP-RU and its precursor 5-A-RU.(15,16) We have selected 4 important parameters for display in this figure (molecular weight; LogP, corresponding to the partition coefficient in octanol/water; TPSA, total polar surface area; number of "Lipinski's rule" violations). A higher bioavailability score corresponds to higher probability of intestinal absorption. The score was calculated using an online tool for bioavailability. (17)

Supplementary Videos

Supplementary Videos V1-7. Killing efficiency of MAIT cells in response to activation by hepatocytes. Co-culture of hepatocytes with liver-derived MAIT cell line MAIT-BSL-19, using a mixture of 5-OP-RU (3 nM) and *E. coli* lysate (3e9 CFU/ml) as Ags. V1 - V3, cells co-cultured in the presence of Ags (labelled + Ag). V4 and V5, cells co-cultured in the absence of Ags (labelled - Ag). V6 and V7, hepatocytes cultured alone (labelled CTRL). Starting with the addition of MAIT cells to the culture, videos were taken for 15 h. The quantification of hepatocyte killing is shown in Supplementary Figure 6B.

References

1. Portmann S, Fahrner R, Lechleiter A, Keogh A, Overney S, Laemmle A, Mikami K, et al. Antitumor effect of SIRT1 inhibition in human HCC tumor models in vitro and in vivo. Mol Cancer Ther 2013;12:499-508.
2. Shetty S, Weston CJ, Oo YH, Westerlund N, Stamataki Z, Youster J, Hubscher SG, et al. Common lymphatic endothelial and vascular endothelial receptor-1 mediates the transmigration of regulatory T cells across human hepatic sinusoidal endothelium. J Immunol 2011;186:4147-4155.
3. Fabris L, Strazzabosco M, Crosby HA, Ballardini G, Hubscher SG, Kelly DA, Neuberger JM, et al. Characterization and isolation of ductular cells coexpressing neural cell adhesion molecule and Bcl-2 from primary cholangiopathies and ductal plate malformations. Am J Pathol 2000;156:1599-1612.
4. Boyum A. Separation of leukocytes from blood and bone marrow. Introduction. Scand J Clin Lab Invest Suppl 1968;97:7.
5. Schindelin J, Rueden CT, Hiner MC, Eliceiri KW. The ImageJ ecosystem: An open platform for biomedical image analysis. Mol Reprod Dev 2015;82:518-529.
6. Lepore M, Kalinichenko A, Calogero S, Kumar P, Paleja B, Schmaler M, Narang V, et al. Functionally diverse human T cells recognize non-microbial antigens presented by MR1. Elife 2017;6.
7. Huang S, Gilfillan S, Cella M, Miley MJ, Lantz O, Lybarger L, Fremont DH, et al. Evidence for MR1 antigen presentation to mucosal-associated invariant T cells. J Biol Chem 2005;280:21183-21193.
8. Lepore M, Kalinichenko A, Colone A, Paleja B, Singhal A, Tschumi A, Lee B, et al. Parallel T-cell cloning and deep sequencing of human MAIT cells reveal stable oligoclonal TCRbeta repertoire. Nat Commun 2014;5:3866.
9. **Corbett AJ**, **Eckle SB**, **Birkinshaw RW**, **Liu L**, Patel O, Mahony J, Chen Z, et al. T-cell activation by transitory neo-antigens derived from distinct microbial pathways. Nature 2014;509:361-365.
10. Grubman SA, Perrone RD, Lee DW, Murray SL, Rogers LC, Wolkoff LI, Mulberg AE, et al. Regulation of intracellular pH by immortalized human intrahepatic biliary epithelial cell lines. Am J Physiol 1994;266:G1060-1070.
11. Aden DP, Fogel A, Plotkin S, Damjanov I, Knowles BB. Controlled synthesis of HBsAg in a differentiated human liver carcinoma-derived cell line. Nature 1979;282:615-616.
12. Nakabayashi H, Taketa K, Miyano K, Yamane T, Sato J. Growth of human hepatoma cells lines with differentiated functions in chemically defined medium. Cancer Res 1982;42:3858-3863.

13. Xu L, Hui AY, Albanis E, Arthur MJ, O'Byrne SM, Blaner WS, Mukherjee P, et al. Human hepatic stellate cell lines, LX-1 and LX-2: new tools for analysis of hepatic fibrosis. Gut 2005;54:142-151.
14. Matsumura T, Takesue M, Westerman KA, Okitsu T, Sakaguchi M, Fukazawa T, Totsugawa T, et al. Establishment of an immortalized human-liver endothelial cell line with SV40T and hTERT. Transplantation 2004;77:1357-1365.
15. Lipinski CA, Lombardo F, Dominy BW, Feeney PJ. Experimental and computational approaches to estimate solubility and permeability in drug discovery and development settings. Adv Drug Deliv Rev 2001;46:3-26.
16. Martin YC. A bioavailability score. J Med Chem 2005;48:3164-3170.
17. Daina A, Michielin O, Zoete V. SwissADME: a free web tool to evaluate pharmacokinetics, drug-likeness and medicinal chemistry friendliness of small molecules. Sci Rep 2017;7:42717.

Author names in bold designate shared co-first authorship.

VII. References

Aagaard, B.D., Heyworth, M.F., Oesterle, A.L., Jones, A.L., and Way, L.W. (1996). Intestinal immunisation with Escherichia coli protects rats against Escherichia coli induced cholangitis. Gut *39*, 136–140.

Aizarani, N., Saviano, A., Sagar, null, Mailly, L., Durand, S., Herman, J.S., Pessaux, P., Baumert, T.F., and Grün, D. (2019). A human liver cell atlas reveals heterogeneity and epithelial progenitors. Nature *572*, 199–204.

Aldemir, H., Prod'homme, V., Dumaurier, M.-J., Retiere, C., Poupon, G., Cazareth, J., Bihl, F., and Braud, V.M. (2005). Cutting edge: lectin-like transcript 1 is a ligand for the CD161 receptor. J. Immunol. *175*, 7791–7795.

Aliyari Serej, Z., Ebrahimi Kalan, A., Mehdipour, A., and Nozad Charoudeh, H. (2017). Regulation and roles of CD26/DPPIV in hematopoiesis and diseases. Biomedicine & Pharmacotherapy *91*, 88–94.

Aust, J.G., Gays, F., Mickiewicz, K.M., Buchanan, E., and Brooks, C.G. (2009). The Expression and Function of the NKRP1 Receptor Family in C57BL/6 Mice. The Journal of Immunology *183*, 106–116.

Awad, W., Ler, G.J.M., Xu, W., Keller, A.N., Mak, J.Y.W., Lim, X.Y., Liu, L., Eckle, S.B.G., Le Nours, J., McCluskey, J., et al. (2020). The molecular basis underpinning the potency and specificity of MAIT cell antigens. Nat. Immunol. *21*, 400–411.

Baba, T., Ishizu, A., Iwasaki, S., Suzuki, A., Tomaru, U., Ikeda, H., Yoshiki, T., and Kasahara, M. (2006). CD4+/CD8+ macrophages infiltrating at inflammatory sites: a population of monocytes/macrophages with a cytotoxic phenotype. Blood *107*, 2004–2012.

Bailey, S.R., Nelson, M.H., Majchrzak, K., Bowers, J.S., Wyatt, M.M., Smith, A.S., Neal, L.R., Shirai, K., Carpenito, C., June, C.H., et al. (2017). Human CD26 high T cells elicit tumor immunity against multiple malignancies via enhanced migration and persistence. Nat Commun *8*, 1–13.

Balaban, Y.H., Korkusuz, P., Simsek, H., Gokcan, H., Gedikoglu, G., Pinar, A., Hascelik, G., Asan, E., Hamaloglu, E., and Tatar, G. (2007). Dipeptidyl peptidase IV (DDP IV) in NASH patients. Ann Hepatol *6*, 242–250.

Bambard, N.D., Mathew, S.O., and Mathew, P.A. (2010). LLT1-mediated Activation of IFN-γ Production in Human Natural Killer Cells Involves ERK Signalling Pathway. Scandinavian Journal of Immunology *71*, 210–219.

Bansal, T., Alaniz, R.C., Wood, T.K., and Jayaraman, A. (2010). The bacterial signal indole increases epithelial-cell tight-junction resistance and attenuates indicators of inflammation. Proc. Natl. Acad. Sci. U.S.A. *107*, 228–233.

Barathan, M. (2016). Peripheral loss of CD8+ CD161++ TCRValpha7.2+ mucosal-associated invariant T cells in chronic hepatitis C virus-infected patients. Eur. J. Clin. Invest. *46*.

Barcelo, A., Claustre, J., Toumi, F., Burlet, G., Chayvialle, J.-A., Cuber, J.-C., and Plaisancié, P. (2001). Effect of Bile Salts on Colonic Mucus Secretion in Isolated Vascularly Perfused Rat Colon. Dig Dis Sci *46*, 1223–1231.

Baskaran, S., Prasanna Rajan, D., and Balasubramanian, K.A. (1989). Formation of methylglyoxal by bacteria isolated from human faeces. Journal of Medical Microbiology *28*, 211–215.

Bedin, A.-S., Molès, J.-P., Rutagwera, D., Nagot, N., Kankasa, C., Tylleskär, T., Valverde-Villegas, J.M., Durand, M., Van de Perre, P., and Tuaillon, E. (2019). MAIT cells, TCR γδ+ cells and ILCs cells in human breast milk and blood from HIV infected and uninfected women. Pediatr Allergy Immunol *30*, 479–487.

Begley, M., Gahan, C.G.M., and Hill, C. (2005). The interaction between bacteria and bile. FEMS Microbiology Reviews *29*, 625–651.

Bertrand, C.P., and Ponath, P.D. (2000). CCR3 blockade as a new therapy for asthma. Expert Opin Investig Drugs *9*, 43–52.

Billerbeck, E. (2010). Analysis of CD161 expression on human CD8+ T cells defines a distinct functional subset with tissue-homing properties. Proc. Natl Acad. Sci. USA *107*.

Blériot, C., and Ginhoux, F. (2019). Understanding the Heterogeneity of Resident Liver Macrophages. Front Immunol *10*.

Boles, K.S., Barten, R., Kumaresan, P.R., Trowsdale, J., and Mathew, P.A. (1999). Cloning of a new lectin-like receptor expressed on human NK cells. Immunogenetics *50*, 1–7.

Bolte, F.J. (2017). Intra-hepatic depletion of mucosal-associated invariant T cells in hepatitis C virus-induced liver inflammation. Gastroenterology *153*.

Booijink, C.C.G.M., El-Aidy, S., Rajilić-Stojanović, M., Heilig, H.G.H.J., Troost, F.J., Smidt, H., Kleerebezem, M., De Vos, W.M., and Zoetendal, E.G. (2010). High temporal and inter-individual variation detected in the human ileal microbiota. Environ. Microbiol. *12*, 3213–3227.

Böttcher, K., Rombouts, K., Saffioti, F., Roccarina, D., Rosselli, M., Hall, A., Luong, T., Tsochatzis, E.A., Thorburn, D., and Pinzani, M. (2018). MAIT cells are chronically activated in patients with autoimmune liver disease and promote profibrogenic hepatic stellate cell activation. Hepatology *68*, 172–186.

Boursier, J., Mueller, O., Barret, M., Machado, M., Fizanne, L., Araujo-Perez, F., Guy, C.D., Seed, P.C., Rawls, J.F., David, L.A., et al. (2016). The severity of NAFLD is associated with gut dysbiosis and shift in the metabolic function of the gut microbiota. Hepatology *63*, 764–775.

Braakman, E., van de Winkel, J.G.J., van Krimpen, B.A., Jansze, M., and Bolhuis, R.L.H. (1992). CD16 on human γδ T lymphocytes: Expression, function, and specificity for mouse IgG isotypes. Cellular Immunology *143*, 97–107.

Brozova, J., Karlova, I., and Novak, J. (2016). Analysis of the Phenotype and Function of the Subpopulations of Mucosal-Associated Invariant T Cells. Scandinavian Journal of Immunology *84*, 245–251.

Brunt, E.M., Wong, V.W.-S., Nobili, V., Day, C.P., Sookoian, S., Maher, J.J., Bugianesi, E., Sirlin, C.B., Neuschwander-Tetri, B.A., and Rinella, M.E. (2015). Nonalcoholic fatty liver disease. Nat Rev Dis Primers *1*, 1–22.

Bryceson, Y.T., March, M.E., Ljunggren, H.-G., and Long, E.O. (2006). Synergy among receptors on resting NK cells for the activation of natural cytotoxicity and cytokine secretion. Blood *107*, 159–166.

Bunker, J.J., Erickson, S.A., Flynn, T.M., Henry, C., Koval, J.C., Meisel, M., Jabri, B., Antonopoulos, D.A., Wilson, P.C., and Bendelac, A. (2017). Natural polyreactive IgA antibodies coat the intestinal microbiota. Science *358*.

Casrouge, A., Sauer, A.V., Silva, R.B. da, Tejera-Alhambra, M., Sánchez-Ramón, S., ICAReB, Cancrini, C., Ingersoll, M.A., Aiuti, A., and Albert, M.L. (2018). Lymphocytes are a major source of circulating soluble dipeptidyl peptidase 4. Clinical and Experimental Immunology *194*, 166.

Catalfamo, M., and Henkart, P.A. (2003). Perforin and the granule exocytosis cytotoxicity pathway. Curr. Opin. Immunol. *15*, 522–527.

Celinski, K., Konturek, P.C., Slomka, M., Cichoz-Lach, H., Brzozowski, T., Konturek, S.J., and Korolczuk, A. (2014). Effects of treatment with melatonin and tryptophan on liver enzymes, parameters of fat metabolism and plasma levels of cytokines in patients with non-alcoholic fatty liver disease--14 months follow up. J. Physiol. Pharmacol. *65*, 75–82.

Chambers, W.H., Vujanovic, N.L., DeLeo, A.B., Olszowy, M.W., Herberman, R.B., and Hiserodt, J.C. (1989). Monoclonal antibody to a triggering structure expressed on rat natural killer cells and adherent lymphokine-activated killer cells. J. Exp. Med. *169*, 1373–1389.

Chan, W.K., Rujkijyanont, P., Neale, G., Yang, J., Bari, R., Gupta, N.D., Holladay, M., Rooney, B., and Leung, W. (2013). Multiplex and Genome-Wide Analyses Reveal Distinctive Properties of KIR+ and CD56+ T Cells in Human Blood. The Journal of Immunology *191*, 1625–1636.

Chaplen, F.W.R., Fahl, W.E., and Cameron, D.C. (1998). Evidence of high levels of methylglyoxal in cultured Chinese hamster ovary cells. Proc Natl Acad Sci U S A *95*, 5533–5538.

Chen, P., Deng, W., Li, D., Zeng, T., Huang, L., Wang, Q., Wang, J., Zhang, W., Yu, X., Duan, D., et al. (2019). Circulating Mucosal-Associated Invariant T Cells in a Large Cohort of Healthy Chinese Individuals From Newborn to Elderly. Front. Immunol. *10*.

Chen, X., Li, X., Zhai, X., Zhi, X., Cao, L., Qin, L., and Su, J. (2018). Shikimic Acid Inhibits Osteoclastogenesis in Vivo and in Vitro by Blocking RANK/TRAF6 Association and Suppressing NF-κB and MAPK Signaling Pathways. Cell. Physiol. Biochem. *51*, 2858–2871.

Chiba, A. (2017). Activation status of mucosal-associated invariant T cells reflects disease activity and pathology of systemic lupus erythematosus. Arthritis Res. Ther. *19*.

Cho, Y.N. (2014). Mucosal-associated invariant T cell deficiency in systemic lupus erythematosus. J. Immunol. *193*.

Chou, L.S., and Weimer, B. (1999). Isolation and characterization of acid- and bile-tolerant isolates from strains of Lactobacillus acidophilus. J. Dairy Sci. *82*, 23–31.

Cisternas, I.S., Torres, A., Flores, A.F., and Angulo, V.A.G. (2017). Differential regulation of riboflavin supply genes in Vibrio cholerae. Gut Pathogens *9*, 10.

Clémenceau, B., Vivien, R., Debeaupuis, E., Esbelin, J., Biron, C., Levy, Y., and Vié, H. (2011). FcγRIIIa (CD16) Induction on Human T Lymphocytes and CD16pos T-Lymphocyte Amplification. Journal of Immunotherapy *34*, 542–549.

Clemente Carmine D. Anatomy: A Regional Atlas of the Human Body.

Constantinides, M.G., Link, V.M., Tamoutounour, S., Wong, A.C., Perez-Chaparro, P.J., Han, S.-J., Chen, Y.E., Li, K., Farhat, S., Weckel, A., et al. (2019). MAIT cells are imprinted by the microbiota in early life and promote tissue repair. Science *366*.

Corbett, A.J., Eckle, S.B.G., Birkinshaw, R.W., Liu, L., Patel, O., Mahony, J., Chen, Z., Reantragoon, R., Meehan, B., Cao, H., et al. (2014). T-cell activation by transitory neo-antigens derived from distinct microbial pathways. Nature *509*, 361–365.

Correia, M.P., Costa, A.V., Uhrberg, M., Cardoso, E.M., and Arosa, F.A. (2011). IL-15 induces CD8+ T cells to acquire functional NK receptors capable of modulating cytotoxicity and cytokine secretion. Immunobiology *216*, 604–612.

Crowther, M.D., Dolton, G., Legut, M., Caillaud, M.E., Lloyd, A., Attaf, M., Galloway, S.A.E., Rius, C., Farrell, C.P., Szomolay, B., et al. (2020). Genome-wide CRISPR–Cas9 screening reveals ubiquitous T cell cancer targeting via the monomorphic MHC class I-related protein MR1. Nature Immunology *21*, 178–185.

De Boever, P., Wouters, R., Verschaeve, L., Berckmans, P., Schoeters, G., and Verstraete, W. (2000). Protective effect of the bile salt hydrolase-active Lactobacillus reuteri against bile salt cytotoxicity. Appl. Microbiol. Biotechnol. *53*, 709–714.

Depommier, C., Everard, A., Druart, C., Plovier, H., Van Hul, M., Vieira-Silva, S., Falony, G., Raes, J., Maiter, D., Delzenne, N.M., et al. (2019). Supplementation with Akkermansia muciniphila in overweight and obese human volunteers: a proof-of-concept exploratory study. Nat. Med. *25*, 1096–1103.

Derrien, M., Vaughan, E.E., Plugge, C.M., and de Vos, W.M. (2004). Akkermansia muciniphila gen. nov., sp. nov., a human intestinal mucin-degrading bacterium. Int. J. Syst. Evol. Microbiol. *54*, 1469–1476.

Di Rienzi, S.C., Sharon, I., Wrighton, K.C., Koren, O., Hug, L.A., Thomas, B.C., Goodrich, J.K., Bell, J.T., Spector, T.D., Banfield, J.F., et al. (2013). The human gut and groundwater harbor non-photosynthetic bacteria belonging to a new candidate phylum sibling to Cyanobacteria. ELife *2*.

Dias, J. (2018). The CD4−CD8− MAIT cell subpopulation is a functionally distinct subset developmentally related to the main CD8+ MAIT cell pool. Proc. Natl Acad. Sci. USA *115*.

Dias, J., Hengst, J., Parrot, T., Leeansyah, E., Lunemann, S., Malone, D.F.G., Hardtke, S., Strauss, O., Zimmer, C.L., Berglin, L., et al. (2019). Chronic hepatitis delta virus infection leads to functional impairment and severe loss of MAIT cells. Journal of Hepatology *71*, 301–312.

Dobie, R., Wilson-Kanamori, J.R., Henderson, B.E.P., Smith, J.R., Matchett, K.P., Portman, J.R., Wallenborg, K., Picelli, S., Zagorska, A., Pendem, S.V., et al. (2019). Single-Cell Transcriptomics Uncovers Zonation of Function in the Mesenchyme during Liver Fibrosis. Cell Rep *29*, 1832-1847.e8.

Dupont, A., Heinbockel, L., Brandenburg, K., and Hornef, M.W. (2014). Antimicrobial peptides and the enteric mucus layer act in concert to protect the intestinal mucosa. Gut Microbes *5*, 761–765.

Dusseaux, M., Martin, E., Serriari, N., Péguillet, I., Premel, V., Louis, D., Milder, M., Le Bourhis, L., Soudais, C., Treiner, E., et al. (2011). Human MAIT cells are xenobiotic-resistant, tissue-targeted, CD161hi IL-17-secreting T cells. Blood *117*, 1250–1259.

Eadala, P., Matthews, S.B., Waud, J.P., Green, J.T., and Campbell, A.K. (2011). Association of lactose sensitivity with inflammatory bowel disease--demonstrated by analysis of genetic polymorphism, breath gases and symptoms. Aliment. Pharmacol. Ther. *34*, 735–746.

Eckle, S.B.G., Birkinshaw, R.W., Kostenko, L., Corbett, A.J., McWilliam, H.E.G., Reantragoon, R., Chen, Z., Gherardin, N.A., Beddoe, T., Liu, L., et al. (2014). A molecular basis underpinning the T cell receptor heterogeneity of mucosal-associated invariant T cells. J Exp Med *211*, 1585–1600.

Esser, C., Bargen, I., Weighardt, H., Haarmann-Stemmann, T., and Krutmann, J. (2013). Functions of the aryl hydrocarbon receptor in the skin. Semin Immunopathol *35*, 677–691.

Exley, M., Garcia, J., Balk, S.P., and Porcelli, S. (1997). Requirements for CD1d recognition by human invariant Valpha24+ CD4-CD8- T cells. J. Exp. Med. *186*, 109–120.

Exley, M., Porcelli, S., Furman, M., Garcia, J., and Balk, S. (1998). CD161 (NKR-P1A) Costimulation of CD1d-dependent Activation of Human T Cells Expressing Invariant Vα24JαQ T Cell Receptor α Chains. J Exp Med *188*, 867–876.

Fantuzzi, G., Puren, A.J., Harding, M.W., Livingston, D.J., and Dinarello, C.A. (1998). Interleukin-18 Regulation of Interferon γ Production and Cell Proliferation as Shown in Interleukin-1β–Converting Enzyme (Caspase-1)-Deficient Mice. Blood *91*, 2118–2125.

Fantuzzi, L., Tagliamonte, M., Gauzzi, M.C., and Lopalco, L. (2019). Dual CCR5/CCR2 targeting: opportunities for the cure of complex disorders. Cell Mol Life Sci *76*, 4869–4886.

Fergusson, J.R. (2016). CD161int CD8+ T cells: a novel population of highly functional, memory CD8+ T cells enriched within the gut. Mucosal Immunol. *9*.

Fergusson, J.R., Smith, K.E., Fleming, V.M., Rajoriya, N., Newell, E.W., Simmons, R., Marchi, E., Björkander, S., Kang, Y.-H., Swadling, L., et al. (2014). CD161 defines a transcriptional and functional phenotype across distinct human T cell lineages. Cell Rep *9*, 1075–1088.

Flahaut, S., Hartke, A., Giard, J.C., Benachour, A., Boutibonnes, P., and Auffray, Y. (1996). Relationship between stress response toward bile salts, acid and heat treatment in Enterococcus faecalis. FEMS Microbiol. Lett. *138*, 49–54.

Flint, H.J., Scott, K.P., Duncan, S.H., Louis, P., and Forano, E. (2012). Microbial degradation of complex carbohydrates in the gut. Gut Microbes *3*, 289–306.

Floch, M.H., Gershengoren, W., Elliott, S., and Spiro, H.M. (1971). Bile Acid inhibition of the intestinal microflora—A function for simple bile acids? Gastroenterology *61*, 228–233.

Freeman, M.L., Morris, S.R., and Lederman, M.M. (2017). CD161 Expression on Mucosa-Associated Invariant T Cells is Reduced in HIV-Infected Subjects Undergoing Antiretroviral Therapy Who Do Not Recover CD4+ T Cells. Pathog Immun *2*, 335–351.

Furie, B., Bouchard, B.A., and Furie, B.C. (1999). Vitamin K-dependent biosynthesis of gamma-carboxyglutamic acid. Blood *93*, 1798–1808.

Garcia, K.C., Scott, C.A., Brunmark, A., Carbone, F.R., Peterson, P.A., Wilson, I.A., and Teyton, L. (1996). CD8 enhances formation of stable T-cell receptor/MHC class I molecule complexes. Nature *384*, 577–581.

Geerts, A. (2001). History, heterogeneity, developmental biology, and functions of quiescent hepatic stellate cells. Semin. Liver Dis. *21*, 311–335.

Georgel, P., Radosavljevic, M., Macquin, C., and Bahram, S. (2011). The non-conventional MHC class I MR1 molecule controls infection by Klebsiella pneumoniae in mice. Mol. Immunol. *48*.

Gherardin, N.A., Loh, L., Admojo, L., Davenport, A.J., Richardson, K., Rogers, A., Darcy, P.K., Jenkins, M.R., Prince, H.M., Harrison, S.J., et al. (2018). Enumeration, functional responses and cytotoxic capacity of MAIT cells in newly diagnosed and relapsed multiple myeloma. Sci Rep *8*, 1–14.

Gibbs, A. (2017). MAIT cells reside in the female genital mucosa and are biased towards IL-17 and IL-22 production in response to bacterial stimulation. Mucosal Immunol. *10*.

Gierahn, T.M., Wadsworth, M.H., Hughes, T.K., Bryson, B.D., Butler, A., Satija, R., Fortune, S., Love, J.C., and Shalek, A.K. (2017). Seq-Well: portable, low-cost RNA sequencing of single cells at high throughput. Nat. Methods *14*, 395–398.

Gill, S.R., Pop, M., DeBoy, R.T., Eckburg, P.B., Turnbaugh, P.J., Samuel, B.S., Gordon, J.I., Relman, D.A., Fraser-Liggett, C.M., and Nelson, K.E. (2006). Metagenomic Analysis of the Human Distal Gut Microbiome. Science *312*, 1355–1359.

Glaser, S., Francis, H., DeMorrow, S., LeSage, G., Fava, G., Marzioni, M., Venter, J., and Alpini, G. (2006). Heterogeneity of the intrahepatic biliary epithelium. World J Gastroenterol *12*, 3523–3536.

Gnoth, M.J., Kunz, C., Kinne-Saffran, E., and Rudloff, S. (2000). Human milk oligosaccharides are minimally digested in vitro. J. Nutr. *130*, 3014–3020.

Gold, M.C., Cerri, S., Smyk-Pearson, S., Cansler, M.E., Vogt, T.M., Delepine, J., Winata, E., Swarbrick, G.M., Chua, W.-J., Yu, Y.Y.L., et al. (2010). Human mucosal associated invariant T cells detect bacterially infected cells. PLoS Biol. *8*, e1000407.

Gold, M.C., Eid, T., Smyk-Pearson, S., Eberling, Y., Swarbrick, G.M., Langley, S.M., Streeter, P.R., Lewinsohn, D.A., and Lewinsohn, D.M. (2013). Human thymic MR1-restricted MAIT cells are innate pathogen-reactive effectors that adapt following thymic egress. Mucosal Immunol *6*, 35–44.

Goldfinch, N., Reinink, P., Connelley, T., Koets, A., Morrison, I., and Van Rhijn, I. (2010). Conservation of mucosal associated invariant T (MAIT) cells and the MR1 restriction element in ruminants, and abundance of MAIT cells in spleen. Vet. Res. *41*, 62.

Goronzy, J.J., and Weyand, C.M. (2008). T-cell co-stimulatory pathways in autoimmunity. Arthritis Research & Therapy *10*, S3.

Gracey, E. (2016). IL-7 primes IL-17 in mucosal-associated invariant T (MAIT) cells, which contribute to the Th17-axis in ankylosing spondylitis. Ann. Rheum. Dis. *75*.

Greene, J.M. (2017). MR1-restricted mucosal-associated invariant T (MAIT) cells respond to mycobacterial vaccination and infection in nonhuman primates. Mucosal Immunol. *10*.

Grimaldi, D. (2014). Specific MAIT cell behaviour among innate-like T lymphocytes in critically ill patients with severe infections. Intensive Care Med. *40*.

Guia, S., Cognet, C., de Beaucoudrey, L., Tessmer, M.S., Jouanguy, E., Berger, C., Filipe-Santos, O., Feinberg, J., Camcioglu, Y., Levy, J., et al. (2008). A role for interleukin-12/23 in the maturation of human natural killer and CD56+ T cells in vivo. Blood *111*, 5008–5016.

Gustafsson, B.E., Daft, F.S., Mcdaniel, E.G., Smith, J.C., and Fitzgerald, R.J. (1962). Effects of vitamin K-active compounds and intestinal microorganisms in vitamin K-deficient germfree rats. J. Nutr. *78*, 461–468.

Gutierrez-Arcelus, M., Teslovich, N., Mola, A.R., Polidoro, R.B., Nathan, A., Kim, H., Hannes, S., Slowikowski, K., Watts, G.F.M., Korsunsky, I., et al. (2019). Lymphocyte innateness defined by transcriptional states reflects a balance between proliferation and effector functions. Nat Commun *10*.

Hansson, G.C. (2012). Role of mucus layers in gut infection and inflammation. Curr Opin Microbiol *15*, 57–62.

Hartmann, N., McMurtrey, C., Sorensen, M.L., Huber, M.E., Kurapova, R., Coleman, F.T., Mizgerd, J.P., Hildebrand, W., Kronenberg, M., Lewinsohn, D.M., et al. (2018). Riboflavin Metabolism Variation among Clinical Isolates of Streptococcus pneumoniae Results in Differential Activation of Mucosal-associated Invariant T Cells. Am J Respir Cell Mol Biol *58*, 767–776.

Hayashi, E. (2016). Involvement of mucosal-associated invariant T cells in ankylosing spondylitis. J. Rheumatol *43*.

He, T., Zhang, N., Wang, L., Wan, B., Wang, X., and Zhang, L. (2020). GPR43 regulates HBV X protein (HBx)-induced inflammatory response in human LO2 hepatocytes. Biomed. Pharmacother. *123*, 109737.

Hegde, P., Weiss, E., Paradis, V., Wan, J., Mabire, M., Sukriti, S., Rautou, P.-E., Albuquerque, M., Picq, O., Gupta, A.C., et al. (2018). Mucosal-associated invariant T cells are a profibrogenic immune cell population in the liver. Nat Commun *9*, 2146.

Hegen, M., Mittrücker, H.W., Hug, R., Demuth, H.U., Neubert, K., Barth, A., and Fleischer, B. (1993). Enzymatic activity of CD26 (dipeptidylpeptidase IV) is not required for its signalling function in T cells. Immunobiology *189*, 483–493.

Hegen, M., Kameoka, J., Dong, R.P., Schlossman, S.F., and Morimoto, C. (1997). Cross-linking of CD26 by antibody induces tyrosine phosphorylation and activation of mitogen-activated protein kinase. Immunology *90*, 257–264.

Henao-Mejia, J., Elinav, E., Jin, C., Hao, L., Mehal, W.Z., Strowig, T., Thaiss, C.A., Kau, A.L., Eisenbarth, S.C., Jurczak, M.J., et al. (2012). Inflammasome-mediated dysbiosis regulates progression of NAFLD and obesity. Nature *482*, 179–185.

Hendrikx, T., and Schnabl, B. (2019). Indoles: metabolites produced by intestinal bacteria capable of controlling liver disease manifestation. J. Intern. Med. *286*, 32–40.

Hengst, J. (2016). Nonreversible MAIT cell-dysfunction in chronic hepatitis C virus infection despite successful interferon-free therapy. Eur. J. Immunol. *46*.

Hinks, T.S.C., Marchi, E., Jabeen, M., Olshansky, M., Kurioka, A., Pediongco, T.J., Meehan, B.S., Kostenko, L., Turner, S.J., Corbett, A.J., et al. (2019). Activation and In Vivo Evolution of the MAIT Cell Transcriptome in Mice and Humans Reveals Tissue Repair Functionality. Cell Reports *28*, 3249-3262.e5.

Howson, L.J., Salio, M., and Cerundolo, V. (2015). MR1-Restricted Mucosal-Associated Invariant T Cells and Their Activation during Infectious Diseases. Front Immunol *6*, 303.

Huang, J.Y., Lee, S.M., and Mazmanian, S.K. (2011). The human commensal Bacteroides fragilis binds intestinal mucin. Anaerobe *17*, 137–141.

Huang, S., Gilfillan, S., Cella, M., Miley, M.J., Lantz, O., Lybarger, L., Fremont, D.H., and Hansen, T.H. (2005). Evidence for MR1 antigen presentation to mucosal-associated invariant T cells. J. Biol. Chem. *280*, 21183–21193.

Huang, S., Martin, E., Kim, S., Yu, L., Soudais, C., Fremont, D.H., Lantz, O., and Hansen, T.H. (2009). MR1 antigen presentation to mucosal-associated invariant T cells was highly conserved in evolution. Proc Natl Acad Sci U S A *106*, 8290–8295.

Hughes, T.K., Wadsworth, M.H., Gierahn, T.M., Do, T., Weiss, D., Andrade, P.R., Ma, F., de Andrade Silva, B.J., Shao, S., Tsoi, L.C., et al. (2019). Highly Efficient, Massively-Parallel Single-Cell RNA-Seq Reveals Cellular States and Molecular Features of Human Skin Pathology. BioRxiv.

Idris, I., and Donnelly, R. (2007). Dipeptidyl peptidase-IV inhibitors: a major new class of oral antidiabetic drug. Diabetes Obes Metab *9*, 153–165.

Ishimori, A. (2017). Circulating activated innate lymphoid cells and mucosal-associated invariant T cells are associated with airflow limitation in patients with asthma. Allergol. Int. *66*.

Itou, M., Kawaguchi, T., Taniguchi, E., and Sata, M. (2013). Dipeptidyl peptidase-4: A key player in chronic liver disease. World J Gastroenterol *19*, 2298–2306.

Jarry, A., Cerf-bensussan, N., Brousse, N., Selz, F., and Guy-grand, D. (1990). Subsets of CD3+ (T cell receptor α/β or γ/δ) and CD3− lymphocytes isolated from normal human gut epithelium display phenotypical features different from their counterparts in peripheral blood. European Journal of Immunology *20*, 1097–1103.

Jeffery, H.C., van Wilgenburg, B., Kurioka, A., Parekh, K., Stirling, K., Roberts, S., Dutton, E.E., Hunter, S., Geh, D., Braitch, M.K., et al. (2016). Biliary epithelium and liver B cells exposed to bacteria activate intrahepatic MAIT cells through MR1. J. Hepatol. *64*, 1118–1127.

Jia, E., Liu, Z., Pan, M., Lu, J., and Ge, Q. (2019). Regulation of bile acid metabolism-related signaling pathways by gut microbiota in diseases. J Zhejiang Univ Sci B *20*, 781–792.

Jiang, X., Lian, M., Li, Y., Zhang, W., Wang, Q., Wei, Y., Zhang, J., Chen, W., Xiao, X., Miao, Q., et al. (2018). The immunobiology of mucosal-associated invariant T cell (MAIT) function in primary biliary cholangitis: Regulation by cholic acid-induced Interleukin-7. J. Autoimmun. *90*, 64–75.

Jo, J., Tan, A.T., Ussher, J.E., Sandalova, E., Tang, X.-Z., Tan-Garcia, A., To, N., Hong, M., Chia, A., Gill, U.S., et al. (2014). Toll-Like Receptor 8 Agonist and Bacteria Trigger Potent Activation of Innate Immune Cells in Human Liver. PLoS Pathog *10*.

Jungermann, K., and Keitzmann, T. (1996). Zonation of Parenchymal and Nonparenchymal Metabolism in Liver. Annual Review of Nutrition *16*, 179–203.

Kalra, A., and Tuma, F. (2020). Physiology, Liver. In StatPearls, (Treasure Island (FL): StatPearls Publishing), p.

Karamooz, E., Harriff, M.J., and Lewinsohn, D.M. (2018). MR1-dependent antigen presentation. Semin. Cell Dev. Biol. *84*.

Karamooz, E., Harriff, M.J., Narayanan, G.A., Worley, A., and Lewinsohn, D.M. (2019). MR1 recycling and blockade of endosomal trafficking reveal distinguishable antigen presentation pathways between Mycobacterium tuberculosis infection and exogenously delivered antigens. Sci Rep *9*, 1–11.

Karlstadt, R.G., Hogan, D.L., and Foxx-orenstein, A. (2004). 36 - Normal Physiology of the Gastrointestinal Tract and Gender Differences. In Principles of Gender-Specific Medicine, M.J. Legato, ed. (San Diego: Academic Press), pp. 377–396.

Kau, A.L., Planer, J.D., Liu, J., Rao, S., Yatsunenko, T., Trehan, I., Manary, M.J., Liu, T.-C., Stappenbeck, T.S., Maleta, K.M., et al. (2015). Functional characterization of IgA-targeted bacterial taxa from undernourished Malawian children that produce diet-dependent enteropathy. Sci Transl Med *7*, 276ra24.

Kawachi, I., Maldonado, J., Strader, C., and Gilfillan, S. (2006). MR1-Restricted Vα19i Mucosal-Associated Invariant T Cells Are Innate T Cells in the Gut Lamina Propria That Provide a Rapid and Diverse Cytokine Response. The Journal of Immunology *176*, 1618–1627.

Kawaguchi, T., Izumi, N., Charlton, M.R., and Sata, M. (2011). Branched-chain amino acids as pharmacological nutrients in chronic liver disease. Hepatology *54*, 1063–1070.

Keller, A.N., Eckle, S.B.G., Xu, W., Liu, L., Hughes, V.A., Mak, J.Y.W., Meehan, B.S., Pediongco, T., Birkinshaw, R.W., Chen, Z., et al. (2017). Drugs and drug-like molecules can modulate the function of mucosal-associated invariant T cells. Nat. Immunol. *18*, 402–411.

Kim, N.H., Park, J.H., Park, J., and Joung, Y.-H. (2017). The Effect of Deoxycholic Acid on Secretion and Motility in the Rat and Guinea Pig Large Intestine. J Neurogastroenterol Motil *23*, 606–615.

Kimoto, H., Ohmomo, S., and Okamoto, T. (2002). Enhancement of bile tolerance in lactococci by Tween 80. J. Appl. Microbiol. *92*, 41–46.

Kirkham, C.L., and Carlyle, J.R. (2014). Complexity and Diversity of the NKR-P1:Clr (Klrb1:Clec2) Recognition Systems. Front Immunol *5*.

Kitajima, Y., Takahashi, H., Akiyama, T., Murayama, K., Iwane, S., Kuwashiro, T., Tanaka, K., Kawazoe, S., Ono, N., Eguchi, T., et al. (2018). Supplementation with branched-chain amino acids ameliorates hypoalbuminemia, prevents sarcopenia, and reduces fat accumulation in the skeletal muscles of patients with liver cirrhosis. J. Gastroenterol. *53*, 427–437.

Kjer-Nielsen, L., Patel, O., Corbett, A.J., Le Nours, J., Meehan, B., Liu, L., Bhati, M., Chen, Z., Kostenko, L., Reantragoon, R., et al. (2012). MR1 presents microbial vitamin B metabolites to MAIT cells. Nature *491*, 717–723.

Knolle, P.A. (2016). Staying local-antigen presentation in the liver. Curr. Opin. Immunol. *40*, 36–42.

Kristiansen, T.Z., Bunkenborg, J., Gronborg, M., Molina, H., Thuluvath, P.J., Argani, P., Goggins, M.G., Maitra, A., and Pandey, A. (2004). A Proteomic Analysis of Human Bile. Molecular & Cellular Proteomics *3*, 715–728.

Kuric, E. (2018). No evidence for presence of mucosal-associated invariant T cells in the insulitic lesions in patients recently diagnosed with type 1 diabetes. Am. J. Pathol. *188*.

Kurioka, A., Jahun, A.S., Hannaway, R.F., Walker, L.J., Fergusson, J.R., Sverremark-Ekström, E., Corbett, A.J., Ussher, J.E., Willberg, C.B., and Klenerman, P. (2017). Shared and Distinct Phenotypes and Functions of Human CD161++ Vα7.2+ T Cell Subsets. Front Immunol *8*.

Kuwabara, T., Ishikawa, F., Kondo, M., and Kakiuchi, T. (2017). The Role of IL-17 and Related Cytokines in Inflammatory Autoimmune Diseases. Mediators Inflamm *2017*.

Lai, J.-J., Cruz, F.M., and Rock, K.L. (2020). Immune Sensing of Cell Death through Recognition of Histone Sequences by C-Type Lectin-Receptor-2d Causes Inflammation and Tissue Injury. Immunity *52*, 123-135.e6.

Lamichhane, R., Schneider, M., de la Harpe, S.M., Harrop, T.W.R., Hannaway, R.F., Dearden, P.K., Kirman, J.R., Tyndall, J.D.A., Vernall, A.J., and Ussher, J.E. (2019). TCR- or Cytokine-Activated CD8+ Mucosal-Associated Invariant T Cells Are Rapid Polyfunctional Effectors That Can Coordinate Immune Responses. Cell Reports *28*, 3061-3076.e5.

Lanier, L.L., Chang, C., and Phillips, J.H. Human NKR-P1A. A disulfide-linked homodimer of the C-type lectin superfamily expressed by a subset of NK and T lymphocytes. 13.

Lantz, O., and Legoux, F. (2018). MAIT cells: an historical and evolutionary perspective. Immunol. Cell Biol. *96*, 564–572.

Larsson, J.M.H., Karlsson, H., Sjövall, H., and Hansson, G.C. (2009). A complex, but uniform O-glycosylation of the human MUC2 mucin from colonic biopsies analyzed by nanoLC/MSn. Glycobiology *19*, 756–766.

Lazarova, D.L., Chiaro, C., Wong, T., Drago, E., Rainey, A., O'Malley, S., and Bordonaro, M. (2013). CBP Activity Mediates Effects of the Histone Deacetylase Inhibitor Butyrate on WNT Activity and Apoptosis in Colon Cancer Cells. J Cancer *4*, 481–490.

Le Bourhis, L., Martin, E., Péguillet, I., Guihot, A., Froux, N., Coré, M., Lévy, E., Dusseaux, M., Meyssonnier, V., Premel, V., et al. (2010). Antimicrobial activity of mucosal-associated invariant T cells. Nat. Immunol. *11*, 701–708.

Le Bourhis, L., Dusseaux, M., Bohineust, A., Bessoles, S., Martin, E., Premel, V., Coré, M., Sleurs, D., Serriari, N.-E., Treiner, E., et al. (2013). MAIT Cells Detect and Efficiently Lyse Bacterially-Infected Epithelial Cells. PLoS Pathog *9*.

Le Roy, T., Llopis, M., Lepage, P., Bruneau, A., Rabot, S., Bevilacqua, C., Martin, P., Philippe, C., Walker, F., Bado, A., et al. (2013). Intestinal microbiota determines development of non-alcoholic fatty liver disease in mice. Gut *62*, 1787–1794.

Lécuyer, E., Rakotobe, S., Lengliné-Garnier, H., Lebreton, C., Picard, M., Juste, C., Fritzen, R., Eberl, G., McCoy, K.D., Macpherson, A.J., et al. (2014). Segmented filamentous bacterium uses secondary and tertiary lymphoid tissues to induce gut IgA and specific T helper 17 cell responses. Immunity *40*, 608–620.

Lee, C.H., Zhang, H.H., Singh, S.P., Koo, L., Kabat, J., Tsang, H., Singh, T.P., and Farber, J.M. C/EBPδ drives interactions between human MAIT cells and endothelial cells that are important for extravasation. ELife *7*.

Legoux, F., Bellet, D., Daviaud, C., Morr, Y.E., Darbois, A., Niort, K., Procopio, E., Salou, M., Gilet, J., Ryffel, B., et al. (2019). Microbial metabolites control the thymic development of mucosal-associated invariant T cells. Science eaaw2719.

Leng, T., Akther, H.D., Hackstein, C.-P., Powell, K., King, T., Friedrich, M., Christoforidou, Z., McCuaig, S., Neyazi, M., Arancibia-Cárcamo, C.V., et al. (2019). TCR and Inflammatory Signals Tune Human MAIT Cells to Exert Specific Tissue Repair and Effector Functions. Cell Reports *28*, 3077-3091.e5.

Lepore, M., Kalinichenko, A., Kalinicenko, A., Colone, A., Paleja, B., Singhal, A., Tschumi, A., Lee, B., Poidinger, M., Zolezzi, F., et al. (2014). Parallel T-cell cloning and deep sequencing of human MAIT cells reveal stable oligoclonal TCRβ repertoire. Nat Commun *5*, 3866.

Lepore, M., Kalinichenko, A., Calogero, S., Kumar, P., Paleja, B., Schmaler, M., Narang, V., Zolezzi, F., Poidinger, M., Mori, L., et al. (2017). Functionally diverse human T cells recognize non-microbial antigens presented by MR1. ELife *6*, e24476.

Leverrier, P., Dimova, D., Pichereau, V., Auffray, Y., Boyaval, P., and Jan, G. (2003). Susceptibility and adaptive response to bile salts in Propionibacterium freudenreichii: physiological and proteomic analysis. Appl. Environ. Microbiol. *69*, 3809–3818.

Lezmi, G. (2018). Circulating IL-17-producing mucosal-associated invariant T cells (MAIT) are associated with symptoms in children with asthma. Clin. Immunol. *188*.

Li, Y., Huang, B., Jiang, X., Chen, W., Zhang, J., Wei, Y., Chen, Y., Lian, M., Bian, Z., Miao, Q., et al. (2018). Mucosal-Associated Invariant T Cells Improve Nonalcoholic Fatty Liver Disease Through Regulating Macrophage Polarization. Front Immunol *9*.

Linnemann, C., Schildberg, F.A., Schurich, A., Diehl, L., Hegenbarth, S.I., Endl, E., Lacher, S., Müller, C.E., Frey, J., Simeoni, L., et al. (2009). Adenosine regulates CD8 T-cell priming by inhibition of membrane-proximal T-cell receptor signalling. Immunology *128*, e728–e737.

Lipinski, C.A., Lombardo, F., Dominy, B.W., and Feeney, P.J. (2001). Experimental and computational approaches to estimate solubility and permeability in drug discovery and development settings. Adv. Drug Deliv. Rev. *46*, 3–26.

Llibre, A., Klenerman, P., and Willberg, C.B. (2016a). Multi-functional lectin-like transcript-1: A new player in human immune regulation. Immunology Letters *177*, 62–69.

Llibre, A., López-Macías, C., Marafioti, T., Mehta, H., Partridge, A., Kanzig, C., Rivellese, F., Galson, J.D., Walker, L.J., Milne, P., et al. (2016b). LLT1 and CD161 Expression in Human Germinal Centers Promotes B Cell Activation and CXCR4 Downregulation. J Immunol *196*, 2085–2094.

Llibre, A., Garner, L., Partridge, A., Freeman, G.J., Klenerman, P., and Willberg, C.B. (2016c). Expression of lectin-like transcript-1 in human tissues. F1000Research *5*, 2929.

Llorente, C., and Schnabl, B. (2015). The gut microbiota and liver disease. Cell Mol Gastroenterol Hepatol *1*, 275–284.

Loh, L. (2016). Human mucosal-associated invariant T cells contribute to antiviral influenza immunity via IL-18-dependent activation. Proc. Natl Acad. Sci. USA *113*.

López-Sagaseta, J., Dulberger, C.L., Crooks, J.E., Parks, C.D., Luoma, A.M., McFedries, A., Van Rhijn, I., Saghatelian, A., and Adams, E.J. (2013). The molecular basis for Mucosal-Associated Invariant T cell recognition of MR1 proteins. Proc. Natl. Acad. Sci. U.S.A. *110*, E1771-1778.

Lu, F., Yin, D., Pu, Y., Liu, W., Li, Z., Shao, Q., He, C., and Cao, L. (2019). Shikimic Acid Promotes Oligodendrocyte Precursor Cell Differentiation and Accelerates Remyelination in Mice. Neurosci Bull *35*, 434–446.

Mack, M., van Loon, A.P.G.M., and Hohmann, H.-P. (1998). Regulation of Riboflavin Biosynthesis in Bacillus subtilis Is Affected by the Activity of the Flavokinase/Flavin Adenine Dinucleotide Synthetase Encoded by ribC. J Bacteriol *180*, 950–955.

Macosko, E.Z., Basu, A., Satija, R., Nemesh, J., Shekhar, K., Goldman, M., Tirosh, I., Bialas, A.R., Kamitaki, N., Martersteck, E.M., et al. (2015). Highly Parallel Genome-wide Expression Profiling of Individual Cells Using Nanoliter Droplets. Cell *161*, 1202–1214.

Macpherson, A.J., and Uhr, T. (2004). Induction of protective IgA by intestinal dendritic cells carrying commensal bacteria. Science *303*, 1662–1665.

Maekawa, T., Osawa, Y., Okada, Y., Tachi, N., Teramoto, M., Kawamura, T., Horiuchi, T., Kato, S., Kobayashi, A., Kobayashi, S., et al. (2018). Low mucosal-associated invariant T-cell number in peripheral blood of patients with immune thrombocytopenia and their response to prednisolone. PLoS One *13*.

Magalhaes, I. (2015). Mucosal-associated invariant T cell alterations in obese and type 2 diabetic patients. J. Clin. Invest. *125*.

Magnúsdóttir, S., Ravcheev, D., de Crécy-Lagard, V., and Thiele, I. (2015). Systematic genome assessment of B-vitamin biosynthesis suggests co-operation among gut microbes. Front Genet *6*.

Marcobal, A., Barboza, M., Sonnenburg, E.D., Pudlo, N., Martens, E.C., Desai, P., Lebrilla, C.B., Weimer, B.C., Mills, D.A., German, J.B., et al. (2011). Bacteroides in the Infant Gut Consume Milk Oligosaccharides via Mucus-Utilization Pathways. Cell Host Microbe *10*, 507–514.

Marrufo, A.M., Mathew, S.O., Chaudhary, P., Malaer, J.D., Vishwanatha, J.K., and Mathew, P.A. (2018). Blocking LLT1 (CLEC2D, OCIL)-NKRP1A (CD161) interaction enhances natural killer cell-mediated lysis of triple-negative breast cancer cells. Am J Cancer Res *8*, 1050–1063.

Martens, E.C., Chiang, H.C., and Gordon, J.I. (2008). Mucosal glycan foraging enhances fitness and transmission of a saccharolytic human gut bacterial symbiont. Cell Host Microbe *4*, 447–457.

Martens, E.C., Neumann, M., and Desai, M.S. (2018). Interactions of commensal and pathogenic microorganisms with the intestinal mucosal barrier. Nat. Rev. Microbiol. *16*, 457–470.

Martin, Y.C. (2005). A Bioavailability Score. Journal of Medicinal Chemistry *48*, 3164–3170.

Martin, E., Treiner, E., Duban, L., Guerri, L., Laude, H., Toly, C., Premel, V., Devys, A., Moura, I.C., Tilloy, F., et al. (2009). Stepwise Development of MAIT Cells in Mouse and Human. PLOS Biology *7*, e1000054.

Mathew, P.A., Chuang, S.S., Vaidya, S.V., Kumaresan, P.R., Boles, K.S., and Pham, H.-T.K. (2004). The LLT1 receptor induces IFN-gamma production by human natural killer cells. Mol. Immunol. *40*, 1157–1163.

Mathew, S.O., Chaudhary, P., Powers, S.B., Vishwanatha, J.K., and Mathew, P.A. (2016). Overexpression of LLT1 (OCIL, CLEC2D) on prostate cancer cells inhibits NK cell-mediated killing through LLT1-NKRP1A (CD161) interaction. Oncotarget *7*, 68650–68661.

McIntyre, C.W., Harrison, L.E.A., Eldehni, M.T., Jefferies, H.J., Szeto, C.-C., John, S.G., Sigrist, M.K., Burton, J.O., Hothi, D., Korsheed, S., et al. (2011). Circulating endotoxemia: a novel factor in systemic inflammation and cardiovascular disease in chronic kidney disease. Clin J Am Soc Nephrol *6*, 133–141.

McWilliam, H.E.G., Eckle, S.B.G., Theodossis, A., Liu, L., Chen, Z., Wubben, J.M., Fairlie, D.P., Strugnell, R.A., Mintern, J.D., McCluskey, J., et al. (2016). The intracellular pathway for the presentation of vitamin B-related antigens by the antigen-presenting molecule MR1. Nat. Immunol. *17*, 531–537.

Medina-Vera, I., Sanchez-Tapia, M., Noriega-López, L., Granados-Portillo, O., Guevara-Cruz, M., Flores-López, A., Avila-Nava, A., Fernández, M.L., Tovar, A.R., and Torres, N. (2019). A dietary intervention with functional foods reduces metabolic endotoxaemia and attenuates biochemical abnormalities by modifying faecal microbiota in people with type 2 diabetes. Diabetes Metab. *45*, 122–131.

Mei, Q.-X., Huang, C.-L., Luo, S.-Z., Zhang, X.-M., Zeng, Y., and Lu, Y.-Y. (2018). Characterization of the duodenal bacterial microbiota in patients with pancreatic head cancer vs. healthy controls. Pancreatology *18*, 438–445.

Meierovics, A.I., and Cowley, S.C. (2016). MAIT cells promote inflammatory monocyte differentiation into dendritic cells during pulmonary intracellular infection. J. Exp. Med. *213*.

Meierovics, A., Yankelevich, W.J., and Cowley, S.C. (2013). MAIT cells are critical for optimal mucosal immune responses during in vivo pulmonary bacterial infection. Proc. Natl Acad. Sci. USA *110*.

Mendler, A., Pierzchalski, A., Bauer, M., Röder, S., Sattler, A., Standl, M., Borte, M., Bergen, M. von, Rolle-Kampczyk, U., and Herberth, G. MAIT cell activation in adolescents is impacted by bile acid concentrations and body weight. Clinical & Experimental Immunology *n/a*.

Metzemaekers, M., Van Damme, J., Mortier, A., and Proost, P. (2016). Regulation of Chemokine Activity – A Focus on the Role of Dipeptidyl Peptidase IV/CD26. Front Immunol *7*.

Michail, S., Lin, M., Frey, M.R., Fanter, R., Paliy, O., Hilbush, B., and Reo, N.V. (2015). Altered gut microbial energy and metabolism in children with non-alcoholic fatty liver disease. FEMS Microbiol. Ecol. *91*, 1–9.

Mitsdoerffer, M., Lee, Y., Jäger, A., Kim, H.-J., Korn, T., Kolls, J.K., Cantor, H., Bettelli, E., and Kuchroo, V.K. (2010). Proinflammatory T helper type 17 cells are effective B-cell helpers. PNAS *107*, 14292–14297.

Moro-Sibilot, L., Blanc, P., Taillardet, M., Bardel, E., Couillault, C., Boschetti, G., Traverse-Glehen, A., Defrance, T., Kaiserlian, D., and Dubois, B. (2016). Mouse and Human Liver Contain Immunoglobulin A–Secreting Cells Originating From Peyer's Patches and Directed Against Intestinal Antigens. Gastroenterology *151*, 311–323.

Munukka, E., Pekkala, S., Wiklund, P., Rasool, O., Borra, R., Kong, L., Ojanen, X., Cheng, S.M., Roos, C., Tuomela, S., et al. (2014). Gut-adipose tissue axis in hepatic fat accumulation in humans. J. Hepatol. *61*, 132–138.

Nakanishi, K., Yoshimoto, T., Tsutsui, H., and Okamura, H. (2001). Interleukin-18 regulates both Th1 and Th2 responses. Annu. Rev. Immunol. *19*, 423–474.

Nardone, G., and Compare, D. (2015). The human gastric microbiota: Is it time to rethink the pathogenesis of stomach diseases? United European Gastroenterol J *3*, 255–260.

Negrotto, L., Cantó, E., Río, J., Tintoré, M., Montalban, X., and Comabella, M. (2015). Peripheral blood non-MAIT CD8+CD161hi cells are decreased in relapsing-remitting multiple sclerosis patients treated with interferon beta. J. Neuroimmunol. *288*, 98–101.

Neuberger, G., and Bacher, A. (1986). Biosynthesis of riboflavin. enzymatic formation of 6,7-dimethyl-8-ribityllumazine by heavy riboflavin synthase from Bacillus subtilis. Biochemical and Biophysical Research Communications *139*, 1111–1116.

Newgard, C.B., An, J., Bain, J.R., Muehlbauer, M.J., Stevens, R.D., Lien, L.F., Haqq, A.M., Shah, S.H., Arlotto, M., Slentz, C.A., et al. (2009). A branched-chain amino acid-related metabolic signature that differentiates obese and lean humans and contributes to insulin resistance. Cell Metab. *9*, 311–326.

Ning, L., Liu, R., Lou, X., Du, H., Chen, W., Zhang, F., Li, S., Chen, X., and Xu, G. (2019). Association between Helicobacter pylori infection and nonalcoholic fatty liver disease: a systemic review and meta-analysis. Eur J Gastroenterol Hepatol *31*, 735–742.

Nishiyama, M., Ohtake, N., Kaneko, A., Tsuchiya, N., Imamura, S., Iizuka, S., Ishizawa, S., Nishi, A., Yamamoto, M., Taketomi, A., et al. (2020). Increase of Akkermansia muciniphila by a Diet Containing Japanese Traditional Medicine Bofutsushosan in a Mouse Model of Non-Alcoholic Fatty Liver Disease. Nutrients *12*.

Nistal, E., Caminero, A., Herrán, A.R., Pérez-Andres, J., Vivas, S., Ruiz de Morales, J.M., Sáenz de Miera, L.E., and Casqueiro, J. (2016). Study of duodenal bacterial communities by 16S rRNA gene analysis in adults with active celiac disease vs non-celiac disease controls. J. Appl. Microbiol. *120*, 1691–1700.

Niwa, T. (2011). Role of indoxyl sulfate in the progression of chronic kidney disease and cardiovascular disease: experimental and clinical effects of oral sorbent AST-120. Ther Apher Dial *15*, 120–124.

Noh, D.O., and Gilliland, S.E. (1993). Influence of bile on cellular integrity and beta-galactosidase activity of Lactobacillus acidophilus. J. Dairy Sci. *76*, 1253–1259.

Oa, A., Is, S., Mma, R., Jd, S., Me, T., M, K., B, P., M, B., A, K., B, T., et al. (2019). Mouse Cytomegalovirus m153 Protein Stabilizes Expression of the Inhibitory NKR-P1B Ligand Clr-b (J Virol).

O'Hara, A.M., and Shanahan, F. (2006). The gut flora as a forgotten organ. EMBO Rep *7*, 688–693.

Ohnuma, K., Yamochi, T., Uchiyama, M., Nishibashi, K., Yoshikawa, N., Shimizu, N., Iwata, S., Tanaka, H., Dang, N.H., and Morimoto, C. (2004). CD26 up-regulates expression of CD86 on antigen-presenting cells by means of caveolin-1. PNAS *101*, 14186–14191.

Ohnuma, K., Uchiyama, M., Yamochi, T., Nishibashi, K., Hosono, O., Takahashi, N., Kina, S., Tanaka, H., Lin, X., Dang, N.H., et al. (2007). Caveolin-1 Triggers T-cell Activation via CD26 in Association with CARMA1. J. Biol. Chem. *282*, 10117–10131.

Omoto, Y., Yamanaka, K., Tokime, K., Kitano, S., Kakeda, M., Akeda, T., Kurokawa, I., Gabazza, E.C., Tsutsui, H., Katayama, N., et al. (2010). Granzyme B is a novel interleukin-18 converting enzyme. J. Dermatol. Sci. *59*, 129–135.

Pala, L., Mannucci, E., Pezzatini, A., Ciani, S., Sardi, J., Raimondi, L., Ognibene, A., Cappadona, A., Vannelli, B.G., and Rotella, C.M. (2003). Dipeptidyl peptidase-IV expression and activity in human glomerular endothelial cells. Biochem. Biophys. Res. Commun. *310*, 28–31.

Paquin-Proulx, D., Greenspun, B.C., Costa, E.A.S., Segurado, A.C., Kallas, E.G., Nixon, D.F., and Leal, F.E. (2017). MAIT cells are reduced in frequency and functionally impaired in human T lymphotropic virus type 1 infection: Potential clinical implications. PLoS ONE *12*, e0175345.

Pedersen, H.K., Gudmundsdottir, V., Nielsen, H.B., Hyotylainen, T., Nielsen, T., Jensen, B.A.H., Forslund, K., Hildebrand, F., Prifti, E., Falony, G., et al. (2016). Human gut microbes impact host serum metabolome and insulin sensitivity. Nature *535*, 376–381.

Porcelli, S., Yockey, C.E., Brenner, M.B., and Balk, S.P. (1993). Analysis of T cell antigen receptor (TCR) expression by human peripheral blood CD4-8- alpha/beta T cells demonstrates preferential use of several V beta genes and an invariant TCR alpha chain. J. Exp. Med. *178*, 1–16.

Portmann, S., Fahrner, R., Lechleiter, A., Keogh, A., Overney, S., Laemmle, A., Mikami, K., Montani, M., Tschan, M.P., Candinas, D., et al. (2013). Antitumor effect of SIRT1 inhibition in human HCC tumor models in vitro and in vivo. Mol. Cancer Ther. *12*, 499–508.

Provine, N.M., and Klenerman, P. (2020). MAIT Cells in Health and Disease. 26.

Puche, J.E., Saiman, Y., and Friedman, S.L. (2013). Hepatic stellate cells and liver fibrosis. Compr Physiol *3*, 1473–1492.

Quesada-Vázquez, S., Aragonès, G., Del Bas, J.M., and Escoté, X. (2020). Diet, Gut Microbiota and Non-Alcoholic Fatty Liver Disease: Three Parts of the Same Axis. Cells *9*.

Rabot, S., Membrez, M., Bruneau, A., Gérard, P., Harach, T., Moser, M., Raymond, F., Mansourian, R., and Chou, C.J. (2010). Germ-free C57BL/6J mice are resistant to high-fat-diet-induced insulin resistance and have altered cholesterol metabolism. FASEB J. *24*, 4948–4959.

Racanelli, V., and Rehermann, B. (2006). The liver as an immunological organ. Hepatology *43*, S54–S62.

Raghavan, M., Cid, N.D., Rizvi, S.M., and Peters, L.R. (2008). MHC class I assembly: out and about. Trends Immunol *29*, 436–443.

Rai, A.K., Thakur, C.P., Kumar, P., and Mitra, D.K. (2012). Impaired expression of CD26 compromises T-cell recruitment in human visceral leishmaniasis. European Journal of Immunology *42*, 2782–2791.

Ramachandran, P., Dobie, R., Wilson-Kanamori, J.R., Dora, E.F., Henderson, B.E.P., Luu, N.T., Portman, J.R., Matchett, K.P., Brice, M., Marwick, J.A., et al. (2019). Resolving the fibrotic niche of human liver cirrhosis at single-cell level. Nature *575*, 512–518.

Reantragoon, R. (2013). Antigen-loaded MR1 tetramers define T cell receptor heterogeneity in mucosal-associated invariant T cells. J. Exp. Med. *210*.

Reantragoon, R., Kjer-Nielsen, L., Patel, O., Chen, Z., Illing, P.T., Bhati, M., Kostenko, L., Bharadwaj, M., Meehan, B., Hansen, T.H., et al. (2012). Structural insight into MR1-mediated recognition of the mucosal associated invariant T cell receptor. J Exp Med *209*, 761–774.

Reinholdt, J., and Husby, S. (2013). IgA and Mucosal Homeostasis (Landes Bioscience).

Renand, A., Habes, S., Mosnier, J.-F., Aublé, H., Judor, J.-P., Vince, N., Hulin, P., Nedellec, S., Métairie, S., Archambeaud, I., et al. (2018). Immune Alterations in Patients With Type 1 Autoimmune Hepatitis Persist Upon Standard Immunosuppressive Treatment. Hepatol Commun *2*, 968–981.

Ridlon, J.M., Kang, D.-J., and Hylemon, P.B. (2006). Bile salt biotransformations by human intestinal bacteria. J. Lipid Res. *47*, 241–259.

Riegert, P., Wanner, V., and Bahram, S. (1998). Genomics, isoforms, expression, and phylogeny of the MHC class I-related MR1 gene. J. Immunol. *161*, 4066–4077.

Rodrigues, P.M., Afonso, M.B., Simão, A.L., Borralho, P.M., Rodrigues, C.M.P., and Castro, R.E. (2015). Inhibition of NF-κB by deoxycholic acid induces miR-21/PDCD4-dependent hepatocellular apoptosis. Sci Rep *5*, 17528.

Rosen, D.B., Cao, W., Avery, D.T., Tangye, S.G., Liu, Y.-J., Houchins, J.P., and Lanier, L.L. (2008). Functional Consequences of Interactions between Human NKR-P1A and Its Ligand LLT1 Expressed on Activated Dendritic Cells and B Cells. J Immunol *180*, 6508–6517.

Rosen, F., Huff, J.W., and Perlzweig, W.A. (1946). THE EFFECT OF TRYPTOPHANE ON THE SYNTHESIS OF NICOTINIC ACID IN THE RAT. J. Biol. Chem. *163*, 343–344.

Rouxel, O. (2017). Cytotoxic and regulatory roles of mucosal-associated invariant T cells in type 1 diabetes. Nat. Immunol. *18*.

Ruijing, X. (2012). Jα33+ MAIT cells play a protective role in TNBS induced intestinal inflammation. Hepatogastroenterology *59*.

Sakanaka, M., Gotoh, A., Yoshida, K., Odamaki, T., Koguchi, H., Xiao, J.-Z., Kitaoka, M., and Katayama, T. (2019). Varied Pathways of Infant Gut-Associated Bifidobacterium to Assimilate Human Milk Oligosaccharides: Prevalence of the Gene Set and Its Correlation with Bifidobacteria-Rich Microbiota Formation. Nutrients *12*.

Salyers, A.A., Palmer, J.K., and Wilkins, T.D. (1977). Laminarinase (beta-glucanase) activity in Bacteroides from the human colon. Appl. Environ. Microbiol. *33*, 1118–1124.

Santos-Juanes, J., Fernández-Vega, I., Lorenzo-Herrero, S., Sordo-Bahamonde, C., Martínez-Camblor, P., García-Pedrero, J.M., Vivanco, B., Galache-Osuna, C., Vazquez-Lopez, F., Gonzalez, S., et al. (2019). Lectin-like transcript 1 (LLT1) expression is associated with nodal metastasis in patients with head and neck cutaneous squamous cell carcinoma. Arch. Dermatol. Res. *311*, 369–376.

Satkunanathan, S., Kumar, N., Bajorek, M., Purbhoo, M.A., and Culley, F.J. (2014). Respiratory Syncytial Virus Infection, TLR3 Ligands, and Proinflammatory Cytokines Induce CD161 Ligand LLT1 Expression on the Respiratory Epithelium. Journal of Virology *88*, 2366–2373.

Sattler, A., Dang-Heine, C., Reinke, P., and Babel, N. (2015). IL-15 dependent induction of IL-18 secretion as a feedback mechanism controlling human MAIT-cell effector functions. Eur. J. Immunol. *45*, 2286–2298.

Sawa, Y., Arima, Y., Ogura, H., Kitabayashi, C., Jiang, J.-J., Fukushima, T., Kamimura, D., Hirano, T., and Murakami, M. (2009). Hepatic interleukin-7 expression regulates T cell responses. Immunity *30*, 447–457.

Schmaler, M., Colone, A., Spagnuolo, J., Zimmermann, M., Lepore, M., Kalinichenko, A., Bhatia, S., Cottier, F., Rutishauser, T., Pavelka, N., et al. (2018). Modulation of bacterial metabolism by the microenvironment controls MAIT cell stimulation. Mucosal Immunology *11*, 1060–1070.

Sekirov, I., Russell, S.L., Antunes, L.C.M., and Finlay, B.B. (2010). Gut Microbiota in Health and Disease. Physiological Reviews *90*, 859–904.

Serriari, N.E. (2014). Innate mucosal-associated invariant T (MAIT) cells are activated in inflammatory bowel diseases. Clin. Exp. Immunol. *176*.

Setsu, T., Yamagiwa, S., Tominaga, K., Kimura, N., Honda, H., Kamimura, H., Tsuchiya, A., Takamura, M., and Terai, S. (2018). Persistent reduction of mucosal-associated invariant T cells in primary biliary cholangitis. Journal of Gastroenterology and Hepatology *33*, 1286–1294.

Sharma, P.K., Wong, E.B., Napier, R.J., Bishai, W.R., Ndung'u, T., Kasprowicz, V.O., Lewinsohn, D.A., Lewinsohn, D.M., and Gold, M.C. (2015). High expression of CD26 accurately identifies human bacteria-reactive MR1-restricted MAIT cells. Immunology *145*, 443–453.

Shi, J., Gao, W., and Shao, F. (2017). Pyroptosis: Gasdermin-Mediated Programmed Necrotic Cell Death. Trends Biochem. Sci. *42*, 245–254.

Shimada, Y., Kinoshita, M., Harada, K., Mizutani, M., Masahata, K., Kayama, H., and Takeda, K. (2013). Commensal bacteria-dependent indole production enhances epithelial barrier function in the colon. PLoS ONE *8*, e80604.

Shortman, K., and Heath, W.R. (2010). The CD8+ dendritic cell subset. Immunol. Rev. *234*, 18–31.

Smirnoff, N. (2018). Ascorbic acid metabolism and functions: A comparison of plants and mammals. Free Radic Biol Med *122*, 116–129.

Spadoni, I., Zagato, E., Bertocchi, A., Paolinelli, R., Hot, E., Di Sabatino, A., Caprioli, F., Bottiglieri, L., Oldani, A., Viale, G., et al. (2015). A gut-vascular barrier controls the systemic dissemination of bacteria. Science *350*, 830–834.

Struyf, S., De Meester, I., Scharpé, S., Lenaerts, J.P., Menten, P., Wang, J.M., Proost, P., and Van Damme, J. (1998). Natural truncation of RANTES abolishes signaling through the CC chemokine receptors CCR1 and CCR3, impairs its chemotactic potency and generates a CC chemokine inhibitor. Eur. J. Immunol. *28*, 1262–1271.

Suck, G., Chu, S., Niam, M., Lim, T., Hui, K., and Koh, M. (2007). Highly cytotoxic CD56+CD8+ NK cells as potential novel candidates for cancer cellular therapy. Clin Cancer Res *13*, B13–B13.

Sundin, O.H., Mendoza-Ladd, A., Zeng, M., Diaz-Arévalo, D., Morales, E., Fagan, B.M., Ordoñez, J., Velez, P., Antony, N., and McCallum, R.W. (2017). The human jejunum has an endogenous microbiota that differs from those in the oral cavity and colon. BMC Microbiol. *17*, 160.

Sung, J.J., Leung, J.C., Tsui, C.P., Chung, S.S., and Lai, K.N. (1995). Biliary IgA secretion in obstructive jaundice: the effects of endoscopic drainage. Gastrointest. Endosc. *42*, 439–444.

Sung, J.Y., Costerton, J.W., and Shaffer, E.A. (1992). Defense system in the biliary tract against bacterial infection. Dig. Dis. Sci. *37*, 689–696.

Tang, X.-Z., Jo, J., Tan, A.T., Sandalova, E., Chia, A., Tan, K.C., Lee, K.H., Gehring, A.J., Libero, G.D., and Bertoletti, A. (2013). IL-7 Licenses Activation of Human Liver Intrasinusoidal Mucosal-Associated Invariant T Cells. The Journal of Immunology *190*, 3142–3152.

Targher, G., Bertolini, L., Padovani, R., Rodella, S., Tessari, R., Zenari, L., Day, C., and Arcaro, G. (2007). Prevalence of Nonalcoholic Fatty Liver Disease and Its Association With Cardiovascular Disease Among Type 2 Diabetic Patients. Diabetes Care *30*, 1212–1218.

Teunissen, M.B.M., Yeremenko, N.G., Baeten, D.L.P., Chielie, S., Spuls, P.I., de Rie, M.A., Lantz, O., and Res, P.C.M. (2014). The IL-17A-Producing CD8+ T-Cell Population in Psoriatic Lesional Skin Comprises Mucosa-Associated Invariant T Cells and Conventional T Cells. Journal of Investigative Dermatology *134*, 2898–2907.

Tilg, H., and Kaser, A. (2011). Gut microbiome, obesity, and metabolic dysfunction. J Clin Invest *121*, 2126–2132.

Toubal, A., Nel, I., Lotersztajn, S., and Lehuen, A. (2019). Mucosal-associated invariant T cells and disease. Nature Reviews Immunology *19*, 643–657.

Toussirot, E., Laheurte, C., Gaugler, B., Gabriel, D., and Saas, P. (2018). Increased IL-22- and IL-17A-producing mucosal-associated invariant T cells in the peripheral blood of patients with ankylosing spondylitis. Front. Immunol. *9*.

Treiner, E., Duban, L., Bahram, S., Radosavljevic, M., Wanner, V., Tilloy, F., Affaticati, P., Gilfillan, S., and Lantz, O. (2003). Selection of evolutionarily conserved mucosal-associated invariant T cells by MR1. Nature *422*, 164–169.

Tsuchida, T., and Friedman, S.L. (2017). Mechanisms of hepatic stellate cell activation. Nat Rev Gastroenterol Hepatol *14*, 397–411.

Turtle, C.J., Delrow, J., Joslyn, R.C., Swanson, H.M., Basom, R., Tabellini, L., Delaney, C., Heimfeld, S., Hansen, J.A., and Riddell, S.R. (2011). Innate signals overcome acquired TCR signaling pathway regulation and govern the fate of human CD161(hi) CD8α^+ semi-invariant T cells. Blood *118*, 2752–2762.

Uchimura, Y., Fuhrer, T., Li, H., Lawson, M.A., Zimmermann, M., Yilmaz, B., Zindel, J., Ronchi, F., Sorribas, M., Hapfelmeier, S., et al. (2018). Antibodies Set Boundaries Limiting Microbial Metabolite Penetration and the Resultant Mammalian Host Response. Immunity *49*, 545-559.e5.

Ushio, S., Namba, M., Okura, T., Hattori, K., Nukada, Y., Akita, K., Tanabe, F., Konishi, K., Micallef, M., Fujii, M., et al. (1996). Cloning of the cDNA for human IFN-gamma-inducing factor, expression in Escherichia coli, and studies on the biologic activities of the protein. J. Immunol. *156*, 4274–4279.

Ussher, J.E., Bilton, M., Attwod, E., Shadwell, J., Richardson, R., de Lara, C., Mettke, E., Kurioka, A., Hansen, T.H., Klenerman, P., et al. (2014). CD161++ CD8+ T cells, including the MAIT cell subset, are specifically activated by IL-12+IL-18 in a TCR-independent manner. Eur. J. Immunol. *44*, 195–203.

Ussher, J.E., van Wilgenburg, B., Hannaway, R.F., Ruustal, K., Phalora, P., Kurioka, A., Hansen, T.H., Willberg, C.B., Phillips, R.E., and Klenerman, P. (2016). TLR signaling in human antigen-presenting cells regulates MR1-dependent activation of MAIT cells. Eur. J. Immunol. *46*, 1600–1614.

Ussher, J.E., Willberg, C.B., and Klenerman, P. (2018). MAIT cells and viruses. Immunol. Cell Biol. *96*.

Utzny, C., Coombs, D., Müller, S., and Valitutti, S. (2006). Analysis of peptide/MHC-induced TCR downregulation: deciphering the triggering kinetics. Cell Biochem. Biophys. *46*, 101–111.

Van Acker, H.H., Capsomidis, A., Smits, E.L., and Van Tendeloo, V.F. (2017). CD56 in the Immune System: More Than a Marker for Cytotoxicity? Front Immunol *8*.

Van Herreweghe, F., Mao, J., Chaplen, F.W.R., Grooten, J., Gevaert, K., Vandekerckhove, J., and Vancompernolle, K. (2002). Tumor necrosis factor-induced modulation of glyoxalase I activities through phosphorylation by PKA results in cell death and is accompanied by the formation of a specific methylglyoxal-derived AGE. Proceedings of the National Academy of Sciences *99*, 949–954.

Villmones, H.C., Haug, E.S., Ulvestad, E., Grude, N., Stenstad, T., Halland, A., and Kommedal, Ø. (2018). Species Level Description of the Human Ileal Bacterial Microbiota. Sci Rep *8*.

Walker, L.J., Kang, Y.-H., Smith, M.O., Tharmalingham, H., Ramamurthy, N., Fleming, V.M., Sahgal, N., Leslie, A., Oo, Y., Geremia, A., et al. (2012). Human MAIT and CD8αα cells develop from a pool of type-17 precommitted CD8+ T cells. Blood *119*, 422–433.

Wang, H. (2018). MAIT cells protect against pulmonary Legionella longbeachae infection. Nat. Commun. *9*.

Wanless, I.R., and Lentz, J.S. (1990). Fatty liver hepatitis (steatohepatitis) and obesity: An autopsy study with analysis of risk factors. Hepatology *12*, 1106–1110.

Waumans, Y., Baerts, L., Kehoe, K., Lambeir, A.-M., and De Meester, I. (2015). The Dipeptidyl Peptidase Family, Prolyl Oligopeptidase and Prolyl Carboxypeptidase in the Immune System and Inflammatory Disease, including Atherosclerosis. Front. Immunol. *6*.

Weisburg, W.G., Barns, S.M., Pelletier, D.A., and Lane, D.J. (1991). 16S ribosomal DNA amplification for phylogenetic study. J. Bacteriol. *173*, 697–703.

Wilgenburg, B.V. (2018). MAIT cells contribute to protection against lethal influenza infection in vivo. Nat. Commun. *9*.

van Wilgenburg, B., Scherwitzl, I., Hutchinson, E.C., Leng, T., Kurioka, A., Kulicke, C., de Lara, C., Cole, S., Vasanawathana, S., Limpitikul, W., et al. (2016). MAIT cells are activated during human viral infections. Nat Commun *7*, 11653.

Yamagata, K., Daitoku, H., Shimamoto, Y., Matsuzaki, H., Hirota, K., Ishida, J., and Fukamizu, A. (2004). Bile acids regulate gluconeogenic gene expression via small heterodimer partner-mediated repression of hepatocyte nuclear factor 4 and Foxo1. J. Biol. Chem. *279*, 23158–23165.

Yan, S., Marguet, D., Dobers, J., Reutter, W., and Fan, H. (2003). Deficiency of CD26 results in a change of cytokine and immunoglobulin secretion after stimulation by pokeweed mitogen. Eur. J. Immunol. *33*, 1519–1527.

Yano, J.M., Yu, K., Donaldson, G.P., Shastri, G.G., Ann, P., Ma, L., Nagler, C.R., Ismagilov, R.F., Mazmanian, S.K., and Hsiao, E.Y. (2015). Indigenous bacteria from the gut microbiota regulate host serotonin biosynthesis. Cell *161*, 264–276.

Yasuda, K., Nakanishi, K., and Tsutsui, H. (2019). Interleukin-18 in Health and Disease. Int J Mol Sci *20*.

Yoshimoto, T., Takeda, K., Tanaka, T., Ohkusu, K., Kashiwamura, S., Okamura, H., Akira, S., and Nakanishi, K. (1998). IL-12 up-regulates IL-18 receptor expression on T cells, Th1 cells, and B cells: synergism with IL-18 for IFN-gamma production. J. Immunol. *161*, 3400–3407.

Yu, J., Lo, J.-L., Huang, L., Zhao, A., Metzger, E., Adams, A., Meinke, P.T., Wright, S.D., and Cui, J. (2002). Lithocholic acid decreases expression of bile salt export pump through farnesoid X receptor antagonist activity. J. Biol. Chem. *277*, 31441–31447.

Yuan, J., Chen, C., Cui, J., Lu, J., Yan, C., Wei, X., Zhao, X., Li, N., Li, S., Xue, G., et al. (2019). Fatty Liver Disease Caused by High-Alcohol-Producing Klebsiella pneumoniae. Cell Metab. *30*, 675-688.e7.

von Zastrow, M. (2001). Endocytosis and downregulation of G protein-coupled receptors. Parkinsonism Relat. Disord. *7*, 265–271.

Ze, X., Duncan, S.H., Louis, P., and Flint, H.J. (2012). Ruminococcus bromii is a keystone species for the degradation of resistant starch in the human colon. ISME J *6*, 1535–1543.

Zhao, S., Liu, W., Wang, J., Shi, J., Sun, Y., Wang, W., Ning, G., Liu, R., and Hong, J. (2017). Akkermansia muciniphila improves metabolic profiles by reducing inflammation in chow diet-fed mice. J. Mol. Endocrinol. *58*, 1–14.

Zheng, H., Pomyen, Y., Hernandez, M.O., Li, C., Livak, F., Tang, W., Dang, H., Greten, T.F., Davis, J.L., Zhao, Y., et al. (2018). Single-cell analysis reveals cancer stem cell heterogeneity in hepatocellular carcinoma. Hepatology *68*, 127–140.

Zhu, J., Peng, T., Johnston, C., Phasouk, K., Kask, A.S., Klock, A., Jin, L., Diem, K., Koelle, D.M., Wald, A., et al. (2013a). Immune Surveillance by CD8αα+ Skin Resident T Cells in Human Herpesvirus Infection. Nature *497*, 494–497.

Zhu, L., Baker, S.S., Gill, C., Liu, W., Alkhouri, R., Baker, R.D., and Gill, S.R. (2013b). Characterization of gut microbiomes in nonalcoholic steatohepatitis (NASH) patients: a connection between endogenous alcohol and NASH. Hepatology *57*, 601–609.

Zumwalde, N.A., Haag, J.D., Gould, M.N., and Gumperz, J.E. (2018). Mucosal associated invariant T cells from human breast ducts mediate a Th17-skewed response to bacterially exposed breast carcinoma cells. Breast Cancer Res. *20*.

Martin Lett

27/01/1991
6 Rue du Jura● 68300 Saint-Louis, France
Phone: +33676745039 ● E-Mail: martin.lett@unibas.ch

Work Experience

PhD student at the University of Basel **April 2016 to August 2020**

Liver Immunology lab (PD Dr. med. Dr. phil. M. Filipowicz Sinnreich, Department of Biomedicine)

Project: Role of Mucosal associated invariant T cells in liver diseases

- Isolation, culture and analysis of patient derived liver cells by flow cytometry and single cell RNA-sequencing
- Investigating potential therapeutic interventions by functional assays using blocking ligands and antibodies
- Establishing new techniques of bacterial metabolite detection
- Presenting scientific results at national and international meetings

Research Internship at the University of Strasbourg **January to July 2015**

Invasion, Migration, and Microenvironment Team (UMR 7213), Prof. P. Ronde

Project: Study of the effect of the microenvironment composition on cell motility

- Handled cell migration studies in addition to zymography and image treatment in relation to melanoma, cell migration, and invasion involving the tumour microenvironment
- Investigated the CD47 pharmacological pathway by Western Blotting, immunoprecipitation, and immunostaining.

Research Internship at the University of Strasbourg **March to August 2014**

Invasion, Migration, and Microenvironment Team (UMR 7213), Prof. Y. Mély, Dr. E. Sick

Project: CD47 role in cancer cell migration

- Performed Western Blot analyses, immunostaining and cell transfection with labelled proteins to understand the effect of the receptor activation
- Responsible for the culture of five cell types including human tumour cells and human astrocytes

Internal Medicine / Emergency Services Unit **September to February 2014**

New Civil Hospital of Strasbourg

- Verified incoming medical prescriptions of the patients, and discussed the prescription with the medical team
- Analysed drug misprescriptions in the Emergency Service

Volunteer Research Internship at the University of Strasbourg **June to July 2014**

Invasion, Migration, and Microenvironment Team (UMR 7213)

- Cell culture preparation, proliferation, and viability assays in research on the role of the CD47 receptor in cell multiplication

Education

PhD in Cell Biology, University of Basel **2016 – 2020**

Dissertation: *Role of liver cells in bacterial antigen metabolism and MAIT cell activation*

Master degree in Pharmacology, University of Strasbourg **2013 - 2015**

Master achieved in 2015 in conjunction with a PharmD

Dissertation: *The role of the CD47 receptor in cell invasion and migration.*

National qualification as a Doctor of Pharmacy, University of Strasbourg **2009 - 2015**

Dissertation: *Targeting cell migration to prevent metastasis; current status* **(First class Honours)**

Degree consists of six years of theoretical and practical studies with a competitive exam following the first year of higher education.

Scientific baccalaureate, St. Augustin, Bitche, France **2006 - 2009**

Attained a scientific baccalaureate with First Honours (**valedictorian**)

Seminars / Presentations

19th Hepatobiliary and Gastrointestinal Research Retreat, Pontresina, CH **January 2020**

Oral presentation: "Towards a characterization of the gut microbiome and its influence on MAIT cells in non-alcoholic fatty liver disease"

CD1-MR1 EMBO Workshop, Oxford, UK **September 2019**

Poster presentation: "Robust Mucosal-associated invariant T cell (MAIT) activation in response to interactions with primary human liver cell subsets"

University of Oxford - Peter Medawar Building Seminars, Oxford, UK **June 2019**

Invited speaker: "Robust Mucosal-associated invariant T cell (MAIT) cell activation in response to interactions with primary human liver cell subsets"

EASL International Liver Conference, Vienna, Austria **April 2019**

Late breaker **poster** presentation: "Robust Mucosal-associated invariant T cell (MAIT) activation in response to interactions with primary human liver cell subsets"

University of Basel Immunology Community (UBICO) retreat 2018, CH **March 2019**

Oral presentation: "Robust MAIT cell activation in response to interactions with primary human liver cell subsets"

18th Hepatobiliary and Gastrointestinal Research Retreat, Les Diablerets, CH **January 2019**

Oral presentation: "Robust MAIT cell activation in response to interactions with primary human liver cell subsets"

Gastro-Regio meeting 2018, Freiburg i. Br., Germany **September 2018**

Oral presentation: "Towards a characterisation of MAIT cell populations in non-alcoholic fatty liver disease"

Gastro-Regio meeting 2017, Strasbourg, France **September 2017**

Oral presentation: "Intrahepatic interaction partners of Mucosal-associated invariant T cells"

Funding

University of Basel travel fund for early career researchers **September 2019**
CD1-MR1 EMBO Workshop, Oxford, UK

University of Basel travel fund for early career researchers **April 2019**
EASL International Liver Conference, Vienna, Austria

Extracurricular Activities

Immuno-PhD Club University of Basel

- Member of the organizing committee for three years
- Coordinated monthly internal seminar
- Organized journal club with international invited speakers

Association «*Association des étudiants en Pharmacie de Strasbourg*» (AAEPS/H2S):

- Presided over the student association "H2S" in 2013 after four years as an active member
- Managed a team of 19 dedicated student volunteers
- Spearheaded several initiatives advocating healthy sexual decisions among students at the University of Strasbourg, and orchestrated blood drives
- Ensured proper management of the campus canteen and the association's shop
- Handled the €170,000 annual budget and supervised the association's employee

Leadership:

- Elected by the students of the College to the council of Pharmacy in 2011
- Nominated for and joined the CFVU "*commission de la formation et de la vie universitaire"* (University council) in 2013.
- Elected by the council of Pharmacy to the College Direction Committee as the Student Assistant Director in 2014

Skills

Instruction:

- Volunteered as a peer tutor in 2010
- Joined Supexam©, a tutoring company, as chemistry teacher

Language Proficiencies:

- French: Native speaker
- English: C2 (mastery of written and spoken English)
- German: B1 (conversational fluency and moderate writing skills)